Journal of Diabetes Research

Genomics and Metabolomics in Obesity and Type 2 Diabetes

Guest Editors: Adam Kretowski, Francisco J. Ruperez, and Michal Ciborowski

Genomics and Metabolomics in Obesity and Type 2 Diabetes

Journal of Diabetes Research

Genomics and Metabolomics in Obesity and Type 2 Diabetes

Guest Editors: Adam Kretowski, Francisco J. Ruperez, and Michal Ciborowski

Editorial Board

Contents

Hindawi Publishing Corporation
Journal of Diabetes Research
Volume 2016, Article ID 9415645, 2 pages
http://dx.doi.org/10.1155/2016/9415645

Editorial

Genomics and Metabolomics in Obesity and Type 2 Diabetes

Adam Kretowski,[1,2] Francisco J. Ruperez,[3] and Michal Ciborowski[2]

[1]*Department of Endocrinology, Diabetology and Internal Medicine, Medical University of Bialystok, Sklodowskiej-Curie 24a, 15-276 Bialystok, Poland*
[2]*Clinical Research Centre, Medical University of Bialystok, Sklodowskiej-Curie 24a, 15-276 Bialystok, Poland*
[3]*Center for Metabolomics and Bioanalysis (CEMBIO), Faculty of Pharmacy, University San Pablo-CEU, Montepríncipe Campus, Boadilla del Monte, 28668 Madrid, Spain*

Correspondence should be addressed to Adam Kretowski; adamkretowski@wp.pl

Received 11 April 2016; Accepted 12 April 2016

Obesity and associated diseases are responsible for the global burden of morbidity and mortality, consequently having a huge impact on the economy of healthcare system. Obesity is the leading risk factor for type 2 diabetes (T2DM), and both conditions currently affect millions of individuals worldwide, being considered as epidemic. The risk for development of obesity and consequently T2DM depends on multiple factors, such as genetic susceptibility [1], composition of the gut microbiota [2], or environmental factors, that is, increased consumption of "unhealthy" food, rich in either saturated fat or refined carbohydrates, as well as reduced physical activity or exposition to pesticides, phenols, phthalates, or heavy metals [3, 4]. Over the past decade a number of common genetic susceptibility loci for obesity and T2DM have been identified [5, 6] and the estimated heritability of obesity/T2DM ranges from 20% to 80% [7, 8]. However, considering the rapid rise of obesity prevalence in the last decade and the radical differences in BMI among individuals living in the same "obesity promoting" environment, it can be suggested that the risk for obesity development depends on complex interactions between genes and the environment [4].

The metabolome is influenced by genetic variants, epigenetic factors, changes in gene expression, or enzyme activity, as well as by environmental factors (diet, physical activity, and pharmaceuticals) and aging [9]. Consequently, metabolomics is a valuable tool to study environment-related modifications of the genetic susceptibility. Currently, based on metabolomics studies, several small molecules are proposed as related to diabetes and/or obesity [10], and the utility of metabolomics for diet-related studies has already been shown [11]. However, as the prevalence of obesity is continually increasing, more research is needed for better understanding of the mechanisms of obesity and the evolution to T2DM. Moreover, novel treatment strategies for obesity/T2DM are sought, while the already known effective treatments such as life style modification (physical activity, diet) or weight loss surgeries should be studied in more detail to explore the molecular pathways lying underneath the weight loss and the T2DM remission.

This special issue is devoted to genetic and molecular biomarkers of obesity and diabetes, as well as to studies in which novel holistic approaches are applied to improve the knowledge on molecular aspects of the evolution or treatment of obesity and diabetes.

Among small molecule metabolites, branched-chain amino acids and acylcarnitines have been linked to obesity-associated insulin resistance (IR). C. Hellmuth et al. performed a longitudinal study on obese children participating in a lifestyle intervention trial for inducing weight loss, to explore changes in amino acids, carnitines, and insulin resistance after the intervention. Only tyrosine was significantly associated with HOMA before and after the intervention and was found to change during the intervention. In addition, BCAA levels were negatively related to insulin resistance in cross-sectional analyses but not in the longitudinal profiling.

The authors concluded that tyrosine alterations in association with insulin resistance precede the alteration in BCAA metabolism.

Another group of metabolites shown to be altered in diabetes are short-chain fatty acids (SCFAs). In their article, E. Lachmandas et al. showed the relationship between diabetes, SCFAs, and increased susceptibility to tuberculosis. Diabetes is associated with a threefold increased risk of tuberculosis, while butyrate producing bacteria are known to be decreased in gut microbiota of patients with diabetes. The authors linked these observations and performed several experiments in which they showed that SCFAs exhibit anti-inflammatory properties, while low doses of butyrate decreased *Mycobacterium tuberculosis*-induced proinflammatory cytokine responses and increased production of IL-10. IL-10 may play a role in mediating the inhibitory effects of butyrate on the host immune response to *M. tuberculosis*.

M.-O. Guzmán-Ornelas et al. investigated the relationship between CCL2 G-2518A and CCR2Val64Ile polymorphisms and the levels of soluble chemokine (C-C motif) ligand-2 (sCCL2), metabolic markers, and adiposity in a Mexican population with insulin resistance. The CCL2 polymorphism was found to be associated with IR, and the CCL2-phenotype carriers (A+) had lower body mass and fat indexes, insulin, and HOMA-IR, as well as higher adiponectin levels. Furthermore, individuals with IR presented higher sCCL2 level. The double-polymorphic phenotype carriers (A+/Ile+) exhibited higher sCCL2 than double wild type-phenotype carriers (A−/Ile−). The present findings allow the authors to suggest a possible association of sCCL2 production with the adiposity and polymorphic phenotypes of CCL2 and CCR2, in Mexican-Mestizos with IR.

Other articles included in this special issue discuss the treatment of obesity and diabetes. Although several natural (green tea polyphenols, cocoa, and chitin/chitosan) antiobesity agents have been already proposed, researchers are still interested in finding phytochemical strategies to treat obesity. N. G. S. Jambocus et al. used an NMR-based metabolomics approach to evaluate mechanisms of antiobesity effect of one extract from the leaves of *Morinda citrifolia* L. The study was performed on an animal model of obesity, Sprague-Dawley rats with high fat diet. Changes in metabolic pathways such as glucose metabolism and TCA cycle, amino acid, choline, creatinine, and gut microbiome metabolism were observed. Treatment with *M. citrifolia* L. leaves extract resulted in significant improvement in the metabolic perturbations caused by obesity.

However, in the case of morbidly obese individuals, more radical interventions are necessary to overcome diabetes. Currently, the most effective treatment for obesity and type 2 diabetes is bariatric surgery. In the article by K. Sarosiek et al., nontargeted global metabolomics analysis was performed to evaluate changes occurring in nondiabetic and type 2 diabetic patients experiencing standard preoperative liquid weight loss diet, less extreme sleeve gastrectomy, or a full gastric bypass surgery. Preoperative weight loss diet was associated with strong changes in lipid metabolism showing glucose usage that shifted away from glycolytic pyruvate production towards pentose phosphate pathway, via glucose-6-phosphate. These modifications appeared to be shared by all patients regardless of T2D status or bariatric surgery procedure. Results obtained by the authors suggest that bariatric surgery might promote antioxidant defense and insulin sensitivity through increased heme synthesis and HO activity or expression. Other changes in histidine and its metabolites following surgery might indicate alteration in gut microbiome ecology or liver function.

Articles included in this special issue cover a broad range of topics, which we hope the readers of the journal will find important and interesting.

Adam Kretowski
Francisco J. Ruperez
Michal Ciborowski

References

[1] F. R. Day and R. J. F. Loos, "Developments in obesity genetics in the era of genome-wide association studies," *Journal of Nutrigenetics and Nutrigenomics*, vol. 4, no. 4, pp. 222–238, 2011.

[2] G. M. Barlow, A. Yu, and R. Mathur, "Role of the gut microbiome in obesity and diabetes mellitus," *Nutrition in Clinical Practice*, vol. 30, no. 6, pp. 787–797, 2015.

[3] R. Villegas, R. Delahanty, Y.-T. Gao et al., "Joint effect of genetic and lifestyle risk factors on type 2 diabetes risk among Chinese men and women," *PLoS ONE*, vol. 7, no. 11, Article ID e49464, 2012.

[4] S. Bouret, B. E. Levin, and S. E. Ozanne, "Gene-environment interactions controlling energy and glucose homeostasis and the developmental origins of obesity," *Physiological Reviews*, vol. 95, no. 1, pp. 47–82, 2015.

[5] S. Li, J. H. Zhao, J. Luan et al., "Genetic predisposition to obesity leads to increased risk of type 2 diabetes," *Diabetologia*, vol. 54, no. 4, pp. 776–782, 2011.

[6] K. J. Basile, M. E. Johnson, Q. Xia, and S. F. A. Grant, "Genetic susceptibility to type 2 diabetes and obesity: follow-up of findings from genome-wide association studies," *International Journal of Endocrinology*, vol. 2014, Article ID 769671, 13 pages, 2014.

[7] A. J. Walley, A. I. F. Blakemore, and P. Froguel, "Genetics of obesity and the prediction of risk for health," *Human Molecular Genetics*, vol. 15, supplement 2, pp. R124–R130, 2006.

[8] V. Lyssenko and M. Laakso, "Genetic screening for the risk of type 2 diabetes: worthless or valuable?" *Diabetes Care*, vol. 36, supplement 2, pp. S120–S126, 2013.

[9] J. Zierer, C. Menni, G. Kastenmüller, and T. D. Spector, "Integration of 'omics' data in aging research: from biomarkers to systems biology," *Aging Cell*, vol. 14, no. 6, pp. 933–944, 2015.

[10] A.-H. Zhang, S. Qiu, H.-Y. Xu, H. Sun, and X.-J. Wang, "Metabolomics in diabetes," *Clinica Chimica Acta*, vol. 429, pp. 106–110, 2014.

[11] K. A. Guertin, S. C. Moore, J. N. Sampson et al., "Metabolomics in nutritional epidemiology: identifying metabolites associated with diet and quantifying their potential to uncover diet-disease relations in populations," *The American Journal of Clinical Nutrition*, vol. 100, no. 1, pp. 208–217, 2014.

Hindawi Publishing Corporation
Journal of Diabetes Research
Volume 2016, Article ID 6238526, 15 pages
http://dx.doi.org/10.1155/2016/6238526

Research Article

Transcriptome Profiles Using Next-Generation Sequencing Reveal Liver Changes in the Early Stage of Diabetes in Tree Shrew (*Tupaia belangeri chinensis*)

Xiaoyun Wu,[1,2] Haibo Xu,[3,4] Zhiguo Zhang,[1,5] Qing Chang,[1] Shasha Liao,[1,4] Linqiang Zhang,[1,5] Yunhai Li,[1] Dongdong Wu,[3] and Bin Liang[1]

[1]*Key Laboratory of Animal Models and Human Disease Mechanisms of the Chinese Academy of Sciences and Yunnan Province, Kunming Institute of Zoology, Chinese Academy of Sciences, Kunming, Yunnan 650223, China*
[2]*Key Laboratory of Puer Tea Science, Ministry of Education, Yunnan Agricultural University, Kunming, Yunnan 650201, China*
[3]*State Key Laboratory of Genetic Resources and Evolution, Kunming Institute of Zoology, Chinese Academy of Sciences, Kunming, Yunnan 650223, China*
[4]*School of Life Sciences, Anhui University, Hefei, Anhui 230601, China*
[5]*Kunming College of Life Science, University of Chinese Academy of Sciences, Kunming, Yunnan 650204, China*

Correspondence should be addressed to Dongdong Wu; wudongdong@mail.kiz.ac.cn and Bin Liang; liangb@mail.kiz.ac.cn

Received 18 August 2015; Revised 6 February 2016; Accepted 18 February 2016

Academic Editor: Kim Connelly

Determining the liver changes during the early stages of diabetes is critical to understand the nature of the disease and development of novel treatments for it. Advances in the use of animal models and next-generation sequencing technologies offer a powerful tool in connection between liver changes and the diabetes. Here, we created a tree shrew diabetes model akin to type 1 diabetes by using streptozotocin to induce hyperglycemia and hyperlipidemia. Using RNA-seq, we compiled liver transcriptome profiles to determine the differentially expressed genes and to explore the role of hyperglycemia in liver changes. Our results, respectively, identified 14,060 and 14,335 genes in healthy tree shrews and those with diabetes, with 70 genes differentially expressed between the two groups. Gene orthology and KEGG annotation revealed that several of the main biological processes of these genes were related to translational processes, steroid metabolic processes, oxidative stress, inflammation, and hypertension, all of which are highly associated with diabetes and its complications. These results collectively suggest that STZ induces hyperglycemia in tree shrew and that hyperglycemia induced oxidative stress led to high expression of aldose reductase, inflammation, and even cell death in liver tissues during the early stage of diabetes.

1. Introduction

Decades of research into diabetes mellitus, a disease characterized by chronic hyperglycemia in the blood resulting from insulin resistance or insulin deficiency, paint a grim picture for the next 20 years. In 2010, 258 million adults had diabetes, but, despite ongoing searches for treatments paired with prevention efforts, that number is still expected to rise to nearly 439 million people by 2030, about 7.7% of the global adult population [1]. The seriousness of increasing diabetes is underscored by chronic hyperglycemia being among the most important factors involved in the complications and organ injuries that accompany diabetes, including cardiovascular disease, kidney disease, neuropathy, blindness, and liver injury, all of which are major risk factors for morbidity and mortality [2].

Given the connections between diabetes, chronic hyperglycemia, and their comorbidities, researchers have increasingly focused on exploring the liver, the primary organ involved in glucose metabolism and regulation, and the

major target organ of insulin action. Previous reports found a heightened prevalence of liver diseases among diabetic patients to the extent that liver disease ranks as a key cause of death among patients with type 2 diabetes [3–5]. Indeed, the entire spectrum of liver disease, abnormal liver enzymes, nonalcoholic fatty liver disease (NAFLD), cirrhosis, hepatocellular carcinoma, and acute liver failure are frequently observed among these patients. Unfortunately, precisely why these associations exist is not well understood.

During the progression of diabetic liver diseases, increasing oxidative stress induced by the hyperglycemia plays several key roles in promoting liver changes or injury [2, 4] and is particularly critical in inducing the cellular dysfunction of liver tissues [6]. Other studies reported that diabetic liver diseases can also be induced by several other factors, for example, activation of the stress signaling pathways, increased cytokine levels, impairment of protective mechanisms, or dysregulation of glucose and lipid metabolism [4, 7, 8]. Curiously, these factors all appear to be driven by hyperglycemia, so the possibility that they may contribute individually or collectively to induce liver injuries exists. To verify if such a possibility exists, pinpointing gene expression changes within the liver may be critical in fully characterizing the underlying mechanisms of diabetes-induced liver diseases. To date, several studies have investigated these changes at the transcriptional level in streptozotocin (STZ) treated rats, db/db mice and hepatic cell lines using qPCR [4], and microarray analysis in Zucker diabetic fatty (ZDF) rats [9, 10], but these models proved to be poorly suited to characterizing the associations in humans. Ultimately, detecting the initial changes to the liver, and thereby improving the outcomes of early therapeutic interventions and preventing organ failure and reducing overall mortality, requires a more sensitive technique for conducting whole genome transcriptional analysis, and such analyses need to be conducted on species more closely related to human beings, such as the nonhuman primates or their close relatives.

Recent advances in both animal models and genomic research may be able to overcome the shortcomings of early studies and allow researchers to draw meaningful, translational results. In terms of technique, RNA sequencing (RNA-seq) has become a powerful tool for conducting transcriptome characterization and gene expression profiling in a high-throughput manner [11, 12], allowing for an unbiased survey of the entire transcriptome and *de novo* assembly that does not require genomic sequences to produce a genome-scale transcription map [11]. With deep coverage and single nucleotide resolution, RNA-seq provides a platform to determine differential expression of genes or isoforms [13] that can also identify novel genes and alternative splicing events (AS) [14], noncoding RNAs [15], and posttranscriptional modifications [16]. Similarly, the increasingly popular use of tree shrews has been shown to overcome some of the inherent limitations in more popular animal models such as mice or rodents. Being a close relative to the primates [17, 18], the tree shrew (*Tupaia belangeri chinensis*) has been successfully used as an animal model of several human diseases, including cancer [19–21], hepatitis B virus (HBV) [22], and metabolism syndromes [23].

To date, the number of RNA-Seq analyses on diabetes is scarce, and studies of diabetes in the tree shrew model are nearly nonexistent. The existing RNA-Seq analyses have primarily focused on the pancreatic islet from both type 1 diabetes and type 2 diabetes subjects [24, 25] and identified putative candidate genes under the proinflammatory cytokines [25] and the saturated fatty acid palmitate [24] and also identified novel mechanisms of β-cell dysfunction and death. However, none of these studies has been able to fully explicate the gene expression changes in the liver cells on the early stage of diabetes. The characterization of the transcriptome landscape of the liver may be partially helpful in solving this problem, but without an effective animal model from which results can be accurately extrapolated, such findings would be limited at best. One of our previous studies suggested that streptozotocin (STZ), a glucosamine derivative of nitrosourea and preferentially toxic to pancreatic beta cells, can be used to induce tree shrew diabetes [26]. We found that diabetic tree shrews exhibited higher concentrations of blood glucose, triglyceride (TAG), total cholesterol (CHOL), and impaired glucose intolerance, similar to the symptoms found in humans [26]. Accordingly, applying modern RNA-Seq techniques to a tree shrew type 1 diabetes model may bring promise to better understand the pathogenesis of diabetes-induced liver diseases.

In this study, we first used STZ to induce tree shrews diabetes akin to type 1 diabetes and then took RNA-seq techniques to determine the transcriptome characterization and gene expression profiling of the diabetic and wild type tree shrews. The results of these analyses identified 14,060 and 14,335 genes, respectively, in healthy tree shrews and those with diabetes, with 70 genes differentially expressed between the two groups. Further GO and KEGG annotation revealed that several of the main biological processes of these genes were related to translational processes, steroid metabolic processes, oxidative stress, inflammation, and hypertension, all of which are highly associated with diabetes and its complications.

2. Material and Methods

2.1. Induction of Diabetes by STZ and Samples Collection. Sixteen male tree shrews captured from the wild near the Animal Centre of Kunming Institute of Zoology and housed in captivity for more than 1 year were collected and then separated into two groups, a control group and a group treated with streptozotocin (STZ) used to induce diabetes which was akin to type 1 diabetes. After overnight fasting (14 hr), body weight and fasting blood glucose were measured prior to injection. The animals in the STZ-induced diabetic group received two intraperitoneal injections of a freshly prepared solution of STZ (Sigma-Aldrich) in 10 mM sodium citrate buffer (PH = 4.2–4.5) at 80 mg/kg of body weight given one week apart while the animals in control group were intraperitoneally injected 10 mM sodium citrate buffer (PH = 4.2–4.5) in comparable amounts. Following injection of either the sodium citrate buffer or STZ, body weight and the fasting blood glucose concentration were measured weekly.

All animal care and experimental protocols were approved by the Animal Ethics Committee of Kunming Institute of Zoology, the Chinese Academy of Sciences (Approval number: SYBW20110101-1).

At 4 and 8 weeks after injection, 0.5 mL of femoral vein blood was collected from animals in both groups. The blood samples were treated with heparin lithium salt to anticoagulation, centrifuged at 3000 g for 3 min. The plasma triglycerides (TG), total cholesterol (TC), low-density lipoproteins (LDL), high-density lipoproteins (HDL), and glycated hemoglobin A1c (HbA1c) were assayed by an automatic blood biochemistry analyzer (Ci16200, Abbott, USA) at the First People's Hospital of Yunnan Province, China. The diabetic animals were verified by the concentration of fasting blood glucose and HbA1c. Finally, 5 of the original 8 animals in the STZ-induced diabetic group were regarded as the diabetic animals. At 8 weeks, a total of 6 trees shrews in the control group and 5 diabetic tree shrews were anesthetized, and tissue samples were harvested for further analyses. Each tissue sample was divided into several pieces and snap frozen using liquid nitrogen.

2.2. Oral Glucose Tolerance Test (OGTT). OGTT was followed as previously described [23]. Briefly, tree shrews were fasted overnight (14 hr) prior to the OGTT. Approximately 1 mL of 50% glucose (g/v) base on 3.5 mg/kg (glucose/body weight) was orally administered for the OGTT in all tree shrews. Blood samples were collected from the tail vein and plasma glucose levels were immediately measured at 0, 20, 40, 60, 120, and 180 min after glucose administration using automatic blood glucose test meter (Accu-Chek Performa Blood Glucose Meter, Roche).

2.3. RNA Isolation, Library Preparation, and Sequencing. Total RNA was extracted and purified from the frozen liver tissues of each animal using TRIzol (TRansgene) according to the manufacture's protocols. Total RNA was then quantified using the nucleic acid-protein quantitative instrument (Bio-RAD), before the samples from each group were mixed into one sample at the equivalent concentrations. Afterward, the mixed total RNA samples from both the control and diabetic group were packed in dry ice and sent on to Macrogen Millennium Genomics for further library preparation and sequencing. Sequencing was performed using Illumina HiSeq2000 instrument.

2.4. Transcriptomic Construction. All reads were mapped to the tree shrew genome (NCBI Ref. database: GCA_000334495.1) [27] using Tophat v2.0.9 [28, 29] with the newest tree shrew annotation file. Reads quality control and statistics were confirmed with FASTQC (http://www.bioinformatics.babraham.ac.uk/projects/fastqc/). Transcripts were assembled and quantified by Cufflinks 2.0.2 [13]. Isoforms assembled by Cufflinks from the two samples were then sent to the Cuffcompare utility, along with the gene annotation file, to generate an integrated combined gtf annotation file. To minimize annotation artifacts, all single exon transcripts mapped to known genes with transcripts lengths shorter than 200 bp were excluded. Transcripts labeled with class code "j" by Cuffcompare software were considered as new isoforms of known genes and added to the original tree shrew annotation file, and the resulting new annotation file was used as the reference file and sent to Cuffcompare utility to generate following events: "annotated exons," "unknown, generic overlap with reference," "potentially novel isoforms of genes," "intergenic transcripts," "intron retention events," and "exonic overlap with reference on the opposite strand." Cuffdiff was used to calculate the FPKM (fragments per kilobase of exon per million fragments mapped) values of each gene in both samples using the new reference file.

2.5. Orthology Detection and Gene Functional Enrichment. The Coding Potential Calculator (CPC) [30] was used to determine the coding potential of the transcripts which came from the new loci. Transcript sequences were extracted by gffread, a utility within the Cufflinks package [13]. All probable coding transcript sequences were blasted against the UniProt database using BLASTP with the following parameters and criteria: E-value hit filter $1.00E-5$, at least 80% sequence identity, and at least 70% query sequence coverage. Database for Annotation, Visualization, and Integrated Discovery (DAVID; http://david.abcc.ncifcrf.gov/) [31] was used to perform gene function enrichment analysis based on GO and KEGG annotation for the significantly expressed genes.

2.6. Validation of Differentially Expressed Genes by Quantitative Real Time PCR. Quantitative RT-PCR analysis of selected genes was performed using SYBR green method (TransStart Top Green qPCR SuperMix, TransGen Biotech, Beijing, China) on an ABI PRISM 7900HT (Applied Biosystems, Inc.). The isolated RNA of 3 individuals either from the control group or from the diabetic animals was reverse-transcribed into cDNA using the RT reagent Kit with gDNA Eraser (Takara, DRR047A) in a total volume of 20 μL containing 2 μg of total RNA, following the manufacturer protocol. The cDNA was diluted 20-fold and 2 μL was used as template in subsequent qRT-PCR reactions. Each sample was analyzed in triplicate with the following reaction conditions: 30 seconds at 95°C, followed by 40 cycles of 5 seconds at 95°C, 30 seconds at 60°C, and 20 seconds at 72°C. A dissociation curve was drawn for each primer pair. Relative expression levels of interested genes were determined using $2^{-\Delta\Delta Ct}$ method, and the gene expression levels were normalized to *β-actin* measured in parallel.

2.7. Data Availability. The raw dataset have been submitted to NCBI Sequence Read Archive (SRA) under Accession SRX1009946 and SRX1017387, Bioproject: PRJNA282350.

3. Results

3.1. Diabetic Symptoms of STZ-Induced Tree Shrew. The average body weights of tree shrews in the control group and the diabetic group induced by STZ did not change significantly

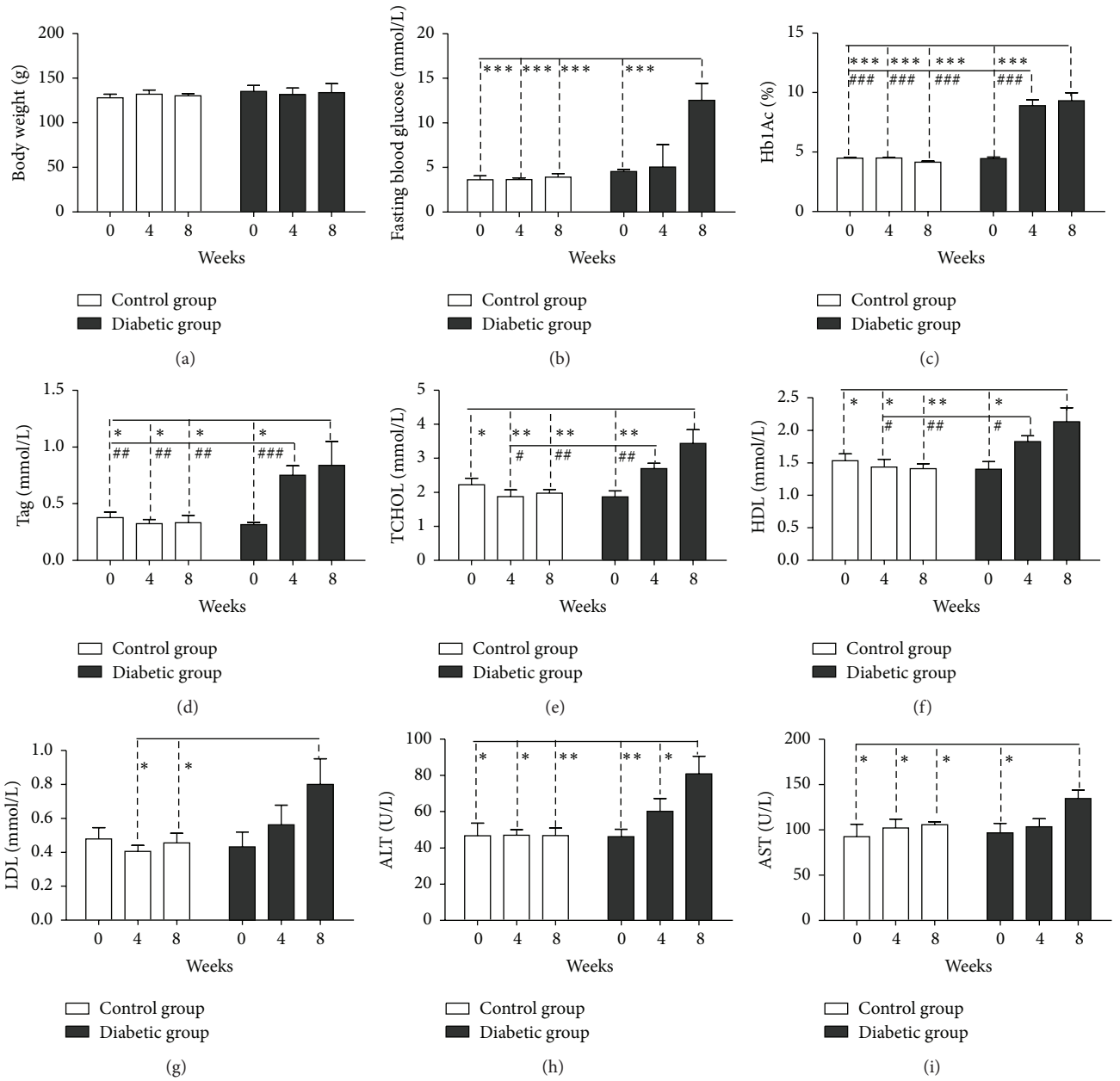

Figure 1: Biochemical parameters in healthy control tree shrews and STZ-induced diabetic tree shrews over 8 weeks. (a) Body weight; (b) plasma concentration of fasting blood glucose; (c) serum concentration of HbA1c; (d) serum concentration of triglycerides (TAG); (e) serum concentration of cholesterol (CHOL); (f) serum concentration of high-density lipoprotein cholesterol (HDL); (g) serum concentration of low-density lipoprotein cholesterol (LDL); (h) serum concentration of alanine aminotransferase (ALT); (i) serum concentration of aspartate aminotransferase (AST). $n = 6$ in control group; $n = 5$ in diabetic group. Significance between two groups. Control group versus 8 weeks of diabetic group: $^{*}P < 0.05$, $^{**}P < 0.01$, and $^{***}P < 0.001$; control group versus 4 weeks of diabetic group: $^{\#}P < 0.05$, $^{\#\#}P < 0.01$, and $^{\#\#\#}P < 0.001$.

over the 8 wk testing period (Figure 1(a)). Similarly, the fasting blood glucose concentration over the 4 wk period in the diabetic group did not increase significantly (5.03 ± 2.27 mmol/L) as compared with the control group (3.62 ± 0.18 mmol/L) (Figure 1(b)), but the average concentration of the glycosylated hemoglobin (HbA1c) was significantly higher in the diabetic group than that in the control group ($P < 0.0001$) over the 4 wk period (Figure 1(c)). These results indicate a higher postprandial blood glucose concentration in the diabetic group. The oral glucose tolerance test (OGTT) administered at week 5 showed a significant impairment of glucose tolerance in the diabetic group with the significant higher glucose concentration from 20 min to 120 min after glucose administration (Figure 2). At 8 wk, the fasting blood glucose concentration and the value of HbA1c were both significantly higher in the diabetic group (10.42 ± 2.57 mmol/L

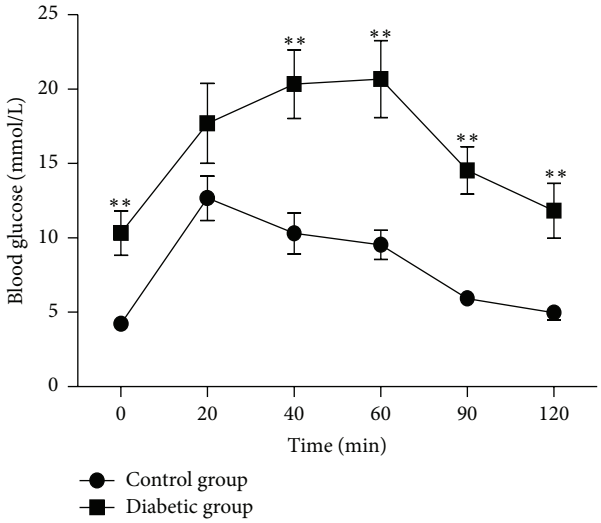

Figure 2: Oral glucose tolerance test (OGTT) in the healthy control group and diabetic group at week 5. $n = 6$ in control group; $n = 5$ in diabetic group. $^{**}P < 0.01$.

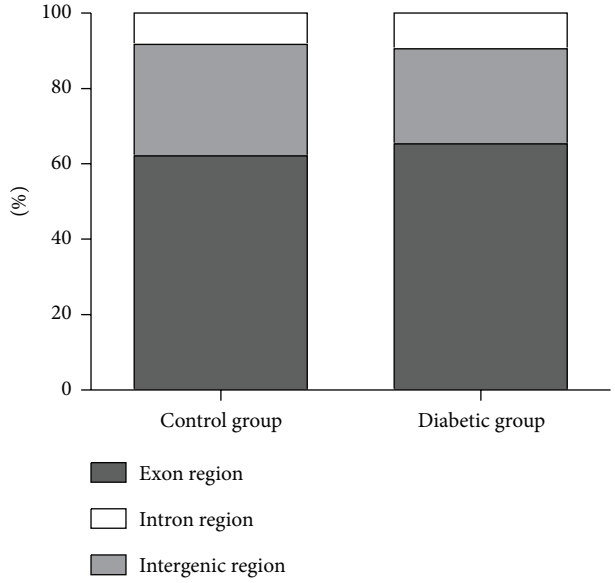

Figure 3: Proportion of reads mapped to the exons, introns, and intergenic regions in liver tissues of the control and diabetic groups.

and 9.31 ± 0.66 mmol/L) than in the control group (3.90 ± 0.38 mmol/L and 4.14 ± 0.09 mmol/L) (Figure 1(b)). These results indicated that STZ-induced tree shrew diabetic model is more likely type 1 diabetes.

The serum total triglycerides (TAG) and total cholesterol (TC) in diabetic animals were both significantly higher than those in the control group animals over the total 8-week period ($P < 0.05$) (Figures 1(d) and 1(e)). Additionally, serum concentrations of the high-density lipoprotein (HDL) and the low-density lipoprotein (LDL) were also highly increased among the diabetic group as compared to the control (Figures 1(f) and 1(g)). To examine the liver injury in the diabetic animals, the serum concentrations of the alanine aminotransferase (ALT) and the aspartate aminotransferase (AST) were detected. The concentrations of ALT and AST increased significantly in the diabetic group at week 8, but not at week 4 (Figures 1(h) and 1(i)).

3.2. Mapping and Annotation. To obtain comprehensive liver transcripts of the tree shrew and an expression profile in the diabetic tree shrew, total RNAs were isolated from the livers of the control animals and the diabetic animals for RNA-seq using the Illumina instrument. Overall 89,212,358 pair-end 110 bp reads corresponding to more than 18.0 billion base pairs and 73,656,617 pair-end 110 bp reads corresponding to more than 14.8 billion base pairs were obtained in the liver tissues of the control animals and the diabetic animals, respectively. The Tophat software was employed to map the reads against the tree shrew genome [27]. And about 71.5% reads of the control dataset and 75.5% reads of the diabetic dataset, separately, could be mapped to the Chinese tree shrew genome. The mapped reads covered over 90% of the tree shrew genome. Additionally, we calculated the proportion of reads mapped to the exons, introns, and intergenic regions using intersectBed tool from BEDtools package [32]. The highest percentages of reads were mapped to exons (62.1% in control group and 65.3% in diabetic group); and 29.6% of reads in control group and 25.2% of reads in diabetic group were mapped to the intergenic regions; and the lowest percentages of reads (8.3% in control group and 9.5% in diabetic group) fell in the intron regions (Figure 3).

The total numbers of nonredundant assembled transcripts with Cufflinks were 63,748 transcripts from 89,212,358 sequence reads in the control dataset and 55,985 transcripts from 73,656,617 sequence reads in the diabetic dataset. From the Cuffcompare output, these transcripts fall into several categories: annotated exons (35.6% in control group, 31.2% in diabetic group), intron retention events (5.5% in control group, 9.0% in diabetic group), intergenic transcripts (12.5% in control group, 15.5% in diabetic group), potentially novel isoforms of genes (33.6% in control group, 32.0% in diabetic group), pre-mRNA molecules (2.2% in control group, 2.5% in diabetic group), and polymerase run-on fragments (1.7% in control group, 1.7% in diabetic group) (Table 1).

In sum, the total amount of expressed transcripts was 55,976, which generated a total of 24,694 genes in the liver tissues of the control and diabetic groups. A total amount of 7,036 noncoding genes and 2,834 potential coding genes was detected using Coding Potential Calculator (CPC). BLASTP analysis of the 2,834 potential coding genes finally yielded 943 annotated genes.

3.3. Gene Expression Analysis. With a total of 14,060 and 14,335 genes, respectively, expressed in the control and diabetic groups, we separately set the threshold value of FPKM to 0.1, 0.2, and 0.3 to balance the numbers of false positives and false negatives and obtained, respectively, 12,418, 11,811, and 11,411 in the control group and 12,578, 11,912, and 11,485 in the diabetic group (Figure 4). Approximately 800 and 600 genes were highly abundant (FPKM > 100) in hepatic

Table 1: Transcripts assembled with Cufflinks and percentage from both the control and diabetic groups.

Code	Control group		Diabetic group	
	Number	%	Number	%
e	1249	2.2	1611	2.5
=	19938	35.6	19904	31.2
x	556	1	657	1
s	2	0	3	0
j	18793	33.6	20376	32
c	3	0	4	0
u	6997	12.5	9910	15.5
p	941	1.7	1101	1.7
.	3251	5.8	3251	5.1
o	1171	2.1	1212	1.9
i	3084	5.5	5719	9
Total	**55985**	**100**	**63748**	**100**

Class codes described by Cuffcompare: "=": exactly equal to the reference annotation; "c": contained in the reference annotation; "e": possible pre-mRNA molecule; "i": an exon falling into an intron of the reference; "j": new isoforms; "o": unknown, generic overlap with reference; "p": possible polymerase run-on fragment; "s": an intron of the transfrag overlaps a reference intron on the opposite strand; "u": unknown intergenic transcript; "x": exonic overlap with reference on the opposite strand; ".": tracking file only, which indicates multiple classifications.

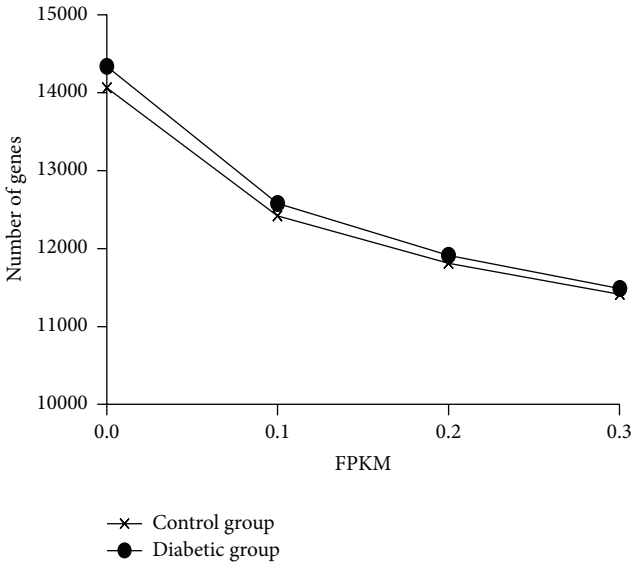

Figure 4: Number of expressed genes with different minimum expression thresholds.

tissues of the control and diabetic groups, respectively. To determine the biological functions of genes of the liver cells, we investigated the total cellular mRNA allocating to genes involved in different biological processes in the liver tissues of tree shrew. The categories of biological processes were defined according to [33]. In the liver tissues of tree shrew, three biological processes, including signal transduction, metabolic process, and macromolecular turnover, showed a far higher fraction of transcriptions allocated to genes than

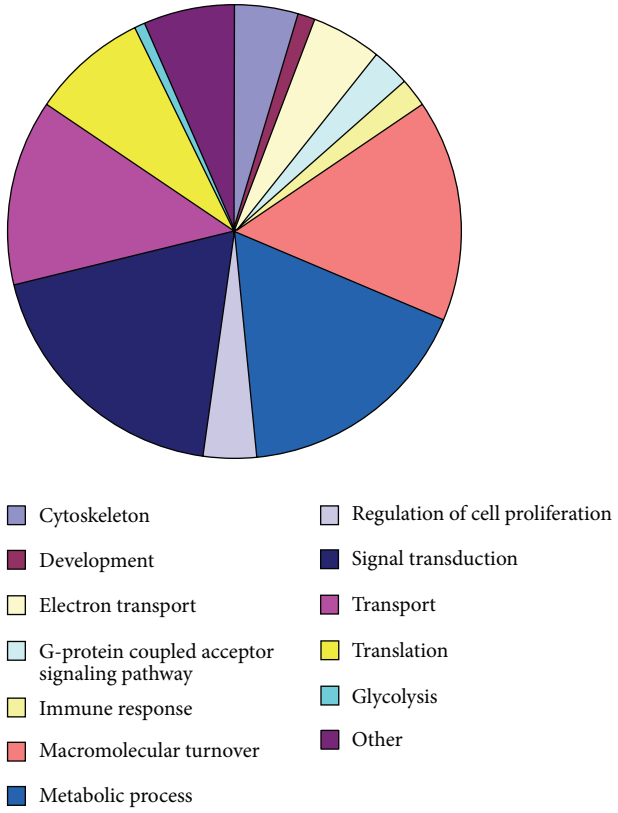

Figure 5: Estimated fractions of cellular transcripts based on gene ontology in the liver tissues of control and diabetic groups. Biological process categories for liver tissues of control tree shrews.

other processes (Figure 5), while glycolysis, development, and immune response processes showed a much lower fraction (Figure 5).

3.4. Analysis of Differential Gene Expression. Cuffdiff was used to calculate the differentially expressed gene between the control and diabetic groups, yielding 75 differentially expressed genes (Table 2). Among these genes, 23 were upregulated in the diabetic group while the remaining 47 were downregulated (Table 2). To validate the expression level of genes obtained from RNA-Seq, 8 genes (*adrb2*, *akr1b1*, *cox5b*, *crp*, *prlr*, *mcp1*, *prdx1,* and *romo1*) involved in different biological processes were selected for quantitative Real Time PCR (qRT-PCR) (Figure 6). The expression trend of these genes was similar to RNA-Seq platforms.

To explore differences in the biological processes between the healthy and diabetic groups, DAVID [31] was used to perform gene function enrichment analysis based on GO and KEGG annotation for the significantly differentiated genes in both groups (Tables 2 and 3). The main biological functions identified were related to translational process, steroid metabolic process, blood circulation, and so froth, (Table 3). Additionally, several physiological processes and biological processes associated with diabetes, oxidation reduction, electron carrier activity, lipid metabolism, apoptosis regulation,

Table 2: Genes differentially expressed in liver tissues of tree shrew.

ID	Gene name	Gene symbol	Fold changes*	Biological process	KEGG pathway
XLOC_001420	Acetyl coenzyme A acyltransferase 2	*Acaa2*	(−) 8.01	Metabolic process	hsa00062:Fatty acid elongation in mitochondria
TSDBG00010707	Beta-2-adrenergic receptor	*Adrb2*	(+) 4.61	G-protein coupled receptor signaling pathway	
TSDBG00019059	Angiotensin II receptor, type 2	*Agtr2*	(+) 693.72	G-protein coupled receptor signaling pathway	
TSDBG00005129	Aldo-keto reductase family 1, member B1	*Akr1b1*	(+) 6.08	Electron transport	
TSDBG00003625	Beta-2-microglobulin	*B2m*	(−) 4.58	Immune response	
TSDBG00006817	Beta-2-bradykinin receptor	*Bdkrb2*	(+) 8.08	Transport	
TSDBG00021527	Calneuron 1	*Caln1*	(+) 18.60	NA	
TSDBG00019726	Cadherin 3	*Cdh3*	(+) 85.20	Cytoskeleton	
TSDBG00017230	Chromogranin A	*Chga*	(+) 47.78	Regulation of blood pressure	
TSDBG00004640	Chromogranin B	*Chgb*	(+) 84.21	Signal transduction	
TSDBG00013910	Cytochrome c oxidase subunit VA	*Cox5a*	(−) 8.05	Electron transport	
TSDBG00011477	Cytochrome c oxidase subunit VB	*Cox5b*	(−) 11.26	Electron transport	
TSDBG00013437	Cytochrome c oxidase subunit VIc	*Cox6c*	(−) 5.81	Electron transport	
TSDBG00018314	C-reactive protein	*Crp*	(+) 5.86	Inflammatory response	
TSDBG00007703	Chemokine (C-X-C motif) ligand 13	*Cxcl13*	(−) 10.59	Immune response	
TSDBG00022385	Cytochrome P450, family 11, subfamily A, polypeptide 1	*Cyp11a1*	(+) 71.64	Electron response	hsa00140:Steroid hormone biosynthesis
TSDBG00016058	Cytochrome P450, family 11, subfamily B, polypeptide 2	*Cyp11b2*	(+) 76.51	Electron response	hsa00141:Steroid hormone biosynthesis
TSDBG00016058	Cytochrome P450, family 11, subfamily B, polypeptide 2	*Cyp11b2*	(+) 68.25	Electron response	hsa00143:Steroid hormone biosynthesis
TSDBG00016479	Cytochrome P450, family 17, subfamily A, polypeptide 1	*Cyp17a1*	(+) 95.77	Electron response	hsa00144:Steroid hormone biosynthesis
TSDBG00010507	Cytochrome P450, family 7, subfamily A, polypeptide 1	*Cyp7a1*	(+) 5.74	Electron response	hsa00144:Steroid hormone biosynthesis
XLOC_008932	Dynein, light chain, LC8-type 1	*Dynll1*	(−) 14.05	Cytoskeleton	
TSDBG00020294	Enoyl CoA hydratase, short chain, 1,	*Echs1*	(−) 19.90	Metabolic process	hsa00062:Fatty acid elongation in mitochondria
TSDBG00018541	Eukaryotic translation elongation factor 1 alpha 1	*Eef1a1*	(−) 5.15	Macromolecular turnover	
XLOC_007804	Ferritin, heavy chain, polypeptide 1	*Fth1*	(−) 12.76	Metabolic process	
TSDBG00003452	G0/G1 switch 2	*G0s2*	(−) 26.68	Signal transduction	
TSDBG00020849	Glial cell derived neurotrophic factor	*Gdnf*	(+) 273.86	Signal transduction	
TSDBG00001160	Hemoglobin, alpha 1	*Hba1*	(−) 6.70	Transport	
TSDBG00005453	Hemoglobin, beta	*Hbb*	(+) 11.90	Transport	
TSDBG00021208	High mobility group nucleosome binding domain 1	*Hmgn1*	(−) 15.39	Cytoskeleton	
XLOC_002257	Heat shock protein 1	*Hspd1*	(−) 5.54	Other	
TSDBG00002459	Kruppel-like factor 6	*Klf6*	(+) 4.90	Macromolecular turnover	
TSDBG00018913	Leukocyte cell-derived chemotaxin 2	*Lect2*	(−) 19.18	Immune response	
TSDBG00013095	Lysozyme	*Lyz*	(−) 10.04	Metabolic process	
TSDBG00002162	Melanocortin 2 receptor	*Mc2r*	(+) 116.92	G-protein coupled receptor signaling pathway	
TSDBG00024122	Mitochondrially encoded ATP synthase 6	*MT-Atp6*	(−) 187.11	Metabolic process	
TSDBG00024207	Mitochondrially encoded cytochrome c oxidase I	*Mt-co1*	(−)	Metabolic process	

Table 2: Continued.

ID	Gene name	Gene symbol	Fold changes*	Biological process	KEGG pathway
TSDBG00024123	Mitochondrially encoded cytochrome c oxidase III	*Mt-co3*	(−)	Metabolic process	
TSDBG00024119	Mitochondrially encoded NADH dehydrogenase 4	*Mt-nd4*	(−)	Metabolic process	
TSDBG00013867	Myomesin 1	*Myom1*	(−) 9.47	Muscle contraction	
TSDBG00014996	Nucleolin	*Ncl*	(−) 22.79	NA	
XLOC_009534	Nucleolar protein interacting with the FHA domain of MKI67	*Nifk*	(−) 20.77	Macromolecular turnover	
XLOC_009785	Nucleophosmin 1	*Npm1*	(−) 23.49	Signal transduction	
TSDBG00009363	Nuclear receptor subfamily 5, group A, member 1	*Nr5a1*	(+) 31.23	Translation	
XLOC_007808	Poly(rC) binding protein 2	*Pcbp2*	(−) 5.67	Immune response	
XLOC_008508	Peroxiredoxin 1	*Prdx1*	(−) 4.40	Response to ROS	
TSDBG00020861	Prolactin receptor	*Prlr*	(+) 8.54	Metabolic process	
TSDBG00023696	Prostate stem cell antigen	*Psca*	(−) 6.50	NA	
TSDBG00017201	Proteasome (prosome, macropain) subunit, alpha type, 6	*Psma6*	(−) 17.58	Other	
XLOC_008889	18S ribosomal RNA	*Rn18s*	(−) 8.17	NA	
XLOC_008890	RNA, 45S pre-ribosomal 5	*Rna45s5*	(−) 6.86	NA	
TSDBG00008648	Reactive oxygen species modulator 1	*Romo1*	(−) 3.84	Response to ROS	
TSDBG00000016	Ribosomal protein L21	*Rpl21*	(−) 16.72	Translation	hsa03013:Ribosome
TSDBG00015118	Ribosomal protein L21	*Rpl21*	(−) 13.55	Translation	hsa03013:Ribosome
TSDBG00021103	Ribosomal protein L21	*Rpl21*	(−) 14.86	Translation	hsa03013:Ribosome
TSDBG00010811	Ribosomal protein L21	*Rpl21*	(−) 78.98	Translation	hsa03013:Ribosome
TSDBG00013239	Ribosomal protein L21	*Rpl21*	(−) 8.21	Translation	hsa03013:Ribosome
TSDBG00008910	Ribosomal protein L22	*Rpl22*	(−) 5.38	Translation	hsa03013:Ribosome
TSDBG00013442	Ribosomal protein L30	*Rpl30*	(−) 5.32	Translation	hsa03013:Ribosome
XLOC_009108	Ribosomal protein L31	*Rpl31*	(−) 11.86	Translation	hsa03013:Ribosome
TSDBG00008508	Ribosomal protein L34	*Rpl34*	(−) 100.22	Translation	hsa03013:Ribosome
XLOC_006890	Ribosomal protein L35a	*Rpl35a*	(−) 16.94	Translation	hsa03013:Ribosome
TSDBG00016157	Ribosomal protein L4	*Rpl4*	(−) 8.55	Translation	hsa03013:Ribosome
TSDBG00001838	Ribosomal protein S24	*Rps24*	(−) 4.50	Translation	hsa03013:Ribosome
TSDBG00006238	Ribosomal protein S24	*Rps24*	(−) 14.75	Translation	hsa03013:Ribosome
TSDBG00013032	Ribosomal protein S26	*Rps26*	(−) 5.76	Translation	hsa03013:Ribosome
XLOC_003904	Methylsterol monooxygenase 1	*Sc4mol*	(−) 4.43	Metabolic process	
TSDBG00006015	Secretogranin II	*Scg2*	(+) 156.25	Signal transduction	
TSDBG00002295	Secretoglobin, family 2A, member 2	*Scgb2a2*	(−) 138.70	NA	
XLOC_008362	Small ubiquitin-like modifier 1	*Sumo1*	(−) 16.29	Regulation of cell proliferation	
TSDBG00017904	Trefoil factor 3	*Tff3*	(−) 15.12	Immune response	
XLOC_010510	Translocase of inner mitochondrial membrane 13	*Timm13*	(−) 5.71	Transport	
TSDBG00009988	Transmembrane protein 252	*Tmem252*	(+) 5.85	NA	
XLOC_004969	Ubiquitin-conjugating enzyme E2D 2A	*Ube2d2a*	(−) 6.67	Other	
TSDBG00019547	Vestigial-like family member 3	*Vgll3*	(+) 17.36	Macromolecular turnover	
XLOC_003709	Vimentin	*Vim*	(−) 13.65	Regulation of cell proliferation	
TSDBG00009142	WAP four-disulfide core domain 2	*Wfdc2*	(+) 8.18	Proteolysis	

*Diabetic group/control group; (+): upregulated; (−): downregulated.

Table 3: Biological processes and genes likely affected among tree shrews with STZ-induced diabetes.

Function	Genes	*P* value
Translational process	*RPL35A*, *RPS26*, *EEF1A1*, *RPL30*, *RPL31*, *RPL22*, *RPL34*, *RPL21*, *RPL4*, *RPS24*	$9.76E-06$
Regulation of blood pressure	*ADRB2*, *AGTR2*, *CHGA*, *CYP11B2*, *BDKRB2*, *HBB*	$8.53E-04$
Steroid metabolic process	*ACAA2*, *CYP17A1*, *PRLR*, *CYP11A1*, *CYP7A1*, *CYP11B2*, *SC4MOL*	$1.46E-04$
Mitochondrion	*ACAA2*, *CYP11A1*, *CYP11B2*, *ECHS1*, *ROMO1*, *TIMM13*, *COX5A*, *COX5B*, *PRDX1*, *COX6C*, *CYP17A1*, *PSMA6*, *HSPD1*, *MTCO1*, *MTCO3*, *MTND4*, *MTATP6*	0.0019
Electron carrier activity	*CYP7A1*, *CYP17A1*, *CYP11A1*, *CYP11B2*, *AKR1B1*, *COX5A*	0.0019
Oxidation reduction	*CYP7A1*, *CYP17A1*, *CYP11A1*, *CYP11B2*, *AKR1B1*, *COX5A*, *PRDX1*, *FTH1*, *SC4MOL*, *AGTR2*, *GDNF*	0.0036
Regulation of apoptosis	*ADRB2*, *AGTR2*, *PRLR*, *DYNLL1*, *NPM1*, *BDKRB2*, *HSPD1*, *GDNF*, *PRDX1*, *SCG2*	0.0042
Cytochrome c oxidase activity	*COX5A*, *COX5B*, *COX6C*	0.0056
Lipid biosynthetic process	*ACAA2*, *CYP17A1*, *PRLR*, *CYP11A1*, *CYP11B2*, *SC4MOL*	0.0091
Steroid binding	*CYP11A1*, *CYP11B2*, *SCGB2A2*	0.027
Response to reactive oxygen species	*CYP11A1*, *ROMO1*, *PRDX1*	0.036
Inflammatory response	CXCL13, CRP, LYZ, BDKRB2, SCG2	0.040
Fatty acid elongation in mitochondria	*ACAA2*, *ECHS1*	0.046

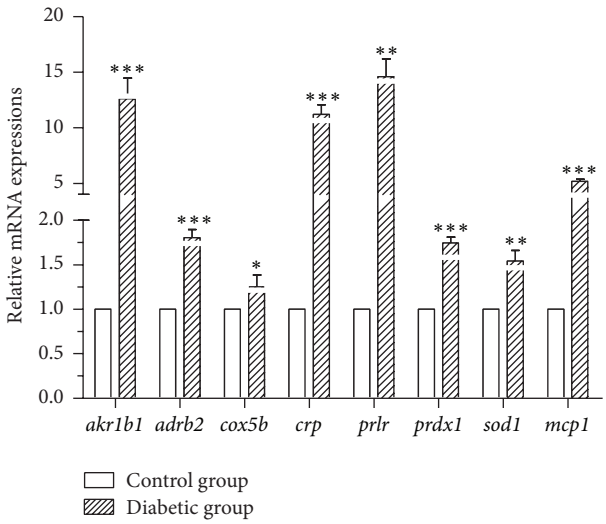

Figure 6: Quantitative-PCR mRNA expression of the randomly selected genes from differentially expressed genes in liver tissues of control and diabetic tree shrews. Significance between two groups; $^{*}P < 0.05$, $^{**}P < 0.01$, and $^{***}P < 0.001$.

reactive oxygen species response, and inflammatory response were also examined (Table 3).

Our results showed that two genes involved in lipid metabolism were significantly downregulated, potentially due the diabetic status of the tree shrews in the STZ-induced group. The enzymes, acetyl coenzyme A acyltransferase 2 (*acaa2*) (fold difference = −8.01, *P* value = 5.77×10^{-5}) and the enoyl coenzyme A hydratase, short chain, 1, mitochondrial (*echs1*) (fold difference = −19.90, *P* value = 1.36×10^{-6}), involved in mitochondrial fatty acid beta-oxidation, showed a markedly lower expression in the diabetic group, implying that the fatty acid breakdown ability was decreased in the diabetic tree shrews. The enzymes *echs1* and *acaa2*, which separately catalyze the second and last steps of the mitochondrial fatty acid beta-oxidation spiral and produce acetyl coenzyme A, were previously reported to candidate genes in type 2 diabetes [34]. Additionally, the downregulation of enzymes *echs1* and *acaa2* inhibits the production of acetyl coenzyme A, leading to the production of ketone bodies and oxidative phosphorylation [34, 35]. We further found that the expression of several genes in the cytochrome P450 family (e.g., *cyp7a1*, *cyp11a1*, *cyp11b2,* and *cyp17a1*) was upregulated in the diabetic group but not in the control group. These genes appear to be involved in the steroid metabolic process; for example, *cyp7a1* encodes the enzyme cholesterol 7α-hydroxylase, which catalyzes the initial step in cholesterol catabolism and bile acid synthesis, while *cyp11a1*, *cyp11b2,* and *cyp17a1* are involved in the process of steroid hormone synthesis. Collectively, this upregulation of genes within the cytochrome P450 family may suggest an increased biosynthesis from cholesterol to the bile acid and steroid hormone.

We also found that several genes associated with the process of oxidative phosphorylation (*cox5a*, *cox5b*, *cox6c*, *mtco1*, *mtco3*, *mtnd4,* and *mtatp6*) were all downregulated in the diabetic group as compared to the control group. Of these genes, *cox5a*, *cox5b,* and *cox6c* are involved in complex IV of the mitochondrial electron transport chain, and downregulation may block the electron transfer through the mitochondrial electron transport chain to generate superoxide. Additionally, within the diabetic group of tree shrews, genes promoting cell apoptosis (*adrb2*, *agtr2*, and *bdkrb2*) were found to be upregulated, while antiapoptotic genes (*npm1*, *dynll1*, and *hspd1*) were downregulated. Likewise, genes associated with

the inflammatory process were detected in the RNA-seq data for the diabetic group, including *cxcl13* and *crp*. The *cxcl13* gene, a biomarker of B-cell, displayed a decrease mRNA expression (fold difference = −10.59, P value = 4.06×10^{-5}) in the diabetic group. *crp*, the inflammatory biomarker, showed a significantly higher expression (fold difference = 5.86, P value = 1.52×10^{-4}) in the diabetic group. Finally, we also determined that the genes putatively involved in feeding behavior (*cartpt* and *gal*) were expressed in the diabetic group, but the expression was markedly low among the healthy control group.

4. Discussion

4.1. Diabetic Dyslipidemia. Among the diabetic tree shrews, we observed significantly higher concentrations of serum TAG, CHOL, HDL, and LDL (Figures 1(d), 1(e), 1(f), and 1(g)), all of which are considered major risk factors for subsequent cardiovascular disease that accompany diabetes mellitus. Earlier reports also found similarly elevated serum TAG, CHOL, and LDL in STZ-induced diabetic rats and mice [36, 37], suggesting that our present tree shrew model induced via STZ replicates the dyslipidemia seen in those test models. In this study, we also observed higher concentration of HDL in the diabetic tree shrews. The increased level of HDL was also commonly observed in type 1 diabetic patients [38, 39]. Some studies reported that the higher HDL cholesterol in type 1 diabetic patients may be related to increased lipoprotein lipase activity and adiponectin [38, 40, 41]. However, STZ-induced rodent diabetes commonly exhibited lower levels of HDL [42, 43]. These results indicate that tree shrew diabetic model might be more appropriate to diabetic research with higher level HDL and to investigate the mechanisms underlying the higher concentration of HDL in type 1 diabetes. Although the precise pathogenesis of diabetic dyslipidemia is not known, a growing number of studies have found that insulin deficiency or insulin resistance and hyperglycemia seem to be key contributors to the disorder [3–7]. Since STZ is preferentially toxic to pancreatic beta cells, the main changes of these upheavals are seen in a reduction of insulin concentration in the blood, suggesting that insulin deficiency and hyperglycemia may also play a critical role during the occurrence of diabetic dyslipidemia within tree shrews, as well as other animal models. More importantly, the serum concentration of AST and ALT increased significantly at week 8 (Figures 1(h) and 1(i)), indicating that diabetic tree shrews appeared to suffer from the same types of liver injury that accompany human diabetes. While this finding may limit some translational aspects of using the tree shrew model, it does provide a novel opportunity to explore the liver changes in diabetic tree shrews that may accompany the early onset of diabetes and help better identify the nature of early changes in the liver tissues that affect diabetic patients with liver diseases.

4.2. Transcriptional Profile of Tree Shrew Liver. When applying the threshold value of FPKM to 0.3, our results showed a total of 11,411 and 11,485 genes expressed, respectively, in the control and diabetic groups (Figure 4). On the whole, these numbers are quite similar to those detected in human and mice liver tissues (11,392 and 11,201, resp.) via Ensembl and the proteomic analysis of murine liver cells [33, 44] and in the liver tissues of cows (about 12,500) and pigs (about 10,200) [45, 46]. After examining the categories of biological processes associated with genes expressed in the liver tissues of the tree shrews, we found that three biological processes, signal transduction, metabolic process, and macromolecular turnover, had a far higher fraction of transcriptions allocated to genes than other processes (Figure 5). This transcriptional result is consistent with previous proteomic results, which also found enrichment in the metabolic process and biosynthetic process in the tree shrew liver tissues [44, 47]. Additionally, the fractions of biological processes in the differentiated genes were associated with metabolic processes, translation, electron transport, and inflammatory response. These results are consistent with earlier microarray analyses of liver tissue of ZDF rats, wherein differentially expressed genes were highly associated with metabolic process, signal transduction, inflammatory response [10], and electron transport [9].

4.3. Liver Changes during the Early Stage of Diabetes. In the present study we detected a significantly increased expression of the aldose reductase (*akr1b1*), the rate-limiting enzyme of the polyol pathway, which suggests that hyperglycemia may upregulate the expression of aldose reductase (AR) and increase the flux through the polyol pathway in liver tissue of diabetic tree shrews. Accumulation of intracellular sorbitol as a consequence of increased aldose reductase activity was previously implicated in the development of various secondary complications of diabetes. Several studies using experimental animals reported that inhibition of *akr1b1* may be effective in the prevention of some diabetic complications, including kidney, retina, lens, and peripheral neuron tissues [48–50]. However, among animal models with hyperglycemia, increasing of polyol pathway is scarcely observed in the liver tissues. Indeed, a higher expression of *akr1b1* was only observed in liver tissues of STZ-induced type 1 diabetic mice on 4-week period [51], though increased flux of polyol pathway was not detected using microarray analysis in the liver tissues of ZDF rats which are characterized by obesity and type 2 diabetes with a point mutation in the leptin receptor [9, 10]. The reasons for this discrepancy are not entirely clear, but we speculate that the mechanisms used to induce diabetes are different between STZ-induced animal models and the obesity diabetic animal models. Several lines of evidence indicate that the inhibition of AR can prevent oxidative stress induced activation of inflammation that lead to cell death [52], suggesting that oxidative stress may actually be capable of upregulating the expression of AR. Accordingly, the higher expression of AR may be caused by oxidative stress among our diabetic tree shrews.

Impaired mitochondrial oxidative phosphorylation is the primary source of oxidation products (such as reactive oxygen species, ROS), which plays pivotal roles in the genesis of diabetic chronic liver diseases [53, 54]. In this study, three genes involved in the oxidative phosphorylation showed a

higher expression differentiation between the control and the diabetic group; within the diabetic group, *cox5a*, *cox5b*, and *cox6c* (complex IV) manifested a significantly lower expression as compared with the control group. This result suggests that the block of electron transfer through the mitochondrial electron transport chain immediately led to the overproduction of superoxide [55]. However, proteomic analysis of liver mitochondria found that most of the genes associated with oxidative phosphorylation were upregulated during the progression of diabetes in GK rats [56]. This discrepancy between the two animal models may be due to either different mechanisms used to induce diabetes or different methods to analyze the data. Likely further replication or comparative studies would be needed to verify this possibility.

Diabetes and hyperglycemia are both known to increase oxidative stress [57, 58]. Convincing experimental and clinical data suggests that the generation of reactive oxygen species increased with diabetes and that the onset of diabetes and its comorbidities and complications are closely associated with oxidative stress [55, 59–63]. High glucose has also been shown to increase oxidative stress, due to combination of increased production of excessive free radicals, ROS along with decreased antioxidant function, which further damaged all components of the cell, including proteins, lipids, and DNA. Here, STZ-induced high glucose levels in the diabetic tree shrews were associated with oxidative stress, consistent with the differential expressed genes of P450 side chain cleavage, P450scc (*cyp11a1*), reactive oxygen species modulator 1 (*romo1*), and peroxiredoxin 1 (*prdx1*). Mitochondrial cytochrome P450 systems have been suggested as a source of mitochondrial ROS production that can play a role in the induction of mitochondrial apoptosis [64]. Moreover, the upregulated expression of *cyp11a1* was purported to potentially indicate an increased ROS in mitochondria of diabetic animals [64]; and the forced expression of *romo1* increased the level of cellular ROS that originate from the mitochondria [65]. Additionally, *prdx1*, ROS scavenging enzymes, was upregulated in diabetic animals, indicating the increasing ability to clean out the free radical, which would alleviate the accumulation of free radical in diabetic liver. Subsequent identification of these genes indicates that oxidative stress in liver tissues occurred during the early stage of diabetes, a finding that may be critical in elucidating the mechanisms that generate the liver changes seen in diabetic patients.

Increased oxidative stress and the simultaneous decline of antioxidant defense mechanisms can lead to inflammation, damage of cellular organelle, and cell death [66–68]. The production of ROS induces inflammatory reactions, and the reverse is also true [66]. The interaction between oxidative stress and inflammatory reactions seems to lead to a vicious circle that eventually induces pathogenesis of diabetic complications. Here, several highly differentiated genes associated with the inflammatory process were detected in the RNA-seq data of the diabetic tree shews, including *cxcl13* and *crp*. The gene *cxcl13*, a biomarker of B-cell, displayed a marked decrease of mRNA expression in the diabetic group, while, *crp*, the inflammatory biomarker, showed significantly higher expression in the same group. Together, these results suggest that inflammatory reactions also occurred in the liver tissues during the early stage of diabetes and that the observed inflammation was mainly induced by ROS. Following this line of evidence, attenuating the oxidative stress and inflammation may prove a useful target for therapeutics aimed at preventing liver injury among diabetes patients.

Mitochondria are thought to be the primary target of oxidative damage, as ROS are generated mainly as by-products of mitochondrial respiration [69]. Several studies also observed mutations in mtDNA and impaired oxidative phosphorylation in diabetic patients [70, 71]. Consistently, the mitochondrial DNA (mtDNA) has been hypothesized to act as a major target for ROS damage [72, 73]. Our analysis of the tree shrew RNA-seq data uncovered several mtDNA genes (*mtco1*, *mtco3*, *mtnd4*, and *mtatp6*) downregulated among the diabetic tree shrews (Table 2). Since these genes are highly associated with the essential components of mitochondria respiration chain [74], the dysfunction of mtDNA genes should impair either the assembly or the function of the respiratory chain. This impairment should in turn trigger further accumulation of ROS, thereby creating a vicious cycle leading to energy depletion in the cell and ultimately cell death [69, 73]. Likewise, mitochondrion dysfunction can result in cell apoptosis [75]. Consistent with this hypothesis, here we observed the upregulation of several genes that promote cell apoptosis (*adrb2*, *agtr2*, *bdkrb2*, and *gdnf*) and a concurrent downregulation of antiapoptotic genes (*npm1*, *dynll1*, *hspd1*, and *prdx1*) among the STZ-induced tree shrews, as compared to the control group. This discrepancy implies that mitochondria may be more vulnerable than other organelles in the hepatic cells during the early stage of diabetes. Furthermore, the dysfunction of mitochondria may further promote inflammation and cell death in the diabetic liver cells. Numerous studies have demonstrated that mitochondrial factors are critical in the development of diabetes [56]. Microarray assay in liver tissues of diabetic ZDF rats and proteomic analysis of liver mitochondria in GK rats previously found impaired oxidative phosphorylation and apoptosis during the development of diabetes [9, 10, 56]. These results collectively indicate that the oxidative phosphorylation of mitochondria likely plays crucial roles in the development of diabetes and in diabetes-induced liver injury.

The liver plays a critical role in regulation of lipid metabolism, accounting for the generation and degradation of fatty acids, steroids, triacylglycerols, cholesterols, bile salts, and so forth, and it is also the central synthetic site of the *de novo* cholesterol biosynthesis in the body. Here, we observed a downregulation of *sc4mol*, a gene involved in the cholesterol biosynthetic process, among diabetic group (Table 2). This result may suggest a decreased synthesis of total cholesterol in the liver. Additionally, we also observed that several genes in cytochrome P450 family (e.g., *cyp7a1*, *cyp11a1*, *cyp11b2*, and *cyp17a1*) were upregulated in the diabetic group. These genes were previously reported to be involved in the steroid metabolic process, which were in the synthetic processes from cholesterol to the bile acid and steroid hormone. Pullinger et al. [76] demonstrated that the deficiency of *cyp7a1* led to the hypercholesterolemic

phenotype among humans, but conversely Pandak et al. [77] found that overexpression of *cyp7a1* in human liver cells might help to lower the concentration of serum cholesterol. By extension, the upregulation of these genes may be helpful in lowering the concentration of serum cholesterol in tree shrew. These results may also hint at a protective mechanism capable of decreasing the concentration of total cholesterol in the liver tissue of the diabetic group, because the high circulation concentration of total cholesterol is the main risk factor for development of cardiovascular diseases. We also observed an increase in the circulation HDL cholesterol particles among the diabetic tree shrews, further hinting at some sort of a protection that prevents the development of atherosclerosis. She et al. [78] previously reported the higher serum HDL in tree shrews after a long period of cholesterol intake, indicating that high serum HDL may play an important role in retarding the development of atherosclerosis, potentially due to the overexcretion of bile acid to degrade large amount of cholesterol in liver of tree shrew. Unfortunately, compared with the hepatic transcriptome profiles of ZDF rats and GK rats, we did not observe the gene changes associated with sucrose/glucose metabolism and tricarboxylic acid cycle, ketone body metabolism, phospholipid/glucolipid metabolism, insulin signaling pathway, ppar signaling pathway, Jak-STAT signaling pathway, and so froth [9, 10, 56]. These discrepancies might be due to the different diabetic phenotypes and different pathognomies. It has reported that STZ-induced type 1 diabetes contributed greatly to the liver dysfunction and cellular damage in rats [79]. Their results are similar to our results in STZ-induced diabetic tree shrews. However, ZDF rat is an obese type 2 diabetes model with a point mutation in the leptin receptor, which makes it an ideal model for studying insulin resistance related to obesity. Additionally, adult GK rats exhibit spontaneous type 2 diabetes with impaired glucose-induced insulin secretion, decreased β-cell mass, and hepatic glucose overproduction in the liver [80]. Therefore, genes involved in sucrose/glucose metabolism and tricarboxylic acid cycle, ketone body metabolism, insulin signaling pathway, and ppar signaling pathway could be determined in these models [9, 56]. However, the difference in terms of hepatic gene profiles between type 1 diabetes and type 2 diabetes is still unclear. Further studies still need to investigate this problem.

5. Conclusion

In summary, the present study found that STZ can adequately induce diabetes in the tree shrew model, accompanied by higher serum TAG, CHOL, HDL, and LDL. The number of expressed genes and the dominant categories of biological processes in liver transcriptional profile of tree shrew were quite similar to other mammary animals, including humans, pigs, and cows. The differentially expressed genes between the two tested groups of tree shrews also indicated that liver changes accompanied the early stage of diabetes in tree shrew, and hyperglycemia-induced oxidative stress can further lead to higher expression of AR, inflammation, and even cell death in liver tissues.

Competing Interests

The authors declare that there are no competing interests regarding the publication of this paper.

Authors' Contributions

Xiaoyun Wu and Haibo Xu contribute equally to this work.

Acknowledgments

This work was supported by the National Natural Science Foundation of China (U1202223 and Y301261041), the Strategic Priority Research Program of the Chinese Academy of Sciences (XDB13030600), the Application Program of Basic Research of Yunnan Province (2014FB180), and the National 863 Project of China (2012AA021801 and 2012AA022402). The authors would also like to thank Andrew Willden of the Kunming Institute of Zoology for assistance with the paper.

References

[1] J. E. Shaw, R. A. Sicree, and P. Z. Zimmet, "Global estimates of the prevalence of diabetes for 2010 and 2030," *Diabetes Research and Clinical Practice*, vol. 87, no. 1, pp. 4–14, 2010.

[2] A. D. Deshpande, M. Harris-Hayes, and M. Schootman, "Epidemiology of diabetes and diabetes-related complications," *Physical Therapy*, vol. 88, no. 11, pp. 1254–1264, 2008.

[3] D. S. H. Bell and E. Allbright, "The multifaceted associations of hepatobiliary disease and diabetes," *Endocrine Practice*, vol. 13, no. 3, pp. 300–312, 2007.

[4] A. Dey and K. Chandrasekaran, "Hyperglycemia induced changes in liver: in vivo and in vitro studies," *Current Diabetes Reviews*, vol. 5, no. 2, pp. 67–78, 2009.

[5] N. Vasdev, A. G. Kakati, S. Saigal, and N. C. Nayak, "Spectrum of histological features in non-alcoholic fatty liver disease," *National Medical Journal of India*, vol. 20, no. 6, pp. 282–287, 2007.

[6] H. Kaneto, N. Katakami, D. Kawamori et al., "Involvement of oxidative stress in the pathogenesis of diabetes," *Antioxidants and Redox Signaling*, vol. 9, no. 3, pp. 355–366, 2007.

[7] H. Kaneto, T.-A. Matsuoka, N. Katakami et al., "Oxidative stress and the JNK pathway are involved in the development of type 1 and type 2 diabetes," *Current Molecular Medicine*, vol. 7, no. 7, pp. 674–686, 2007.

[8] J. L. Evans, I. D. Goldfine, B. A. Maddux, and G. M. Grodsky, "Are oxidative stress—activated signaling pathways mediators of insulin resistance and β-cell dysfunction?" *Diabetes*, vol. 52, no. 1, pp. 1–8, 2003.

[9] Y. N. Kim, S. Kim, I.-Y. Kim et al., "Transcriptomic analysis of insulin-sensitive tissues from anti-diabetic drug treated ZDF rats, a T2DM animal model," *PLoS ONE*, vol. 8, no. 7, Article ID e69624, 2013.

[10] Y. H. Suh, Y. Kim, J. H. Bang et al., "Analysis of gene expression profiles in insulin-sensitive tissues from pre-diabetic and diabetic Zucker diabetic fatty rats," *Journal of Molecular Endocrinology*, vol. 34, no. 2, pp. 299–315, 2005.

[11] Z. Wang, M. Gerstein, and M. Snyder, "RNA-Seq: a revolutionary tool for transcriptomics," *Nature Reviews Genetics*, vol. 10, no. 1, pp. 57–63, 2009.

[12] B. T. Wilhelm and J.-R. Landry, "RNA-Seq-quantitative measurement of expression through massively parallel RNA-sequencing," *Methods*, vol. 48, no. 3, pp. 249–257, 2009.

[13] C. Trapnell, B. A. Williams, G. Pertea et al., "Transcript assembly and quantification by RNA-Seq reveals unannotated transcripts and isoform switching during cell differentiation," *Nature Biotechnology*, vol. 28, no. 5, pp. 511–515, 2010.

[14] E. T. Wang, R. Sandberg, S. Luo et al., "Alternative isoform regulation in human tissue transcriptomes," *Nature*, vol. 456, no. 7221, pp. 470–476, 2008.

[15] M. N. Cabili, C. Trapnell, L. Goff et al., "Integrative annotation of human large intergenic noncoding RNAs reveals global properties and specific subclasses," *Genes and Development*, vol. 25, no. 18, pp. 1915–1927, 2011.

[16] M. Li, I. X. Wang, Y. Li et al., "Widespread RNA and DNA sequence differences in the human transcriptome," *Science*, vol. 333, no. 6038, pp. 53–58, 2011.

[17] W. J. Murphy, E. Eizirik, S. J. O'Brien et al., "Resolution of the early placental mammal radiation using Bayesian phylogenetics," *Science*, vol. 294, no. 5550, pp. 2348–2351, 2001.

[18] J. E. Janečka, W. Miller, T. H. Pringle et al., "Molecular and genomic data identify the closest living relative of primates," *Science*, vol. 318, no. 5851, pp. 792–794, 2007.

[19] H.-J. Xia and C.-S. Chen, "Progress of non-human primate animal models of cancers," *Zoological Research*, vol. 32, no. 1, pp. 70–80, 2011.

[20] Y. Peng, Z. Ye, R. Zou et al., *Biology of Tree Shrew*, Yunnan Science and Technology Press, Kunming, China, 1991.

[21] J. Cao, E.-B. Yang, J.-J. Su, Y. Li, and P. Chow, "The tree shrews: adjuncts and alternatives to primates as models for biomedical research," *Journal of Medical Primatology*, vol. 32, no. 3, pp. 123–130, 2003.

[22] H. Yan, G. Zhong, G. Xu et al., "Sodium taurocholate cotransporting polypeptide is a functional receptor for human hepatitis B and D virus," *eLife*, vol. 2012, no. 1, Article ID e00049, 2012.

[23] X. Wu, Q. Chang, Y. Zhang et al., "Relationships between body weight, fasting blood glucose concentration, sex and age in tree shrews (*Tupaia belangeri chinensis*)," *Journal of Animal Physiology and Animal Nutrition*, vol. 97, no. 6, pp. 1179–1188, 2013.

[24] M. Cnop, B. Abdulkarim, G. Bottu et al., "RNA sequencing identifies dysregulation of the human pancreatic islet transcriptome by the saturated fatty acid palmitate," *Diabetes*, vol. 63, no. 6, pp. 1978–1993, 2014.

[25] D. L. Eizirik, M. Sammeth, T. Bouckenooghe et al., "The human pancreatic islet transcriptome: expression of candidate genes for type 1 diabetes and the impact of pro-inflammatory cytokines," *PLoS Genetics*, vol. 8, no. 3, Article ID e1002552, 2012.

[26] X.-Y. Wu, Y.-H. Li, Q. Chang, L.-Q. Zhang, S.-S. Liao, and B. Liang, "Streptozotocin induced type 2 diabetes in tree shrew (*Tupaia belangeri* chinensis)," *Zoological Research*, vol. 34, no. 2, pp. 108–115, 2013.

[27] Y. Fan, Z. Y. Huang, C. C. Cao et al., "Genome of the Chinese tree shrew," *Nature Communications*, vol. 4, p. 1426, 2013.

[28] C. Trapnell, L. Pachter, and S. L. Salzberg, "TopHat: discovering splice junctions with RNA-Seq," *Bioinformatics*, vol. 25, no. 9, pp. 1105–1111, 2009.

[29] D. Kim, G. Pertea, C. Trapnell, H. Pimentel, R. Kelley, and S. L. Salzberg, "TopHat2: accurate alignment of transcriptomes in the presence of insertions, deletions and gene fusions," *Genome Biology*, vol. 14, no. 4, article R36, 2013.

[30] L. Kong, Y. Zhang, Z.-Q. Ye et al., "CPC: assess the protein-coding potential of transcripts using sequence features and support vector machine," *Nucleic Acids Research*, vol. 35, no. 2, pp. W345–W349, 2007.

[31] D. W. Huang, B. T. Sherman, and R. A. Lempicki, "Bioinformatics enrichment tools: paths toward the comprehensive functional analysis of large gene lists," *Nucleic Acids Research*, vol. 37, no. 1, pp. 1–13, 2009.

[32] A. R. Quinlan and I. M. Hall, "BEDTools: a flexible suite of utilities for comparing genomic features," *Bioinformatics*, vol. 26, no. 6, Article ID btq033, pp. 841–842, 2010.

[33] D. Ramsköld, E. T. Wang, C. B. Burge, and R. Sandberg, "An abundance of ubiquitously expressed genes revealed by tissue transcriptome sequence data," *PLoS Computational Biology*, vol. 5, no. 12, Article ID e1000598, 2009.

[34] N. Tiffin, E. Adie, F. Turner et al., "Computational disease gene identification: a concert of methods prioritizes type 2 diabetes and obesity candidate genes," *Nucleic Acids Research*, vol. 34, no. 10, pp. 3067–3081, 2006.

[35] J. D. McGarry, G. P. Mannaerts, and D. W. Foster, "A possible role for malonyl-CoA in the regulation of hepatic fatty acid oxidation and ketogenesis," *The Journal of Clinical Investigation*, vol. 60, no. 1, pp. 265–270, 1977.

[36] K. E. Knoll, J. L. Pietrusz, and M. Liang, "Tissue-specific transcriptome responses in rats with early streptozotocin-induced diabetes," *Physiological Genomics*, vol. 21, no. 2, pp. 222–229, 2005.

[37] L. Qiu, H. Ye, L. Chen, Y. Hong, F. Zhong, and T. Zhang, "Red clover extract ameliorates dyslipidemia in streptozotocin-induced diabetic C57BL/6 mice by activating hepatic PPARα," *Phytotherapy Research*, vol. 26, no. 6, pp. 860–864, 2012.

[38] H. M. Colhoun, M. B. Rubens, S. R. Underwood, and J. H. Fuller, "The effect of type 1 diabetes mellitus on the gender difference in coronary artery calcification," *Journal of the American College of Cardiology*, vol. 36, no. 7, pp. 2160–2167, 2000.

[39] T. Alessa, A. Szeto, W. Chacra, A. Mendez, and R. B. Goldberg, "High HDL-C prevalence is common in type 1 diabetes and increases with age but is lower in Hispanic individuals," *Journal of Diabetes and its Complications*, vol. 29, no. 1, pp. 105–107, 2015.

[40] M.-R. Taskinen, J. Kahri, V. Koivisto, J. Shepherd, and C. J. Packard, "Metabolism of HDL apolipoprotein A-I and A-II in Type 1 (insulin-dependent) diabetes mellitus," *Diabetologia*, vol. 35, no. 4, pp. 347–356, 1992.

[41] R. M. Calderon, S. Diaz, A. Szeto et al., "Elevated lipoprotein lipase activity does not account for the association between adiponectin and HDL in type 1 diabetes," *The Journal of Clinical Endocrinology and Metabolism*, vol. 100, no. 7, pp. 2581–2588, 2015.

[42] O. A. Komolafe, D. O. Adeyemi, S. O. Adewole, and E. M. Obuotor, "Streptozotocin-induced diabetes alters the serum lipid profiles of adult wistar rats," *The Internet Journal of Cardiovascular Research*, vol. 7, no. 1, 2009.

[43] S. Skovsø, "Modeling type 2 diabetes in rats using high fat diet and streptozotocin," *Journal of Diabetes Investigation*, vol. 5, no. 4, pp. 349–358, 2014.

[44] S. B. Azimifar, N. Nagaraj, J. Cox, and M. Mann, "Cell-type-resolved quantitative proteomics of murine liver," *Cell Metabolism*, vol. 20, no. 6, pp. 1076–1087, 2014.

[45] M. McCabe, S. Waters, D. Morris, D. Kenny, D. Lynn, and C. Creevey, "RNA-seq analysis of differential gene expression in liver from lactating dairy cows divergent in negative energy balance," *BMC Genomics*, vol. 13, article 193, 2012.

[46] Y. Ramayo-Caldas, N. Mach, A. Esteve-Codina et al., "Liver transcriptome profile in pigs with extreme phenotypes of intramuscular fatty acid composition," *BMC Genomics*, vol. 13, article 547, 2012.

[47] R. Li, W. Xu, Z. Wang, B. Liang, J.-R. Wu, and R. Zeng, "Proteomic characteristics of the liver and skeletal muscle in the Chinese tree shrew (*Tupaia belangeri chinensis*)," *Protein & Cell*, vol. 3, no. 9, pp. 691–700, 2012.

[48] A. Bhatnagar and S. K. Srivastava, "Aldose reductase: congenial and injurious profiles of an enigmatic enzyme," *Biochemical Medicine and Metabolic Biology*, vol. 48, no. 2, pp. 91–121, 1992.

[49] P. F. Kador, W. G. Robison Jr., and J. H. Kinoshita, "The pharmacology of aldose reductase inhibitors," *Annual Review of Pharmacology and Toxicology*, vol. 25, pp. 691–714, 1985.

[50] M. A. Pfeifer, M. P. Schumer, and D. A. Gelber, "Aldose reductase inhibitors: the end of an era or the need for different trial designs?" *Diabetes*, vol. 46, supplement 2, pp. S82–S89, 1997.

[51] S.-M. Jang, M.-J. Kim, M.-S. Choi, E.-Y. Kwon, and M.-K. Lee, "Inhibitory effects of ursolic acid on hepatic polyol pathway and glucose production in streptozotocin-induced diabetic mice," *Metabolism*, vol. 59, no. 4, pp. 512–519, 2010.

[52] K. V. Ramana, "Aldose reductase: new insights for an old enzyme," *BioMolecular Concepts*, vol. 2, no. 1-2, pp. 103–114, 2011.

[53] J. St-Pierre, J. A. Buckingham, S. J. Roebuck, and M. D. Brand, "Topology of superoxide production from different sites in the mitochondrial electron transport chain," *Journal of Biological Chemistry*, vol. 277, no. 47, pp. 44784–44790, 2002.

[54] A. N. Lucchesi, N. T. de Freitas, L. L. Cassettari, S. F. G. Marques, and C. T. Spadella, "Diabetes mellitus triggers oxidative stress in the liver of alloxan-treated rats: a mechanism for diabetic chronic liver disease," *Acta Cirurgica Brasileira*, vol. 28, no. 7, pp. 502–508, 2013.

[55] M. Brownlee, "The pathobiology of diabetic complications: a unifying mechanism," *Diabetes*, vol. 54, no. 6, pp. 1615–1625, 2005.

[56] W.-J. Deng, S. Nie, J. Dai, J.-R. Wu, and R. Zeng, "Proteome, phosphoproteome, and hydroxyproteome of liver mitochondria in diabetic rats at early pathogenic stages," *Molecular and Cellular Proteomics*, vol. 9, no. 1, pp. 100–116, 2010.

[57] D. Giugliano, A. Ceriello, and G. Paolisso, "Oxidative stress and diabetic vascular complications," *Diabetes Care*, vol. 19, no. 3, pp. 257–267, 1996.

[58] S. M. Son, M. K. Whalin, D. G. Harrison, W. R. Taylor, and K. K. Griendling, "Oxidative stress and diabetic vascular complications," *Current Diabetes Reports*, vol. 4, no. 4, pp. 247–252, 2004.

[59] J. W. Baynes, "Role of oxidative stress in development of complications in diabetes," *Diabetes*, vol. 40, no. 4, pp. 405–412, 1991.

[60] T. Nishikawa, D. Edelstein, X. L. Du et al., "Normalizing mitochondrial superoxide production blocks three pathways of hyperglycaemic damage," *Nature*, vol. 404, no. 6779, pp. 787–790, 2000.

[61] J. S. Johansen, A. K. Harris, D. J. Rychly, and A. Ergul, "Oxidative stress and the use of antioxidants in diabetes: linking basic science to clinical pratice," *Cardiovascular Diabetology*, vol. 4, article 5, 2005.

[62] J. W. Baynes and S. R. Thorpe, "Role of oxidative stress in diabetic complications: a new perspective on an old paradigm," *Diabetes*, vol. 48, no. 1, pp. 1–9, 1999.

[63] P. Rösen, P. P. Nawroth, G. King, W. Möller, H.-J. Tritschler, and L. Packer, "The role of oxidative stress in the onset and progression of diabetes and its complications: a summary of a congress series sponsored by UNESCO-MCBN, the American diabetes association and the German Diabetes Society," *Diabetes/Metabolism Research and Reviews*, vol. 17, no. 3, pp. 189–212, 2001.

[64] E. Derouet-Hümbert, K. Roemer, and M. Bureik, "Adrenodoxin (Adx) and CYP11A1 (P450scc) induce apoptosis by the generation of reactive oxygen species in mitochondria," *Biological Chemistry*, vol. 386, no. 5, pp. 453–461, 2005.

[65] Y. M. Chung, J. S. Kim, and Y. D. Yoo, "A novel protein, Romo1, induces ROS production in the mitochondria," *Biochemical and Biophysical Research Communications*, vol. 347, no. 3, pp. 649–655, 2006.

[66] J. Hakim, "Reactive oxygen species and inflammation," *Comptes Rendus des Seances de la Societe de Biologie et de Ses Filiales*, vol. 187, no. 3, pp. 286–295, 1993.

[67] A. C. Maritim, R. A. Sanders, and J. B. Watkins III, "Diabetes, oxidative stress, and antioxidants: a review," *Journal of Biochemical and Molecular Toxicology*, vol. 17, no. 1, pp. 24–38, 2003.

[68] S. W. Ryter, P. K. Hong, A. Hoetzel et al., "Mechanisms of cell death in oxidative stress," *Antioxidants and Redox Signaling*, vol. 9, no. 1, pp. 49–89, 2007.

[69] H. Cui, Y. Kong, and H. Zhang, "Oxidative stress, mitochondrial dysfunction, and aging," *Journal of Signal Transduction*, vol. 2012, Article ID 646354, 13 pages, 2012.

[70] D. E. Kelley, J. He, E. V. Menshikova, and V. B. Ritov, "Dysfunction of mitochondria in human skeletal muscle in type 2 diabetes," *Diabetes*, vol. 51, no. 10, pp. 2944–2950, 2002.

[71] R. Becker, H. Laube, T. Linn, and M. S. Damian, "Insulin resistance in patients with the mitochondrial tRNA(Leu(UUR)) gene mutation at position 3243," *Experimental and Clinical Endocrinology and Diabetes*, vol. 110, no. 6, pp. 291–297, 2002.

[72] L. A. Esposito, S. Melov, A. Panov, B. A. Cottrell, and D. C. Wallace, "Mitochondrial disease in mouse results in increased oxidative stress," *Proceedings of the National Academy of Sciences of the United States of America*, vol. 96, no. 9, pp. 4820–4825, 1999.

[73] I. Shokolenko, N. Venediktova, A. Bochkareva, G. I. Wilson, and M. F. Alexeyev, "Oxidative stress induces degradation of mitochondrial DNA," *Nucleic Acids Research*, vol. 37, no. 8, pp. 2539–2548, 2009.

[74] M. Falkenberg, N.-G. Larsson, and C. M. Gustafsson, "DNA replication and transcription in mammalian mitochondria," *Annual Review of Biochemistry*, vol. 76, pp. 679–699, 2007.

[75] N. R. Madamanchi and M. S. Runge, "Mitochondrial dysfunction in atherosclerosis," *Circulation Research*, vol. 100, no. 4, pp. 460–473, 2007.

[76] C. R. Pullinger, C. Eng, G. Salen et al., "Human cholesterol 7α-hydroxylase (CYP7A1) deficiency has a hypercholesterolemic phenotype," *The Journal of Clinical Investigation*, vol. 110, no. 1, pp. 109–117, 2002.

[77] W. M. Pandak, C. Schwarz, P. B. Hylemon et al., "Effects of CYP7A1 overexpression on cholesterol and bile acid homeostasis," *The American Journal of Physiology—Gastrointestinal and Liver Physiology*, vol. 281, no. 4, pp. G878–G889, 2001.

[78] M. P. She, Y. Z. Lu, R. Y. Xia et al., "The role of α-lipoprotein in preventing atherosclerosis plaques developed in tree shrew associating with induced hypercholesterinemia," *Chinese Journal of Pathology*, vol. 11, no. 1, pp. 23–28, 1982.

[79] P. Manna, J. Das, J. Ghosh, and P. C. Sil, "Contribution of type 1 diabetes to rat liver dysfunction and cellular damage via activation of NOS, PARP, IκBα/NF-κB, MAPKs, and mitochondria-dependent pathways: prophylactic role of arjunolic acid," *Free Radical Biology and Medicine*, vol. 48, no. 11, pp. 1465–1484, 2010.

[80] F. Picarel-Blanchot, C. Berthelier, D. Bailbé, and B. Portha, "Impaired insulin secretion and excessive hepatic glucose production are both early events in the diabetic GK rat," *The American Journal of Physiology—Endocrinology and Metabolism*, vol. 271, no. 4, pp. E755–E762, 1996.

Hindawi Publishing Corporation
Journal of Diabetes Research
Volume 2016, Article ID 3467403, 10 pages
http://dx.doi.org/10.1155/2016/3467403

Research Article

Conserved Metabolic Changes in Nondiabetic and Type 2 Diabetic Bariatric Surgery Patients: Global Metabolomic Pilot Study

Konrad Sarosiek,[1] Kirk L. Pappan,[2] Ankit V. Gandhi,[1] Shivam Saxena,[1] Christopher Y. Kang,[1] Heather McMahon,[1] Galina I. Chipitsyna,[3] David S. Tichansky,[1] and Hwyda A. Arafat[3]

[1]*Department of Surgery, Thomas Jefferson University, Philadelphia, PA 19107, USA*
[2]*Metabolon, Inc., Research Triangle Park, Durham, NC 27713, USA*
[3]*Department of Biomedical Sciences, University of New England, Biddeford, ME 04005, USA*

Correspondence should be addressed to Galina I. Chipitsyna; gchipitsyna@une.edu

Received 17 September 2015; Revised 15 November 2015; Accepted 25 November 2015

Academic Editor: Michal Ciborowski

The goal of this study was to provide insight into the mechanism by which bariatric surgical procedures led to weight loss and improvement or resolution of diabetes. Global biochemical profiling was used to evaluate changes occurring in nondiabetic and type 2 diabetic (T2D) patients experiencing either less extreme sleeve gastrectomy or a full gastric bypass. We were able to identify changes in metabolism that were affected by standard preoperation liquid weight loss diet as well as by bariatric surgery itself. Preoperation weight-loss diet was associated with a strong lipid metabolism signature largely related to the consumption of adipose reserves for energy production. Glucose usage shift away from glycolytic pyruvate production toward pentose phosphate pathway, via glucose-6-phosphate, appeared to be shared across all patients regardless of T2D status or bariatric surgery procedure. Our results suggested that bariatric surgery might promote antioxidant defense and insulin sensitivity through both increased heme synthesis and HO activity or expression. Changes in histidine and its metabolites following surgery might be an indication of altered gut microbiome ecology or liver function. This initial study provided broad understanding of how metabolism changed globally in morbidly obese nondiabetic and T2D patients following weight-loss surgery.

1. Introduction

Diabetes is a major public health concern in the United States because of its prevalence, considerable morbidity and mortality, and economic burden with total medical costs of 245 billion dollars in 2012 alone [1, 2]. In 2010, the prevalence rate of diabetes in the US was 9.3%, affecting older population (65 years or older) even more dramatically with the rate of 25.9% [1]. Diabetes is associated with serious complications, including coronary heart disease, stroke, kidney failure, neuropathy, blindness, and amputation, and was the seventh leading cause of death in 2010 [1, 2]. Type 2 diabetes (T2D) accounts for 90–95% of all diagnosed cases [1]. Obesity is a major risk factor for T2D [2, 3], and the risk of diabetes increases directly with BMI [2, 4, 5]. According to National Center for Health Statistics (NCHS) more than one-third of US adults (34.9 percent) were obese in 2011-2012 [6]. The medical care costs of obesity in the United States are staggering, totaling about $147 billion dollars in 2008 alone [7].

Weight loss is important therapeutic goal in obese patients with T2D, because even moderate weight loss (5%) improves insulin sensitivity [2, 8]. Bariatric surgery is the most effective weight-loss therapy and has considerable beneficial effects on diabetes and other obesity-related comorbidities [2, 9–11].

Weight-loss surgery by laparoscopic sleeve gastrectomy (SG) leads to a 40–65% reduction in excess weight and,

amazingly, 56% of patients achieve resolution in their type 2 diabetes and 37% see improvement in their T2D symptoms [12]. Laparoscopic gastric bypass (GB) is a more intense surgery that typically results in a 60–70% loss of excess weight and is also characterized by improvement or resolution of diabetes [9, 12, 13].

The objective of this study was to provide insight into the mechanism by which gut/stomach rerouting leads to weight loss and the improvement or resolution of diabetes. In metabolomics, an individual's metabolic state is profiled by multiplexed measurement of many low-molecular-weight metabolites [14]. Over 4,000 such metabolites have been identified in human serum [15]. Two complementary approaches, targeted and nontargeted analyses, have evolved [16]. In targeted analysis discrete groups of chemically related metabolites (e.g., amino acids) are quantified in a biological sample. In contrast, nontargeted analysis is a more qualitative approach that surveys as many different metabolites as possible [14]. Using primarily targeted approaches, multiple studies have identified higher levels of branched-chain and aromatic amino acids in insulin-resistant, obese, and T2D individuals [17]. More recent studies demonstrated that higher levels of these amino acids are predictive of progression to T2D as well as future insulin resistance and hyperglycemia [14, 18–22]. Recently, Gall and colleagues [23] used nontargeted approach to identify plasma metabolites associated with development of insulin resistance and/or glucose intolerance. Two top-ranked metabolites were an organic acid, α-hydroxybutyrate (α-HB), and a lipid, 1-linoleoyl-glycerophosphocholine (L-GPC). Ferrannini et al. proposed fasting α-HB and L-GPC levels as new biomarkers to help predict dysglycemia and T2D [14, 24]. This nontargeted global metabolomic profiling represents new tool that allows the comprehensive survey of metabolism and metabolic networks to gain insight into phenotype and identify biomarker candidates. So far this approach was used to find a way to predict the progression to T2D as well as future insulin resistance and impaired glucose tolerance by serum analysis of insulin-resistant, obese individuals who progressed to T2D [14]. We took an opposite approach utilizing bariatric surgery tool as the most promising way to affect weight loss and to rectify T2D symptoms in morbidly obese patients. The range of metabolic changes that accompany weight reduction is not fully characterized. It is not known whether metabolic response is the same for all bariatric procedures, nor is it known whether there are any differences between nondiabetic and T2D patients.

2. Research Design and Methods

2.1. Serum Samples Collection. 15 patients represented three disease-surgery groups: nondiabetic (non-T2D) receiving SG and T2D receiving either SG or GB surgery (Table 1). Blood samples were collected over the course of treatment for each patient at the following times: at baseline (BL) prior to dieting/surgery, 14 days after baseline with adherence to strict preoperation weight-loss liquid diet (preop diet), and 28 days after surgery recovery after bariatric surgery (postop). Blood samples were collected in serum separator tubes, allowed to stand at room temperature for 15–20 minutes, centrifuged at 2500 rpm for 10 minutes at 4°C, aliquoted, snap frozen in liquid nitrogen, and stored at −80°C until analysis.

2.2. Global Metabolomic Analysis. Nontargeted global metabolomic analysis was performed by Metabolon, Inc. (Durham, NC), using two independent platforms: ultrahigh performance liquid chromatography/tandem mass spectrometry (UHPLC-MS/MS) optimized for basic species or acidic species, and gas chromatography/mass spectrometry (GC/MS). General platform methods are described in details in Online Supplemental Data section (see Supplementary Methods and Materials available online at http://dx.doi.org/10.1155/2016/3467403).

Following log transformation and imputation with minimum observed values for each compound, repeated measures 2-way ANOVA with posttest contrasts was used to identify biochemicals that differed significantly between experimental groups and across study time points with statistical cut-offs for P value ($P < 0.05$). Multiple comparisons were accounted for by estimating the false discovery rate using q-values of less than 5% ($q < 0.05$) [25].

3. Results and Discussion

3.1. Metabolite Summary and Significantly Altered Biochemicals. The search continues to identify biomarkers capable of predicting the onset of T2D [14]. Genome-wide association studies have identified many T2D susceptibility genes [14, 26] but generally failed to improve risk prediction over that provided by routine clinical measures [14, 27]. Global nontargeted analysis performed in this study is the first study to provide the insight into mechanism by which bariatric surgery leads to weight loss and resolution or improvement of T2D. This approach might also be used to identify T2D biomarker candidates and find new, cost effective treatments that can replace surgery itself.

Since metabolomic profiling generates a wealth of data that must be parsed to extract information, we chose statistical cut-offs at both the level of individual metabolites—P values—and the level of multiple testing across the 476 metabolites detected in the serum samples—q-values. By narrowing in on metabolites meeting the conservative criteria of $P < 0.05$ and an estimated false discovery rate of less than 5% ($q < 0.05$), we were able to reduce the complexity of the dataset and observed a number of statistically significant changes that occurred in common in nondiabetic and T2D patients with SG or GB. Furthermore, we were able to identify concerted changes of related metabolites that pointed to areas of metabolism that were affected by standard preop diet as well as by bariatric surgery itself. A list of all 476 metabolites detected and heat map of the statistical comparisons across time and patient groups are presented in Online Supplemental Tables A1 and A2.

Comparison of serum profiles at baseline, following a preop weight reduction diet, and after weight-loss surgery revealed several key metabolic differences as highlighted below.

Table 1: Clinicopathological characteristics of the patients.

Average	Gastric sleeve with T2D	Gastric sleeve without T2D	Gastric bypass with T2D
M, number of patients	2	0	1
F, number of patients	3	5	4
Age, years	46 ± 12.84	45.2 ± 14.24	44.4 ± 17.57
Weight, lb	306.28 ± 46.27	250.4 ± 18.58	304.4 ± 44.11
BMI	48.74 ± 8.2	43.54 ± 4.13	47.56 ± 6.61
Fasting blood sugar, mg/dL	140.6 ± 26.03	87 ± 2.92	98.8 ± 21.71
HTN, number of patients	2	3	3

Fat mobilization and oxidation were the key signatures associated with preop diet. Prior to surgery, patients were subjected to 2-week clear liquid diet that promoted weight loss on the order of 3–5% of body weight. The preoperative liquid diet is a 14-day high protein, very low calorie diet (VLCD) designed to deplete glycogen and fat stores in the liver or "shrink the liver" which is lifted to access the stomach during surgery. This VLCD includes 800 kcal with 80 g protein and typically produces a 10–20-pound weight loss. High protein drinks with less than 200 calories and at least 20 g protein are consumed 3-4x daily; no solid food is allowed on this diet. In addition, at least 64 ounces of sugar-free decaffeinated clear liquids a day are recommended along with a multivitamin and a calcium + vitamin D supplement. Medications, such as antihyperglycemics, are adjusted during this preoperative weight-loss phase to account for decreased calorie and carbohydrate intake. The study found that patients who follow a preoperative liquid diet effectively reduced visceral fat and achieve greater weight loss [28].

Examination of preop metabolic profiles, serum samples taken immediately before surgery, showed a profound mobilization of fat as attested by statistically significant elevations of ketones, monoacylglycerols, oleate, and an acyl-carnitine (Online Supplemental Table A3, Figure 1). These are compounds associated with lipolysis and fatty acid oxidation which suggested that a major metabolic effect of the preop diet was to stimulate fat tissue triglyceride hydrolysis, transport of fatty acids to the liver, and subsequent liver fatty acid oxidation and ketogenesis to supply energy substrates for peripheral tissues. The elevation of the markers associated with lipolysis and ketone production was transient and, in most cases, returned to near baseline levels by day 28 postsurgery time point. These results suggest that 3–5% weight loss experienced by patients during preop diet is largely due to the consumption of adipose reserves for energy production.

Another interesting observation is that preop diet led to a transient elevation of alpha-hydroxybutyrate (α-HB) and its precursor alpha-ketobutyrate (Online Supplemental Table A3, Figure 1). α-HB is a sensitive biomarker of insulin resistance [23, 24] which suggests that both nondiabetic and T2D patients experienced a temporary relative increase in insulin resistance during preop diet.

Compounds that changed in a statistically significant manner after 28 days of recovery from bariatric surgery, relative to baseline, were more numerous and diverse than observed in response to the preoperation diet. 62 compounds in the postsurgery to baseline comparison represented $P < 0.05$ and showed $q < 0.05$ in at least one of the disease-surgery groups (Online Supplemental Table A4). 28 compounds showed P and q-value cut-offs across all three disease-surgery groups at the 28-day postsurgery sample collection time point relative to baseline. 13 of the compounds that changed across all three groups had fold-change increases—including 100-fold + increases for *trans*-urocanate, *cis*-urocanate, pyroglutamylvaline, and heme in most or all of the groups. The remaining fifteen compounds that changed across all three groups were reduced at the postsurgery time point compared to baseline. Levels of ascorbate and various tocopherols were substantially reduced with ascorbate showing a 12.5-fold or greater decrease in each of the groups (Online Supplemental Table A4, Figure 2). Difficulty in absorbing micronutrients, such as vitamin C, following bariatric surgery has been reported previously [29, 30] and appeared to be confirmed at a shorter follow-up time point in this study.

Glutathione and its precursors were more abundant following weight-loss surgery. Weight-loss surgery led to concerted changes in compounds related to sulfur-containing amino acid metabolism that were largely shared across the groups. Glutathione (GSH) is a tripeptide comprised of glutamate, cysteine, and glycine. These amino acids along with the recycling intermediates Cys-Gly and 5-oxoproline were increased in all groups following surgery (Online Supplemental Table A4), suggesting a greater potential availability of substrates for GSH production. Oxidized forms of glutathione and cysteine, such as the mixed heterodimer cysteine-glutathione and glutathione homodimer GSSG, were elevated following surgery (Online Supplemental Table A4, Figure 2) and could be a sign of increased oxidative stress following surgery. However, an alternate interpretation is that a greater availability of glutathione and sulfur-containing amino acids following weight-loss surgery led to the greater formation of these oxidized compounds.

Weight-loss surgery appeared to shift glucose usage away from glycolytic pyruvate production. Pyruvate—the terminal product of glucose metabolism via the glycolysis pathway—dropped sharply after bariatric surgery (Online Supplemental Table A4, Figure 3), likely indicating its more efficient mitochondrial utilization. The reduction of pyruvate was matched by increases in fumarate, in all T2D patients, and malate perhaps indicating an inadequate supply of acetyl-CoA, which is derived from pyruvate, relative to

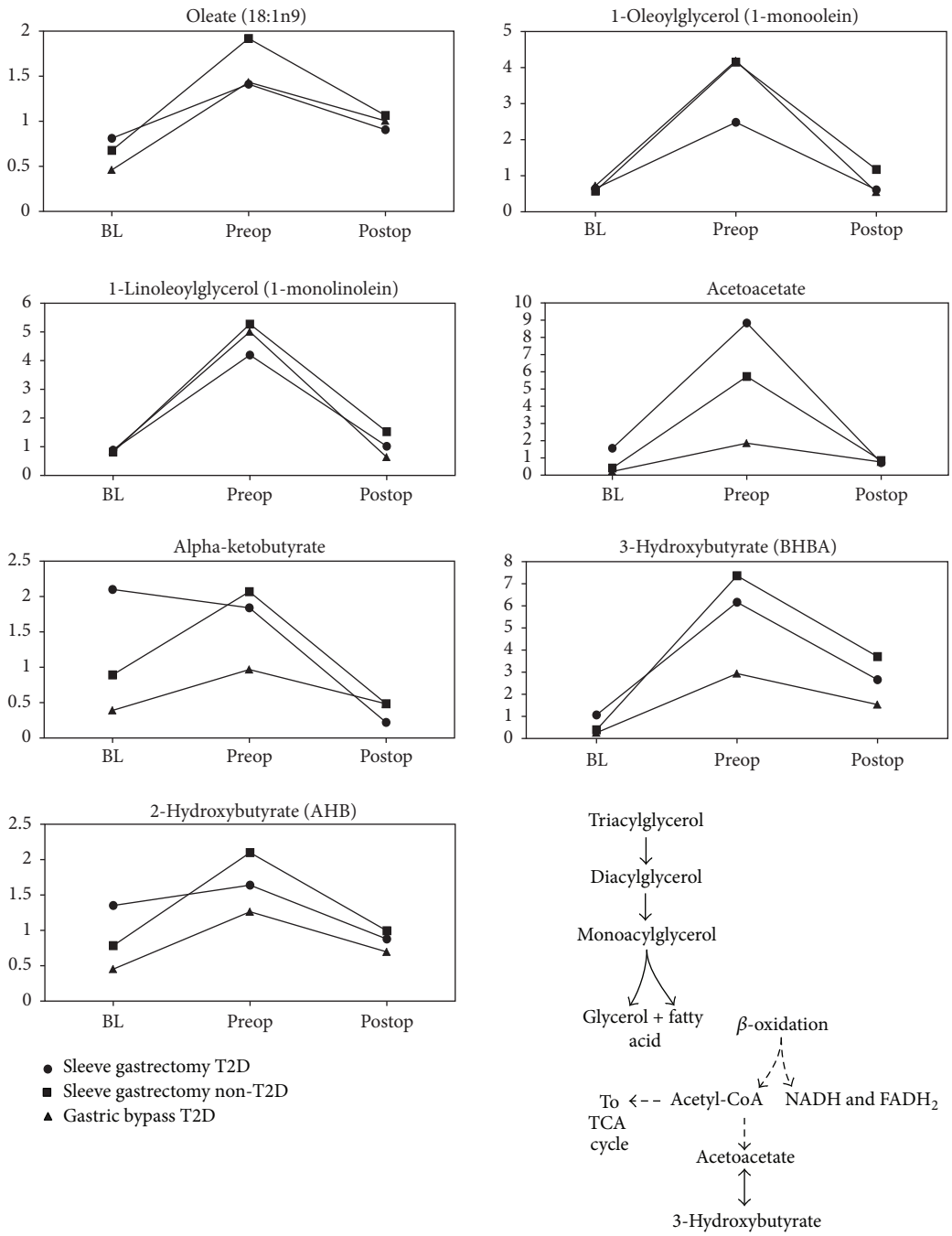

Figure 1: Fat mobilization and oxidation: key signatures associated with preop diet. All shown metabolites meet the conservative criteria of $P < 0.05$ and an estimated false discovery rate of less than 5% ($q < 0.05$).

the level of TCA cycle components. However, levels of the glycolytic intermediate 3-phosphoglycerate (3-PG) increased after surgery as did nonglycolytic products—glycerol and serine—potentially derived from 3-PG.

In addition to changes in pyruvate production, glucose usage via the pentose phosphate pathway (PPP) was also shifted following bariatric surgery. The PPP is a key source of pentose sugars used for nucleotide synthesis as well as NADPH which is used for reductive synthesis reactions and regeneration of reduced glutathione. PPP intermediates and derivative pentose sugars, including ribulose-5-phosphate and xylulose-5-phosphate that are isobars that cannot be differentiated by our platform, and their nonphosphorylated products, such as xylulose, were significantly increased in all groups following surgery (Online Supplemental Table A4, Figure 3). Glucose carbons, via glucose-6-phosphate, may have been directed toward the pentose phosphate pathway in the face of the proposed decrease in glycolysis pathway activity. Glucose metabolism was likely confounded by the use of antidiabetic medications. For example, at baseline,

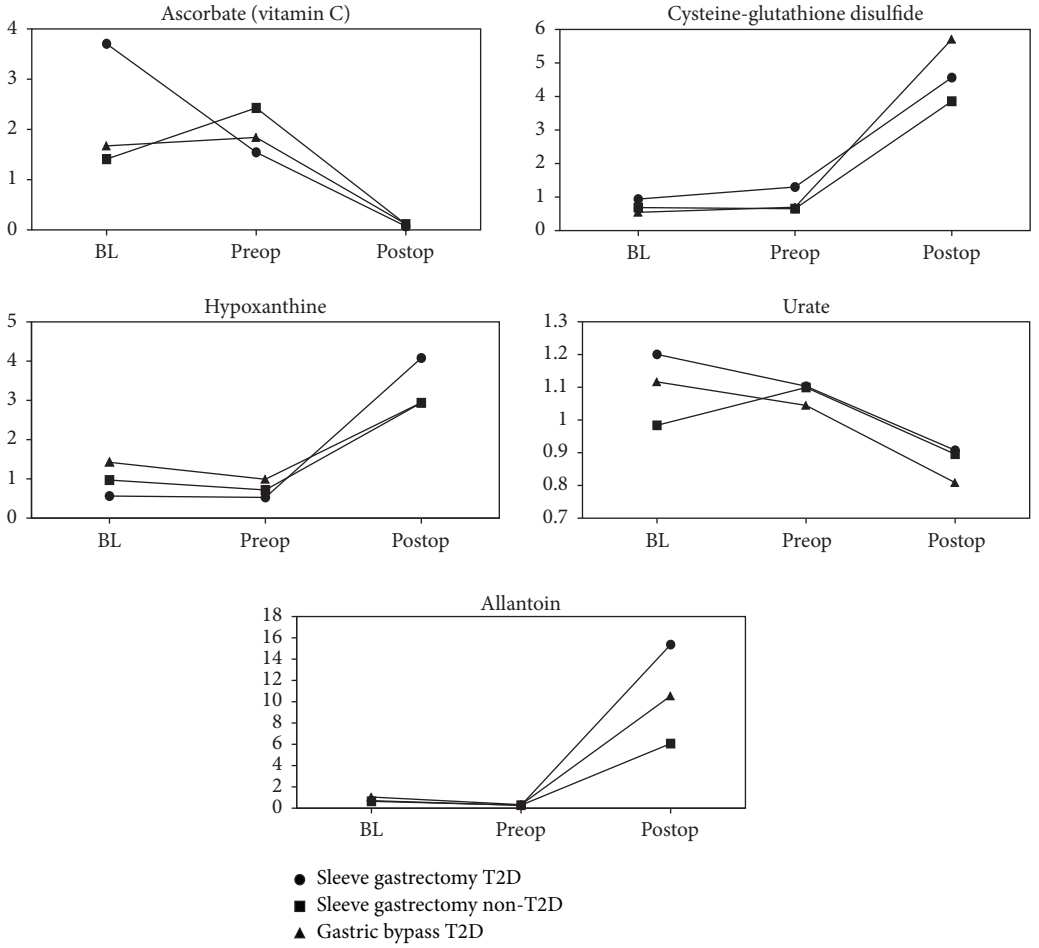

Figure 2: Postsurgery metabolic changes. All shown metabolites meet the conservative criteria of $P < 0.05$ and an estimated false discovery rate of less than 5% ($q < 0.05$).

metformin was detected in 100% of the T2D SG patient samples, 60% of the T2D GB samples, and none of the nondiabetic SG samples. After bariatric surgery, metformin was only detected in 20% of the T2D SG and GB serum samples. Postsurgery serum glucose levels decreased relative to baseline but this change only reached statistical significance ($P < 0.05$) in the T2D SG group (Online Supplemental Table A4, Figure 3). In total, the results suggest that bariatric surgery affected glucose metabolism through glycolytic and nonglycolytic pathways similarly for all three of the disease-surgery groups.

Increased serum heme levels were a possible indication of improved liver function following surgery. Each of the patient groups experienced an increase in serum heme levels around 100-fold compared to their respective baseline levels following surgery (Online Supplemental Table A4). A couple of interesting possibilities, such as a reduced level of heme breakdown by heme oxygenase (HO) or an increased level of synthesis by 5-aminolevulinate synthase (ALA synthase), could explain these changes. The understanding of HO-1 function has evolved beyond a simple disposal of heme to include cytoprotective, anti-inflammatory, and antioxidant functions. For instance, endogenous carbon monoxide produced by HO-1 engages multiple signal transduction pathways to confer antiapoptotic and anti-inflammatory effects and biliverdin and bilirubin are potent antioxidants. HO activation has been shown to have insulin sensitizing and anti-inflammation effects in T2D [31]. So the increase in heme and biliverdin following surgery could represent an increase in heme oxidation by HO leading to greater antioxidant protection and insulin sensitivity. On the other hand, the greater availability of glycine, which shows a relative deficiency in T2D [23, 32], could also serve as the basis for greater heme production by ALA synthase—the rate-limiting enzyme of heme formation whose expression is repressed by glucose [33]. On the other hand, biliverdin catabolism—which can reflect red blood cell turnover and heme disposal—was less evident following surgery as indicated by reductions in bilirubin ZZ and its EE photoisomer (Online Supplemental Table A4). Together, these exciting results suggest that bariatric surgery may promote antioxidant defense and insulin sensitivity through both increased heme synthesis and HO activity or expression.

Diabetes and obesity are chronic conditions associated with elevated oxidative/inflammatory activities with a

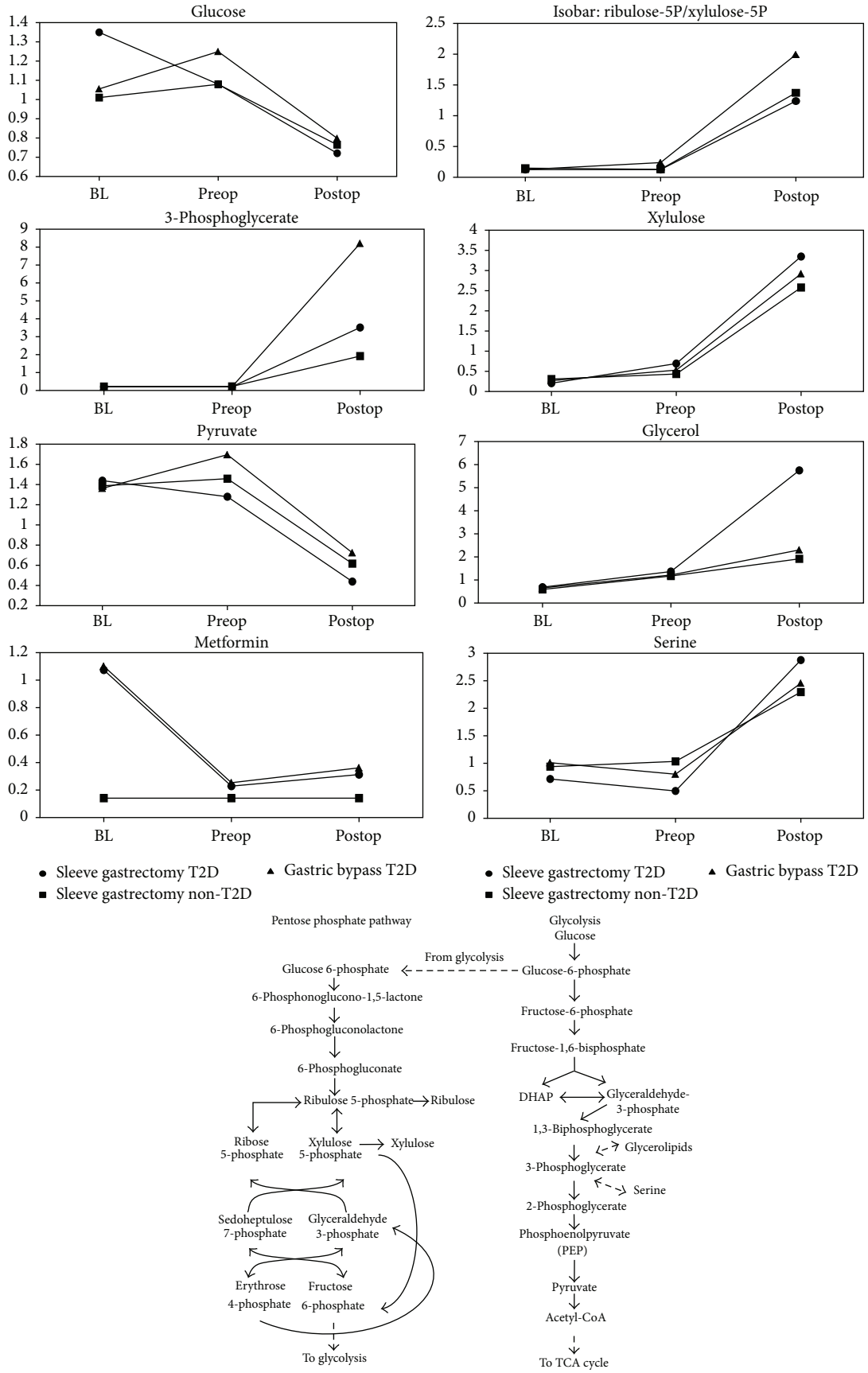

Figure 3: Postsurgery glucose usage shift towards pentose phosphate pathway. All shown metabolites meet the conservative criteria of $P < 0.05$ and an estimated false discovery rate of less than 5% ($q < 0.05$).

continuum of tissue insults leading to more severe cardiometabolic and renal complications including myocardial infarction and end-stage-renal damage [31]. A common denominator of these chronic conditions is the enhanced levels of cytokines like tumour necrosis factor-alpha (TNF-α), interleukin (IL-6), IL-1beta, and resistin, which in turn activates the c-Jun-N-terminal kinase (JNK) and NF-κB, pathways, creating a vicious cycle that exacerbates insulin resistance, type-2 diabetes, and related complications [31]. Emerging evidence indicates that heme oxygenase (HO) inducers are endowed with potent antidiabetic and insulin sensitizing effects besides their ability to suppress immune/inflammatory response [31]. Importantly, the HO system abates inflammation through several mechanisms including the suppression of macrophage-infiltration and abrogation of oxidative/inflammatory transcription factors like NF-κB, JNK, and activating protein-1 [31]. Thus, HO system could be explored in the search for novel remedies against T2D and its complications.

Ferrannini et al. proposed using fasting α-HB and L-GPC levels as new biomarkers to help predict dysglycemia and T2D [14, 24]. Both were detected in this study but postsurgery results do not bear out an improvement in insulin resistance based on these markers. α-HB is positively but L-GPC is negatively correlated with insulin resistance, so a postsurgery signature of improved insulin sensitivity would be expected to show a decrease of α-HB and an increase of L-GPC. Our findings showed an opposite pattern: α-HB was increased during the liquid weight-loss diet and then returned to near baseline levels after the surgery, while L-GPC levels showed significant postsurgery decrease across all three disease-surgery groups (Online Supplemental Table A4, Figure 1). There could be several reasons for this to occur, including the assumption that α-HB will drop after bariatric surgery is incorrect, or the 28-day time point is too soon to register a change. For the T2D subjects, there is the potential that metformin therapy also altered the baseline levels of α-HB and L-GPC. Future research is needed to clarify these findings.

Large increases in histidine derivatives were possibly due to altered gut microbiome composition or increased liver histidine-ammonia lyase activity. Histidine and several catabolites, such as imidazole propionate and urocanate isomers, both *trans*- and *cis*-urocanate, were significantly elevated ($P < 0.05$, $q < 0.00001$, including 100-fold + increases for *trans*-urocanate and *cis*-urocanate) in all three groups (Online Supplemental Table A4, Figure 4). Histidine is classified as an essential amino acid but gut bacteria can synthesize it, perhaps using precursors supplied by the human host. These markers may be an indication of changes in gut microbiome as the direct participation of the rat intestinal flora in the degradation of urocanate to imidazole propionate has been demonstrated previously [34].

Although the sample size was very small, these results suggested that histidine metabolites could also be important marker candidates to monitor metabolic changes associated with weight-loss surgery. Recently, Ryan and colleagues [35] found that vertical sleeve gastrectomy that led to weight loss and improvement of diabetes also resulted in changes in the gut bacteria. The researchers observed changes in several key bacterial groups that have been previously linked to the risk of T2D, and these changes were related to increase in circulating of bile acids that are known to bind to the nuclear receptor FXR. Interesting is the researches proposal that manipulating the gut bacteria might be another way to mimic the surgery [35].

On the other hand, urocanate is also formed in the liver by histidine-ammonia lyase (HAL) which converts histidine into urocanate and ammonia. Interestingly, HAL gene expression in hepatocytes can be stimulated by glucagon [36], so it is also possible that the increase of urocanate following surgery reflects a change in circulating glucagon levels. *trans*-Urocanate is converted to *cis*-urocanate by sunlight. *cis*-Urocanate has interesting immunosuppressive properties that are believed to help protect the skin during sun exposure and perhaps sites distal from the skin [37]. Little is known about imidazole propionate but it is a reported constituent of urine and has been proposed as a marker of intestinal dysfunction [38]. It may be useful to validate the ability of *trans*-urocanate, *cis*-urocanate, and imidazole propionate to serve as markers to monitor bariatric surgery in a larger independent cohort of patients and targeted quantitative assay. It will also be interesting to determine what, if any, utility such markers have for predicting long-term patient outcomes following surgery.

Comparing the postsurgery to the preoperation diet time point revealed 18 compounds that met the P and q-value cut-off criteria across all three disease-surgery groups (Online Supplemental Table A5). Thirteen were increased postsurgery samples relative to the samples collected at the preoperation diet time point and *trans*-urocanate, *cis*-urocanate, and pyroglutamylvaline displayed 100-fold or greater increases in nearly all of the groups.

Ascorbate and 1-linolenoylglycerol showed the greatest reductions among the 5 compounds that decreased in postsurgery samples relative to preoperation diet samples following surgery, but these reductions could also reflect altered gut absorption of these vitamins in addition to their consumption via the quenching of reactive oxygen species.

There were 29 additional compounds that represented $P < 0.05$ in all groups but did not reach $q < 0.05$ for all of the disease-surgery combinations. Histidine and several catabolites, such as imidazole propionate and urocanate isomers, were increased in T2D patients and the urocanate isomers were also likewise increased in nondiabetic patients after surgery (Online Supplemental Tables A4 and A5). Again, these results suggest that histidine metabolites could be important markers to monitor metabolic changes associated with weight-loss surgery.

4. Conclusions

Global metabolomic analysis was used to evaluate the changes occurring in nondiabetic and T2D patients experiencing either less extreme sleeve gastrectomy or a full gastric bypass. This study allowed gaining insights into the metabolic changes during both the preoperation weight-loss diet and early postsurgery recovery that accompany bariatric surgery.

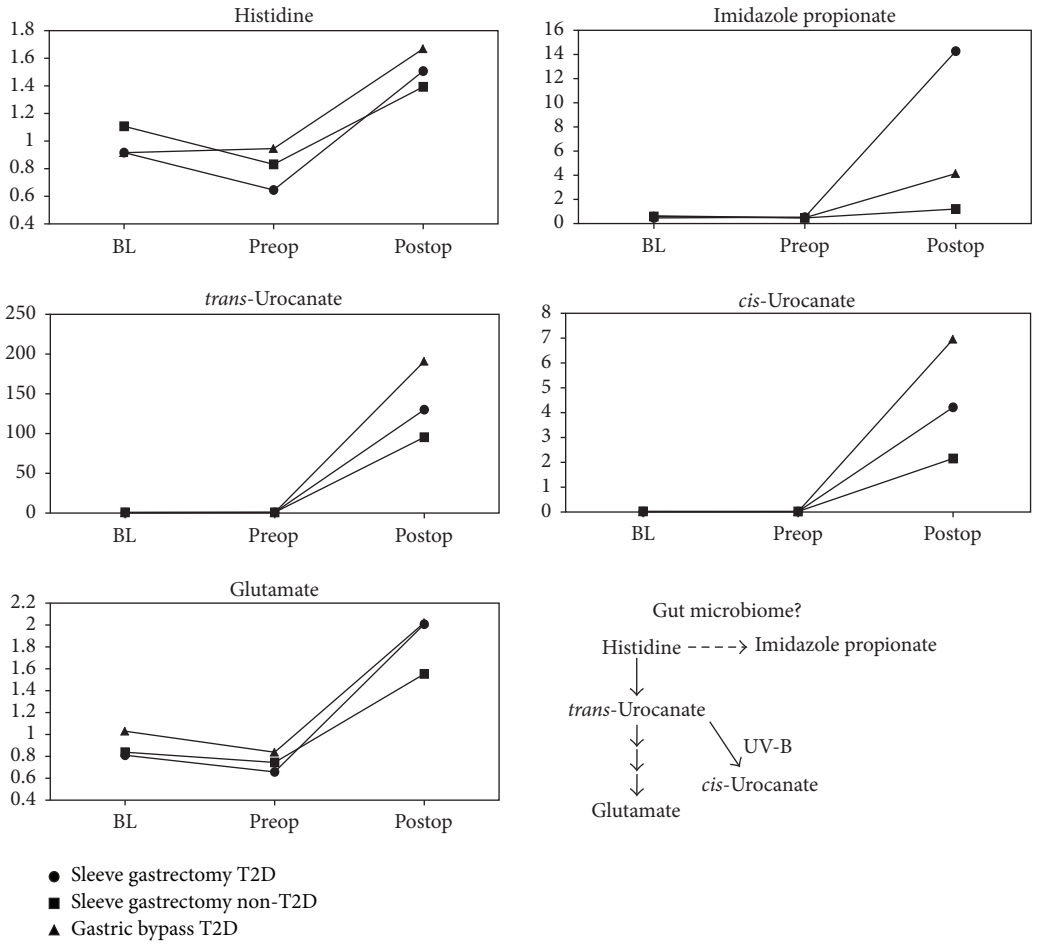

Figure 4: Postsurgery increase in histidine derivatives. All shown metabolites meet the conservative criteria of $P < 0.05$ and an estimated false discovery rate of less than 5% ($q < 0.05$).

To identify metabolic changes that were conserved across nondiabetic and T2D patients and different bariatric surgery procedures—sleeve gastrectomy (SG) versus gastric bypass (GB)—the metabolomic data collected for each disease-surgery combination were filtered according to statistical cut-offs for P value ($P < 0.05$) and to establish an estimated false discovery rate of less than 5% ($q < 0.05$).

It is important to point out that, despite age and sex difference, T2D status or bariatric surgery procedure, and coexistence of other associated diseases, all patients demonstrated striking similarity in major metabolome changes associated with preoperation weight-loss diet and bariatric surgery itself.

The preoperation weight-loss diet was associated with a strong lipid metabolism signature related to triglyceride hydrolysis, fatty acid oxidation, and ketone formation.

Diverse changes across a variety of metabolic areas were observed after bariatric surgery. Glucose metabolism via glycolytic and nonglycolytic pathways appeared to share a similar response across all patients regardless of baseline T2D status or the bariatric surgery procedure. Glycolysis pathway appeared to be suppressed and perhaps led to an accumulation of the TCA cycle components: malate and fumarate. Glucose derivatives in the pentose phosphate pathway were elevated following surgery. Such increases might indicate a greater demand for pentose sugars and NADPH and the redirection of glucose-6-phosphate away from glycolysis.

Increased heme levels were a likely sign of improved antioxidant defense via the action of heme oxygenase and liver function through increased heme biosynthesis in the liver. The increased availability of glutathione precursors suggested a greater capacity to synthesize glutathione. The simultaneous postsurgery disappearance of vitamin C and surge in oxidative stress markers such as allantoin and cysteine-glutathione disulfide suggest that micronutrient status should be monitored and supported by nutritional supplementation. This initial study provided a broad understanding of how metabolism changed globally in morbidly obese subjects following weight-loss surgery. Future serum metabolomic profiling studies focusing on baseline and 28 days (or other) after surgery with a greater number of patients in each group might help to further resolve differences between diabetic and nondiabetic patients. Additionally, profiling of baseline and postsurgery fecal samples might provide a more focused manner to interrogate changes associated with gut and microbiome function. Finally, the significance of this

study lays in the exploration of future treatments for obesity and T2D that can mimic bariatric surgery weight loss and improvement and resolution of T2D.

Conflict of Interests

The authors declare that they have no competing interests or other interests that might be perceived to influence the results and/or discussion reported in this paper.

Acknowledgments

The authors acknowledge research support and funding they have received from the Department of Surgery, Thomas Jefferson University Hospital, Philadelphia, PA, relevant to the work described. This work was funded by the Robert Saligman Charitable Trust.

References

[1] *National Diabetes Statistics Report: Estimates of Diabetes and Its Burden in the United States*, Department of Health and Human Services, US Centers for Disease Control and Prevention, Atlanta, Ga, USA, 2014.

[2] S. Klein, A. Ghosh, P. Y. Cremieux, S. Eapen, and T. J. McGavock, "Economic impact of the clinical benefits of bariatric surgery in diabetes patients with BMI $\geq$ 35 kg/m^2," *Obesity (Silver Spring)*, vol. 19, pp. 581–587, 2011.

[3] E. S. Ford, D. F. Williamson, and S. Liu, "Weight change and diabetes incidence: findings from a national cohort of US adults," *American Journal of Epidemiology*, vol. 146, no. 3, pp. 214–222, 1997.

[4] G. A. Colditz, W. C. Willett, A. Rotnitzky, and J. E. Manson, "Weight gain as a risk factor for clinical diabetes mellitus in women," *Annals of Internal Medicine*, vol. 122, no. 7, pp. 481–486, 1995.

[5] N. T. Nguyen, X.-M. T. Nguyen, J. Lane, and P. Wang, "Relationship between obesity and diabetes in a US adult population: findings from the national health and nutrition examination survey, 1999–2006," *Obesity Surgery*, vol. 21, no. 3, pp. 351–355, 2011.

[6] *Obesity Data*, National Health and Nutrition Examination Survey (NHANES), Centers for Disease Control and Prevention, National Center for Health Statistics (NCHS), 2014.

[7] E. A. Finkelstein, J. G. Trogdon, J. W. Cohen, and W. Dietz, "Annual medical spending attributable to obesity: payer-and service-specific estimates," *Health Affairs*, vol. 28, no. 5, pp. w822–w831, 2009.

[8] R. R. Wing, R. Koeske, L. H. Epstein, M. P. Nowalk, W. Gooding, and D. Becker, "Long-term effects of modest weight loss in type II diabetic patients," *Archives of Internal Medicine*, vol. 147, no. 10, pp. 1749–1753, 1987.

[9] W. J. Pories, M. S. Swanson, K. G. MacDonald et al., "Who would have thought it? An operation proves to be the most effective therapy for adult-onset diabetes mellitus," *Annals of Surgery*, vol. 222, no. 3, pp. 339–352, 1995.

[10] J. B. Dixon, P. E. O'Brien, J. Playfair et al., "Adjustable gastric banding and conventional therapy for type 2 diabetes," *Journal of the American Medical Association*, vol. 299, no. 3, pp. 316–323, 2008.

[11] P. R. Schauer, S. Ikramuddin, W. Gourash, R. Ramanathan, and J. Luketich, "Outcomes after laparoscopic Roux-en-Y gastric bypass for morbid obesity," *Annals of Surgery*, vol. 232, no. 4, pp. 515–529, 2000.

[12] H. Buchwald, R. Estok, K. Fahrbach et al., "Weight and type 2 diabetes after bariatric surgery: systematic review and meta-analysis," *American Journal of Medicine*, vol. 122, no. 3, pp. 248–256, 2009.

[13] J. B. Dixon, P. E. O'Brien, J. Playfair et al., "Adjustable gastric banding and conventional therapy for type 2 diabetes: a randomized controlled trial," *The Journal of the American Medical Association*, vol. 299, no. 3, pp. 316–323, 2008.

[14] W. L. Lowe Jr. and J. R. Bain, "'Prediction is very hard, especially about the future': new biomarkers for type 2 diabetes?" *Diabetes*, vol. 62, no. 5, pp. 1384–1385, 2013.

[15] N. Psychogios, D. D. Hau, J. Peng et al., "The human serum metabolome," *PLoS ONE*, vol. 6, no. 2, Article ID e16957, 2011.

[16] J. R. Bain, R. D. Stevens, B. R. Wenner, O. Ilkayeva, D. M. Muoio, and C. B. Newgard, "Metabolomics applied to diabetes research: moving from information to knowledge," *Diabetes*, vol. 58, no. 11, pp. 2429–2443, 2009.

[17] C. B. Newgard, "Interplay between lipids and branched-chain amino acids in development of insulin resistance," *Cell Metabolism*, vol. 15, no. 5, pp. 606–614, 2012.

[18] T. J. Wang, M. G. Larson, R. S. Vasan et al., "Metabolite profiles and the risk of developing diabetes," *Nature Medicine*, vol. 17, no. 4, pp. 448–453, 2011.

[19] P. Wurtz, P. Soininen, A. J. Kangas et al., "Branched-chain and aromatic amino acids are predictors of insulin resistance in young adults," *Diabetes Care*, vol. 36, no. 3, pp. 648–655, 2013.

[20] P. Würtz, M. Tiainen, V. P. Mäkinen et al., "Circulating metabolite predictors of glycemia in middle-aged men and women," *Diabetes Care*, vol. 35, pp. 1749–1756, 2012.

[21] A. Floegel, N. Stefan, Z. Yu et al., "Identification of serum metabolites associated with risk of type 2 diabetes using a targeted metabolomic approach," *Diabetes*, vol. 62, no. 2, pp. 639–648, 2013.

[22] S. E. Mccormack, O. Shaham, M. A. Mccarthy et al., "Circulating branched-chain amino acid concentrations are associated with obesity and future insulin resistance in children and adolescents," *Pediatric Obesity*, vol. 8, no. 1, pp. 52–61, 2013.

[23] W. E. Gall, K. Beebe, K. A. Lawton et al., "α-hydroxybutyrate is an early biomarker of insulin resistance and glucose intolerance in a nondiabetic population," *PLoS ONE*, vol. 5, no. 5, Article ID e10883, 2010.

[24] E. Ferrannini, A. Natali, S. Camastra et al., "Early metabolic markers of the development of dysglycemia and type 2 diabetes and their physiological significance," *Diabetes*, vol. 62, no. 5, pp. 1730–1737, 2013.

[25] J. D. Storey and R. Tibshirani, "Statistical significance for genomewide studies," *Proceedings of the National Academy of Sciences of the United States of America*, vol. 100, no. 16, pp. 9440–9445, 2003.

[26] A. P. Morris, B. F. Voight, T. M. Teslovich et al., "Large-scale association analysis provides insights into the genetic architecture and pathophysiology of type 2 diabetes," *Nature Genetics*, vol. 44, no. 9, pp. 981–990, 2012.

[27] J. L. Vassy, N. H. Durant, E. K. Kabagambe et al., "A genotype risk score predicts type 2 diabetes from young adulthood: the CARDIA study," *Diabetologia*, vol. 55, no. 10, pp. 2604–2612, 2012.

[28] S. L. Faria, O. P. Faria, M. D. A. Cardeal, and M. K. Ito, "Effects of a very low calorie diet in the preoperative stage of bariatric surgery: a randomized trial," *Surgery for Obesity and Related Diseases*, vol. 11, no. 1, pp. 230–237, 2015.

[29] V. R. G. da Silva, E. A. M. Moreira, D. Wilhelm-Filho et al., "Proinflammatory and oxidative stress markers in patients submitted to Roux-en-Y gastric bypass after 1 year of follow-up," *European Journal of Clinical Nutrition*, vol. 66, no. 8, pp. 891–899, 2012.

[30] S. P. Donadelli, M. V. M. Junqueira-Franco, C. A. de Mattos Donadelli et al., "Daily vitamin supplementation and hypovitaminosis after obesity surgery," *Nutrition*, vol. 28, no. 4, pp. 391–396, 2012.

[31] J. F. Ndisang, "Role of heme oxygenase in inflammation, insulin-signalling, diabetes and obesity," *Mediators of Inflammation*, vol. 2010, Article ID 359732, 18 pages, 2010.

[32] R. Wang-Sattler, Z. Yu, C. Herder et al., "Novel biomarkers for pre-diabetes identified by metabolomics," *Molecular Systems Biology*, vol. 8, article 615, 2012.

[33] C. Handschin, J. Lin, J. Rhee et al., "Nutritional regulation of hepatic heme biosynthesis and porphyria through PGC-1alpha," *Cell*, vol. 122, no. 4, pp. 505–515, 2005.

[34] A. V. Emes and H. Hassall, "The degradation of L-histidine in the rat. The formation of imidazolylpyruvate, imidazolyl-lactate and imidazolylpropionate," *Biochemical Journal*, vol. 136, no. 3, pp. 649–658, 1973.

[35] K. K. Ryan, V. Tremaroli, C. Clemmensen et al., "FXR is a molecular target for the effects of vertical sleeve gastrectomy," *Nature*, vol. 509, no. 7499, pp. 183–188, 2014.

[36] G. Alemán, V. Ortíz, E. Langley, A. R. Tovar, and N. Torres, "Regulation by glucagon of the rat histidase gene promoter in cultured rat hepatocytes and human hepatoblastoma cells," *The American Journal of Physiology—Endocrinology and Metabolism*, vol. 289, no. 1, pp. E172–E179, 2005.

[37] N. K. Gibbs and M. Norval, "Urocanic acid in the skin: a mixed blessing," *Journal of Investigative Dermatology*, vol. 131, no. 1, pp. 14–17, 2011.

[38] C. Van der Heiden, S. K. Wadman, P. K. De Bree, and E. A. K. Wauters, "Increased urinary imidazolepropionic acid, n-acetylhistamine and other imidazole compounds in patients with intestinal disorders," *Clinica Chimica Acta*, vol. 39, no. 1, pp. 201–214, 1972.

Hindawi Publishing Corporation
Journal of Diabetes Research
Volume 2016, Article ID 5490258, 7 pages
http://dx.doi.org/10.1155/2016/5490258

Review Article

The Stricter the Better? The Relationship between Targeted HbA_{1c} Values and Metabolic Control of Pediatric Type 1 Diabetes Mellitus

Marcin Braun,[1] Bartlomiej Tomasik,[1] Ewa Wrona,[1] Wojciech Fendler,[1] Przemyslawa Jarosz-Chobot,[2] Agnieszka Szadkowska,[1] Agnieszka Zmysłowska,[1] Jayne Wilson,[3] and Wojciech Mlynarski[1]

[1]*Department of Pediatrics, Oncology, Hematology and Diabetology, Medical University of Lodz, Sporna 36/50, 91-738 Lodz, Poland*
[2]*Department of Pediatrics, Endocrinology and Diabetology, Medical University of Silesia, Medykow 16, 40-752 Katowice, Poland*
[3]*Cancer Research UK Clinical Trials Unit, School of Cancer Sciences, University of Birmingham, Vincent Drive, Edgbaston, Birmingham B15 2TT, UK*

Correspondence should be addressed to Wojciech Mlynarski; wojciech.mlynarski@umed.lodz.pl

Received 7 September 2015; Accepted 14 December 2015

Academic Editor: Francisco J. Ruperez

Introduction. It remains unclear how HbA_{1c} recommendations influence metabolic control of paediatric patients with type 1 diabetes mellitus. To evaluate this we compared reported HbA_{1c} with guideline thresholds. *Materials and Methods*. We searched systematically MEDLINE and EMBASE for studies reporting on HbA_{1c} in children with T1DM and grouped them according to targeted HbA_{1c} obtained from regional guidelines. We assessed the discrepancies in the metabolic control between these groups by comparing mean HbA_{1c} extracted from each study and the differences between actual and targeted HbA_{1c}. *Results*. We included 105 from 1365 searched studies. The median (IQR) HbA_{1c} for the study population was 8.30% (8.00%–8.70%) and was lower in "6.5%" than in "7.5%" as targeted HbA_{1c} level (8.20% (7.85%–8.57%) versus 8.40% (8.20%–8.80%); $p = 0.028$). Median difference between actual and targeted HbA_{1c} was 1.20% (0.80%–1.70%) and was higher in "6.5%" than in "7.5%" (1.70% (1.30%–2.07%) versus 0.90% (0.70%–1.30%), resp.; $p < 0.001$). *Conclusions*. Our study indicates that the 7.5% threshold results in HbA_{1c} levels being closer to the therapeutic goal, but the actual values are still higher than those observed in the "6.5%" group. A meta-analysis of raw data from national registries or a prospective study comparing both approaches is warranted as the next step to examine this subject further.

1. Introduction

Despite the crucial role of HbA_{1c} in the management of diabetes, substantial differences among diabetic associations regarding targeted levels of this parameter are still present. The stricter approach is represented by the European Society of Cardiology (ESC) and recommends 6.5% (48 mmol/mol) of HbA_{1c} [1], whilst the International Society for Pediatric and Adolescent Diabetes (ISPAD), International Diabetes Federation (IDF), and American Diabetes Association (ADA) advocate 7.5% (58 mmol/mol) as the valid target of HbA_{1c} [2, 3].

The Hvidøre Study Group on Childhood Diabetes observed significant differences in average HbA_{1c} levels among 21 large pediatric diabetes centres from 17 countries in Europe, Japan, and North America [4]. The authors of this study suggested that there might be several reasons for these discrepancies. One possible explanation might be bound to guideline values of desirable HbA_{1c} level that differ depending on the diabetic association.

Both the Diabetes Control and Complications Trial (DCCT) and the Epidemiology of Diabetes Interventions and Complications Study (EDIC) have shown that early intensive therapy of patients with type 1 diabetes results in better metabolic control [5, 6]. The differences in metabolic control between conventional therapy and functional intensive insulin treatment cohorts were directly correlated with strikingly different treatment outcomes (e.g., any cardiovascular

disease event was reduced by 42% in the intensive metabolic control arm). Taking into consideration the results of DCCT and EDIC studies, if the difference among targeted HbA_{1c} levels of 1% was related to a different metabolic control, this would have an impact on long-term complications of diabetes mellitus. Recent cohort studies have shown that metabolic control of patients with T1DM has significantly improved during the last decade and better metabolic control resulted in superior outcome which supports aforementioned observations [7, 8].

In view of the controversy of the role of HbA_{1c} guidelines and the fact that, in majority of cases, they are set arbitrarily, we have conducted this study to examine the influence of HbA_{1c} targets on metabolic control of type 1 diabetes in pediatric population [9].

2. Materials and Methods

2.1. Guideline Identification. The data on guideline HbA_{1c} values in each country or region at the time of the study were obtained from official websites of national/regional diabetic associations. In case of lack of information consultants were contacted by phone or e-mail.

2.2. Reported HbA_{1c} Levels: Data Sources and Searches. Publications which reported HbA_{1c} levels were sought using systematic review techniques. A systematic search was undertaken using terms for pediatric/children/juvenile diabetes mellitus type 1, glycated haemoglobin A_{1c}, and insulin-based therapy in the following databases: OVID MEDLINE, EMBASE, Cochrane Database of Systematic Reviews (CDSR), National Institute for Health and Clinical Excellence (NICE) database, Scottish Intercollegiate Guidelines (SIGN) database, Database of Reviews of Effects (DARE), and Health Technology Assessment (HTA/NHS EED). The searches were conducted between 1st January 2008 and 26th August 2013, with no language restrictions. We searched for studies with T1DM pediatric patients (≤18 years) being treated for at least 1 year. The patients had to have at least one HbA_{1c} level measurement taken after December 2007. In cases of interventional studies, we utilized the HbA_{1c} levels recorded prior to the planned intervention. We excluded studies with less than 50 participants. The study design and search strategy are available in the Supporting Information, available online at http://dx.doi.org/10.1155/2016/5490258.

2.3. Study Selection. Two reviewers independently assessed searched papers for eligibility: firstly by screening titles and abstracts and secondly by examining full-text papers of studies included after screening. The same strategy was used for both data bits' extraction. All disagreements were resolved by the discussion between reviewers.

In order to reduce bias caused by overlapping studies we contacted corresponding authors of papers, which we found to be based on common national diabetic registries or which had at least one common author or when the research was done in the same institution. When we detected that the results of several papers overlapped each other and we could not obtain separated data, we chose the study with the largest sample.

2.4. Data Extraction. Data were extracted onto a predefined form. HbA_{1c} levels representing populations of each study were calculated by combining the mean values for all investigated groups. If applicable, all values were transformed and presented as percentage of the total haemoglobin level by using standard HbA_{1c} units' converter [10]. HbA_{1c} measurements had to be performed using high-performance liquid chromatography meeting the DCCT standard. For interventional studies HbA_{1c} values were extracted before implementation of preplanned intervention.

2.5. Data Synthesis and Statistical Analysis. Subgroup analyses were undertaken according to the following: gross domestic product (GDP; high-income country is defined to have a GDP above US$12,746 in 2013) [11], number of patients in each study, age, duration of type 1 diabetes mellitus, prevalence of acute complications (hypoglycaemia and ketoacidosis), and type of therapy (continuous subcutaneous insulin infusion and multiple daily injection). If studies were conducted across multiple countries we checked whether guideline values were homogenous among them and allocated to appropriate groups. If targeted values were different in individual studies and we could not extract separate data for each country we excluded such studies from the quantitative analyses. In order to compare compliance, the difference between actual and targeted guideline HbA_{1c} value was calculated for each study (ΔHbA_{1c}).

Nominal variables were given as numbers with appropriate percentage whereas continuous variables were given as medians with interquartile ranges (IQR). For pairwise comparisons of continuous variables, the Mann-Whitney U (MWU) test was used. For multigroup comparisons Kruskal-Wallis one-way analysis of variance with additional post hoc tests within subgroups was used. Correlations were assessed using Spearman's rank correlation coefficient. Multivariate analyses were made using linear regression (GLM) weighted by the logarithm of number of participants in included studies. The multivariate model was fitted including all the variables that had reached statistical significance in the univariate analyses. Meta-analysis for comparison of adherence to guideline values was conducted using differences between mean and guideline HbA_{1c} levels. I^2 values to assess the heterogeneity between studies were calculated and results above 50% were considered as being of high heterogeneity. Statistical significance was set at $p \leq 0.05$; 95% confidence intervals were calculated. Statistical analysis was performed with usage of STATISTICA 10.0 software (StatSoft, Tulsa, OK, USA).

3. Results

3.1. Studies' Selection. The systematic searches for published HbA_{1c} levels yielded 1365 records. Eight hundred thirty of them were excluded after screening by title and abstract and further 77 were excluded due to duplication. Three hundred and fifty-three papers were excluded after full-text paper analysis. One hundred five studies were included for the final analyses, involving 91393 patients. In 25 studies only the abstract was available. The flowchart for the study selection

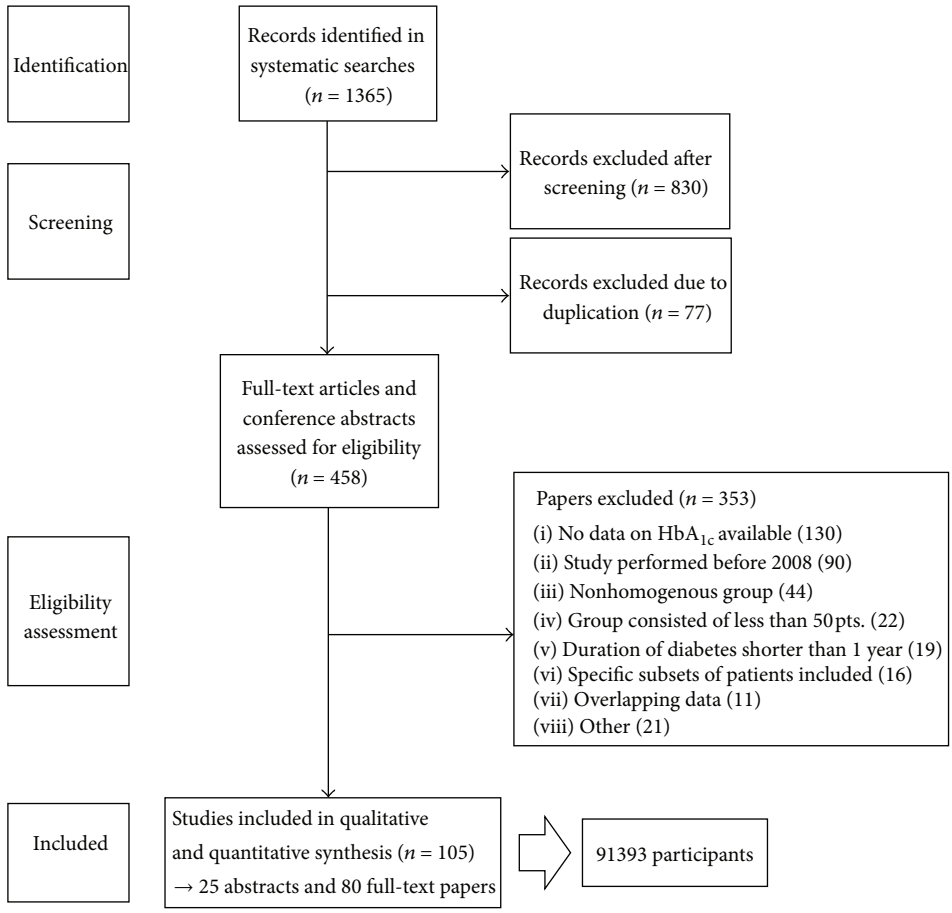

Figure 1: Flowchart for studies' selection process.

process with detailed reasons for exclusion is presented in Figure 1.

3.2. Studies' Characteristics and Allocation of Countries and Regions regarding Guideline Values. Of the 105 studies yielding HbA_{1c} level data 47 (44.76%) were cross-sectional, 40 (38.10%) were cohort, 9 (8.57%) were case-series or case-control, and 9 (8.57%) were interventional (including 5 randomized clinical trials). The eligible studies came from 18 countries (at least one country from Africa, Asia, Australia, Europe, South America, and North America). Forty-three (40.95%) studies were from European Union (21 of them (48.84%) were represented by 3 countries—UK (9 studies), Poland (6 studies), and Germany (6 studies)), whilst 39 (37.14%) were from the USA. Fifty-five (52.38%) studies were allocated to the group of "7.5% (58 mmol/mol)" as guideline HbA_{1c} value; 42 (40.00%) were allocated to the group of "6.5% (48 mmol/mol)." The guideline values from remaining studies (7.62%) were not homogenous and thus we excluded them from further analyses (the complete data for comparisons among all three study groups are available in Supporting Information). Ninety-five (90.48%) studies were conducted in high-income countries. The smallest study enrolled 50 patients [12], whilst the biggest one included 42881 individuals (cross-sectional study from Germany, Austria, and Switzerland) [13]. The median number of enrolled patients was 146 (IQR: 90–368). Median age within the studies was 12.79 (IQR: 11.60–13.77) years and median duration of diabetes was 5.20 (IQR: 3.90–6.30) years. In 26 studies (24.76%) patients were treated more frequently with MDI; in 30 (28.57%) of studies CSII was the preferred method of therapy. Only in 5 (4.76%) and in 8 (7.62%) of included studies did acute complications of diabetes mellitus (hypoglycaemia and diabetic ketoacidosis, resp.) occur more frequently in comparison to the prevalence reported in the literature. A detailed table with studies' characteristics and references can be seen in Supporting Information.

3.3. Comparison of HbA_{1c} Levels regarding HbA_{1c} Guideline Values. The median (IQR) HbA_{1c} level in the whole study population was 8.30% (IQR: 8.00%–8.70%) (67 (IQR: 63–72) mmol/mol). Median values for HbA_{1c} in groups regarding guideline values were significantly lower in "6.5" group than in "7.5" group and equalled 8.20% (IQR: 7.85%–8.57%; 66 (IQR: 62–70) mmol/mol) versus 8.40% (IQR: 8.20%–8.80%) (68 (IQR: 66–73) mmol/mol), respectively (MWU—$p = 0.028$, Figure 2(a); GLM—$p = 0.001$; beta for "6.5" group = −0.22 (95% CI: −0.34, −0.09)). This difference was significant in linear regression model with studies weighted by logarithm

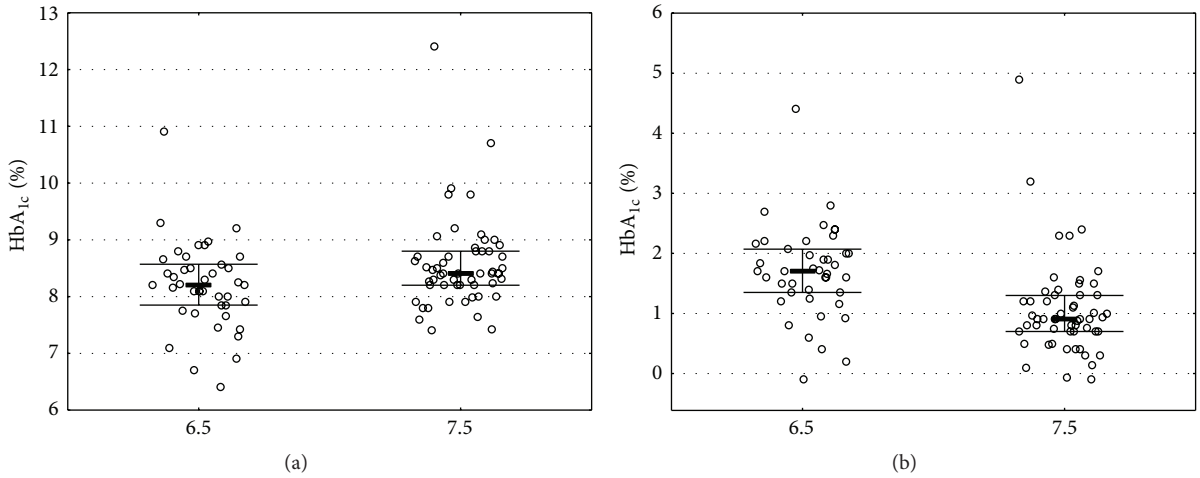

Figure 2: (a) Comparison for HbA_{1c} levels between regions of 6.5% and 7.5% as guideline values (MWU test, $p = 0.0162$). (b) Comparison of the difference between HbA_{1c} levels and guideline HbA_{1c} values between regions of 6.5% and 7.5% as guideline values (MWU test, $p < 0.0001$). Bolded line represents median; whiskers represent IQR.

from the number of patients ($p = 0.025$, beta for "6.5" group = −0.16 (95% CI: −0.29, −0.22)).

3.4. Comparison of the Difference between HbA_{1c} Levels and Guideline HbA_{1c} Values. The median ΔHbA_{1c} in the whole study population was 1.20% (IQR: 0.80%–1.70%). Median values for ΔHbA_{1c} in groups regarding guideline values were significantly higher in "6.5" group than in "7.5" group and equalled 1.70% (IQR: 1.30%–2.07%) versus 0.9% (IQR: 0.70%–1.30%) respectively (MWU—$p < 0.001$, Figure 2(b); GLM—$p < 0.001$; beta for "6.5" group = 0.40). The forest plots for meta-analysis of ΔHbA_{1c} are available in the Supporting Information.

3.5. Evaluation of the Effect of Other Variables on HbA_{1c} Level. Study design, publication type, percentage of patients with severe diabetic ketoacidosis or severe hypoglycaemia, type of therapy, GDP per capita, and number of patients did not have a significant impact on HbA_{1c} levels. HbA_{1c} values were significantly lower in countries from Europe (in comparison with the USA). We observed a positive correlation between HbA_{1c} levels and duration of type 1 diabetes and age of patients. All results for discussed comparisons are available in Table 1.

4. Discussion

Taking into consideration the debate regarding the role of HbA_{1c} guidelines and the fact that in majority of cases they are set arbitrarily, we decided to conduct this study to examine the impact of HbA_{1c} targets on metabolic control of type 1 diabetes in pediatric population [14]. Our work suggests that patients treated in centres with lower HbA_{1c} targets have better metabolic control despite being further from reaching their goal than patients from higher target countries. We found that the diabetic populations in countries with 6.5% (48 mmol/mol) as the targeted HbA_{1c} values are represented by actual median levels of HbA_{1c} of 0.2% lower than countries with 7.5% (58 mmol/mol) as targeted levels. Although the adherence was better in the centres with less strict aims of the therapy (median ΔHbA_{1c} 1.70% (1.30%–2.07%) versus 0.90% (0.70%–1.30%), resp.) the final outcome in terms of metabolic control was better in the more strict centres. We found also discrepancies between centres included in our study and this result tends to agree with the main observation of the Hvidøre Study Group [4].

The real reason for discrepancies between guideline levels for HbA_{1c} is likely to be linked to different aims and priorities in the management of diabetes [4, 15]. The teams, which set higher HbA_{1c} goals, are more concerned about risks of intensive therapy, such as hypoglycaemia. Although the previously strong association of low HbA_{1c} with severe hypoglycemia in young individuals with type 1 diabetes has substantially decreased in the last decade [16] this complication is one of the most common fatal acute diabetic complications [17]. Therefore the supporters of less strict metabolic control are willing to make concessions in order to avoid the risk. Higher HbA_{1c} values are also easier to accept and may lead to a better compliance. On the other hand, other teams focus on avoidance of hyperglycaemia, because they are devoted to minimalize the risk of long-term complications from the very first day after the diagnosis of diabetes mellitus. The crucial issue of this approach is to convince patients and their families to put an effort in pursuing stricter metabolic control [15, 18]. Additionally, since recently developed technologies including insulin pumps with low glucose suspend software reduce the risk of hypoglycaemia, the restricted goal is safely achievable [19, 20].

The differences in average HbA_{1c} levels among large diabetic centres have been the area of interest of researchers in pediatric diabetology for years [4, 15, 21–23]. The authors from the Hvidøre Study Group on Childhood Diabetes indicated several reasons, which could lead to discrepancies. The majority of these issues are relatively hard to assess in

Table 1: Univariate and multivariate linear model results for HbA_{1c} values regarding HbA_{1c} guideline groups (6.5% and 7.5%) and the other covariates. NA means not applied.

Variable	Groups	Number of studies included in analysis	p value from univariate analysis	p value from multivariate analysis with β parameter (95% CI)	The effect on HbA_{1c} level
HbA_{1c} targeted levels	6.5 (48 mmol/mol) versus 7.5 (58 mmol/mol)	97	0.028	<0.001 $\beta = -0.26$ (−0.40, −0.12)	Lower in "6.5% (48 mmol/mol) countries"
Publication type	Article versus abstract	97	0.967	NA	NA
Hypoglycemia	More versus less frequent	30	0.427	NA	NA
Diabetic ketoacidosis	More versus less frequent	26	0.261	NA	NA
Type of therapy	MDI versus CSII	56	0.249	NA	NA
Study design	Five groups	97	0.356	NA	NA
Location	Europe versus USA	82	0.022	NA	Lower in Europe
GDP per capita ($)	Continuous variable	97	0.127	NA	NA
Number of patients in the study	Continuous variable	97	0.985	NA	NA
Mean age in the study (years)	Continuous variable	93	0.016	0.001 $\beta = 0.29$ (0.12, 0.47)	Positive correlation ($r = 0.25$)
Mean duration of DM in the study (years)	Continuous variable	85	0.037	0.753 $\beta = -0.03$ (−0.20, −0.15)	Positive correlation ($r = 0.23$)

a robust way (e.g., the role of multidisciplinary approach, self-care behaviours, educational models, ethnic or cultural aspects, socioeconomic status, etc.) [24]. Recent findings suggest that the phenomenon of seasonal HbA_{1c} variability in schoolchildren could also affect the results of reported HbA_{1c} results [25]. According to Hvidøre Study Group different guideline values of HbA_{1c} among centres also appear to play a significant role in explaining the differences in metabolic outcomes among pediatric population [15]. The results of our study supports this hypothesis.

Although this is the first study that systematically examines the influence of different guideline HbA_{1c} values on the actual HbA_{1c} levels, it should be stated that our work has several limitations. The problem of overlapping populations in the enrolled studies was particularly hard to eliminate in our review. Although we tried to contact with the authors of the studies, in which such problem might have occurred, the response rate level was lower than 20%. Another issue which affects our study is the fact that more than a half of enrolled studies concerned several countries. Studies from United States of America constituted 37% of all included studies and studies from Poland, Germany, and United Kingdom constituted further 20% when considered together. Additionally it should be mentioned that we included both studies based on national registries (e.g., Germany and Austria or Sweden) and single centre studies. In the major analyses, which we are presenting in this report, we excluded 8 studies due to heterogenous HbA_{1c} guideline values. In our opinion such small number of studies is not representative and analysis of their results would be burdened with high risk of bias. Because we included studies of various designs, from which neither aimed directly to compare groups of different HbA_{1c} guidelines, we found linear regression model weighted by number of participants in each study as most appropriate for our comparisons. We present the results for all comparisons in the Supporting Information. Furthermore, our search was not restricted to studies that contained data on other variables that might have an impact on DMI control. Hence, the results on, for example, acute complications (ketoacidosis and hypoglycemia) were not fully covered in the included papers and our subgroup analysis should be treated with caution. Nevertheless we conducted the analyses on those aspects within representative studies. Only in 5 (4.76%) and in 8 (7.62%) of included studies hypoglycaemia and diabetic ketoacidosis occurred more frequently in comparison to the prevalence reported in the literature. Although this is an ecological study, with its inherent limitations (i.e., cause and effect cannot be proven and confounding factors cannot be eliminated) we attempted to strengthen the data used by employing systematic review techniques to identify and process the published data set that was used for HbA_{1c} levels. By using systematic review techniques for our searches we have attempted to reduce selection and publication biases and by using double data extraction we have reduced possible errors in data collection and analysis. Therefore our study is a robust piece of work for ascertaining the impact of

discrepancies between major diabetic associations regarding targeted HbA_{1c} levels in children with type 1 diabetes.

5. Conclusions

Our study shows that the targeted HbA_{1c} level plays an important role in terms of metabolic control in children with type 1 diabetes. The consequences of this observation should be discussed among health care professionals. Target values for HbA_{1c} levels for children and adolescents suffering from type 1 diabetes vary between countries and centres which, in the light of our study, affects metabolic control of the patients and may have an impact on long-term complications in the future. Our study provides a solid basis for rational discussion on the impact of guideline HbA_{1c} values on the metabolic control. According to our findings the "6.5% approach" results in better outcomes, but other factors such as multidisciplinary approach, self-care behaviours, educational models, ethnic or cultural aspects, socioeconomic status, and seasonal variability should be taken into consideration. In our opinion a metaregression of raw data from national registries is warranted as a next step to corroborate our results and finally ascertain the effect of HbA_{1c} guideline values on the metabolic control among children with type 1 diabetes mellitus.

Disclosure

This research received no specific grant from any funding agency in the public, commercial, or not-for-profit sectors.

Conflict of Interests

The authors declare that there is no duality of interest associated with this paper.

Authors' Contribution

Wojciech Mlynarski, Przemyslawa Jarosz-Chobot, Agnieszka Szadkowska, Agnieszka Zmysłowska, and Wojciech Fendler conceived this study. Marcin Braun, Bartlomiej Tomasik, and Ewa Wrona did the searches, selection of studies, data extraction, and statistical analysis. Wojciech Fendler contributed to statistical analysis. Jayne Wilson critically assessed the design and realization of the study. All authors critically reviewed various drafts of the paper, and all authors approved the final version. Wojciech Mlynarski is responsible for the integrity of the work as a whole. Marcin Braun, Bartlomiej Tomasik, and Ewa Wrona contributed equally.

References

[1] ESC Clinical Practice Guidelines, 2013, http://www.escardio.org/Guidelines-&-Education/Clinical-Practice-Guidelines/Diabetes-Pre-Diabetes-and-Cardiovascular-Diseases-developed-with-the-EASD.

[2] Global IDF/ISPAD Guideline for Diabetes in Childhood and Adolescence, 2011, http://www.idf.org/sites/default/files/Diabetes-in-Childhood-and-Adolescence-Guidelines.pdf.

[3] American Diabetes Association, "Standards of medical care in diabetes: children and adolescents," *Diabetes Care*, vol. 38, supplement 1, pp. S70–S76, 2015.

[4] T. Danne, H. B. Mortensen, P. Hougaard et al., "Persistent differences among centers over 3 years in glycemic control and hypoglycemia in a study of 3,805 children and adolescents with type 1 diabetes from the Hvidøre Study Group," *Diabetes Care*, vol. 24, no. 8, pp. 1342–1347, 2001.

[5] The Diabetes Control and Complications Trial Research Group, "The effect of intensive treatment of diabetes on the development and progression of long-term complications in insulin-dependent diabetes mellitus. The Diabetes Control and Complications Trial Research Group," *The New England Journal of Medicine*, vol. 329, pp. 977–986, 1993.

[6] D. M. Nathan, P. A. Cleary, J.-Y. C. Backlund et al., "Intensive diabetes treatment and cardiovascular disease in patients with type 1 diabetes," *The New England Journal of Medicine*, vol. 353, no. 25, pp. 2643–2653, 2005.

[7] K. Dovc, S. S. Telic, L. Lusa et al., "Improved metabolic control in pediatric patients with type 1 diabetes: a nationwide prospective 12-year time trends analysis," *Diabetes Technology and Therapeutics*, vol. 16, no. 1, pp. 33–40, 2014.

[8] D. M. Maahs, J. M. Hermann, S. N. DuBose et al., "Contrasting the clinical care and outcomes of 2,622 children with type 1 diabetes less than 6 years of age in the United States T1D Exchange and German/Austrian DPV registries," *Diabetologia*, vol. 57, no. 8, pp. 1578–1585, 2014.

[9] D. F. Stroup, J. A. Berlin, S. C. Morton et al., "Meta-analysis of observational studies in epidemiology: a proposal for reporting. Meta-analysis of Observational Studies in Epidemiology (MOOSE) group," *Journal of the American Medical Association*, vol. 283, no. 15, pp. 2008–2012, 2000.

[10] NSGP, International Federation of Clinical Chemistry (IFCC) Standardization of HbA1c, 2010, http://www.ngsp.org/docs/IFCCstd.pdf.

[11] Country and Lending Groups, 2015, http://data.worldbank.org/about/country-and-lending-groups#High_income.

[12] Juvenile Diabetes Research Foundation Continuous Glucose Monitoring Study Group, "Effectiveness of continuous glucose monitoring in a clinical care environment: evidence from the Juvenile Diabetes Research Foundation Continuous Glucose Monitoring (JDRF-CGM) trial," *Diabetes Care*, vol. 33, no. 1, pp. 17–22, 2010.

[13] T. R. Rohrer, P. Hennes, A. Thon et al., "Down's syndrome in diabetic patients aged <20 years: an analysis of metabolic status, glycaemic control and autoimmunity in comparison with type 1 diabetes," *Diabetologia*, vol. 53, no. 6, pp. 1070–1075, 2010.

[14] P. Jarosz-Chobot, J. Polańska, M. Myśliwiec et al., "Multicenter cross-sectional analysis of values of glycated haemoglobin (HbA1c) in Polish children and adolescents with long-term type 1 diabetes in Poland: PolPeDiab study group," *Pediatric Endocrinology, Diabetes, and Metabolism*, vol. 18, no. 4, pp. 125–129, 2012.

[15] P. G. F. Swift, T. C. Skinner, C. E. de Beaufort et al., "Target setting in intensive insulin management is associated with metabolic control: the Hvidoere Childhood Diabetes Study Group Centre Differences Study 2005," *Pediatric Diabetes*, vol. 11, no. 4, pp. 271–278, 2010.

[16] B. Karges, J. Rosenbauer, T. Kapellen et al., "Hemoglobin A1c levels and risk of severe hypoglycemia in children and young adults with type 1 diabetes from Germany and Austria: a trend

analysis in a cohort of 37,539 patients between 1995 and 2012," *PLoS Medicine*, vol. 11, no. 10, Article ID e1001742, 2014.

[17] A. Morimoto, Y. Onda, R. Nishimura, H. Sano, K. Utsunomiya, and N. Tajima, "Cause-specific mortality trends in a nationwide population-based cohort of childhood-onset type 1 diabetes in Japan during 35 years of follow-up: the DERI Mortality study," *Diabetologia*, vol. 56, no. 10, pp. 2171–2175, 2013.

[18] M. Boot, L. K. Volkening, D. A. Butler, and L. M. B. Laffel, "The impact of blood glucose and HbA_{1c} goals on glycaemic control in children and adolescents with Type 1 diabetes," *Diabetic Medicine*, vol. 30, no. 3, pp. 333–337, 2013.

[19] T. T. Ly, A. J. M. Brnabic, A. Eggleston et al., "A cost-effectiveness analysis of sensor-augmented insulin pump therapy and automated insulin suspension versus standard pump therapy for hypoglycemic unaware patients with type 1 diabetes," *Value in Health*, vol. 17, no. 5, pp. 561–569, 2014.

[20] M. Stenerson, F. Cameron, D. M. Wilson et al., "The impact of accelerometer and heart rate data on hypoglycemia mitigation in type 1 diabetes," *Journal of Diabetes Science and Technology*, vol. 8, no. 1, pp. 64–69, 2014.

[21] H. B. Mortensen and P. Hougaard, "Comparison of metabolic control in a cross-sectional study of 2,873 children and adolescents with IDDM from 18 countries," *Diabetes Care*, vol. 20, no. 5, pp. 714–720, 1997.

[22] L. Schwartz and D. Drotar, "Defining the nature and impact of goals in children and adolescents with a chronic health condition: a review of research and a theoretical framework," *Journal of Clinical Psychology in Medical Settings*, vol. 13, no. 4, pp. 390–402, 2006.

[23] H. A. Wolpert and B. J. Anderson, "Metabolic control matters: why is the message lost in the translation? The need for realistic goal-setting in diabetes care," *Diabetes Care*, vol. 24, no. 7, pp. 1301–1303, 2001.

[24] F. J. Cameron, T. C. Skinner, C. E. de Beaufort et al., "Are family factors universally related to metabolic outcomes in adolescents with type 1 diabetes?" *Diabetic Medicine*, vol. 25, no. 4, pp. 463–468, 2008.

[25] B. Mianowska, W. Fendler, A. Szadkowska et al., "HbA1c levels in schoolchildren with type 1 diabetes are seasonally variable and dependent on weather conditions," *Diabetologia*, vol. 54, no. 4, pp. 749–756, 2011.

Hindawi Publishing Corporation
Journal of Diabetes Research
Volume 2016, Article ID 5675739, 11 pages
http://dx.doi.org/10.1155/2016/5675739

Research Article

CCL2 Serum Levels and Adiposity Are Associated with the Polymorphic Phenotypes -2518A on CCL2 and 64ILE on CCR2 in a Mexican Population with Insulin Resistance

Milton-Omar Guzmán-Ornelas,[1,2] Marcelo Heron Petri,[1,3] Mónica Vázquez-Del Mercado,[1,4,5] Efraín Chavarría-Ávila,[1,2,6] Fernanda-Isadora Corona-Meraz,[1,2] Sandra-Luz Ruíz-Quezada,[2,7] Perla-Monserrat Madrigal-Ruíz,[1,2,4] Jorge Castro-Albarrán,[2] Flavio Sandoval-García,[1] and Rosa-Elena Navarro-Hernández[1,2,4,7]

[1] *Instituto de Investigación en Reumatología y del Sistema Musculo Esquelético, Centro Universitario de Ciencias de la Salud, Universidad de Guadalajara, Sierra Mojada No. 950, Colonia Independencia, 44340 Guadalajara, JAL, Mexico*
[2] *UDG-CA-701, Grupo de Investigación Inmunometabolismo en Enfermedades Emergentes (GIIEE), Centro Universitario de Ciencias de la Salud, Universidad de Guadalajara, Sierra Mojada No. 950, Colonia Independencia, 44340 Guadalajara, JAL, Mexico*
[3] *Translational Cardiology, Center for Molecular Medicine, Department of Medicine, Karolinska Institutet, L8:03, 17176 Stockholm, Sweden*
[4] *Departamento de Biología Molecular y Genómica, Centro Universitario de Ciencias de la Salud, Universidad de Guadalajara, Sierra Mojada No. 950, Colonia Independencia, 44340 Guadalajara, JAL, Mexico*
[5] *Servicio de Reumatología, División de Medicina Interna, Hospital Civil "Dr. Juan I. Menchaca", Universidad de Guadalajara, Salvador de Quevedo y Zubieta No. 750, 44340 Guadalajara, JAL, Mexico*
[6] *Departamento de Disciplinas Filosófico, Metodológico e Instrumentales, Centro Universitario de Ciencias de la Salud, Universidad de Guadalajara, Sierra Mojada No. 950, Colonia Independencia, 44340 Guadalajara, JAL, Mexico*
[7] *Departamento de Farmacobiología, Centro Universitario de Ciencias Exactas e Ingenierías, Universidad de Guadalajara, Boulevard Marcelino García Barragán No. 1421, 44430 Guadalajara, JAL, Mexico*

Correspondence should be addressed to Rosa-Elena Navarro-Hernández; rosa_elena_n@hotmail.com

Received 17 July 2015; Revised 5 October 2015; Accepted 15 October 2015

Academic Editor: Michal Ciborowski

Genetic susceptibility has been described in insulin resistance (IR). Chemokine (C-C motif) ligand-2 (CCL2) is overexpressed in white adipose tissue and is the ligand of C-C motif receptor-2 (CCR2). The *CCL2* G-2518A polymorphism is known to regulate gene expression, whereas the physiological effects of the *CCR2*Val64Ile polymorphism are unknown. The aim of the study is to investigate the relationship between these polymorphisms with soluble CCL2 levels (sCCL2), metabolic markers, and adiposity. In a cross-sectional study we included 380 Mexican-Mestizo individuals, classified with IR according to Stern criteria. Polymorphism was identified using PCR-RFLP/sequence-specific primers. Anthropometrics and metabolic markers were measured by routine methods and adipokines and sCCL2 by ELISA. The CCL2 polymorphism was associated with IR (polymorphic *A*+ phenotype frequencies were 70.9%, 82.6%, in individuals with and without IR, resp.). Phenotype carriers CCL2 (*A*+) displayed lower body mass and fat indexes, insulin and HOMA-IR, and higher adiponectin levels. Individuals with IR presented higher sCCL2 compared to individuals without IR and was associated with CCR2 (*Ile*+) phenotype. The double-polymorphic phenotype carriers (*A*+/*Ile*+) exhibited higher sCCL2 than double-wild-type phenotype carriers (*A*−/*Ile*−). The present findings suggest that sCCL2 production possibly will be associated with the adiposity and polymorphic phenotypes of *CCL2* and *CCR2*, in Mexican-Mestizos with IR.

1. Introduction

The insulin resistance (IR) presents many subclinical manifestations, characterized by alterations in lipids and carbohydrates metabolism at different levels. Most of these changes is due to a low-grade systemic chronic inflammation [1, 2]. Adipose tissue is the primary anatomical site where the disease takes place. In early stage, this tissue became inflamed with the following pathological mechanism: first, monocytes migrate to adipose tissue, these cells express high levels of C-C motif receptor 2 (CCR2) and release monocyte chemoattractant protein-1 (MCP-1), also known as chemokine (C-C motif) ligand 2 (CCL2). This chemokine can promote further local inflammation and/or acts in paracrine way. The signaling through CCR2 may polarize the monocytes to M1 macrophages; these cells present a proinflammatory profile. Nevertheless, CCL2-CCR2 interaction is known to regulate continuous migration of monocytes to adipose tissue [3–5].

CCL2 is produced in soluble form by monocytes and macrophages and binds with high affinity to the CCR2 receptor. The later one is constitutively expressed in monocytes and its levels decrease as it differentiate into macrophages [4].

The human *CCL2* gene is located on chromosome 17q11.2 [6, 7]. It has two remote kappa B binding sites known as A1 (-2640/-2632) and A2 (−2612/−2603) that regulates the transcription of *CCL2* gene. Whereas the *CCR2* belongs to the family of seven transmembrane-spanning receptors that are coupled to heterotrimeric G proteins, the gene is located on the chromosome 3p21 within a cluster of chemokine receptor genes [7, 8].

The IR is considered a multifactor and polygenic disease; nevertheless, it has not determine the environmental and genetic factors contribution. In this context the study of candidate genes to make a contribution in clarifying this point is important. It has been reported that single nucleotide polymorphisms (SNP) in *CCL2* and *CCR2* are related with IR, G-2518A (rs 1024611), and Val64Ile (rs 17998649), respectively. The SNP of *CCL2* is located at 85 base pairs (bp) of remote kappa B binding site A2, while in *CCR2* gene, the SNP is conservative and the amino acid change (Val>Ile) takes place in the first transmembrane domain. This change decreases the affinity CCL2 binding, since the join of CCL2 with CCR2 receptor is through the second transmembrane domain [9–11].

Clinical phenotype has been described with these polymorphisms; type 2 diabetes mellitus (T2DM), cardiometabolic risk factors, obesity indexes, and insulin secretion association were found [12]. Interestingly, another study failed to show effect of this polymorphism in adipokines levels in patients with essential hypertension and T2DM [13]. Studies in animal models were performed to demonstrate the functional effect of these polymorphisms, but the results were not conclusive [14].

With this in mind, the aim of this study is to describe the presence of polymorphism of *CCL2* and *CCR2* in a population with IR, compared to healthy subjects, and to elucidate the clinical/metabolic features that these polymorphisms may present.

2. Material and Methods

2.1. Subjects' Assessment. In this cross-sectional study, a total of 380 nonrelated Mexican-Mestizos (i.e., an individual that were born in Mexico, with a Spanish last name and a family history of Mexican ancestors for at least three generations), and aged 20–69 years, were recruited from population of Western Mexico and classified according to Stern criteria in two groups: group 1 individuals with IR, if any of the following conditions were met: HOMA-IR > 4.65 or BMI > 27.5 kg/m^2 and HOMA-IR > 3.6, and group 2 individuals without IR, therefore negative for those who did not meet the above conditions (i.e., HOMA-IR ≤ 4.65 or BMI ≤ 27.5 kg/m^2 and HOMA-IR ≤ 3.60) [15]. Inclusion criteria for the study were considered as follows: individuals who at the time of the study did not present glucose intolerance, infectious diseases, hypertension, history of cardiovascular disease, malignancy, and renal and metabolic diseases such as T2DM. The subjects were questioned and denied any medication or weight change at least 3 weeks.

2.2. Ethics Conduct. Before enrolment, participants were informed about the study and signed a consent form following the Helsinki declaration guidelines, and the institutional (Guadalajara University) review boards' committees ensured appropriate ethical and biosecurity conduct [16].

2.3. Medical History and Physical Examination. All individuals who fulfil inclusion criteria were clinically evaluated by a physician who performed a complete medical history and assessment of general health status and vital signs were included: blood pressure (executed 3 times with the subject in the sitting position and relaxing for 15 minutes before the measurement), heart and respiratory rate, and body temperature.

2.4. Body Fat Storage Measurements. We evaluated the following body measurements: height, measured to the nearest 1 mm by using a stadiometer (Seca GmbH & Co. KG. Hamburg, Germany), weight, body mass index (BMI), and total body fat, determined by using bioelectrical impedance analysis (TANITA TBF304.Tokio, JPN) to the nearest 0.1 kg. Waist and hip circumferences where measured to the nearest 0.1 cm by using an anthropometric fiberglass tape (GULICK length 0–180 cm precision ±1 mm; USA) following the procedures recommended by the anthropometric indicators measurement guide [17, 18]. We calculated the waist-hip ratio [19] [WHR = waist (cm)/hip (cm)], body fat ratio [BFR = body fat mass (kg)/height^2 (m^2)], and waist to height ratio [WHtR = waist (cm)/height (cm)], as indicators of adiposity [20, 21].

2.5. Laboratory Techniques and Procedures. Individuals included in the study were fasting 12 hours before the blood samples were taken, after allowing them to clot at room temperature; then the blood was centrifuged at 1509 RCF (Rotanta 460R, Andreas Hettich GmbH & Co. KG) for 10 minutes at 20°C. Serum was collected and stored at −86°C until further analysis. We quantified the serum concentration of C reactive protein (CRP, with a limit of detection of 0.15 mg/L), basal glucose, lipid profile that included triglycerides, total cholesterol, HDLc, LDLc, and VLDLc (high, low, and very low density lipoprotein cholesterol, resp.), and apolipoproteins A1 and B (Apo-A1 and Apo-B, Randox Laboratories 55 Diamond Road, Crumlin Co. Antrim, Northern Ireland UK). By using commercial enzyme-linked immunoabsorbent assays (ELISA) were determined soluble levels of insulin (sensitivity of 0.399 μUI/mL), sCCL2 (limit of detection of 2.3 pg/mL), sAdiponectin (limit of detection 0.019 ng/mL) (ALPCO Diagnostics 26-G Keewaydin Drive, Salem, NH), and sResistin (sensitivity 0.026 ng/mL, R&D Systems Inc., Minneapolis, MN, USA).

2.6. SNPs Analysis. Genomic DNA was obtained from total blood using a standard protocol for extraction with the modified Miller method as described previously [22] and was stored at −20°C until being used for genotyping. For each gene studied, polymorphic regions were amplified by polymerase chain reaction (PCR) method as described previously [23, 24].

To analyze the *CCR2* Val64Ile SNP was determined using sequence-specific primers (SSP): forward, Val 5′-TGGGCA-ACATGCTGGTCG-3′, Ile 5′-TGGGCAACATGCTGG-TCA-3′, and reverse: 5′-TGGAAAATAAGGGCCACA-GAC-3′ annealing 62°C, PCR product 413 bp [11], and *CCL2* G-2518A SNP, forward primer 5′-TCACGCCAGCACTGA-CCTCC-3′, and reverse: 5′-ACTTCCCAGCTTTGCTGG-CTGAG-3′ with annealing temperature 56°C, PCR product 250 bp.

The PCR were performed in a 25 μL total volume (mixture with 100 ng of DNA, 2 nM of each primer, 0.20 mM of each dNTP, 0.25 U *Taq* polymerase, and 1x PCR buffer) and 1.5 or 3.0 mM of $MgCl_2$ for *CCL2* or *CCR2*, respectively.

To determine *CCL2* genotypes a PCR was performed and then a digestion of obtained products with *PVU II* restriction enzyme. The lengths of fragments observed were as follows: 175 and 75 bp (allele A) and 250 bp (allele G). Electrophoresis was done at a constant voltage of 180 V on 6% polyacrylamide gels stained with silver nitrate. For quality control, a blank and samples previously confirmed as positive for each genotype were used as controls. To ensure the accuracy of genotype data, we used internal controls and repetitive experiments. In addition, both polymorphisms were identified in duplicate by two different analysts. The genotyping success rate was 100%.

2.7. Statistical Analysis. Data were analyzed with the Statistics program SPSS v21 (IBM Inc., Chicago, IL, USA) and GraphPad Prism v6.01 (2014 Inc. 2236 Beach Avenue Jolla, CA 92037). Results are given as mean ± SD or median with 25, 75 percentiles or percentages based on normal distribution. The data distribution of clinical and laboratory variables of the study group was evaluated with Z Kolmogorov-Smirnov test, and we performed parametric and nonparametric test, as appropriate. The most important variables were adjusted by gender and age with an ANCOVA analysis. About these results we performed multifactorial analysis for the most important variables. The clinical and laboratory characteristics of the study group were performed with the unpaired Student's t-test or Mann-Whitney U test, and to compare quantitative data in four groups, a one-way ANOVA and post hoc Tukey test were used.

Data from serum concentrations of adipokines, the laboratorial assessment, and disease variables were subjected to Pearson or Spearman correlation tests. The Hardy-Weinberg equilibrium text for individual *loci* was performed with http://ihg.gsf.de/cgi-bin/hw/hwa1.pl. Contingency tables (2×2 and 2×3) with χ^2 trend test or Fisher exact test, as appropriate, were used for testing the differences of genotype distribution and allele frequencies between study groups. Two genetic models were used for these analyses: (1) the dominant model where each SNP was modeled categorically and separated into three categories, one for each genotype, and (2) the phenotype model, where each SNP was modeled into two categories, with two genotypes combined into one category (polymorphic homozygotes plus heterozygotes), choosing one genotype (homozygotes wild type) as the reference group. A two-tailed P value less than 0.05 was considered statistically significant.

3. Results

3.1. Adiposity Is Associated with Metabolic Markers. Anthropometrics characteristics and metabolic markers of the subjects included in this study split by IR Stern classification are shown in Table 1. The study group included 380 Mexican-Mestizo individuals of which 237 (62%) were women, they were classified without IR or with IR, ANCOVA was performed, adjusted for sex and age, and no differences were observed (data not showed). Twenty-one percent has been classified with obesity and 32% with IR. Sixty-five percent of individuals, included in the study, were determined with excess body fat according to the Deurenberg criteria [21], and 31% had dyslipidemic profile (data no shown). A positive correlation of soluble levels of sCCL2, adipokines, metabolic markers, and lipid profile (except HDLc, LDLc, and Apo-A1) was observed along body fat storage (Table 2).

3.2. Individuals with IR Presented Inflammatory State. According to IR classification, individuals with IR displayed higher soluble levels of CCL2, resistin, and CRP and lower levels of adiponectin than individuals without IR (Figure 1). Soluble levels of CCL2, CRP, sResistin, and metabolic markers correlated positively with body adiposity, whereas levels of soluble adiponectin correlated negatively (Table 2).

3.3. CCL2 Polymorphism Is Associated with IR. All genotype frequencies were in Hardy-Weinberg equilibrium.

Table 1: Anthropometric characteristics and metabolic markers in individuals included in the study.

Measurement	Study group		P
	Individuals without IR	Individuals with IR	
n (%)	270 (68)	110 (32)	
Age (years)	35 ± 14	34 ± 14	NS
Height (cm)	163.8 ± 5.7	165.7 ± 1.1	NS
Weight (kg)	**68.7 ± 13.2**	**79.4 ± 16.3**	**<0.001***
BMI (kg/m^2)	**24.9 (22.6–28.9)**	**28.6 (24.4–31.7)**	**<0.001**$^+$
Body fat mass (kg)	**20.1 ± 9.2**	**25.9 ± 11.3**	**<0.001***
Total body fat mass (%)	**28.8 ± 9.4**	**32.80 ± 9.2**	**<0.001***
BFR (kg/m^2)	**7.03 (5.24–9.40)**	**9.40 (6.37–12.20)**	**0.001**$^+$
Waist circumference (cm)	**86.5 (77.1–93.1)**	**95.0 (83–103)**	**<0.001**$^+$
Hip circumference (cm)	**99.5 (95–105.9)**	**104 (99–110)**	**0.002**$^+$
WHR	0.854 (0.68–1.17)	0.866 (0.70–1.28)	NS$^+$
WHtR	**0.533 ± 0.076**	**0.568 ± 0.085**	**<0.001***
Glucose (mg/dL)	**89 ± 10**	**98 ± 18**	**<0.001***
Insulin (μUI/mL)	**8.6 ± 3.5**	**35.2 ± 32.5**	**<0.001***
HOMA-IR	**1.86 (1.34–2.58)**	**6.05 (4.40–9.03)**	**<0.001**$^+$
Triglycerides (mg/dL)	**134 ± 83**	**162 ± 95**	**0.005***
Total cholesterol (mg/dL)	184 ± 40	185 ± 34	NS
HDLc (mg/dL)	39.5 ± 15.1	37.6 ± 14.9	NS
LDLc (mg/dL)	111 ± 36	110 ± 31	NS
VLDLc (mg/dL)	**26 ± 16**	**32 ± 19**	**0.005***
Apo-A1 (mg/dL)	114 ± 25	117 ± 27	NS
Apo-B (mg/dL)	111 ± 32	117 ± 32	NS

n = 380. Data are presented as mean ± standard deviation and median (25–75 percentiles). *Student's t-test and $^+$Mann-Whitney U test with P significantly, comparing the groups: individuals with IR versus individuals without IR. IR: insulin resistance; BMI: body mass index; WHR: waist to hip ratio; WHtR: waist to height ratio; BFR: body fat ratio; HOMA-IR: homeostasis model assessment-insulin resistance; HDLc, LDLc, and VLDLc: high, low, and very low density lipoprotein cholesterol, respectively; Apo: apolipoprotein.

Table 2: Correlations soluble levels of adipokines and metabolic markers with body adiposity.

Measurements	*Weight (kg)	$^+$BMI (kg/m^2)	$^+$Body fat mass (%)	$^+$BFR (kg/m^2)	$^+$WC (cm)	$^+$WHtR
	% Correlation					
sCCL2 (pg/mL)	20.1	29.4	21.8	29.3	25.0	24.8
CRP (mg/L)	30.6	52.7	52.8	53.0	44.8	52.8
sAdiponectin (ng/mL)	−34.7	−25.0	−17.5	−25.1	−23.7	−17.2
sResistin (ng/mL)	43.3	27.1	30.1	27.3	32.5	24.9
Glucose (mg/dL)	22.7	38.1	24.0	35.4	32.5	35.6
Insulin (μUI/mL)	23.1	39.8	29.9	40.1	27.1	26.4
HOMA-IR	25.0	43.6	32.4	43.5	30.5	30.6
Triglycerides (mg/dL)	22.5	34.9	16.9	33.7	40.1	36.0
Total cholesterol (mg/dL)	19.5	32.2	27.3	30.8	37.5	39.6
VLDLc (mg/dL)	22.4	34.2	16.4	33.0	39.6	35.4
Apo-B (mg/dL)	21.0	34.5	17.5	34.3	46.7	44.3

n = 380. BMI: body mass index; BFR: body fat ratio; WC: waist circumference; WHtR: waist to height ratio; CCL2: chemokine (C-C motif) ligand 2; HOMA-IR: homeostasis model assessment-insulin resistance; CRP: C reactive protein; VLDLc: very low density lipoprotein cholesterol; Apo: apolipoprotein. Significant differences: $P < 0.05$, *Pearson or $^+$Spearman correlations test.

The individuals without IR presented a higher frequency of the phenotype $A+$ of the *CCL2* polymorphism, while phenotype $A-$ is more common in the individuals with IR. These differences were also observed in genotype and allele frequencies (Table 3). Higher levels of total adiponectin as well as a parallel decrease in insulin levels and HOMA-IR index were associated with $A+$ phenotype carriers (Figure 2), as long as phenotype $A+$ was associated with low measures of BMI and BFR (Table 4).

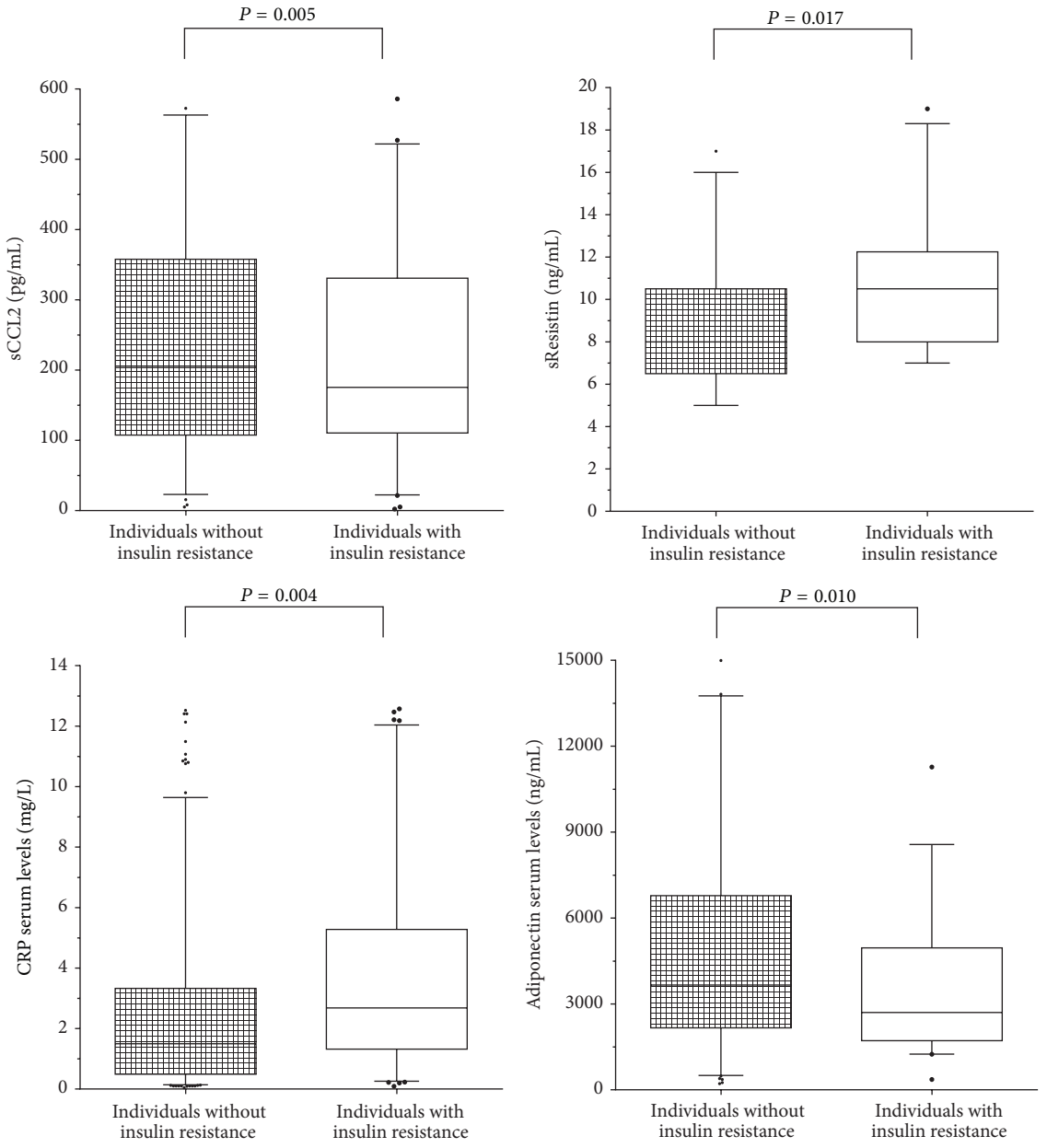

Figure 1: Soluble levels of adipokines and CRP by study group. $n = 380$. Student's t-test with P significantly, comparing the groups: individuals with IR versus individuals without IR.

3.4. CCR2 Polymorphism Was Not Associated with IR but Promoted Clinical Features of IR. None of the *CCR2* variants had an association with IR (Table 3). The detailed analysis showed association of phenotype *Ile*+ with high BMI, levels of glucose and lipids (Table 4). The same as *CCL2 A*+ phenotype, in *CCR2 Ile*+ carriers presented higher levels of CCL2 compared to *Ile*− phenotypes (Figure 2).

3.5. A+ Phenotype of CCL2 and Ile+ of CCR2 Are Associated with High Levels of Circulating CCL2. No metabolic profile explored in this study was associated with A+ phenotype (Table 4). However, significant phenotype-by-phenotype association was observed between the *CCL2*-2518A allele and the *CCR2* 64Ile allele; carriers of the *CCR2* phenotype 64Ile+ who at the same time also were phenotype A+ of *CCL2* (polymorphic genotypes for the both polymorphisms) presented higher levels of soluble CCL2, than any other phenotype combinations (Figure 3).

4. Discussion

The IR is a disease of multifactorial etiology product of the interaction between the genetic component and the environment, epidemiological data describes IR as an emerging disease with epidemic proportions [19, 25, 26]. In prior information it has been postulated that there may exist

Table 3: Distribution of *CCL2* (G-2518A) and *CCR2* (Val64Ile) gene polymorphism in Mexican-Mestizo population.

Study group	Genotype, *n* (%)			Phenotype, *n* (%)		Allele, *n* (%)	
	CCL2 G-2518A						
	G/G	G/A	A/A	A+	A−	G	A
Individuals without IR	47 (17.4)	135 (50.0)	88 (32.6)	223 (82.6)	47 (17.4)	229 (42.4)	311 (57.6)
Individuals with IR	32 (29.0)	51 (46.4)	27 (24.6)	78 (70.9)	32 (29.1)	115 (52.3)	105 (47.7)
$^{*}P$		**0.01378**		**0.01131**		**0.01321**	
Study group	Genotype, *n* (%)			Phenotype, *n* (%)		Allele, *n* (%)	
	CCR2 Val64Ile						
	Val/Val	Val/Ile	Ile/Ile	Ile+	Ile−	Val	Ile
Individuals without IR	173 (64.1)	82 (30.4)	15 (5.5)	97 (35.9)	173 (64.1)	428 (79.3)	112 (20.7)
Individuals with IR	67 (60.9)	37 (33.6)	6 (5.5)	43 (39.1)	67 (60.9)	171 (77.7)	49 (22.3)
$^{*}P$		0.64924		0.94889		0.63925	

$n = 380$. IR: insulin resistance. *Significant differences: Pearson's goodness-of-fit test χ^2 or Fishers' exact test; G or Val: wild-type alleles; A+ phenotype: A/A plus G/A genotypes; Ile+ phenotype: Ile/Ile plus Ile/Val genotypes.

Table 4: Comparisons of body fat measurements and lipid profile between *CCL2* G-2518A and *CCR2* Val64Ile phenotype carriers.

Measurements	*CCL2* G-2518A			*CCR2* Val64Ile		
	Phenotype A+	Phenotype A−	*P*	Phenotype Ile+	Phenotype Ile−	*P*
n (%)	301 (79)	79 (21)		140 (37)	240 (63)	
Weight (kg)	72.0 ± 15.55	72.8 ± 13.56	NS	73.2 ± 14.82	71.5 ± 15.32	NS
BMI (kg/m^2)	**25.9 (22.9–29.1)**	**27.5 (24.3–29.65)**	$^{+}$**0.028**	**27.3 (23.8–29.7)**	**25.4 (23.0–28.9)**	**0.018**$^{+}$
Total body fat (%)	29.6 ± 9.81	31.7 ± 8.57	NS	31.2 ± 9.05	29.4 ± 9.85	NS
BFR (kg/m^2)	**7.31 (5.24–9.92)**	**8.25 (6.24–11.40)**	$^{+}$**0.039**	7.63 (5.57–10.90)	7.37 (5.31–9.93)	NS
Waist circumference (cm)	88.0 (78.4–98.0)	89.4 (79.3–96.5)	NS	89.1 (79.5–99.0)	88.1 (78.3–97.6)	NS
Glucose (mg/dL)	92 ± 12	93 ± 14	NS	**95 ± 13**	**91 ± 12**	**0.004***
Triglycerides (mg/dL)	142 ± 85.6	146 ± 94.2	NS	**156 ± 8.5**	**135 ± 5.0**	**0.039***
Total cholesterol (mg/dL)	181 ± 40.1	185 ± 34.3	NS	**190 ± 43.7**	**180 ± 35.5**	**0.031***
HDLc (mg/dL)	39 ± 14.8	37 ± 15.8	NS	38 ± 13.6	38 ± 15.8	NS
LDLc (mg/dL)	111 ± 35.6	109 ± 30.4	NS	114 ± 39.1	108 ± 31.2	NS
VLDLc (mg/dL)	28 ± 16.9	29 ± 18.8	NS	**31 ± 20.1**	**26 ± 15.3**	**0.032***
Apo-A1 (mg/dL)	114 ± 25.1	121 ± 29.1	NS	117 ± 24.4	114 ± 27.1	NS
Apo-B (mg/dL)	112 ± 30.0	121 ± 41.5	NS	**119 ± 36.8**	**109 ± 27.8**	**0.045***

$n = 380$. BMI: body mass index; BFR: body fat ratio; HDLc, LDLc, and VLDLc: high, low, and very low density lipoprotein cholesterol, respectively; Apo: apolipoprotein. A− or Ile−: wild-type phenotypes; polymorphic A+ phenotype (A/A plus G/A genotypes); polymorphic Ile+ phenotype (Ile/Ile plus Val/Ile genotypes). Data are presented as mean ± standard deviation and median (25–75 percentiles). *Student's *t*-test and $^{+}$Mann-Whitney *U* test with *P* significantly, comparing the polymorphic phenotype carriers versus wild-type phenotypes carriers.

susceptibility genes involved in adipogenesis and energy metabolism [27, 28]; in the current study we explored the distribution of polymorphisms G-2518A and Val64Ile of *CCL2* and *CCR2*, respectively, in individuals with IR.

In addition, the individuals' carriers of different genotypes according to gene dosage were evaluated on the possible association with CCL2 levels, metabolic markers, and adiposity within the population with IR.

In the present work 380 individuals, were classified with or without IR by Stern criteria and obesity by BMI WHO criteria. The frequencies found in IR and obesity, clinical data, and anthropometric measurements are consistent with previous reports in the Mexican population [26, 29].

There are several reasons why a certain obese phenotype possibly will not be equally expressed (e.g., different physical activity levels among participants); however, the aim of the study was to investigate the relationship between the polymorphisms of *CCL2* and *CCR2* with CCL2 soluble levels, metabolic markers, and adiposity (like indicator of body fat status, absolute and/or relative) measured by BIA. Most studies report that the impedance method is reliable and valid. Baumgartner's contribution reviews the assumptions, applicability, equipment, measurement procedure, precision, and accuracy of the BIA method and determined that they were highly recommended [30–32]. Unfortunately we did not evaluate the fat distribution in study subjects; hence, we were not able to include a body fat distribution analysis.

In this set, clinic profile and the ratio of prevalence of IR, presented in the present study, suggest that IR is a complex disease, meaning that different phenotypes are observed with various clinical stages during the development of the pathogenic process. It has been postulated that in

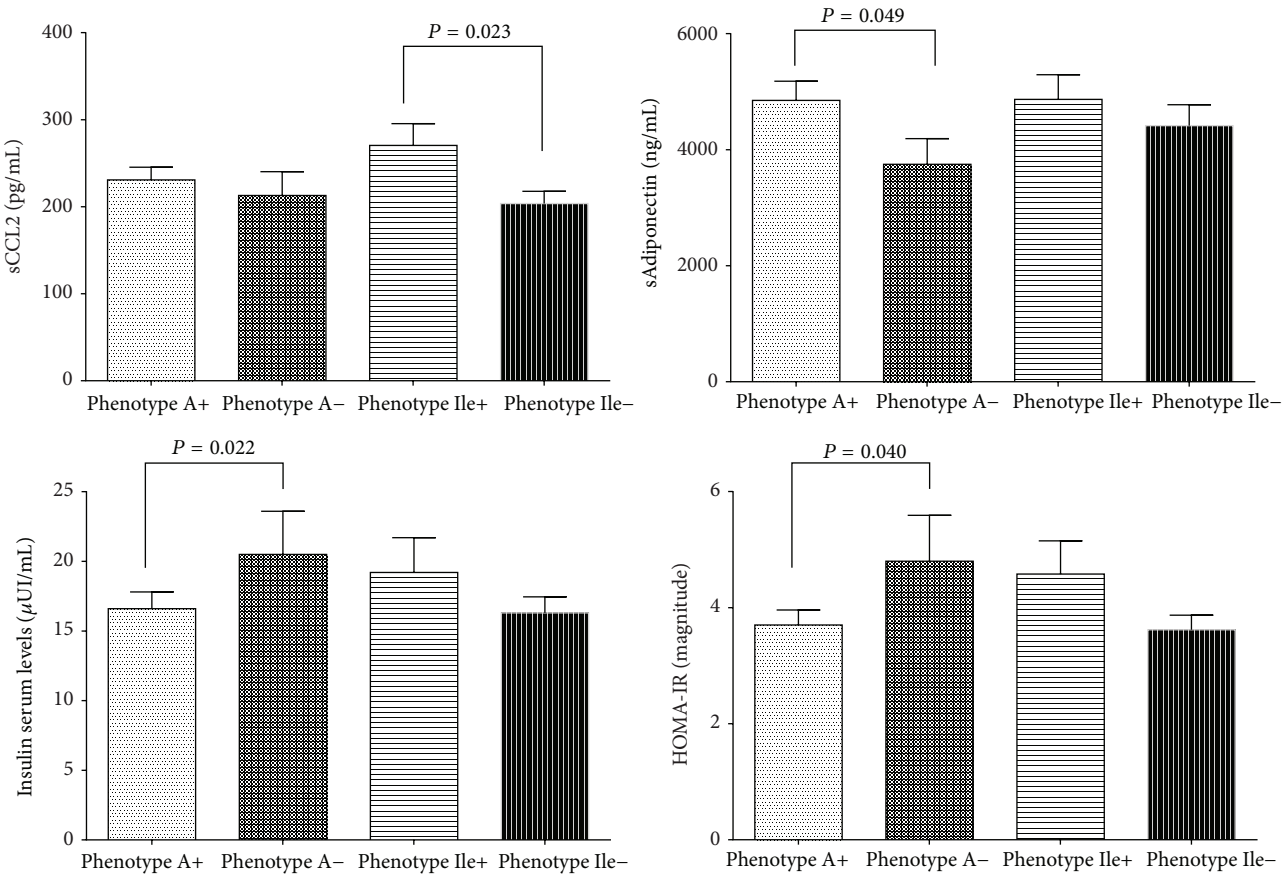

Figure 2: Soluble levels of adipokines, insulin, and HOMA-IR by *CCL2* G-2518A and *CCR2* Val64Ile phenotype carriers. $n = 380$. A+ phenotype: A/A plus G/A genotypes; Ile+ phenotype: Ile/Ile plus Val/Ile genotypes. Student's t-test with P significantly, comparing the polymorphic phenotype carriers versus wild-type phenotypes carriers.

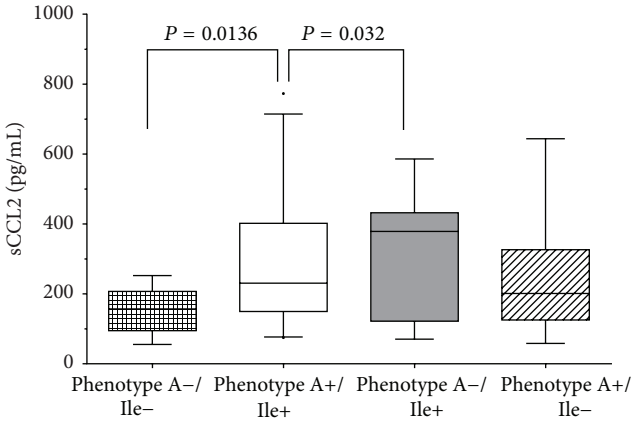

Figure 3: Soluble levels of CCL2 by phenotypes. Phenotype A−/Ile− (genotypes GG/ValVal) $n = 48$; phenotype A+/Ile+ (genotypes AA plus GA/ValIle plus IleIle) $n = 108$; phenotype A−/Ile+ (genotypes GG/ValIle plus IleIle) $n = 32$; phenotype A+/Ile− (genotypes AA plus GA/ValVal) $n = 192$. One way ANOVA and Tukey's post hoc test with P significantly, comparing the double-polymorphic phenotype carriers, (A+/Ile+) versus double-wild-type phenotype carriers (A−/Ile−).

course of the natural history of the IR, the hallmark is a low-grade subclinical inflammatory process, in which circulating monocytes infiltrate to adipose tissue, in a redundant manner, and polarize to M1 macrophages, becoming the main producers of chemokines and their receptors [33].

Two important observations lead this study to supporting that adiposity is associated with metabolic markers, in IR development. First, increased adiposity indicators and triglyceride levels were observed, and secondly no differences were found in other components of lipid profile. The first results are in agreement with previous studies [21, 33–35] that was attributed to the presence of obesity; in this case the expansion and accumulation of fat promotes the progress to IR. The second point given by the present study can be explained by the fact that IR is just component during the development of a mayor disease, since dyslipidemia is a later event, that could generate metabolic syndrome [36].

We observe that IR individuals presented higher inflammatory state, due to increased CCL2 levels in contrast to individuals without IR. These results can be explained by the increased levels of expression of adipokines, chemokines, and proinflammatory cytokines associated with a parallel increase

in the number, macrophages in the adipose tissue. The later ones, mainly macrophages with M1 phenotype, are crucial in IR, based on the fact that these cells are the important source of proinflammatory markers: TNF-α, IL-6, and CRP [2, 33, 37].

Alongside, in the individuals with IR was confirmed the presence of a low-grade inflammatory process represented by the increased levels of sResistin, CRP, and the decreased levels of total adiponectin and the correlation of them with adiposity status, parallel to the increase in BMI, BFR, and metabolic markers.

The importance of the present results lies in the biological relationship that exists between IR and obesity for the development of other diseases, for instance, metabolic syndrome. Insulin has the following functions: on one side, it promotes synthesis of insulin-like growth factor 1, which correlates with fat accumulation, and increase of white adipose tissue; on other side, it is the leader in the deregulations in the secretion of adipokines and metabolic markers that has been associated with certain types of cancer and other chronic diseases such as T2DM [1, 4, 6, 38].

The main pathological mechanism that connect the increase of adipose tissue with IR is the disfunction of the immune system and the establishment of a low-grade subclinical systemic chronic inflammation state, as a result of increased adiposity. This dysregulation of the immune system can be explained on two mechanisms: first, the adipose tissue in obese subjects has an increased amount of infiltrated macrophages who present an M1 phenotype and have an increase in the expression of 4 retinol binding protein (RPB4); and second, it has been found that high concentrations of fatty acids and RPB4 induce the expression of TNF-α and the signaling mediated by the toll-like receptor 4 [1, 27].

In this context, the inflammatory process in IR is an underlying clinical sign in the course of the disease and is identified by an increase in levels of inflammatory markers, as well as deregulation in the production of adipokines; in this respect there is evidence based on animal model studies and in humans, in which the important role of white adipose tissue is demonstrated in the maintenance of an inflammatory response associated with the development of IR [6].

There are numerous studies that have found interactions between polymorphisms and development of diseases such as metabolic syndrome. Due to the link of inflammation with development of IR, numerous genes have been studied [2, 28]. The chemokine CCL2 and their CCR2 receptor have been studied in recent years because of their involvement in the recruitment of macrophages to adipose tissue and subsequent differentiation into proinflammatory M1 phenotype [27, 33, 39].

The polymorphism G-2518A, in *CCL2* gene, was identified as a G to A transition; this change is near to a response site of NF-kB and has been speculated that increases affinity to its ligand; this results in increased levels of CCL2 in the bloodstream and further recruitment of macrophages to adipose tissue compared to those individuals exhibiting wild-type allele. Concerning polymorphism in *CCR2*, Val64Ile, is a transition G to A at position 190 of *CCR2*, changing valine codon (GTC) to isoleucine (ATC) at position 64, a conservative change of neutral nonpolar amino acids. This change makes the CCR2A isoform more stable and increases its half-life but does not affect the stability of the isoform CCR2B [1, 40].

On the stage of genetic diversity between populations, the reported frequencies for polymorphic alleles -2518A and 64Ile ranging from 39.1% to 83.2% and 9.5% to 25.6%, respectively, with differences with the frequencies reported in this study (Tables 5(a) and 5(b)), show that wild-type allele changes in some populations, such as Asiatic. In the present study the allele polymorphic frequencies are similar to those reported in Mexican-Mestizos by González-Enríquez et al. and different from Vázquez-Lavista et al. [41, 42].

We found differences when comparing frequencies of alleles of our Mexican population with other populations of different nations, for example, the Asiatic, Caucasian European, or American populations, with a different genetic background, which is explained by the distribution of alleles as result of their anthropological relationships. Since the conquest by the Spanish, European genetics was introduced on the natures, over the centuries. Hence, individuals included in the present study were not pure endogenous Mexican population. Therefore the differences in genotype distribution with other Mexican populations may be because of the fact that in our study group participants were characterized as Mexican-Mestizos of Western Mexico (Tables 5(a) and 5(b)).

In this study group, *CCL2* polymorphism was associated with IR, according to the results showing differences in the distribution of frequencies of genotypes, phenotypes, and alleles, with a higher contribution of the A+ phenotype than A− phenotype for the presence of IR. A+ phenotype was associated with higher levels of total sAdiponectin and lower levels of insulin and HOMA-IR magnitude, while a decrease was shown in BMI and BFR. The opposite was observed for individuals carrying of polymorphic phenotype Ile+; they had an increase in lipid profile; these results show influence of both polymorphisms in the accumulation of body fat and its relation to the metabolic status of individuals.

This can be explained because this is the main tissue involved in the production of adipokines and increases its volume in the presence of a proinflammatory environment [5, 33]. Previous studies have demonstrated the interference of proinflammatory cytokine in the signaling pathway of insulin receptor [27]. Parallel to this stage, we observed increased levels of glucose in individuals with phenotype Ile+ which indicates involvement of this polymorphism in the establishment of IR.

The adiposity status shown in the individuals of this study regarding the polymorphisms in *CCL2* and *CCR2* and its association with metabolic and inflammatory markers, and levels of adipokines have not been previously described for Mexican-Mestizo population.

Among the most important results of this study are that A+ phenotype of *CCL2* and Ile+ of *CCR2* carriers are associated with higher levels of circulating CCL2; this difference is attributed to the fact that this variant generates a more stable form of the receptor CCR2 membrane which has a longer half-life, allowing for longer signaling that in people with wild-type polymorphism variant [40].

Table 5: (a) Distribution of G-2518A polymorphism in *CCL2* gene in other populations. (b) Distribution of Val64Ile polymorphism in *CCR2* gene in other populations.

(a)

Author	Population	*n*	G	A	G/G	A/G	A/A	*P*
The present study	**Mexican-Mestizo**	**380**	**45.2**	**54.6**	**20.7**	**48.9**	**30.3**	—
Vázquez-Lavista et al. [41]	Mexican-Mestizo	126	57.5	42.5	29.4	56.3	14.3	<**0.001**
González-Enríquez et al. [42]	Mexican-Mestizo	21	52.4	47.6	27.0	50.0	23.0	0.370
Bektas-Kayhan et al. [24]	Caucasian	140	16.8	83.2	0.8	32.1	67.1	<**0.001**
Kruszyna et al. [43]	Caucasian	323	29.9	70.1	7.4	44.9	47.7	<**0.001**
Kucukgergin et al. [44]	Caucasian	197	30.2	69.8	9.1	42.1	48.7	<**0.001**
Kouyama et al. [13]	Asian	361	34.6	65.4	—	—	—	—
Singh et al. [7]	Asian	200	35.3	64.7	11.0	48.5	40.5	<**0.001**
Mandal et al. [45]	Asian	390	37.2	62.8	13.2	48.0	38.8	**0.001**
Chen et al. [23]	Asian	344	51.7	48.3	26.7	50.0	23.3	**0.015**
Wu et al. [46]	Asian	253	60.1	39.1	34.8	52.2	13.0	<**0.001**

Pearson's goodness-of-fit test χ^2 or Fishers' exact test with *P* significantly, comparing alleles and/or genotypes polymorphism distribution in Mexican-Mestizos population in this study versus distribution in other populations. G wild-type allele, A polymorphic allele.

(b)

Author	Population	*n*	Val	Ile	Val/Val	Val/Ile	Ile/Ile	*P*
The present study	**Mexican-Mestizo**	**380**	**78.8**	**21.2**	**63.2**	**31.3**	**5.5**	—
Vázquez-Lavista et al. [41]	Mexican-Mestizo	126	75.8	24.2	58.7	34.1	7.2	0.330
González-Enríquez et al. [42]	Mexican-Mestizo	21	90.5	9.5	82.6	17.3	0	**0.006**
Bektas-Kayhan et al. [24]	Caucasians	140	88.5	11.42	80.0	17.1	2.9	<**0.001**
Kucukgergin et al. [44]	Caucasians	197	89.6	10.4	80.7	17.8	1.5	<**0.001**
González et al. [47]	Caucasians	280	90.0	10.0	80.0	19.0	1.0	<**0.001**
Mandal et al. [45]	Asian	390	74.4	25.6	54.8	39.2	6.0	**0.046**
Wu et al. [46]	Asian	253	80.6	19.4	64.4	32.4	3.2	0.438
Singh et al. [7]	Asian	200	80.5	19.5	63.0	35.0	2.0	0.501
Zandifar et al. [48]	Asian	100	87.5	12.5	75.0	25.0	0	**0.007**
Chen et al. [23]	Asian	344	89.1	10.9	80.2	17.7	2.1	<**0.001**

Pearson's goodness-of-fit test χ^2 or Fishers' exact test with *P* significantly, comparing alleles and/or genotypes polymorphism distribution in Mexican-Mestizos population in this study versus distribution in other populations. Val: wild-type allele; Ile: polymorphic allele.

Taking all results together, the present work shows new evidence that suggests that genetic factors contribute to the development of IR and this triggers pathobiological processes. These changes could influence the clinical course and severity of obesity-related diseases, such as IR. Therefore, the genetic load on individuals could play an important role in the genesis of diseases observed in obese subjects.

5. Conclusions

The most important results in the individuals of the present study are summarized as follows: association of adiposity with metabolic markers alongside with inflammatory state, *CCL2* polymorphism is associated with IR, while *CCR2* was associated with clinical features of IR besides it was seen that the individuals that had both polymorphic phenotypes had increased levels of CCL2.

These data suggests that the *CCL2*A+ phenotype could impact the reduced body fat storage, metabolic and healthy adipokine profile in Mexican-Mestizo individuals. The opposite, *CCR2*64Ile+ phenotype is associated with altered profile of metabolic markers and BMI. All this data suggests that the *CCL2* and *CCR2* polymorphisms and the signaling through this interactions could play a role in the metabolic changes associated with IR in Mexican-Mestizo population.

As a final remark we can conclude that an increase of CCL2 serum levels is associated with the polymorphic phenotypes (A+/Ile+) of the polymorphisms G-2518A in *CCL2* and Val64Ile in *CCR2* in individuals with insulin resistance of Mexican population.

Conflict of Interests

The authors declare that there is no conflict of interests regarding the publication of this paper.

Authors' Contribution

Milton-Omar Guzmán-Ornelas and Marcelo Heron Petri equally contributed to this work.

Acknowledgment

This work was supported by Grant no. PS-2009-552 to Rosa-Elena Navarro-Hernández of the State Council of Science and Technology (COECyTJal-University of Guadalajara).

References

[1] T. Ota, "Chemokine systems link obesity to insulin resistance," *Diabetes & Metabolism Journal*, vol. 37, no. 3, pp. 165–172, 2013.

[2] C. de Luca and J. M. Olefsky, "Inflammation and insulin resistance," *FEBS Letters*, vol. 582, no. 1, pp. 97–105, 2008.

[3] R. A. Bastarrachea, J. C. López-Alvarenga, V. E. Bolado-García, J. Téllez-Mendoza, H. Laviada-Molina, and A. G. Comuzzie, "Macrophages, inflammation, adipose tissue, obesity and insulin resistance," *Gaceta Médica de México*, vol. 143, no. 6, pp. 505–512, 2007.

[4] T. O'Connor, L. Borsig, and M. Heikenwalder, "CCL2-CCR2 signaling in disease pathogenesis," *Endocrine, Metabolic & Immune Disorders-Drug Targets*, vol. 15, no. 2, pp. 105–118, 2015.

[5] B. Gustafson, "Adipose tissue, inflammation and atherosclerosis," *Journal of Atherosclerosis and Thrombosis*, vol. 17, no. 4, pp. 332–341, 2010.

[6] A. Ueda, Y. Ishigatsubo, T. Okubo, and T. Yoshimura, "Transcriptional regulation of the human monocyte chemoattractant protein-1 gene: cooperation of two NF-κB sites and NF-κB/Rel subunit specificity," *Journal of Biological Chemistry*, vol. 272, no. 49, pp. 31092–31099, 1997.

[7] V. Singh, P. Srivastava, N. Srivastava, R. Kapoor, and R. D. Mittal, "Association of inflammatory chemokine gene CCL2I/D with bladder cancer risk in North Indian population," *Molecular Biology Reports*, vol. 39, no. 10, pp. 9827–9834, 2012.

[8] T. Yoshimura and J. J. Oppenheim, "Chemokine-like receptor 1 (CMKLR1) and chemokine (C-C motif) receptor-like 2 (CCRL2); two multifunctional receptors with unusual properties," *Experimental Cell Research*, vol. 317, no. 5, pp. 674–684, 2011.

[9] A. M. Valdes, M. L. Wolfe, E. J. O'Brien et al., "Val64Ile polymorphism in the C-C chemokine receptor 2 is associated with reduced coronary artery calcification," *Arteriosclerosis, Thrombosis, and Vascular Biology*, vol. 22, no. 11, pp. 1924–1928, 2002.

[10] J. Petrkova, Z. Cermakova, J. Drabek, J. Lukl, and M. Petrek, "CC chemokine receptor (CCR)2 polymorphism in Czech patients with myocardial infarction," *Immunology Letters*, vol. 88, no. 1, pp. 53–55, 2003.

[11] K. Chatterjee, C. Dandara, M. Hoffman, and A.-L. Williamson, "CCR2-V64I polymorphism is associated with increased risk of cervical cancer but not with HPV infection or pre-cancerous lesions in African women," *BMC Cancer*, vol. 10, article 278, 2010.

[12] E. Simeoni, M. M. Hoffmann, B. R. Winkelmann et al., "Association between the A-2518G polymorphism in the monocyte chemoattractant protein-1 gene and insulin resistance and Type 2 diabetes mellitus," *Diabetologia*, vol. 47, no. 9, pp. 1574–1580, 2004.

[13] K. Kouyama, K. Miyake, M. Zenibayashi et al., "Association of serum MCP-1 concentration and MCP-1 polymorphism with insulin resistance in Japanese individuals with obese type 2 diabetes," *Kobe Journal of Medical Sciences*, vol. 53, no. 6, pp. 345–354, 2007.

[14] W. R. Bolus, D. A. Gutierrez, A. J. Kennedy, E. K. Anderson-Baucum, and A. H. Hasty, "CCR2 deficiency leads to increased eosinophils, alternative macrophage activation, and type 2 cytokine expression in adipose tissue," *Journal of Leukocyte Biology*, vol. 98, no. 4, pp. 467–477, 2015.

[15] S. E. Stern, K. Williams, E. Ferrannini, R. A. DeFronzo, C. Bogardus, and M. P. Stern, "Identification of individuals with insulin resistance using routine clinical measurements," *Diabetes*, vol. 54, no. 2, pp. 333–339, 2005.

[16] DOF 07-02-1984, ú.r.D., Reglamento de la Ley General de Salud en Materia de Investigación para la Salud.

[17] R. Ness-Abramof and C. M. Apovian, "Waist circumference measurement in clinical practice," *Nutrition in Clinical Practice*, vol. 23, no. 4, pp. 397–404, 2008.

[18] WHO, "Physical status: the use and interpretation of anthropometry. Report of a WHO Expert Committee," World Health Organization Technical Report Series 854, WHO, 1995.

[19] World Health Organization, *Obesity: Preventing and Managing the Global Epidemic*, World Health Organization, Geneva, Switzerland, 1st edition, 2012.

[20] R. Fernandez-Vazquez, Á. Millán Romero, M. Á. Barbancho, and J. R. Alvero-Cruz, "Abdominal bioelectrical impedance analysis and anthropometry for predicting metabolic syndrome in middle aged men," *Nutrición Hospitalaria*, vol. 32, no. 3, pp. 1122–1130, 2015.

[21] P. Deurenberg, M. Yap, and W. A. van Staveren, "Body mass index and percent body fat: a meta analysis among different ethnic groups," *International Journal of Obesity*, vol. 22, no. 12, pp. 1164–1171, 1998.

[22] S. A. Miller, D. D. Dykes, and H. F. Polesky, "A simple salting out procedure for extracting DNA from human nucleated cells," *Nucleic Acids Research*, vol. 16, no. 3, p. 1215, 1988.

[23] M.-K. K. Chen, K.-T. Yeh, H.-L. Chiou, C.-W. Lin, T.-T. Chung, and S.-F. Yang, "CCR2-64I gene polymorphism increase susceptibility to oral cancer," *Oral Oncology*, vol. 47, no. 7, pp. 577–582, 2011.

[24] K. Bektas-Kayhan, M. Unur, Z. Boy-Metin, and B. Cakmakoglu, "MCP-1 and CCR2 gene variants in oral squamous cell carcinoma," *Oral Diseases*, vol. 18, no. 1, pp. 55–59, 2012.

[25] OMS, *Obesity: Preventing and Managing the Global Epidemic*, OMS, 1st edition, 2012.

[26] G. Olaiz-Fernández, J. Rivera, T. Shamah et al., *Encuesta Nacional de Salud y Nutrición 2006*, Instituto Nacional de Salud Pública, 2006.

[27] A. Rull, J. Camps, C. Alonso-Villaverde, and J. Joven, "Insulin resistance, inflammation, and obesity: role of monocyte chemoattractant protein-1 (orCCL2) in the regulation of metabolism," *Mediators of Inflammation*, vol. 2010, Article ID 326580, 11 pages, 2010.

[28] M. L. R. Curti, P. Jacob, M. C. Borges, M. M. Rogero, and S. R. G. Ferreira, "Studies of gene variants related to inflammation, oxidative stress, dyslipidemia, and obesity: implications for a nutrigenetic approach," *Journal of Obesity*, vol. 2011, Article ID 497401, 31 pages, 2011.

[29] J. P. Gutiérrez, J. Rivera, T. Shamah, C. Oropez, and M. H. Ávila, *Encuesta Nacional de Salud y Nutrición 2012. Resultados Nacionales*, Instituto Nacional de Salud Pública, Cuernavaca, México, 2012.

[30] D. Brodie, V. Moscrip, and R. Hutcheon, "Body composition measurement: a review of hydrodensitometry, anthropometry, and impedance methods," *Nutrition*, vol. 14, no. 3, pp. 296–310, 1998.

[31] U. G. Kyle, I. Bosaeus, A. D. de Lorenzo et al., "Bioelectrical impedance analysis—part II: utilization in clinical practice," *Clinical Nutrition*, vol. 23, no. 6, pp. 1430–1453, 2004.

[32] M. Y. Jaffrin and H. Morel, "Body fluid volumes measurements by impedance: a review of bioimpedance spectroscopy (BIS) and bioimpedance analysis (BIA) methods," *Medical Engineering and Physics*, vol. 30, no. 10, pp. 1257–1269, 2008.

[33] B. Feng, T. Zhang, and H. Xu, "Human adipose dynamics and metabolic health," *Annals of the New York Academy of Sciences*, vol. 1281, no. 1, pp. 160–177, 2013.

[34] C. T. Lichtash, J. Cui, X. Guo et al., "Body adiposity index versus body mass index and other anthropometric traits as correlates of cardiometabolic risk factors," *PLoS ONE*, vol. 8, no. 6, Article ID e65954, 2013.

[35] F. Taverne, C. Richard, P. Couture, and B. Lamarche, "Abdominal obesity, insulin resistance, metabolic syndrome and cholesterol homeostasis," *PharmaNutrition*, vol. 1, no. 4, pp. 130–136, 2013.

[36] A. V. Castro, C. M. Kolka, S. P. Kim, and R. N. Bergman, "Obesity, insulin resistance and comorbidities? Mechanisms of association," *Arquivos Brasileiros de Endocrinologia e Metabologia*, vol. 58, no. 6, pp. 600–609, 2014.

[37] M. C. Morrison and R. Kleemann, "Role of macrophage migration inhibitory factor in obesity, insulin resistance, type 2 diabetes, and associated hepatic co-morbidities: a comprehensive review of human and rodent studies," *Frontiers in Immunology*, vol. 6, article 308, 2015.

[38] L. Yao, O. Herlea-Pana, J. Heuser-Baker, Y. Chen, and J. Barlic-Dicen, "Roles of the chemokine system in development of obesity, insulin resistance, and cardiovascular disease," *Journal of Immunology Research*, vol. 2014, Article ID 181450, 11 pages, 2014.

[39] S. L. Deshmane, S. Kremlev, S. Amini, and B. E. Sawaya, "Monocyte chemoattractant protein-1 (MCP-1): an overview," *Journal of Interferon and Cytokine Research*, vol. 29, no. 6, pp. 313–325, 2009.

[40] Y. Huang, H. Chen, J. Wang et al., "Relationship between CCR2-V64I polymorphism and cancer risk: a meta-analysis," *Gene*, vol. 524, no. 1, pp. 54–58, 2013.

[41] L. G. Vázquez-Lavista, G. Lima, F. Gabilondo, and L. Llorente, "Genetic association of monocyte chemoattractant protein 1 (MCP-1)-2518 polymorphism in Mexican patients with transitional cell carcinoma of the bladder," *Urology*, vol. 74, no. 2, pp. 414–418, 2009.

[42] G. V. González-Enríquez, M. I. Rubio-Benítez, V. García-Gallegos, E. Portilla-de Buen, R. Troyo-Sanromán, and C. Á. Leal-Cortés, "Contribution of TNF-308A and CCL2-2518A to carotid intima-media thickness in obese mexican children and adolescents," *Archives of Medical Research*, vol. 39, no. 8, pp. 753–759, 2008.

[43] Ł. Kruszyna, M. Lianeri, B. Rubis et al., "CCL2-2518 A/G single nucleotide polymorphism as a risk factor for breast cancer," *Molecular Biology Reports*, vol. 38, no. 2, pp. 1263–1267, 2011.

[44] C. Kucukgergin, F. K. Isman, S. Dasdemir et al., "The role of chemokine and chemokine receptor gene variants on the susceptibility and clinicopathological characteristics of bladder cancer," *Gene*, vol. 511, no. 1, pp. 7–11, 2012.

[45] R. K. Mandal, T. Agrawal, and R. D. Mittal, "Genetic variants of chemokine CCL2 and chemokine receptor CCR2 genes and risk of prostate cancer," *Tumor Biology*, vol. 36, no. 1, pp. 375–381, 2015.

[46] H.-H. H. Wu, T.-H. Lee, Y.-T. Tee et al., "Relationships of single nucleotide polymorphisms of monocyte chemoattractant protein 1 and chemokine receptor 2 with susceptibility and clinicopathologic characteristics of neoplasia of uterine cervix in Taiwan women," *Reproductive Sciences*, vol. 20, no. 10, pp. 1175–1183, 2013.

[47] P. González, R. Alvarez, A. Batalla et al., "Genetic variation at the chemokine receptors CCR5/CCR2 in myocardial infarction," *Genes and Immunity*, vol. 2, no. 4, pp. 191–195, 2001.

[48] A. Zandifar, M. Taheriun, S. Soleimani, F. Haghdoost, M. Tajaddini, and S. H. Javanmard, "Investigation of chemokine receptor CCR2V64Il gene polymorphism and migraine without aura in the iranian population," *The Scientific World Journal*, vol. 2013, Article ID 836309, 5 pages, 2013.

Hindawi Publishing Corporation
Journal of Diabetes Research
Volume 2016, Article ID 6014631, 15 pages
http://dx.doi.org/10.1155/2016/6014631

Research Article

Diabetes Mellitus and Increased Tuberculosis Susceptibility: The Role of Short-Chain Fatty Acids

Ekta Lachmandas, Corina N. A. M. van den Heuvel, Michelle S. M. A. Damen, Maartje C. P. Cleophas, Mihai G. Netea, and Reinout van Crevel

Department of Internal Medicine and Radboudumc Center for Infectious Diseases, Radboud University Medical Center, Internal Postal Code 463, P.O. Box 9101, 6500 HB Nijmegen, Netherlands

Correspondence should be addressed to Ekta Lachmandas; ekta.lachmandas@radboudumc.nl

Received 17 July 2015; Accepted 18 October 2015

Academic Editor: Francisco J. Ruperez

Type 2 diabetes mellitus confers a threefold increased risk for tuberculosis, but the underlying immunological mechanisms are still largely unknown. Possible mediators of this increased susceptibility are short-chain fatty acids, levels of which have been shown to be altered in individuals with diabetes. We examined the influence of physiological concentrations of butyrate on cytokine responses to *Mycobacterium tuberculosis* (Mtb) in human peripheral blood mononuclear cells (PBMCs). Butyrate decreased Mtb-induced proinflammatory cytokine responses, while it increased production of IL-10. This anti-inflammatory effect was independent of butyrate's well-characterised inhibition of HDAC activity and was not accompanied by changes in Toll-like receptor signalling pathways, the eicosanoid pathway, or cellular metabolism. In contrast blocking IL-10 activity reversed the effects of butyrate on Mtb-induced inflammation. Alteration of the gut microbiota, thereby increasing butyrate concentrations, can reduce insulin resistance and obesity, but further studies are needed to determine how this affects susceptibility to tuberculosis.

1. Introduction

Tuberculosis (TB) is the second leading cause of death from an infectious disease worldwide [1]. Susceptibility to TB can be increased by several comorbidities, one of which is type 2 diabetes mellitus (DM) [2]. DM patients present with an overall threefold increased risk of developing active TB [3]. Globally, 15% of TB cases are estimated to be attributable to DM [4] and thus with a predicted increase of DM by 155% over the next 20 years, DM will become an increasingly important factor challenging TB control [5–7].

DM patients exhibit alterations in the immune response against *Mycobacterium tuberculosis* (Mtb), making them more susceptible to infection or progression towards active TB disease and less responsive to treatment [8–11]. However, the underlying biological mechanisms remain largely unknown [12, 13]. DM patients have been associated with dysregulated cytokine responses to Mtb [14–17]. Whilst proinflammatory cytokines are necessary for protection against Mtb, anti-inflammatory cytokines may counteract these effects. Possible factors that may impact the host response in patients with DM are short-chain fatty acids (SCFAs), the main metabolic products of fermentation of nondigestible dietary fibres by the gut microbiota. Numerous reports have demonstrated that DM patients present with an altered composition of their gut microbiota, which subsequently alters their SCFA levels [18–24]. SCFAs strongly modulate immune and inflammatory responses [22, 25–31], thereby influencing the host response to Mtb. SCFAs, of which butyrate (C4) is the most thoroughly studied, act on immune and endothelial cells via at least two mechanisms: activation of G-protein coupled receptors (GPCRs) and inhibition of histone deacetylase (HDAC) [32]. They affect the function of various cell types such as lymphocytes [33, 34], neutrophils [25, 31, 35], and macrophages [28, 36–38]. In light of the emerging role of the microbiota in inflammation and immunity, we hypothesized that SCFAs, and in particular butyrate, may affect the immune response and susceptibility to Mtb in type 2 DM patients.

In this study we investigated the role of physiological concentrations of SCFAs on the cytokine response against

Mtb in human peripheral blood mononuclear cells (PBMCs). We subsequently examined a number of possible mechanisms via which altered concentrations of one particular SCFA, C4, might affect the host immune response to Mtb in DM patients. To this purpose, we studied the influence of physiological concentrations of C4 on HDAC activity, immune signalling pathways, the eicosanoid pathway, and cellular metabolism. To our knowledge, this is the first study reporting on the effects of physiological plasma concentrations of C4 on Mtb-induced cellular responses. Physiological plasma concentrations of C4 are in the micromolar range [39], whilst in previous studies C4 has been used in the millimolar range. Thus, this study substantially adds to our knowledge of SCFAs as possible mediators of altered immune responses to Mtb in DM patients.

2. Materials and Methods

2.1. Human Samples. PBMCs were isolated from buffy coats donated after written informed consent by healthy volunteers to the Sanquin Blood Bank (http://www.sanquin.nl/en/) in Nijmegen. Experiments were conducted according to the principles expressed in the Declaration of Helsinki. Since blood donations were anonymous no tuberculosis skin test or IFN-γ release assay was performed. However, the incidence of TB in the Dutch population is extremely low (4/100,000), and Bacillus Calmette-Guérin (BCG) vaccination is not part of the routine vaccination program. Blood donors were not screened for DM as prevalence of DM among people under 45 years of age (median age of blood donors) is about 1.5% and therefore DM is unlikely to be a confounding factor [34].

2.2. H37Rv Lysates and Culture. H37Rv Mtb was grown to mid-log phase in Middlebrook 7H9 liquid medium (Difco, Becton Dickinson) supplemented with oleic acid/albumin/dextrose/catalase (OADC) (BBL, Becton Dickinson), washed three times in sterile saline, heat killed, and then disrupted using a bead beater, after which the concentration was measured using a bicinchoninic acid (BCA) assay (Pierce, Thermo Scientific).

2.3. Cell Stimulation Experiments. Isolation of PBMCs was performed by differential centrifugation over Ficoll-Paque (GE Healthcare). Cells were adjusted to 5×10^6 cells/mL (Beckman Coulter) and suspended in RPMI 1640 (Gibco) supplemented with 10 μg/mL gentamicin (Lonza), 10 mM L-glutamine (Life Technologies), and 10 mM pyruvate (Life Technologies). 100 μL of PBMCs was incubated in round-bottom 96-well plates (Greiner), pretreated with SCFAs for 1 h, and stimulated with 1 μg/mL of H37Rv lysate or 10 ng/mL LPS (Sigma-Aldrich, *E. coli* serotype 055:B5). Cells were incubated for 24 h or 7 days at 37°C in a 5% CO_2 environment (n = 6 to 11). Alternatively, PBMCs were pretreated for 1 hour (37°C, 5% CO_2) with ranolazine (ITK Diagnostics), trimetazidine (Sigma), pertussis toxin (Enzo Life Sciences), etomoxir (Sigma) (inhibitors of β-oxidation, n = 3), aspirin (Aspégic injection powder, n = 3), cycloheximide (Sigma, n = 6 to 7), anti-IL-10 antibody IgG2a (BioLegend, n = 10 to 12), or IgG2a isotype control (BioLegend, n = 10 to 12) prior to stimulation. Cell culture supernatants were collected and stored at −20°C for cytokine measurements, performed by ELISA: TNF-α, IL-1β, IL-17A, IL-22, and IL-1Ra (R&D Systems) and IL-6, IFN-γ, and IL-10 (Sanquin).

2.4. Quantification of Gene Expression. For quantitative real-time PCR (qPCR) analysis RNA was isolated from PBMCs using TRIzol reagent (Invitrogen Life Technologies) according to the manufacturer's protocol. RNA was transcribed into complementary DNA (cDNA) by reverse transcription using iScript cDNA synthesis kit (Bio-Rad, Hercules, CA). Primer sequences (Biolegio) are given in Table 1. Power SYBR Green PCR Master Mix (Applied Biosystems) was used for qPCR on an AB StepOnePlus real-time PCR system (Applied Biosystems). qPCR data were normalized to the housekeeping gene human β2M (n = 3 to 10).

2.5. Protein Phosphorylation Measurements. Western blotting was carried out using a Trans-Blot Turbo system (Bio-Rad) according to manufacturer's instructions. 5×10^6 PBMCs were lysed in 100 μL lysis buffer. The resulting lysate was used for Western blot analysis. Equal amounts of protein were separated by SDS-PAGE on 4–15% polyacrylamide gels (Bio-Rad) and transferred to PVDF (Bio-Rad) membranes. Membranes were blocked for 1 h and then incubated overnight with primary antibody (dilution 1 : 1000) in 5% (w/v) BSA or milk in TBS-Tween buffer (TBS-T). Blots were washed in TBS-T 3 times and incubated with HRP-conjugated anti-rabbit antibody (1 : 5000; Sigma) in 5% (w/v) milk in TBS-T for 1 h at room temperature (RT). After washing, blots were developed with ECL (Bio-Rad) following manufacturer's instructions. Primary antibodies used were rabbit anti-p38 MAPK, rabbit anti-phospho-p38 MAPK, rabbit anti-ERK1/2 (p44/p42 MAPK), rabbit anti-phospho-ERK1/2 (P44/42 MAPK, T202/Y204), and rabbit anti-phospho-JNK (T183/Y185) (all Cell Signalling) (n = 2).

2.6. Metabolite Measurements. Lactate was measured from cell culture supernatants using a coupled enzymatic assay in which lactate was oxidised and the resulting H_2O_2 was coupled to the conversion of Amplex Red reagent to fluorescent resorufin by HRP (horseradish peroxidase). 30 μL of lactate standard or 200x diluted sample was added to 30 μL of reaction mix. The 30 μL of reaction mix consisted of 0.6 μL of 10 U/mL HRP (Sigma), 0.6 μL of 100 U/mL lactate oxidase (Sigma), 0.3 μL of 10 mM Amplex Red reagent (Life Technologies), and 28.5 μL PBS. Samples were incubated for 20 min at RT and fluorescence (excitation/emission maxima = 570/585 nm) was measured on an ELISA reader (BioTek) (n = 3 to 5).

Measurements of the NAD^+/NADH redox ratio were adapted from Zhu and Rand [40]. Briefly, 1.5 million stimulated PBMCs were lysed in 75 μL of homogenization buffer (10 mM nicotinamide (Sigma), 10 mM Tris-Cl (Sigma), and 0.05% (w/v) Triton X-100 (Sigma), pH 7.4). The lysate was centrifuged at 12000 g for 1 min. From the resulting supernatants two 18 μL aliquots were removed and either

Table 1: Primer sequences used for gene expression measurements by qPCR.

Target	Forward $5' \rightarrow 3'$	Reverse $5' \rightarrow 3'$
h-β2M	ATGAGTATGCCTGCCGTGTG	CCAAATGCGGCATCTTCAAAC
h-COX-2	CTGGCGCTCAGCCATACAG	CGCACTTATACTGGTCAAATCCC
h-CS	GGTGGCATGAGAGGCATGAA	TAGCCTTGGGTAGCAGTTTCT
h-HDAC1	CCGCATGACTCATAATTTGCTG	ATTGGCTTTGTGAGGGCGATA
h-HDAC8	TCGCTGGTCCCGGTTTATATC	TACTGGCCCGTTTGGGGAT
h-HIF1-α	GAACGTCGAAAAGAAAAGTCTCG	CCTTATCAAGATGCGAACTCACA
h-IDH2	CGCCACTATGCCGACAAAAG	ACTGCCAGATAATACGGGTCA
h-IL-10	CAACCTGCCTAACATGCTTCG	TCATCTCAGACAAGGCTTGGC
h-IL-1β	GCCCTAAACAGATGAAGTGCTC	GAACCAGCATCTTCCTCAG
h-IL12p35	CCTTGCACTTCTGAAGAGATTGA	ACAGGGCCATCATAAAAGAGGT
h-IL23p19	CTCAGGGACAACAGTCAGTTC	ACAGGGCTATCAGGGAGC
h-MDH2	TCGGCCCAGAACAATGCTAAA	GCGGCTTTGGTCTCGATGT
h-SOCS1	TTTTCGCCCTTAGCGTGAAGA	GAGGCAGTCGAAGCTCTCG
h-SOCS3	TGCGCCTCAAGACCTTCAG	GAGCTGTCGCGGATCAGAAA
h-ST2	TTGTCTACCCACGGAACTACA	GCTCTTTCGTATGTTGGTTTCCA
h-TNF-α	CCTCTCTCTAATCAGCCCTCTG	GAGGACCTGGGAGTAGATGAG
h-Tollip	TGGGCCGACTGAACATCAC	GTGGATGACCTTATTCCAGCG

2 μL of 0.2 M HCl or 0.2 M NaOH was added to each aliquot. The samples were heated for 30 min at 65°C and after incubation 2 μL of opposite reagent (NaOH or HCl) was added to each aliquot. 5 μL of sample or NAD^+ (β-nicotinamide adenine dinucleotide hydrate; Sigma) standard was then mixed with 85 μL of reaction mix and 60 μL of fluorescence mix in a black 96-well plate. The reaction mix consisted of 100 mM bicine (N,N-bis(2-hydroxyethyl)glycine; Sigma), 0.6 mM ethanol (Sigma), and 5 mM EDTA (Life Technologies). The fluorescence mix consisted of 0.5 mM PMS (phenazine methosulfate; Sigma), 0.05 mM resazurin (Sigma), and 0.2 mg of ADH (alcohol dehydrogenase; Sigma). The reaction was incubated for 15 min at RT and fluorescence (excitation/emission maxima = 540/586 nm) was measured on an ELISA reader (BioTek) (n = 3 to 5).

2.7. HDAC Activity Assay. HDAC Fluorometric Cellular Activity Assay BML-AK503 (FLUOR DE LYS, Enzo Life Sciences, Inc., Farmingdale, NY) was used to determine HDAC activity in PBMCs pretreated with C4 (30 min) and then stimulated with H37Rv (30 min). Subsequently PBMCs were incubated with acetylated substrate for 2 hours, after which a developer was added to generate a fluorescent signal from the deacetylated substrate. Fluorescence was measured on a microplate reader (BioTek). Trichostatin A (TSA) was used as a positive control for HDAC inhibition (n = 5 to 6).

2.8. Flow Cytometry. PBMCs were treated with 50 μmol C4 for 1 h and stimulated with 1 μg/mL H37Rv or 10 ng/mL LPS for 7 days. Subsequently cells were restimulated with 200 μL RPMI supplemented with 10% serum, Golgi-plug inhibitor (GPI Brefeldin A; 1 μg/mL, BD Pharmingen), PMA (phorbol 12-myristate 13-acetate; 50 μg/mL, Sigma-Aldrich), and ionomycin (1 μg/mL, Sigma-Aldrich) for 4–6 h at 37°C and 5% CO_2. Cells were then washed with PBA (PBS 1% BSA (albumin from bovine serum)) and stained extracellularly for 30 min with CD4-PeCys7 (ITK) for T-helper 17 (Th17) cells at 4°C. Next, cells were washed and permeabilized by fix and perm buffer (eBioscience) according to the manufacturer's protocol for 45–60 min at 4°C. Finally cells were washed and resuspended in 300 μL PBA to be measured using the Cytomics FC500 (Beckman Coulter) (n = 8).

Cell death was measured by staining PBMCs with Annexin V-FITC (BioVision) and Propidium Iodide (PI) (Invitrogen Molecular Probes). Cells were incubated in the dark on ice with Annexin-V staining solution (RPMI supplemented with 5 mM $CaCl_2$ and 0.1 μL/mL Annexin-V) for 15 minutes. Subsequently PBMCs were stained with PI for 5 minutes. Cells were measured with the Cytomics FC500 (Beckman Coulter, Woerden, Netherlands), and data were analysed using CXP analysis software v2.2 (Beckman Coulter) (n = 3 to 5).

2.9. Statistical Analysis. All data were analysed using a paired nonparametric Wilcoxon signed-rank test, as the data were not normally distributed. Differences were considered statistically significant at p value < 0.05. Data are shown as cumulative results of levels obtained in all volunteers (means ± SEM).

3. Results

3.1. Short-Chain Fatty Acids Inhibit Mtb-Induced Cytokine Responses. DM is associated with altered gut microbiota and consequently altered SCFA levels [18–22]. In line with current literature [22, 25–31], we hypothesized that SCFAs have the potential to influence the host inflammatory response against Mtb. In particular we investigated the effects of varying doses of acetate (C2), propionate (C3), and butyrate (C4) on H37Rv-induced cytokine responses, with RPMI as negative

control and LPS as positive control (Figure 1). SCFAs themselves did not induce cytokine production (results not shown) but significantly affected H37Rv-induced cytokine release. C2, C3, and C4 significantly, dose-dependently decreased H37Rv-induced production of proinflammatory cytokines TNF-α, IL-1β, and IL-17, while nonsignificant effects were found for IL-6, IFN-γ, and IL-22 production. In contrast, C3 and C4 induced a significant increase in H37Rv-induced production of the anti-inflammatory cytokine IL-10. Similarly, C3 and C4 but not C2 decreased LPS-induced production of TNF-α and IL-6, while the release of IL-1β was significantly decreased in response to all three SCFAs (results not shown). LPS did not induce production of IFN-γ, IL-17, or IL-22. Moreover, all three SCFAs incurred a dose-dependent, nonsignificant decrease in LPS-induced IL-10 production (results not shown).

Overall, C4 resulted in some of the most significant changes in cytokine responses (Figure 1(b)). Moreover, the potency of butyrate in reducing cytokine responses to H37Rv and LPS was greater than that for the other SCFAs. Importantly, changes in cytokine levels could not be explained by altered pH levels or cell death (Supplementary Figure 1 A and B in Supplementary Material available online at http://dx.doi.org/10.1155/2016/6014631). Therefore, following this screen, we continued our study with C4 at a concentration of 50 μM, which is physiologically relevant because it is comparable to human plasma concentrations [39].

3.2. Influence of Butyrate on HDAC Expression and Activity. Butyrate is reported to be a strong HDAC inhibitor. Since this might account for its anti-inflammatory effects [41–44], we examined the effect of C4 on HDAC expression and activity. C4 significantly decreased HDAC8 but not HDAC1 gene expression upon H37Rv stimulation of PBMCs (Figure 2(a)). Consistent with previous reports [36, 42–44], C4 at a high dose of 1 mM decreased HDAC activity upon both RPMI and H37Rv stimulation. However, different from its effect on gene expression, C4 at a physiological dose of 50 μM had no effect on actual HDAC activity (Figure 2(b)), while trichostatin A (TSA, positive control) strongly decreased HDAC activity. These data suggest that butyrate's inhibition of HDAC activity is unlikely to play a role in the effects of low doses of C4 on Mtb-induced inflammatory responses and stresses the importance of studying the effects of butyrate at physiologically relevant concentrations.

3.3. The Effects of Butyrate on TLR-Signalling Mediators and the Eicosanoid Pathway. Signalling of Toll-like receptors (TLRs), important receptors for Mtb recognition [45–47], is controlled by feedback mechanisms regulated by several intracellular kinases [48, 49]. Because impaired Mtb recognition and insufficient TLR signalling may account for the anti-inflammatory effects of C4, we examined whether C4 affected these feedback loops. However, C4 had no effect on phosphorylation of the MAP kinases p38, ERK (Figure 3(a)), or JNK (Supplementary Figure 2). C4 has also been reported to induce expression of inhibitors of TLR signalling pathways [50], but we found that C4 significantly decreased mRNA expression of TLR signalling inhibitors SOCS1 and Tollip and did not affect expression of SOCS3 or ST2 (Figure 3(b)). Of note, these results were not explained by cell death (Supplementary Figure 1 B).

Aside from TLR signalling, C4 possibly exerts its anti-inflammatory effects through modulation of the eicosanoid pathway. Eicosanoids, oxygenated metabolites of arachidonic acid, modulate the host immune response to Mtb [51–55]. C4 has been reported to upregulate key enzymes of the eicosanoid pathway upon LPS stimulation [30], but a reverse effect has also been described [56]. We did not observe a significant impact of C4 on transcript levels of cyclooxygenase 2 (COX-2), one of the main eicosanoid enzymes, upon H37Rv or LPS stimulation (Supplementary Figure 3 A). Alternatively, C4 has been described to induce release of the anti-inflammatory prostaglandin PGE_2 [26, 30, 57]. Inhibition of PGE_2 with aspirin could not counteract the inhibitory effects of C4 on TNF-α and IL-1β cytokine responses upon either H37Rv or LPS stimulation (Supplementary Figure 3 B). The eicosanoid pathway is therefore unlikely to be the mediator pathway through which C4 exerts its anti-inflammatory effects.

3.4. Influence of Butyrate on Cellular Metabolism. Another possible explanation for butyrate's anti-inflammatory effects is its influence on cellular metabolism. A recent paper described that microbiota have a strong effect on energy homeostasis in the mammalian colon and showed that C4 regulates different aspects of energy metabolism acting as an important energy source for colonocytes [58]. Contrary to this previous study, we observed no effects of C4 on cellular lactate production, the NAD^+/NADH redox ratio, TCA cycle gene expression (Figure 4), or β-oxidation (Supplementary Figure 4). These data strongly suggest that C4 modulates the immune response to Mtb independently of cellular metabolism.

3.5. Butyrate Transcriptionally Influences Cytokine Responses to Mtb, Possibly Mediated through IL-10 Induction. We next examined whether the inhibitory effect of C4 on Mtb-induced proinflammatory cytokine responses, with a concomitant increase in anti-inflammatory IL-10 production (Figure 1) and decrease in Th17 proliferation (Supplementary Figure 5 A), was also present at the level of gene transcription. C4 led to a decrease in TNF-α, IL-12, and IL-23 mRNA levels upon H37Rv stimulation and a parallel increase in IL-10 mRNA (Figure 5(a)), while no effect on production of the anti-inflammatory cytokine IL-1Ra was observed (Supplementary Figure 5 B). These data point to IL-10 as a possible intermediary mediator of the anti-inflammatory effects of C4. We therefore assessed whether removing IL-10 protein from the cellular environment could counteract the inhibitory effects of C4. To this end, we pretreated PBMCs with cycloheximide (CHX), an inhibitor of translation. Stimulation of PBMCs with H37Rv in the presence of C4 in combination with CHX resulted in higher TNF-α responses, as compared to incubation with H37Rv and C4 alone. Upon LPS stimulation, this effect was not present (Figure 5(b)). We subsequently examined whether

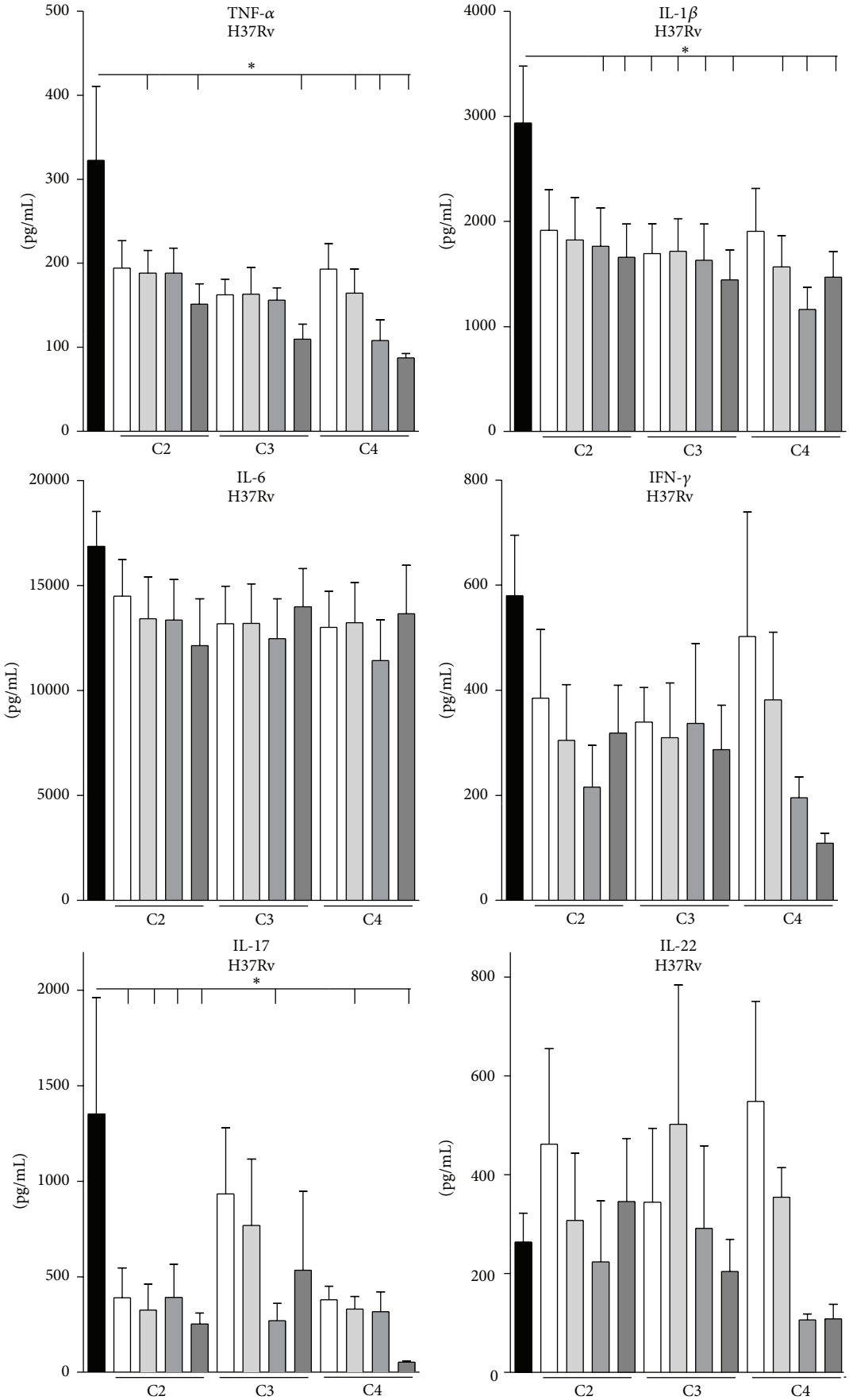

Figure 1: Continued.

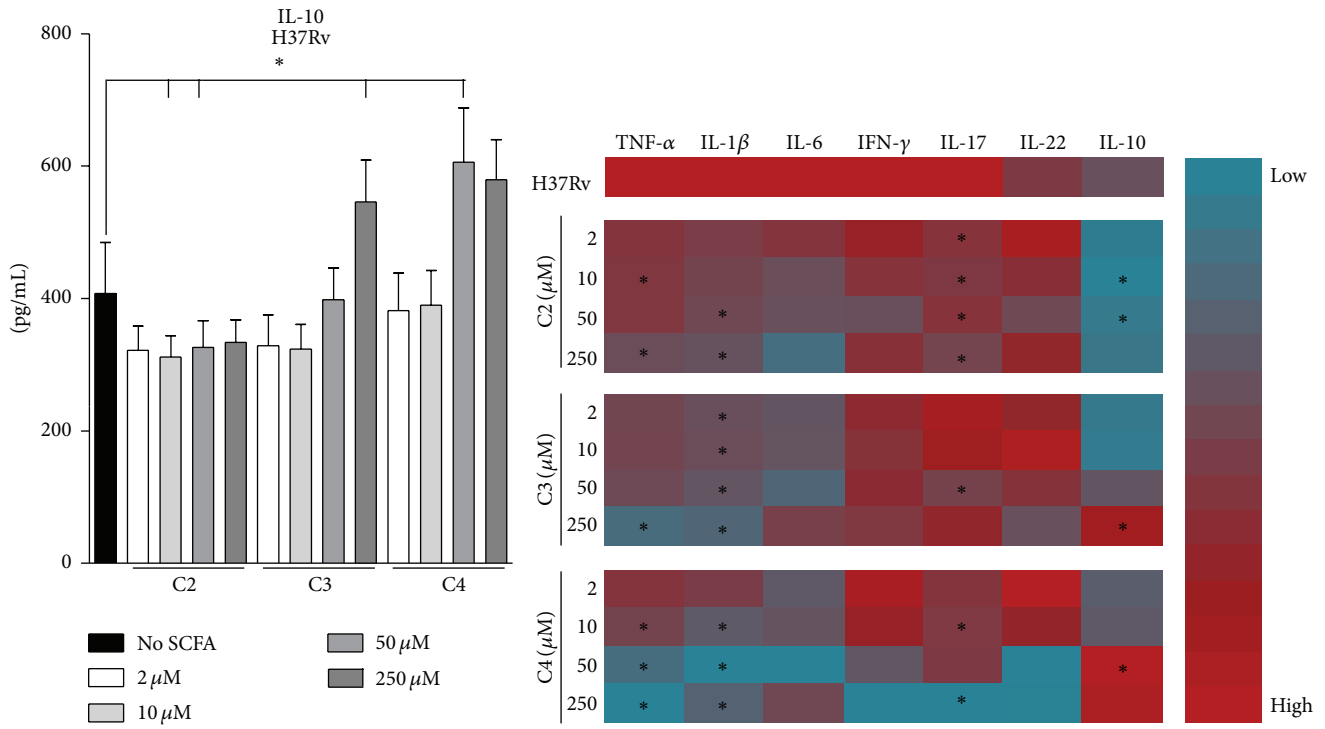

Figure 1: Short-chain fatty acids inhibit Mtb-induced cytokine responses. (a) PBMCs were preincubated with 2–250 μM SCFAs for 1 h prior to stimulation with Mtb lysate for 24 h and 7 d. Hereafter TNF-α, IL-6, IL-10, IFN-γ, IL-17, and IL-22 were measured in supernatants by ELISA. Data are means ± SEM ($n = 6$), using Wilcoxon signed-rank test, representative of 2 independent experiments. $^{*}p < 0.05$. (b) Heat map of log-transformed mean cytokine responses as measured by ELISA, showing cytokines upregulated (red) and downregulated (blue) upon H37Rv stimulation in the presence of different doses of SCFAs. Cytokine responses are shown as compared to H37Rv stimulation alone. $^{*}p < 0.05$.

blocking IL-10 specifically using an anti-IL-10 antibody could counteract the inhibitory effects of C4 on proinflammatory cytokine response. Blocking IL-10 completely restored IL-6 cytokine responses in response to H37Rv and C4, while TNF-α and IL-1β production was partly restored (Figure 5(c)). This suggests an important role for intermediary protein synthesis, specifically IL-10, in mediating the anti-inflammatory effects of C4.

4. Discussion

DM is associated with a threefold increased risk of active TB, but the underlying immunological mechanisms remain largely unknown [3, 12, 13]. Alterations in the gut microbiota of DM patients are associated with changes in plasma SCFA concentrations. Multiple papers have reported a decrease in C4-producing bacteria in type 2 DM patients [18, 19, 21, 23, 24]. We here show that SCFAs, especially C4, exhibit anti-inflammatory properties; low doses of C4 decreased Mtb-induced proinflammatory cytokine responses on both the transcriptional level and the translational level, while production of IL-10 was increased. This anti-inflammatory effect was independent of HDAC activity, Toll-like receptor signalling, the eicosanoid pathway, or cellular metabolism.

We observed a general anti-inflammatory effect of C2, C3, and C4 on Mtb-induced cytokine production. C4 induced some of the most significant and most potent changes in cytokine responses, which is in line with published results [29], although our study is the first to examine the effects of physiological concentrations of SCFAs on Mtb-induced cytokine responses *in vitro*. Several observations were made regarding the effect of SCFA on cytokines. Firstly, the inhibitory effect of all three SCFAs on production of TNF-α and IL-1β was comparable for Mtb and LPS stimulation. However, while C3 and C4 had a clear effect on LPS-induced IL-6 release, this was not found for Mtb. This suggests that SCFAs do not affect Mtb-induced IL-6, although IL-6 has been assigned an important role in Mtb host responses [59–62]. Secondly, C2, C3, and C4 had a much stronger inhibitory effect on T-cell derived cytokine IL-17 than on T-cell derived cytokines IFN-γ and IL-22. Because C4 also strongly decreased Th17 proliferation (Supplementary Figure 5 A), SCFAs may affect Th17 subsets more than other T-cell subsets. This may be of great relevance since Th17 cells, and IL-17 in particular, have been reported to be essential in protective immunity against Mtb [63, 64] but inversely associated with DM complications [65–67]. Lastly, the stimulatory effect of C3 and C4 on anti-inflammatory IL-10 release was Mtb-specific and was not seen with LPS stimulation. IL-10 has

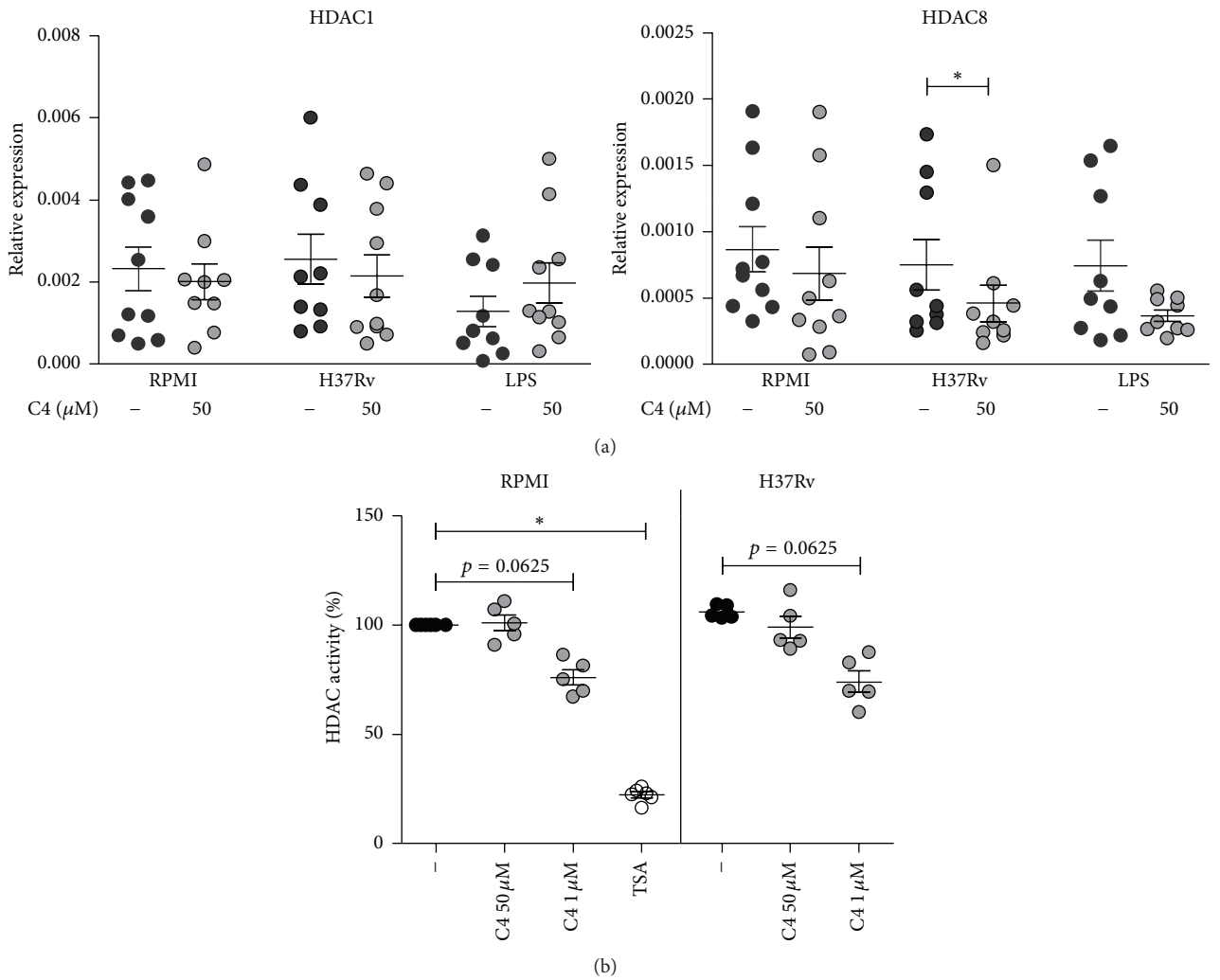

Figure 2: Influence of butyrate on HDAC expression and activity. (a) PBMCs were preincubated with 50 μM C4 for 1 h prior to stimulation with Mtb lysate or LPS for 4 h. Gene expression levels of HDAC1 and HDAC8 were measured by qPCR. Data are means ± SEM ($n = 10$), using Wilcoxon signed-rank test, representative of 3 independent experiments. $^{*}p < 0.05$. (b) Percentage of general HDAC activity relative to RPMI stimulated PBMCs, as measured by levels of substrate deacetylation after 30 min of preincubation with C4 (50 μM) and 30 min of stimulation with Mtb lysate. Data are means ± SEM ($n = 5$ to 6), using Wilcoxon signed-rank test, representative of 3 independent experiments. $^{*}p < 0.05$.

been delineated as an important mediator in Mtb infection: it has been reported to block bacterial killing in Mtb-infected macrophages, suppress multinucleated giant cell formation and cytokine production, and inhibit the development of protective immunity [68–74]. In contrast to TB, IL-10 may have a protective role in type 2 DM by reducing insulin resistance and obesity [75–77]. Therefore, the increase in IL-10 production we see as induced by C4 is very relevant for the course of both DM and TB disease.

We examined several possible mechanisms underlying the effect of C4 on cytokine production, starting with HDAC activity, which is known to be inhibited by SCFAs. C4 at a physiological low dose of 50 μM had little effect, while millimolar concentrations of C4 (as used in other studies [36, 41–44]) decreased HDAC activity upon H37Rv stimulation. This is expected as IC_{50} values of HDAC inhibition by C4 are >100 μM, depending on the class of HDAC [43]. The strongest effect was noted for HDAC8, which is reported to be most sensitive to C4 [43]. This argues that physiological C4 concentrations in human plasma do not exert HDAC inhibition and underlines the importance of using physiological concentrations within *in vitro* experimental models.

In contrast to a previous study [50], we observed a decreased gene expression of the TLR modulatory factors SOCS1 and Tollip when PBMCs were stimulated in the presence of C4, which thus cannot explain the inhibitory effects on cytokine production. This, together with our data showing that C4 does not affect MAP kinase activity, suggests that C4 does not act at the level of TLR signalling, as shown previously [36].

As a third possible mechanism, we assessed whether C4 exerts its effects through eicosanoid metabolism. The eicosanoid pathway is under influence of SCFAs [30, 56] and may modulate the host response to Mtb [51–55]. C4 did not

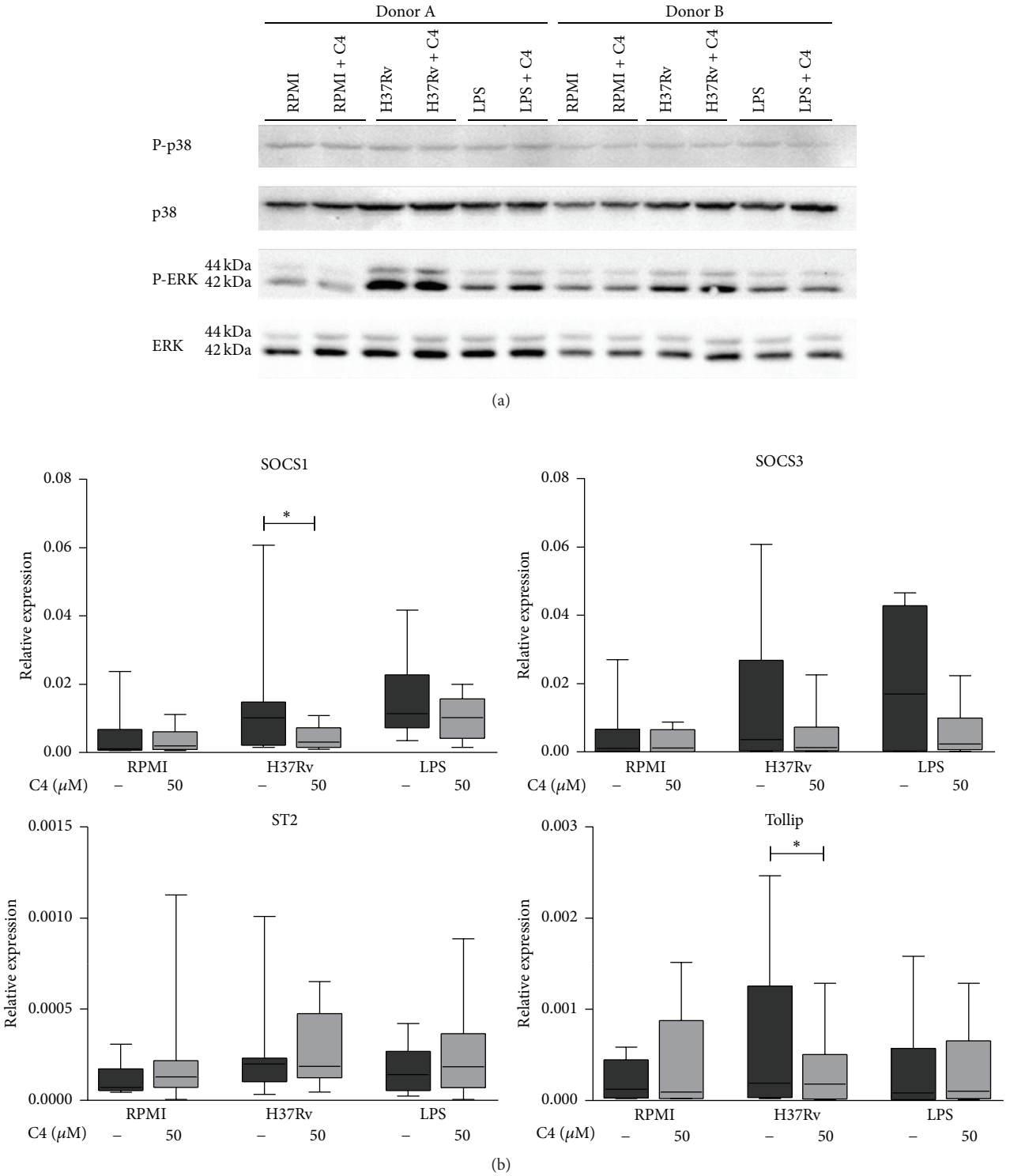

Figure 3: The effects of butyrate on TLR signalling mediators. (a) PBMCs were preincubated with 50 μM C4 (1 h) and stimulated with Mtb lysate or LPS. Cell lysates were harvested at 30 min after stimulation. Phospho-p38, p38, phospho-ERK, and ERK protein levels were determined by Western blot using specific antibodies ($n = 2$). (b) Gene expression levels of SOCS1, SOCS3, ST2, and Tollip in PBMCs preincubated with 50 μM C4 (1 h) and stimulated with Mtb lysate or LPS (4 h) as measured by qPCR. The box plot represents median with first and third quartiles; the whiskers represent minimum and maximum values. $n = 10$, using Wilcoxon signed-rank test, representative of 3 independent experiments. $^{*}p < 0.05$.

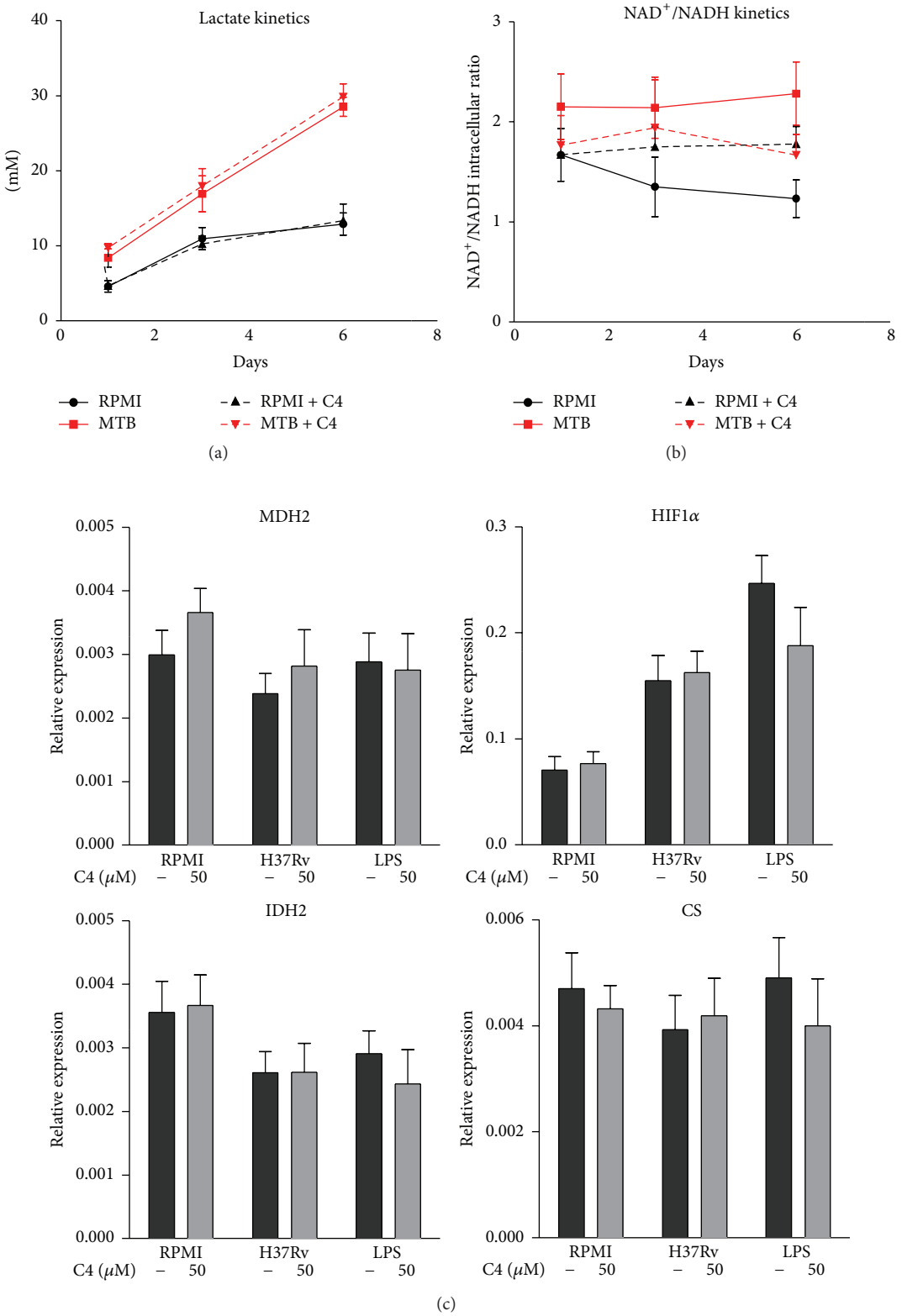

Figure 4: Influence of butyrate on cellular metabolism. (a and b) Kinetics of lactate production (a) and intracellular NAD^+/NADH ratios (b) from days 1, 3, and 7 of PBMCs preincubated with 50 μM C4 (1 h) with and without stimulation with Mtb lysate. Data are means ± SEM (n = 3 to 5), using Wilcoxon signed-rank test, representative of 1-2 independent experiments. (c) Expression levels of glycolysis and TCA cycle genes in PBMCs preincubated with 50 μM C4 (1 h) and stimulated with Mtb lysate or LPS (4 h) as measured by qPCR. Data are means ± SEM (n = 6), using Wilcoxon signed-rank test, representative of 2 independent experiments.

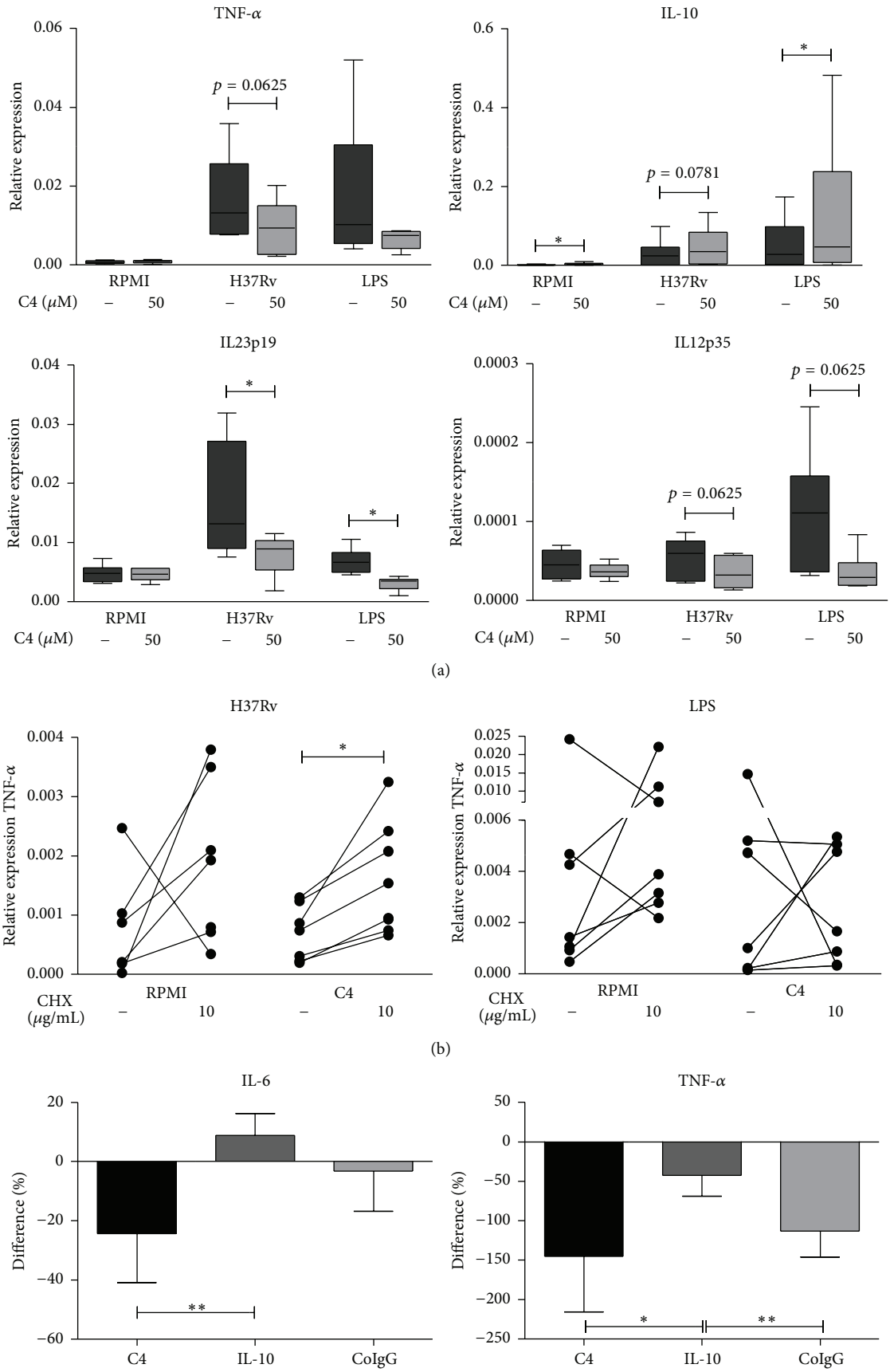

Figure 5: Continued.

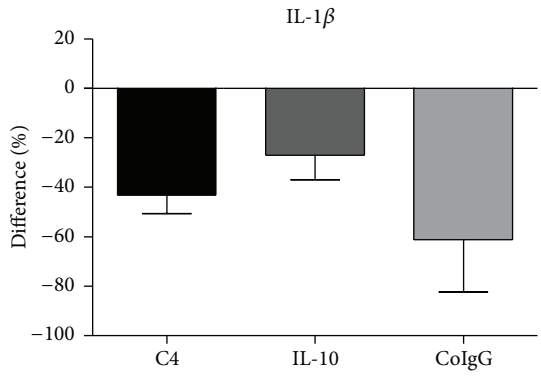

(c)

Figure 5: Butyrate transcriptionally influences cytokine responses to Mtb, possibly mediated through IL-10. (a) Cytokine gene expression levels in PBMCs preincubated with 50 μM C4 for 1 h prior to stimulation with Mtb lysate or LPS for 4 h, as measured by qPCR. The box plot represents median with first and third quartiles; the whiskers represent minimum and maximum values. $n = 6$ to 10, using Wilcoxon signed-rank test, representative of 2+ independent experiments. $^{*}p < 0.05$. (b) To block translation, PBMCs were preincubated with cycloheximide (CHX) for 1 h prior to 1 h incubation with C4 (50 μM). TNF-α transcript levels were measured by qPCR 4 h after stimulation with Mtb lysate or LPS. Data are single values ($n = 6$ to 7), using Wilcoxon signed-rank test, representative of 3 independent experiments. $^{*}p < 0.05$. (c) To block IL-10 activity, PBMCs were preincubated with IL-10 and C4 (50 μM) for 1 h. IL-6, TNF-α, and IL-1β production was measured by ELISA after 24 h of stimulation with Mtb lysate. Data are means ± SEM ($n = 10$ to 12), using Wilcoxon signed-rank test, representative of 4 independent experiments.

affect expression of COX-2, a key enzyme in the eicosanoid pathway, in contrast to previous reports that used supraphysiological C4 concentrations [30, 56]. In addition, inhibition of the eicosanoid pathway using aspirin did not counteract the effects of C4. Therefore, the eicosanoid pathway is unlikely to be involved in mediating the effects of C4.

The effect of diabetes on the host immune response to Mtb might also be explained by altered cellular metabolism, with a possible role for SCFA. Cellular metabolism is increasingly linked to immunology [78–80]. One previous study noted that C4 influences metabolic processes in colonocytes [58], which use butyrate as their primary energy source [58]. However, we did not observe any effect of C4 on lactate production, the redox status, TCA cycle gene expression, or β-oxidation in PBMCs. We therefore conclude that cellular metabolism does not mediate the effect of C4 on Mtb-induced cytokine production.

Finally, we further examined the effect of C4 on the anti-inflammatory cytokine IL-10. IL-10 is detrimental to TB outcome, while it may improve DM symptoms [68–77]. In line with previous studies [33, 81, 82], we report an upregulation in IL-10 production induced by C4. Removal of all intermediary protein, including IL-10, from PBMCs stimulated with H37Rv and C4 led to a significant increase in TNF-α transcript, thereby counteracting the decrease in TNF-α production induced by C4. Moreover, blocking IL-10 specifically fully restored IL-6 responses in PBMCs stimulated with H37Rv and C4 and partly restored TNF-α and IL-1β responses. These data suggest that the anti-inflammatory cytokine IL-10 may play a role in the inhibitory effects of C4 on Mtb-induced inflammatory responses.

Currently, much research focuses on modulation of the gut microbiota in order to treat obesity and type 2 DM [83–86]. Administration of sodium butyrate or butyrate-inducing probiotics in mice significantly increased plasma insulin levels and insulin sensitivity and suppressed body weight gain [87–89]. The anti-inflammatory effects of C4 may attenuate the chronic inflammatory state associated with type 2 DM, thereby improving DM symptoms. If chronic inflammation is a causal factor of the impaired host response to Mtb in type 2 DM patients, attenuation of this hyperinflammatory state may improve not only DM but also TB outcome in patients with coincident DM and TB disease.

Some limitations of our study need to be addressed. Firstly, we studied the effects of C4 on Mtb-induced inflammation in PBMCs *in vitro*. SCFA levels have been shown to be altered in DM patients [18–22], but this *in vitro* model does not include other aspects of the pathophysiology of DM such as hyperglycemia, hyperinsulinemia, or dyslipidemia, phenomena which have also been reported to affect immunity [90–94]. Furthermore, DM medications possibly interfere with the intestinal microbiota and immune responses in patients [95–97]. It is therefore unclear how accurately our *in vitro* model reflects the *in vivo* situation in DM patients.

In conclusion, we show an anti-inflammatory effect of low, physiological doses of C4 on Mtb-induced inflammatory responses. The anti-inflammatory cytokine IL-10 may play a role in mediating the inhibitory effects of C4 on the host immune response to Mtb. Further studies are needed to precisely explore the pathways by which physiological concentrations of C4 exert their anti-inflammatory effects and to define the mechanism of increased TB sensitivity in type 2 DM patients. Moreover, current research on modulating gut microbiota in DM should include its possible effects on TB.

Conflict of Interests

The authors declare that there is no conflict of interests regarding the publication of this paper.

Acknowledgment

This study was supported by the TANDEM (Tuberculosis and Diabetes Mellitus) Grant of the ECFP7 (European Union's Seventh Framework Programme) under Grant Agreement no. 305279.

References

[1] WHO, *Global Tuberculosis Report 2014*, World Health Organization, Geneva, Switzerland, 2014, http://apps.who.int/iris/bitstream/10665/137094/1/9789241564809_eng.pdf?ua=1.

[2] IDF, *IDF Diabetes Atlas Update Poster*, IDF, 6th edition, 2014, http://www.idf.org/sites/default/files/EN_6E_Atlas_Full_0.pdf.

[3] C. Y. Jeon and M. B. Murray, "Diabetes mellitus increases the risk of active tuberculosis: a systematic review of 13 observational studies," *PLoS Medicine*, vol. 5, no. 7, article e152, 2008.

[4] R. Ruslami, R. E. Aarnoutse, B. Alisjahbana, A. J. A. M. Van Der Ven, and R. Van Crevel, "Implications of the global increase of diabetes for tuberculosis control and patient care," *Tropical Medicine and International Health*, vol. 15, no. 11, pp. 1289–1299, 2010.

[5] B. Dixon, "Diabetes and tuberculosis: an unhealthy partnership," *The Lancet Infectious Diseases*, vol. 7, no. 7, p. 444, 2007.

[6] B. I. Restrepo and L. S. Schlesinger, "Impact of diabetes on the natural history of tuberculosis," *Diabetes Research and Clinical Practice*, vol. 106, no. 2, pp. 191–199, 2014.

[7] C. R. Stevenson, N. G. Forouhi, G. Roglic et al., "Diabetes and tuberculosis: the impact of the diabetes epidemic on tuberculosis incidence," *BMC Public Health*, vol. 7, article 234, 2007.

[8] M. A. Baker, H.-H. Lin, H.-Y. Chang, and M. B. Murray, "The risk of tuberculosis disease among persons with diabetes mellitus: a prospective cohort study," *Clinical Infectious Diseases*, vol. 54, no. 6, pp. 818–825, 2012.

[9] C. Y. Jeon, M. B. Murray, and M. A. Baker, "Managing tuberculosis in patients with diabetes mellitus: why we care and what we know," *Expert Review of Anti-Infective Therapy*, vol. 10, no. 8, pp. 863–868, 2012.

[10] M. E. Jimenez-Corona, L. P. Cruz-Hervert, L. García-García et al., "Association of diabetes and tuberculosis: impact on treatment and post-treatment outcomes," *Thorax*, vol. 68, no. 3, pp. 214–220, 2013.

[11] B. Alisjahbana, E. Sahiratmadja, E. J. Nelwan et al., "The effect of type 2 diabetes mellitus on the presentation and treatment response of pulmonary tuberculosis," *Clinical Infectious Diseases*, vol. 45, no. 4, pp. 428–435, 2007.

[12] A. L. Riza, F. Pearson, C. Ugarte-Gil et al., "Clinical management of concurrent diabetes and tuberculosis and the implications for patient services," *The Lancet Diabetes and Endocrinology*, vol. 2, no. 9, pp. 740–753, 2014.

[13] K. Ronacher, S. A. Joosten, R. van Crevel, H. M. Dockrell, G. Walzl, and T. H. M. Ottenhoff, "Acquired immunodeficiencies and tuberculosis: focus on HIV/AIDS and diabetes mellitus," *Immunological Reviews*, vol. 264, no. 1, pp. 121–137, 2015.

[14] N. P. Kumar, V. V. Banurekha, D. Nair et al., "Coincident prediabetes is associated with dysregulated cytokine responses in pulmonary tuberculosis," *PLoS ONE*, vol. 9, no. 11, Article ID e112108, 2014.

[15] N. P. Kumar, P. J. George, P. Kumaran, C. K. Dolla, T. B. Nutman, and S. Babu, "Diminished systemic and antigen-specific type 1, type 17, and other proinflammatory cytokines in diabetic and prediabetic individuals with latent mycobacterium tuberculosis infection," *The Journal of Infectious Diseases*, vol. 210, no. 10, pp. 1670–1678, 2014.

[16] N. P. Kumar, R. Sridhar, V. V. Banurekha, M. S. Jawahar, T. B. Nutman, and S. Babu, "Expansion of pathogen-specific T-helper 1 and T-helper 17 cells in pulmonary tuberculosis with coincident type 2 diabetes mellitus," *Journal of Infectious Diseases*, vol. 208, no. 5, pp. 739–748, 2013.

[17] B. I. Restrepo, S. P. Fisher-Hoch, P. A. Pino et al., "Tuberculosis in poorly controlled type 2 diabetes: altered cytokine expression in peripheral white blood cells," *Clinical Infectious Diseases*, vol. 47, no. 5, pp. 634–641, 2008.

[18] J.-P. Furet, L.-C. Kong, J. Tap et al., "Differential adaptation of human gut microbiota to bariatric surgery-induced weight loss: links with metabolic and low-grade inflammation markers," *Diabetes*, vol. 59, no. 12, pp. 3049–3057, 2010.

[19] F. H. Karlsson, V. Tremaroli, I. Nookaew et al., "Gut metagenome in European women with normal, impaired and diabetic glucose control," *Nature*, vol. 498, no. 7452, pp. 99–103, 2013.

[20] N. Larsen, F. K. Vogensen, F. W. J. van den Berg et al., "Gut microbiota in human adults with type 2 diabetes differs from non-diabetic adults," *PLoS ONE*, vol. 5, no. 2, Article ID e9085, 2010.

[21] J. Qin, J. Wang, Y. Li et al., "A metagenome-wide association study of gut microbiota in type 2 diabetes," *Nature*, vol. 490, no. 7418, pp. 55–60, 2012.

[22] K. M. Maslowski, A. T. Vieira, A. Ng et al., "Regulation of inflammatory responses by gut microbiota and chemoattractant receptor GPR43," *Nature*, vol. 461, no. 7268, pp. 1282–1286, 2009.

[23] M. Remely, E. Aumueller, C. Merold et al., "Effects of short chain fatty acid producing bacteria on epigenetic regulation of FFAR3 in type 2 diabetes and obesity," *Gene*, vol. 537, no. 1, pp. 85–92, 2014.

[24] X. Zhang, D. Shen, Z. Fang et al., "Human gut microbiota changes reveal the progression of glucose intolerance," *PLoS ONE*, vol. 8, no. 8, Article ID e71108, 2013.

[25] U. Böcker, T. Nebe, F. Herweck et al., "Butyrate modulates intestinal epithelial cell-mediated neutrophil migration," *Clinical and Experimental Immunology*, vol. 131, no. 1, pp. 53–60, 2003.

[26] M. A. Cox, J. Jackson, M. Stanton et al., "Short-chain fatty acids act as antiinflammatory mediators by regulating prostaglandin E_2 and cytokines," *World Journal of Gastroenterology*, vol. 15, no. 44, pp. 5549–5557, 2009.

[27] L. Klampfer, J. Huang, T. Sasazuki, S. Shirasawa, and L. Augenlicht, "Inhibition of interferon gamma signaling by the short chain fatty acid butyrate," *Molecular Cancer Research*, vol. 1, no. 11, pp. 855–862, 2003.

[28] M.-C. Maa, M. Y. Chang, M.-Y. Hsieh et al., "Butyrate reduced lipopolysaccharide-mediated macrophage migration by suppression of Src enhancement and focal adhesion kinase activity," *Journal of Nutritional Biochemistry*, vol. 21, no. 12, pp. 1186–1192, 2010.

[29] K. Meijer, P. de Vos, and M. G. Priebe, "Butyrate and other short-chain fatty acids as modulators of immunity: what relevance for health?" *Current Opinion in Clinical Nutrition and Metabolic Care*, vol. 13, no. 6, pp. 715–721, 2010.

[30] J. J. Kovarik, M. A. Hölzl, J. Hofer et al., "Eicosanoid modulation by the short-chain fatty acid n-butyrate in human monocytes," *Immunology*, vol. 139, no. 3, pp. 395–405, 2013.

[31] S. Tedelind, F. Westberg, M. Kjerrulf, and A. Vidal, "Anti-inflammatory properties of the short-chain fatty acids acetate and propionate: a study with relevance to inflammatory bowel disease," *World Journal of Gastroenterology*, vol. 13, no. 20, pp. 2826–2832, 2007.

[32] M. A. R. Vinolo, H. G. Rodrigues, R. T. Nachbar, and R. Curi, "Regulation of inflammation by short chain fatty acids," *Nutrients*, vol. 3, no. 10, pp. 858–876, 2011.

[33] E. Bailón, M. Cueto-Sola, P. Utrilla et al., "Butyrate in vitro immune-modulatory effects might be mediated through a proliferation-related induction of apoptosis," *Immunobiology*, vol. 215, no. 11, pp. 863–873, 2010.

[34] T. Kurita-Ochiai, K. Ochiai, and K. Fukushima, "Butyric acid-induced T-cell apoptosis is mediated by caspase-8 and -9 activation in a Fas-independent manner," *Clinical and Diagnostic Laboratory Immunology*, vol. 8, no. 2, pp. 325–332, 2001.

[35] M. Aoyama, J. Kotani, and M. Usami, "Butyrate and propionate induced activated or non-activated neutrophil apoptosis via HDAC inhibitor activity but without activating GPR-41/GPR-43 pathways," *Nutrition*, vol. 26, no. 6, pp. 653–661, 2010.

[36] P. V. Chang, L. Hao, S. Offermanns, and R. Medzhitov, "The microbial metabolite butyrate regulates intestinal macrophage function via histone deacetylase inhibition," *Proceedings of the National Academy of Sciences of the United States of America*, vol. 111, no. 6, pp. 2247–2252, 2014.

[37] J.-S. Park, E.-J. Lee, J.-C. Lee, W.-K. Kim, and H.-S. Kim, "Anti-inflammatory effects of short chain fatty acids in IFN-gamma-stimulated RAW 264.7 murine macrophage cells: involvement of NF-kappaB and ERK signaling pathways," *International Immunopharmacology*, vol. 7, no. 1, pp. 70–77, 2007.

[38] S. M. Behar, C. J. Martin, M. G. Booty et al., "Apoptosis is an innate defense function of macrophages against *Mycobacterium tuberculosis*," *Mucosal Immunology*, vol. 4, no. 3, pp. 279–287, 2011.

[39] J. H. Cummings, E. W. Pomare, H. W. J. Branch, C. P. E. Naylor, and G. T. MacFarlane, "Short chain fatty acids in human large intestine, portal, hepatic and venous blood," *Gut*, vol. 28, no. 10, pp. 1221–1227, 1987.

[40] C.-T. Zhu and D. M. Rand, "A hydrazine coupled cycling assay validates the decrease in redox ratio under starvation in *Drosophila*," *PLoS ONE*, vol. 7, no. 10, Article ID e47584, 2012.

[41] E. P. M. Candido, R. Reeves, and J. R. Davie, "Sodium butyrate inhibits histone deacetylation in cultured cells," *Cell*, vol. 14, no. 1, pp. 105–113, 1978.

[42] J. R. Davie, "Inhibition of histone deacetylase activity by butyrate," *Journal of Nutrition*, vol. 133, no. 7, supplement, pp. 2485S–2493S, 2003.

[43] M. C. P. Cleophas, T. O. Crisan, H. Lemmers et al., "Suppression of monosodium urate crystal-induced cytokine production by butyrate is mediated by the inhibition of class I histone deacetylases," *Annals of the Rheumatic Diseases*, 2015.

[44] M. Kilgore, C. A. Miller, D. M. Fass et al., "Inhibitors of class 1 histone deacetylases reverse contextual memory deficits in a mouse model of Alzheimer's disease," *Neuropsychopharmacology*, vol. 35, no. 4, pp. 870–880, 2010.

[45] J. Kleinnijenhuis, M. Oosting, L. A. B. Joosten, M. G. Netea, and R. Van Crevel, "Innate immune recognition of *Mycobacterium tuberculosis*," *Clinical and Developmental Immunology*, vol. 2011, Article ID 405310, 12 pages, 2011.

[46] T. K. Means, S. Wang, E. Lien, A. Yoshimura, D. T. Golenbock, and M. J. Fenton, "Human Toll-like receptors mediate cellular activation by *Mycobacterium tuberculosis*," *Journal of Immunology*, vol. 163, no. 7, pp. 3920–3927, 1999.

[47] Y. Bulut, K. S. Michelsen, L. Hayrapetian et al., "*Mycobacterium tuberculosis* heat shock proteins use diverse Toll-like receptor pathways to activate pro-inflammatory signals," *The Journal of Biological Chemistry*, vol. 280, no. 22, pp. 20961–20967, 2005.

[48] L. A. J. O'Neill, D. Golenbock, and A. G. Bowie, "The history of Toll-like receptors—redefining innate immunity," *Nature Reviews Immunology*, vol. 13, no. 6, pp. 453–460, 2013.

[49] M. Y. Peroval, A. C. Boyd, J. R. Young, and A. L. Smith, "A critical role for MAPK signalling pathways in the transcriptional regulation of toll like receptors," *PLoS ONE*, vol. 8, no. 2, Article ID e51243, 2013.

[50] S.-M. Gao, C.-Q. Chen, L.-Y. Wang et al., "Histone deacetylases inhibitor sodium butyrate inhibits JAK2/STAT signaling through upregulation of SOCS1 and SOCS3 mediated by HDAC8 inhibition in myeloproliferative neoplasms," *Experimental Hematology*, vol. 41, no. 3, pp. 261.e4–270.e4, 2013.

[51] S. M. Behar, M. Divangahi, and H. G. Remold, "Evasion of innate immunity by *Mycobacterium tuberculosis*: is death an exit strategy?" *Nature Reviews Microbiology*, vol. 8, no. 9, pp. 668–674, 2010.

[52] M. Chen, M. Divangahi, H. Gan et al., "Lipid mediators in innate immunity against tuberculosis: opposing roles of PGE_2 and LXA_4 in the induction of macrophage death," *Journal of Experimental Medicine*, vol. 205, no. 12, pp. 2791–2801, 2008.

[53] M. Divangahi, M. Chen, H. Gan et al., "Mycobacterium tuberculosis evades macrophage defenses by inhibiting plasma membrane repair," *Nature Immunology*, vol. 10, no. 8, pp. 899–906, 2009.

[54] J. R. Moreno, I. E. García, M. D. L. L. G. Hernández, D. A. Leon, R. Marquez, and R. H. Pando, "The role of prostaglandin E_2 in the immunopathogenesis of experimental pulmonary tuberculosis," *Immunology*, vol. 106, no. 2, pp. 257–266, 2002.

[55] F. G. M. Snijdewint, P. Kaliński, E. A. Wierenga, J. D. Bos, and M. L. Kapsenberg, "Prostaglandin E2 differentially modulates cytokine secretion profiles of human T helper lymphocytes," *The Journal of Immunology*, vol. 150, no. 12, pp. 5321–5329, 1993.

[56] X. Tong, L. Yin, and C. Giardina, "Butyrate suppresses Cox-2 activation in colon cancer cells through HDAC inhibition," *Biochemical and Biophysical Research Communications*, vol. 317, no. 2, pp. 463–471, 2004.

[57] M. Usami, K. Kishimoto, A. Ohata et al., "Butyrate and trichostatin A attenuate nuclear factor kappaB activation and tumor necrosis factor alpha secretion and increase prostaglandin E2 secretion in human peripheral blood mononuclear cells," *Nutrition Research*, vol. 28, no. 5, pp. 321–328, 2008.

[58] D. R. Donohoe, N. Garge, X. Zhang et al., "The microbiome and butyrate regulate energy metabolism and autophagy in the mammalian colon," *Cell Metabolism*, vol. 13, no. 5, pp. 517–526, 2011.

[59] R. K. Dutta, M. Kathania, M. Raje, and S. Majumdar, "IL-6 inhibits IFN-gamma induced autophagy in *Mycobacterium tuberculosis* H37Rv infected macrophages," *International Journal of Biochemistry and Cell Biology*, vol. 44, no. 6, pp. 942–954, 2012.

[60] C. H. Ladel, C. Blum, A. Dreher, K. Reifenberg, M. Kopf, and S. H. E. Kaufmann, "Lethal tuberculosis in interleukin-6-deficient mutant mice," *Infection and Immunity*, vol. 65, no. 11, pp. 4843–4849, 1997.

[61] A. N. Martinez, S. Mehra, and D. Kaushal, "Role of interleukin 6 in innate immunity to *Mycobacterium tuberculosis* infection,"

The Journal of Infectious Diseases, vol. 207, no. 8, pp. 1253–1261, 2013.

[62] V. Nagabhushanam, A. Solache, L.-M. Ting, C. J. Escaron, J. Y. Zhang, and J. D. Ernst, "Innate inhibition of adaptive immunity: *Mycobacterium tuberculosis*-induced IL-6 inhibits macrophage responses to IFN-gamma," *Journal of Immunology*, vol. 171, no. 9, pp. 4750–4757, 2003.

[63] R. Gopal, L. Monin, S. Slight et al., "Unexpected role for IL-17 in protective immunity against hypervirulent *Mycobacterium tuberculosis* HN878 infection," *PLoS Pathogens*, vol. 10, no. 5, Article ID e1004099, 2014.

[64] S. A. Khader, G. K. Bell, J. E. Pearl et al., "IL-23 and IL-17 in the establishment of protective pulmonary CD4+ T cell responses after vaccination and during *Mycobacterium tuberculosis* challenge," *Nature Immunology*, vol. 8, no. 4, pp. 369–377, 2007.

[65] N. Afzal, S. Zaman, F. Shahzad, K. Javaid, A. Zafar, and A. H. Nagi, "Immune mechanisms in type-2 diabetic retinopathy," *Journal of Pakistan Medical Association*, vol. 65, no. 2, pp. 159–163, 2015.

[66] N. Afzal, K. Javaid, W. Sami et al., "Inverse relationship of serum IL-17 with type-II diabetes retinopathy," *Clinical Laboratory*, vol. 59, no. 11-12, pp. 1311–1317, 2013.

[67] N. Afzal, S. Zaman, A. Asghar et al., "Negative association of serum IL-6 and IL-17 with type-II diabetes retinopathy," *Iranian Journal of Immunology*, vol. 11, no. 1, pp. 40–48, 2014.

[68] J. C. Cyktor, B. Carruthers, R. A. Kominsky, G. L. Beamer, P. Stromberg, and J. Turner, "IL-10 inhibits mature fibrotic granuloma formation during *Mycobacterium tuberculosis* infection," *The Journal of Immunology*, vol. 190, no. 6, pp. 2778–2790, 2013.

[69] N. P. Kumar, V. Gopinath, R. Sridhar et al., "IL-10 dependent suppression of type 1, type 2 and type 17 cytokines in active pulmonary tuberculosis," *PLoS ONE*, vol. 8, no. 3, Article ID e59572, 2013.

[70] B. Liang, Y. Guo, Y. Li, and H. Kong, "Association between IL-10 gene polymorphisms and susceptibility of tuberculosis: evidence based on a meta-analysis," *PLoS ONE*, vol. 9, no. 2, Article ID e88448, 2014.

[71] F. W. McNab, J. Ewbank, A. Howes et al., "Type I IFN induces IL-10 production in an IL-27-independent manner and blocks responsiveness to IFN-γ for production of IL-12 and bacterial killing in *Mycobacterium tuberculosis*-infected macrophages," *Journal of Immunology*, vol. 193, no. 7, pp. 3600–3612, 2014.

[72] P. S. Redford, A. Boonstra, S. Read et al., "Enhanced protection to *Mycobacterium tuberculosis* infection in IL-10-deficient mice is accompanied by early and enhanced Th1 responses in the lung," *European Journal of Immunology*, vol. 40, no. 8, pp. 2200–2210, 2010.

[73] P. S. Redford, P. J. Murray, and A. O'Garra, "The role of IL-10 in immune regulation during M. tuberculosis infection," *Mucosal Immunology*, vol. 4, no. 3, pp. 261–270, 2011.

[74] P. Shrivastava and T. Bagchi, "IL-10 modulates in vitro multinucleate giant cell formation in human tuberculosis," *PLoS ONE*, vol. 8, no. 10, Article ID e77680, 2013.

[75] E.-G. Hong, J. K. Hwi, Y.-R. Cho et al., "Interleukin-10 prevents diet-induced insulin resistance by attenuating macrophage and cytokine response in skeletal muscle," *Diabetes*, vol. 58, no. 11, pp. 2525–2535, 2009.

[76] M. Straczkowski, I. Kowalska, A. Nikolajuk, A. Krukowska, and M. Gorska, "Plasma interleukin-10 concentration is positively related to insulin sensitivity in young healthy individuals," *Diabetes Care*, vol. 28, no. 8, pp. 2036–2037, 2005.

[77] E. van Exel, J. Gussekloo, A. J. M. De Craen, M. Frölich, A. B.-V. D. Wiel, and R. G. J. Westendorp, "Low production capacity of interleukin-10 associates with the metabolic syndrome and type 2 diabetes: the Leiden 85-plus study," *Diabetes*, vol. 51, no. 4, pp. 1088–1092, 2002.

[78] K. Ganeshan and A. Chawla, "Metabolic regulation of immune responses," *Annual Review of Immunology*, vol. 32, pp. 609–634, 2014.

[79] D. J. Kominsky, E. L. Campbell, and S. P. Colgan, "Metabolic shifts in immunity and inflammation," *The Journal of Immunology*, vol. 184, no. 8, pp. 4062–4068, 2010.

[80] E. Pearce and E. Pearce, "Metabolic pathways in immune cell activation and quiescence," *Immunity*, vol. 38, no. 4, pp. 633–643, 2013.

[81] M. D. Säemann, G. A. Böhmig, C. H. Osterreicher et al., "Anti-inflammatory effects of sodium butyrate on human monocytes: potent inhibition of IL-12 and up-regulation of IL-10 production," *The FASEB Journal*, vol. 14, no. 15, pp. 2380–2382, 2000.

[82] T. E. Weber and B. J. Kerr, "Butyrate differentially regulates cytokines and proliferation in porcine peripheral blood mononuclear cells," *Veterinary Immunology and Immunopathology*, vol. 113, no. 1-2, pp. 139–147, 2006.

[83] R. Burcelin, M. Serino, C. Chabo, V. Blasco-Baque, and J. Amar, "Gut microbiota and diabetes: from pathogenesis to therapeutic perspective," *Acta Diabetologica*, vol. 48, no. 4, pp. 257–273, 2011.

[84] A. M. Caricilli and M. J. A. Saad, "The role of gut microbiota on insulin resistance," *Nutrients*, vol. 5, no. 3, pp. 829–851, 2013.

[85] B. M. Carvalho and M. J. A. Saad, "Influence of gut microbiota on subclinical inflammation and insulin resistance," *Mediators of Inflammation*, vol. 2013, Article ID 986734, 13 pages, 2013.

[86] A. Puddu, R. Sanguineti, F. Montecucco, and G. L. Viviani, "Evidence for the gut microbiota short-chain fatty acids as key pathophysiological molecules improving diabetes," *Mediators of Inflammation*, vol. 2014, Article ID 162021, 9 pages, 2014.

[87] Z. Gao, J. Yin, J. Zhang et al., "Butyrate improves insulin sensitivity and increases energy expenditure in mice," *Diabetes*, vol. 58, no. 7, pp. 1509–1517, 2009.

[88] H. V. Lin, A. Frassetto, E. J. Kowalik Jr. et al., "Butyrate and propionate protect against diet-induced obesity and regulate gut hormones via free fatty acid receptor 3-independent mechanisms," *PLoS ONE*, vol. 7, no. 4, Article ID e35240, 2012.

[89] H. Yadav, J.-H. Lee, J. Lloyd, P. Walter, and S. G. Rane, "Beneficial metabolic effects of a probiotic via butyrate-induced GLP-1 hormone secretion," *The Journal of Biological Chemistry*, vol. 288, no. 35, pp. 25088–25097, 2013.

[90] S. Devaraj, S. K. Venugopal, U. Singh, and I. Jialal, "Hyperglycemia induces monocytic release of interleukin-6 via induction of protein kinase C-α and -β," *Diabetes*, vol. 54, no. 1, pp. 85–91, 2005.

[91] C. Sun, L. Sun, H. Ma et al., "The phenotype and functional alterations of macrophages in mice with hyperglycemia for long term," *Journal of Cellular Physiology*, vol. 227, no. 4, pp. 1670–1679, 2012.

[92] D. I. Gomez, M. Twahirwa, L. S. Schlesinger, and B. I. Restrepo, "Reduced *Mycobacterium tuberculosis* association with monocytes from diabetes patients that have poor glucose control," *Tuberculosis*, vol. 93, no. 2, pp. 192–197, 2013.

[93] J. M. Han, S. J. Patterson, M. Speck, J. A. Ehses, and M. K. Levings, "Insulin inhibits IL-10-mediated regulatory T cell function: implications for obesity," *The Journal of Immunology*, vol. 192, no. 2, pp. 623–629, 2014.

[94] A. T. Shamshiev, F. Ampenberger, B. Ernst, L. Rohrer, B. J. Marsland, and M. Kopf, "Dyslipidemia inhibits Toll-like receptor-induced activation of CD8alpha-negative dendritic cells and protective Th1 type immunity," *The Journal of Experimental Medicine*, vol. 204, no. 2, pp. 441–452, 2007.

[95] K. A. Pyra, D. C. Saha, and R. A. Reimer, "Prebiotic fiber increases hepatic acetyl CoA carboxylase phosphorylation and suppresses glucose-dependent insulinotropic polypeptide secretion more effectively when used with metformin in obese rats," *Journal of Nutrition*, vol. 142, no. 2, pp. 213–220, 2012.

[96] N.-R. Shin, J.-C. Lee, H.-Y. Lee et al., "An increase in the *Akkermansia* spp. population induced by metformin treatment improves glucose homeostasis in diet-induced obese mice," *Gut*, vol. 63, no. 5, pp. 727–735, 2014.

[97] H. A. Hirsch, D. Iliopoulos, and K. Struhl, "Metformin inhibits the inflammatory response associated with cellular transformation and cancer stem cell growth," *Proceedings of the National Academy of Sciences of the United States of America*, vol. 110, no. 3, pp. 972–977, 2013.

Hindawi Publishing Corporation
Journal of Diabetes Research
Volume 2016, Article ID 6314368, 9 pages
http://dx.doi.org/10.1155/2016/6314368

Research Article

Genetic Analysis and Follow-Up of 25 Neonatal Diabetes Mellitus Patients in China

Bingyan Cao,[1] Chunxiu Gong,[1] Di Wu,[1] Chaoxia Lu,[2] Fang Liu,[2] Xiaojing Liu,[3] Yingxian Zhang,[3] Yi Gu,[1] Zhan Qi,[4] Xiaoqiao Li,[1] Min Liu,[1] Wenjing Li,[1] Chang Su,[1] Xuejun Liang,[1] and Mei Feng[5]

[1]*Department of Pediatric Endocrinology and Genetic Metabolism, Beijing Children's Hospital, Capital Medical University, Beijing 100045, China*
[2]*Institute of Basic Medical Sciences, Peking Union Medical College, Beijing 100730, China*
[3]*Department of Endocrinology and Genetic Metabolism, Zhengzhou Children's Hospital, Zhengzhou 450053, China*
[4]*Department of Pediatrics, Beijing Children's Hospital, Capital Medical University, Beijing 100045, China*
[5]*Department of Endocrinology, Shanxi Children's Hospital, Taiyuan 030013, China*

Correspondence should be addressed to Chunxiu Gong; chunxiugong@163.com

Received 4 July 2015; Revised 29 September 2015; Accepted 30 September 2015

Academic Editor: Adam Kretowski

Aims. To study the clinical features, genetic etiology, and the correlation between phenotype and genotype of neonatal diabetes mellitus (NDM) in Chinese patients. *Methods.* We reviewed the medical records of 25 NDM patients along with their follow-up details. Molecular genetic analysis was performed. We compared the HbA1c levels between PNDM group and infantile-onset T1DM patients. *Results.* Of 25 NDM patients, 18 (72.0%) were PNDM and 7 (28.0%) were TNDM. Among 18 PNDM cases, 6 (33.3%) had known KATP channel mutations (KATP-PNDM). There were six non-KATP mutations, five novel mutations, including *INS*, *EIF2AK3* ($n = 2$), *GLIS3*, and *SLC19A2*, one known *EIF2AK3* mutation. There are two *ABCC8* mutations in TNDM cases and one paternal UPD6q24. Five of the six KATP-PNDM patients were tried for glyburide transition, and 3 were successfully switched to glyburide. Mean HbA1c of PNDM was not significantly different from infantile onset T1DM (7.2% versus 7.4%, $P = 0.41$). *Conclusion.* PNDM accounted for 72% of NDM patients. About one-third of PNDM and TNDM patients had KATP mutations. The genetic etiology could be determined in 50% of PNDM and 43% of TNDM cases. PNDM patients achieved good glycemic control with insulin or glyburide therapy. The etiology of NDM suggests polygenic inheritance.

1. Introduction

Neonatal diabetes mellitus (NDM) occurs within the first six months of life. Depending on clinical outcomes, it is classified into Transient Neonatal Diabetes Mellitus (TNDM) and Permanent Neonatal Diabetes Mellitus (PNDM) [1]. TNDM, which accounts for 50% to 60% of NDM, goes into remission after treatment for an average period of 12 weeks. PNDM, on the other hand, is a lifelong disease without remission. TNDM is usually diagnosed within one month after birth with a median age at diagnosis of 6 days. It is characterized by intrauterine growth retardation (IUGR), less frequent diabetic ketoacidosis, requirement of low initial dose of insulin for treatment, and early remission. About 50% of TNDM patients, however, may have relapse in adulthood and require lifelong insulin maintenance therapy [2]. The clinical features of TNDM and PNDM overlap, and the typing is based on clinical remission on follow-up. PNDM should be considered if insulin requirement persists for up to 18 months [3].

More than 20 pathogenic genes have been identified in PNDM, of which the most common are *KCNJ11* and *ABCC8* encoding the Kir6.2 and SUR1 subunits of KATP channel accounting for 40% to 60% [4, 5]. Mutations in *KCNJ11* and *ABCC8* lead to persistence of KATP channel in the open state inducing membrane hyperpolarization and impaired insulin secretion. The *INS* gene mutation is the secondary cause. Other infrequent mutations include *GCK*, *PDX1*,

EIF2AK3, *PTF1A*, *IPF1*, *GLIS3*, *RFX6*, *SLC2A2*, *SLC19A2*, *FOXP3*, *GATA6*, *MNX1*, *NEUROD1*, and *HNF1B* [6]. TNDM is caused by defects associated with overexpression of paternally expressed genes in the imprinted region of chromosome 6q24 in 70% cases. Three reported defects include (1) paternal uniparental disomy of chromosome 6 (UPD6); (2) paternally inherited duplication of 6q24 (duplication); and (3) maternal hypomethylation at 6q24 [7]. About 26% of the patients contain mutations in *KCNJ11*, *ABCC8*, *INS*, or *HNF1B*. The genetic etiology remains currently unknown in 40% of NDM cases [8].

In vitro and clinical studies suggest that treatment with oral sulfonylurea can close KATP channel and improve glycemic control and neuropsychological development [9, 10]. Only patients with mutations identified in the *KCNJ11* or *ABCC8* genes benefit from sulfonylureas. However, 10% of patients with *KCNJ11* and 15% *ABCC8* mutations fail to achieve glycemic control when insulin therapy is switched to oral sulfonylureas. Therefore, molecular diagnosis is vital not only in accurate typing but also for better prognostication [5].

We summarized the clinical features, molecular typing, treatment, and 1- to 13-year follow-up of 25 cases of NDM in order to better understand the clinical treatment and prognosis.

2. Subjects and Methods

2.1. Patients. The present study included 25 patients diagnosed with NDM including 18 PNDM and 7 TNDM from Beijing Children's Hospital, Zhengzhou Children's Hospital, and Shanxi Children's Hospital, from 2001 to 2013. Diagnostic criteria for NDM [11] were as follows: (1) age at onset <6 months; (2) hyperglycemia sustained for ≥2 weeks; (3) insulin dependence; and (4) exclusion of hyperglycemia caused by stress and infection and drug therapies.

The symptoms at onset and laboratory reports were obtained from medical records. The family history of diabetes mellitus, especially glucose metabolism in parents, was recorded for every patient. Clinical follow-up started with diagnosis at 3- to 6-month intervals, subsequently. Height and weight were measured using normal growth chart of Chinese children. The self-reported frequency of severe hypoglycemia was recorded, and HbA1c was measured at every visit. All the data between years 2012 and 2013 were analyzed.

Patients aged below 18 months, showing normal blood glucose (fasting glucose < 5.6 mmol/L, postprandial glucose < 7.8 mmol/L) and HbA1c (<6.0%) without the need for insulin or oral hypoglycemic treatment, were defined as TNDM. Patients aged more than 18 months and requiring insulin or oral hypoglycemic agents to maintain normal glucose were defined as PNDM [3].

This study was approved by the Ethics Committee of Beijing Children's Hospital of Capital Medical University and all parents have signed the informed consent.

2.2. Sample Collection and DNA Extraction. Upon NDM diagnosis, 2 mL of blood samples was collected in ethylenediaminetetraacetic acid (EDTA) tubes from 25 patients and stored at −20°C. DNA was extracted from peripheral blood leukocytes using kits (QIAGEN, Valencia, CA).

2.3. Gene Mutation Analysis. Samples were tested for *KCNJ11* and *ABCC8* mutations using Sanger sequencing annually, usually within 1 year after diagnosis. Sanger sequencing of the *EIF2AK3* was undertaken in one patient because of the presence of typical features of *Wolcott-Rallison syndrome*. The negative PNDM cases were screened using Ion Torrent platform as described previously [12]. Genes associated with NDM include *KCNJ11*, *ABCC8*, *INS*, *GCK*, *PDX1*, *EIF2AK3*, *PTF1A*, *IPF1*, *GLIS3*, *RFX6*, *SLC2A2*, *SLC19A2*, *FOXP3*, *GATA6*, *MNX1*, *NEUROD1*, and *HNF1B*. Subsequently, Sanger sequencing was used to validate the screened mutations and in parents for inherited or *de novo* mutations. Confirmed mutations were then searched in the human gene mutation database (HGMD), dbSNPl38, thousand genomes, and recent reviews. For all mutations, software Polyphen-2 was used to predict the pathogenicity (http://genetics.bwh.harvard.edu/pph2/).

Microarray comparative genomic hybridization was performed in 5 TNDM patients, in whom *ABCC8* and *KCNJ11* mutations were excluded. We used 4 μL–10 μL of patient DNA for the assay, DNA amplification, tagging, and hybridization according to the manufacturer's protocol. The array slides were scanned on an iScan Reader (Illumina). Data analysis was performed using GenomeStudio version 2010.1, KaryoStudio version 1.2 (Illumina, standard settings), and Nexus Copy Number 5.0 (BioDiscovery, El Segundo, CA, USA). The positive case was subjected to haplotype analysis using highly polymorphic short tandem repeat (STR) markers that span both arms of chromosome 6 [13].

We recalled KATP-PNDM patients to switch from insulin injection to oral glyburide, usually within 18 months of diagnosis. The transfer was carried out using a protocol that was similar to that described previously [8]. Glyburide was started at a dose of 0.1 mg per kilogram twice daily and was increased daily by 0.2 mg per kilogram. The dose of glyburide was increased until insulin independence was achieved or the dose was at least 0.8 mg per kilogram per day. The change to sulfonylureas was considered to be successful if a patient was able to stop insulin treatment completely at any dose of glyburide and was deemed to be unsuccessful if insulin was still required with a dose of glyburide at least 0.8 mg per kilogram per day. All trials were performed during hospitalization.

Type 1 diabetic patients with age of onset between 6 months and 2 years were matched one-to-one with those of PNDM (15 patients with recorded HbA1c). T1DM patients hospitalized during the same period as PNDM group with positive autoimmune antibody (ICA, GAD, or IAA) and comparable age, sex, duration of illness, and time of sample/data collection were selected as the control group. The HbA1c between the two groups was compared. The HbA1c of the PNDM group was tested at least 6 months after glyburide treatment.

2.4. Statistical Analysis. Statistical analysis was performed using chi-square test and Student's t-test using SPSS 19.0

Table 1: Clinical characteristics of NDM patients.

	NDM	PNDM	TNDM
Cases	25	18	7
Male (female)	14 (11)	11 (7)	3 (4)[#]
Birth weight (kg, mean ± SD)	2.6 ± 0.5	2.7 ± 0.5	2.4 ± 0.6[#]
Age at diagnosis (Days, mean ± SD)	74.4 ± 41.4	81.3 ± 42.7	56.7 ± 34.6[#]
DK/DKA (%)	68.0%	77.8%	42.9%[#]
Symptoms (cases)		Infection (6) Decreased responsiveness (5) Polydipsia, polyuria (2) Urine sticky (4) Seizures (2)	Infection (4) Polydipsia, polyuria (1) Seizures (2)
Physical development on follow-up (cases)		Physical and mental retardation (4), others are normal	Intellectual and physical development is normal
Genetic testing (cases)		*KCNJ11* (5) *ABCC8* (1) *INS* (1) *EIF2AK3* (3) *SLC19A2* (1) *GLIS3* (1)	*ABCC8* (2) Paternal uniparental disomy of 6q24 (1)
Therapy (cases)		Glyburide (3) Insulin (15)	Remission in 2 weeks to 1 year after insulin therapy (6)
Average HbA1c at the last follow-up (cases had recorded results)		7.2% (15)	5.5% (5)

[#]No significant differences compared with PNDM ($P > 0.05$).

(SPSS Inc., Chicago, IL, USA) software. Continuous data were analyzed using Student's t-test, and categorical data was analyzed using chi-square test.

3. Results

3.1. Baseline Characteristics of Patients. Table 1 shows the baseline characteristics of 25 NDM patients. Based on follow-up, 18 cases were typed as PNDM (72.0%) and 7 cases as TNDM (28.0%). No statistical differences were found between the two types with age of onset, birth weight, and DK/DKA prevalence ($P > 0.05$) (see Table 1). The clinical features of PNDM and TNDM are summarized in Table 2. All patients were treated with insulin initially. All patients were born to nonconsanguineous parents.

3.2. Genetic Analysis. In PNDM cases, twelve mutations were identified. Direct sequencing identified the most frequent mutations involving KATP channel ($n = 6$) including *KCNJ11* ($n = 5$) and *ABCC8* mutation ($n = 1$), all of which were identified earlier. The non-KATP mutations ($n = 6$) including *INS*, *EIF2AK3* ($n = 3$), *GLIS3*, and *SLC19A2* were identified and five were confirmed as novel mutations. In the TNDM, we found 2 cases harbouring *ABCC8* mutation and 1 case with UPD6. The mutations are summarized in Table 2.

3.3. Follow-Up of NDM Cases

3.3.1. PNDM. All patients were treated with insulin initially. Following stable glucose control with insulin, transition from insulin to oral sulfonylureas was attempted in five of six KATP-PNDM cases. Finally, three cases (60%) were successfully placed on glyburide; one switched back to insulin as there was no response to glyburide; one stopped oral glyburide because of serious gastrointestinal reactions; and in another case glyburide was not tried because of loss of follow-up. The mean HbA1c of PNDM during the last visit was 7.2 ± 0.8%, which was similar to that of the infant-onset T1DM group (Table 3).

Except in 4 PNDM cases, the height and development were found to be normal on follow-up. The patients who presented with convulsion at the onset showed no further convulsions.

Among patients with positive mutations, case 1 carrying *KCNJ11*p.R201H mutation had congenital cataract. Glyburide therapy was also stopped in case 1 due to gastrointestinal reactions and it was switched back to regular insulin treatment with good glycemic control. Case 2 with *KCNJ11*p.R201H mutation and case 3 with *KCNJ11*p.G53S mutation achieved good blood glucose levels with no hypoglycemia with glyburide treatment. Case 5 bearing *KCNJ11*p.E229K mutation was lost to follow-up 1 year after

Table 2: Clinical profile and gene analysis of NDM.

Subtype	Number	Gender	Term or preterm	HbA1c at diagnosis (%)	Age at last visit (yr)	HbA1c (%) at last visit	Height (cm) (percentile)	Weight (kg) (percentile)	Mutant gene	Inherited from		*De novo* mutation	Specific clinical features	Mutation	Zygosity	Insulin/glyburide therapy (age at transfer)
										Father	Mother					
P	1	M	Term	13.7	4.1	6.1%	107.0 (P75)	17.0 (P50)	*KCNJ11*			p.R201H	Congenital cataract	c.602G>A; p.R201H	HET	Insulin/interruption because of side effects (1 yr)
P	2	F	Term	4.0	2.0	6.0%	88.0 (P50–75)	12.5 (P50–75)	*KCNJ11*			p.R201H		c.602G>A; p.R201H	HET	Glyburide response (0.7 mg/kg/d) (3 months)
P	3	M	Term	9.6	1.5	6.5%	81.0 (P25)	11.0 (P10–P25)	*KCNJ11*			p.G53S		c.157C>T; p.G53S	HET	Glyburide response (0.4 mg/kg/d) (7 months)
P	4	M	Term	8.1	2.5	7.5%	85.0 (P3)	11.0 (P3)	*KCNJ11*			p.V59M	iDEND	c.175G>A; p.V59M	HET	Glyburide response (4 months)
P	5	M	Term						*KCNJ11*		p.E229K			c.685G>A; p.E229K	HET	Insulin/no transition because of lost to follow-up
P	6	F	Term	9.6	5.1	8.0%	105.0 (P10)	15.0 (P3–10)	*ABCC8*		p.R825W			c.2473C>T; p.R825W	HET	Insulin/no response (4 months)
P	7	F	Term	9.8	1.5	7.0%	83.0 (P50–75)	11.5 (P25–50)	*INS*					c.293C>A; p.S98I	HET	Insulin
P	8	F	Term	14.2	1.5				*GLIS3*	No sample	No sample		Died of liver and kidney failure at 1.5 years of age	c.2570T>A; p.F857Y	HET	Insulin
P	9	M	Term	10.4	5.0	7.9%	110.0 (P25–P50)	17.5 (P10–P25)	*SLC19A2*	No sample	No sample		Moderate normocytic anemia	c.1213A>G; p.T405A	HET	Insulin
P	10	M	Term	9.5	13.9	7.0%	140.0 (<P3)	30.0 (<P3)	*EIF2AK3*	p.C532STOP			WRS	c.1798A>T; p.C532STOP	HET	Insulin
P	11	F	Term	11.2	1.5	7.5%	74.3 (<P3)	8.0 (<P3)	*EIF2AK3*	p.leu182leufsX19	p.Arg588Ter		WRS	c.1762C>T, p.Arg588Ter; c.544delC, p.leu182leufsX19	HET	Insulin
P	12	F	Term	9.8	4.5	7.5%	106.0 (P50)	15.0 (P10)								Insulin (0.8 IU/kg/d)
P	13	M	Term	15.8	2.0	7.9%	89.5 (P50–P75)	13.0 (P50)								Insulin (based on glucose, injection once every other day)
P	14	M	Term	4.38	0.6		62.0 (<P3)	4.0 (<P3)					Died of DKA at 7 months of age Intellectual and physical retardation			Insulin
P	15	M	Term	5.2	6.0	8.2%	115.0 (P25)	18.5 (P10–P25)								Insulin
P	16	M	Term		5.0	7.4%	113.0 (P75)	20 (P50–75)								Insulin
P	17	M	Term	5.9	3.0	7.3%	98.0 (P50–75)	17.0 (P90)								Insulin
P	18	F	Term		4.0	7.6%	105.0 (P75)	16.0 (P50)								Insulin

Table 2: Continued.

Subtype	Number	Gender	Term or preterm	HbA1c at diagnosis (%)	Age at last visit (yr)	HbA1c (%) at last visit	Height (cm) (percentile)	Weight (kg) (percentile)	Mutant gene	Inherited from Father	Inherited from Mother	*De novo* mutation	Specific clinical features	Mutation	Zygosity	Insulin/glyburide therapy (age at transfer)
T	19	F	Term	7.1	1.8				*ABCC8*		p.G296R			c.886G>A; p.G296R	HET	
T	20	M	Term	10.2	1.8	5.6%	83.6 (P25–50)	11.2 (P25–50)	*ABCC8*		p.D212E			c.636G>T; p.D212E	HET	
T	21	F	Term	9.6	5.8	5.7%	110.5 (P25–50)	20.0 (P50)	UPD6							
T	22	F	Term	7.4	4.8	5.6%	110.0 (P50)	19.0 (P75)								
T	23	M	Term		5.5	5.6%	112.5 (P25–50)	18.0 (P10–25)								
T	24	M	Term	9.9	3.7	5.2%	102.3 (P75)	16.5 (P50–75)								
T	25	F	Term		4.0											

Table 3: Comparison of HbA1c between PNDM and infantile onset T1DM groups.

	PNDM	T1DM	*P* value
N	15	15	
M (F)	10 (5)	10 (5)	1.00
Onset of age (years)	0.2 ± 0.1	1.3 ± 0.5	0.00
Age at follow-up (years)	4.0 ± 2.9	4.4 ± 2.1	0.70
Duration of illness (years)	3.8 ± 2.9	3.1 ± 1.9	0.44
HbA1c at follow-up (%)	7.2 ± 0.8	7.4 ± 0.9	0.41

diagnosis, while he showed good response to initial insulin therapy but failed to undergo glyburide therapy later. Case 6 carrying the *ABCC8* p.R825W mutation failed to respond to glyburide (0.4 mg/kg/d), and the insulin dose was not reduced. During follow-up, insulin therapy once or twice daily was administered to the child depending on the blood glucose level. Case 7 carrying *INS* mutation achieved good glucose control with insulin therapy. All these patients exhibited normal physical and mental development.

PNDM was associated with special syndromes. Case 4 (*KCNJ11*p.V59M) had intellectual and physical retardation without epilepsy and hence was diagnosed as iDEND syndrome. This patient was given intermittent glyburide therapy (following parental request) but died of DKA at 2 years of age in local hospital. Case 8 (*GLIS3* p.F857Y) had liver dysfunction but improved by following supportive therapy. This patient died of liver and kidney failure at 1.5 years of age. Case 9 (*SLC19A2* p.T405A) presented with moderate anemia (hemoglobin, 70 g/L), which improved with oral iron therapy. Case 10 (*EIF2AK3* p.C532STOP) was accompanied with intellectual and physical retardation, short stature, multiple skeletal dysplasia, and hypothyroidism, diagnosed as *Wolcott-Rallison syndrome*. Case 11 who manifested physical retardation and skeletal dysplasia showed compound heterozygous mutations in *EIF2AK3*.

There were three deaths (Cases 4, 8, and 14). Case 14 died of DKA at 7 months of age, several days after diagnosis. The patient also showed weight loss and mental and physical retardation with negative results on genetic screening.

3.3.2. TNDM. Remission among TNDM cases in our cohort was ascertained from 2 weeks to 1 year after diagnosis. None of these patients showed any congenital abnormalities such as macroglossia, umbilical hernia, dysmorphic facial features, hematopoietic dysfunction or abnormal hearing, and heart, liver, or kidney function. The development and height were normal. None of them had acanthosis nigricans. The oldest patient was 5 years old, with no recurrence of diabetes. No specific features were observed in patient carrying *ABCC8* mutations and UPD6 compared with the other TNDM cases carrying negative genetic results.

4. Discussion

The NDM patients generally presented with infection or decreased responsiveness at the onset, without the typical symptoms such as polyuria, polydipsia, polyphagia, and weight loss. In the present study, approximately 30% were TNDM patients, which is similar to the previous reports [4]. There were no differences between PNDM and TNDM patients in age of onset, birth-weight, and prevalence of DKA, making it difficult to clinically distinguish between the two types. Therefore, the typing was based on clinical remission during follow-up. The remission of TNDM cases was from 2 weeks to 1 year. The oldest child on follow-up was 5 years old with no recurrence of diabetes. Of the patients carrying *KCNJ11* and *ABCC8* mutations, there was developmental delay in one patient diagnosed as iDEND, including one with congenital cataract. Busiah et al. [14] found that patients with mutations in KATP channel subunit genes presented with developmental coordination disorders including visual-spatial dyspraxia and attention deficits but not developmental delay or epilepsy. Therefore, adults with a history of neonatal diabetes mellitus should be tested for neuropsychological dysfunction and developmental defects.

We identified six mutations in KATP channel that were previously reported and six non-KATP mutations in PNDM cases, five of which were not identified until now, and found two KATP mutations in TNDM cases. Three cases were placed on glyburide therapy and 15 cases were on insulin therapy, with good glycemic control in most cases.

In this study, we evaluated the gene mutations and clinical manifestations of PNDM cases. We identified two cases of p.R201H mutations, which were the most common *KCNJ11* mutations without neurological abnormalities. These mutations have been confirmed at CpG dinucleotide, resulting in decreased sensitivity of KATP channels to ATP. Glucose stimulation reduces insulin secretion, whereas sulfonylureas stimulate the secretion, explaining the rationale of glyburide therapy. Of the two cases, one was responsive to glyburide and the other presented with severe gastrointestinal reactions and parental worries about side effects and therefore discontinued despite recommendations to the contrary.

The second mutation of *KCNJ11* revealed in the present study was p.V59M. Generally, patients with this mutation cause a triad of developmental delay, epilepsy, and neonatal diabetes (DEND syndrome), or without epilepsy (intermediate DEND (iDEND) syndrome). The neurological symptoms are attributable to the presence of Kir6.2 in nerve and brain tissue. One case with iDEND in the present study responded favorably to oral glyburide therapy. Glyburide not only controls blood glucose levels, but also ameliorates the neurological symptoms. However, this patient died of DKA attributed to glyburide therapy cessation.

The third mutation was *KCNJ11*p.G53S, located between Kir6.2 and SUR1. The patient with this mutation in the present study was successfully switched from insulin to glyburide, leading to HbA1c level of 6.5%.

The fourth mutation was *KCNJ11*p.E229K, which induces NDM without neurological manifestations but was lost to follow-up. As reported, p.E229 and p.G53 mutations cause both PNDM and TNDM [15, 16]. In our study, they were classified as PNDM. The patient with *KCNJ11*p.G53S underwent low dose glyburide (0.4 mg/kg/d), consistent with previous reports [17].

Another case we identified with *ABCC8* p.R825W mutation was not responsive to glyburide transition. The mean effective dosage of glyburide is 0.5~0.6 mg/kg/d for SUR1 mutations [17]. The glyburide dosage of 0.4 mg/kg/d was not effective. The insulin dosage was not reduced during glyburide therapy. The patient manifested nausea and poor appetite. The parents stopped glyburide due to the side effects. At follow-up, the patient was on insulin therapy and refused to be treated with glyburide. Physicians must be cautious before using sulfonylureas as they are not licensed in children and may have side effects. The glyburide transition can only be tried as an inpatient procedure to avoid diabetic ketoacidosis in those young children who may be unresponsive to glyburide and need careful monitoring [18]. Parents who carried the same *KCNJ11* or *ABCC8* mutations showed no neonatal diabetes mellitus symptoms or past history of abnormal glucose metabolism. The phenomenon suggests that KATP mutations have variable clinical phenotypes, with the symptoms varying from TNDM or PNDM. The mild and transient manifestations during neonatal period were missed, with possible risk of relapse in the future. The glucose metabolism of parents carrying the same mutations as their children needs to be monitored.

The success rate of glyburide transition among cases with KATP mutations of 60.0% in the present study is lower than that reported from other countries. One reason for the low success rate could be the side effects of glyburide such as nausea and vomiting that affected its clinical application in infants in the present study. Diarrhea is the common reported side effects of glyburide but has not been seen in our patients. The failed transitions due to side effects were not reported in other studies, suggesting that Chinese children respond differently to glyburide compared with other ethnic groups. The small sample size may be another reason for such a response. We also found a novel *INS* mutation causing simple diabetes.

Other NDM mutations were associated with specific manifestations. Case 1 manifesting mental and physical retardation, hypothyroidism, and multiple epiphyseal dysplasia was diagnosed with WRS, as reported by Sang et al. [19]. Sanger sequencing yielded a sole heterozygous mutation in this patient, which was inherited from father. This nonsense mutation resulted in a truncated protein of 532 amino acid residues. The loss of kinase in the catalytic domain resulted in a complete loss of function. WRS is an autosomal recessive disorder. Therefore, we should also ascertain other genes causing PNDM. The Italian PNDM patient had heterozygous mutations in both *KCNJ11* and *GCK* genes [20], suggesting that NDM may be a polygenic disease. However, no NGS was performed. We decided to monitor the father for diabetic symptoms. Case 18 was also diagnosed as WRS carrying compound heterozygous mutations of *EIF2AK3*, inherited from father and mother, respectively, with one mutation reported and another deletion mutation resulting in a truncated protein. NDM patients with *GLIS3* gene mutation may also manifest congenital hypothyroidism, glaucoma, liver fibrosis, and polycystic kidney disease. The patient with *GLIS3* mutation showed hepatic dysfunction without liver fibrosis and polycystic kidney disease at onset but eventually died of liver and kidney failure 1 year later in a local hospital. The thyroid function was normal in this patient on follow-up. *GLIS3* mutations have been reported to be autosomal recessive resulting in a variable clinical phenotype. Only one heterozygous mutation was found in this patient. Polyphen analysis further indicated a possible causative mutation. Another genetic variant was needed for further study.

SLC19A2 gene mutations causing NDM lead to the development of diabetes, deafness and megaloblastic anemia. This syndrome can be ameliorated by thiamine, so it is called thiamine-responsive megaloblastic anaemia (TRMA) [21]. Our patient with *SLC19A2* mutation exhibited moderate normocytic anemia with no hearing abnormalities at diagnosis. Only one heterozygous mutation was detected by NGS. Polyphen analysis indicated possible causative mutations but not SNP. Another mutation in a non-coding region or a large deletion may be found by Sanger sequencing of the whole gene or with multiplex ligation probe amplification technology (MLPA), respectively.

The genetic etiology of NDM suggests polygenic inheritance. The classification of TNDM and PNDM should be reconsidered. A diagnosis of diabetes in parents who carried the mutations cannot be excluded. We need additional and longer follow-up of cases to establish a TNDM diagnosis or PNDM remission.

Diarrhea is one of the manifestations of IPEX (immune dysregulation, polyendocrinopathy, enteropathy, and X-linked syndrome), which is caused by *FOXP3* mutation. IPEX may also present with autoimmune thyroid disease, exfoliative dermatitis, and sepsis caused by immune dysregulation [22]. Identification of a *FOXP3* mutation suggests possible prenatal testing. Case 14 presenting with diarrhea and fever was negative for *FOXP3* mutations using NGS.

The mutations in KATP channel accounted for 33.3% of PNDM, including 27.8% in *KCNJ11* mutations and 5.6% in *ABCC8* mutations, similar to the reported data. *INS* gene mutation accounted for 5.6%. We diagnosed two cases of WRS (11.2% of all PNDM cases), which is now recognized as the most frequent cause of PNDM in consanguineous children [23, 24]. In addition, rare gene mutations (*GLIS3, SLC19A2*, etc.) also were associated with specific clinical manifestations. Therefore, in view of the high mutation rate of *KCNJ11* in PNDM and high correlation between genotype and phenotype, we suggest screening for *KCNJ11* mutations first in NDM cases, followed by *ABCC8* screen and genes associated with specific complications. It is difficult to distinguish TNDM from PNDM initially during the illness. NGS has been used worldwide to detect mutations in PNDM or TNDM.

PNDM children on insulin and glyburide therapy were found to have good glycemic control (mean HbA1c 7.2%) during follow-up, which is similar to infantile onset T1DM group. It was probably associated with younger age at onset, need for a lower insulin dose, and better residual pancreatic β cell function. The onset age of PNDM and T1DM is usually different, although the duration of illness is comparable, which is the most important factor affecting the HbA1c level.

TNDM is associated with chromosome 6q24 imprinting abnormalities in 70% of cases. The syndrome is associated

with giant tongue, umbilical hernia, facial deformity, kidney abnormalities, congenital heart disease, hypothyroidism, and intrauterine growth retardation (>95%). Array-CGH could be used to detect UPD6 and duplication simultaneously, so it may be a cost-effective genetic analysis method for TNDM cases. In our study, all the TNDM cases did not exhibit the specific manifestations mentioned above. Recurrence of TNDM resulting from *KCNJ11*, *ABCC8*, and 6q24 mutations might respond to treatment with sulfonylurea [3, 25]. It should be noted that the pathophysiological mechanism of 6q24 mutations is not clear and thus the most appropriate treatment remains unclear.

In the present study, PNDM accounted for 72%; the onset symptoms are not typical. Seizure may be seen initially in NDM cases making it remain misdiagnosed. About one-third of PNDM and TNDM patients had KATP mutations. Only one TNDM case had paternal uniparental disomy of chromosome 6q24. The genetic etiology could not be determined in 50% of PNDM and 57% of TNDM cases. However, no maternal hypomethylation at Chr6q24 was detected, which may have affected the mutational analysis of the TNDM cohort. Glyburide was effective in most KATP-PNDM patients. Most NDM patients achieved good glycemic control (HbA1c < 7.5%) and there was no significant difference when compared to infantile onset T1DM.

Conflict of Interests

The authors declare no conflict of interests.

Acknowledgments

A portion of this work was supported by the Open Research Project of Shanghai Key Laboratory of Diabetes Mellitus (SHKLD-KF-1304). The authors thank the patients and their relatives for providing the study samples. They also thank the referring hospitals and clinicians.

References

[1] E. L. Edghill and A. T. Hattersley, "Genetic disorders of the pancreatic beta cell and diabetes (permanent neonatal diabetes and maturity-onset diabetes of the young)," in *Pancreatic Beta Cell in Health and Disease*, S. Seino and G. I. Bell, Eds., pp. 389–420, Springer, Tokyo, Japan, 2008.

[2] I. K. Temple, R. J. Gardner, D. J. G. Mackay, J. C. K. Barber, D. O. Robinson, and J. P. H. Shield, "Transient neonatal diabetes: widening the understanding of the etiopathogenesis of diabetes," *Diabetes*, vol. 49, no. 8, pp. 1359–1366, 2000.

[3] D. J. G. Mackay and I. K. Temple, "Transient neonatal diabetes mellitus type 1," *American Journal of Medical Genetics Part C: Seminars in Medical Genetics*, vol. 154, no. 3, pp. 335–342, 2010.

[4] A. P. Babenko, M. Polak, H. Cavé et al., "Activating mutations in the ABCC8 gene in neonatal diabetes mellitus," *The New England Journal of Medicine*, vol. 355, no. 5, pp. 456–466, 2006.

[5] A. L. Gloyn, E. R. Pearson, J. F. Antcliff et al., "Activating mutations in the gene encoding the ATP-sensitive potassium-channel subunit Kir6.2 and permanent neonatal diabetes," *The New England Journal of Medicine*, vol. 350, no. 18, pp. 1838–1849, 2004.

[6] M. Vaxillaire, A. Bonnefond, and P. Froguel, "The lessons of early-onset monogenic diabetes for the understanding of diabetes pathogenesis," *Best Practice & Research: Clinical Endocrinology & Metabolism*, vol. 26, no. 2, pp. 171–187, 2012.

[7] L. E. Docherty, S. Kabwama, A. Lehmann et al., "Clinical presentation of 6q24 transient neonatal diabetes mellitus (6q24 TNDM) and genotype-phenotype correlation in an international cohort of patients," *Diabetologia*, vol. 56, no. 4, pp. 758–762, 2013.

[8] E. L. Edghill, S. E. Flanagan, A.-M. Patch et al., "Insulin mutation screening in 1,044 patients with diabetes: mutations in the INS gene are a common cause of neonatal diabetes but a rare cause of diabetes diagnosed in childhood or adulthood," *Diabetes*, vol. 57, no. 4, pp. 1034–1042, 2008.

[9] E. R. Pearson, I. Flechtner, P. R. Njølstad et al., "Switching from insulin to oral sulfonylureas in patients with diabetes due to Kir6.2 mutations," *The New England Journal of Medicine*, vol. 355, no. 5, pp. 467–477, 2006.

[10] G. Tonini, C. Bizzarri, R. Bonfanti et al., "Sulfonylurea treatment outweighs insulin therapy in short-term metabolic control of patients with permanent neonatal diabetes mellitus due to activating mutations of the *KCNJ11* (*KIR6.2*) gene," *Diabetologia*, vol. 49, no. 9, pp. 2210–2213, 2006.

[11] International Diabetes Federation, *Global IDF/ISPAD Guideline for Diabetes in Childhood and Adolescents*, International Diabetes Federation, 2011.

[12] C. Gong, S. Huang, C. Su et al., "Congenital hyperinsulinism in Chinese patients: 5-yr treatment outcome of 95 clinical cases with genetic analysis of 55 cases," *Pediatric Diabetes*, 2015.

[13] I. Salahshourifar, A. S. Halim, W. A. W. Sulaiman, and B. A. Zilfalil, "Maternal uniparental heterodisomy of chromosome 6 in a boy with an isolated cleft lip and palate," *American Journal of Medical Genetics Part A*, vol. 152, no. 7, pp. 1818–1821, 2010.

[14] K. Busiah, S. Drunat, L. Vaivre-Douret et al., "Neuropsychological dysfunction and developmental defects associated with genetic changes in infants with neonatal diabetes mellitus: a prospective cohort study," *The Lancet Diabetes & Endocrinology*, vol. 1, no. 3, pp. 199–207, 2013.

[15] T. Klupa, J. Skupien, B. Mirkiewicz-Sieradzka et al., "Efficacy and safety of sulfonylurea use in permanent neonatal diabetes due to KCNJ11 gene mutations: 34-month median follow-up," *Diabetes Technology & Therapeutics*, vol. 12, no. 5, pp. 387–391, 2010.

[16] S. E. Flanagan, A.-M. Patch, D. J. G. Mackay et al., "Mutations in ATP-sensitive K^+ channel genes cause transient neonatal diabetes and permanent diabetes in childhood or adulthood," *Diabetes*, vol. 56, no. 7, pp. 1930–1937, 2007.

[17] M. Rafiq, S. E. Flanagan, A. M. Patch, B. M. Shields, S. Ellard, and A. T. Hattersley, "Effective treatment with oral sulfonylureas in patients with diabetes due to sulfonylurea receptor 1 (SUR1) mutations. Neonatal Diabetes International Collaborative Group," *Diabetes Care*, vol. 31, no. 2, pp. 204–209, 2008.

[18] D. Carmody, C. D. Bell, J. L. Hwang et al., "Sulfonylurea treatment before genetic testing in neonatal diabetes: pros and cons," *Journal of Clinical Endocrinology and Metabolism*, vol. 99, no. 12, pp. E2709–E2714, 2014.

[19] Y. Sang, M. Liu, W. Yang, J. Yan, Chengzhu, and G. Ni, "A novel EIF2AK3 mutation leading to Wolcott-Rallison syndrome

in a Chinese child," *Journal of Pediatric Endocrinology & Metabolism*, vol. 24, no. 3-4, pp. 181–184, 2011.

[20] O. Massa, D. Iafusco, E. D'Amato, A. L. Gloyn, A. T. Hattersley, and B. Pasquino, "KCNJ11 activating mutations in Italian patients with permanent neonatal diabetes. Early onset diabetes study group of the Italian Society of Pediatric Endocrinology and Diabetology," *Human Mutation*, vol. 25, pp. 22–27, 2005.

[21] V. Labay, T. Raz, D. Baron et al., "Mutations in SLC19A2 cause thiamine-responsive megaloblastic anaemia associated with diabetes mellitus and deafness," *Nature Genetics*, vol. 22, no. 3, pp. 300–304, 1999.

[22] R. S. Wildin, S. Smyk-Pearson, and A. H. Filipovich, "Clinical and molecular features of the immunodysregulation, polyendocrinopathy, enteropathy, X linked (IPEX) syndrome," *Journal of Medical Genetics*, vol. 39, no. 8, pp. 537–545, 2002.

[23] H. Demirbilek, V. B. Arya, M. N. Ozbek et al., "Clinical characteristics and molecular genetic analysis of 22 patients with neonatal diabetes from the South-Eastern region of Turkey: predominance of non-KATP channel mutations," *European Journal of Endocrinology*, vol. 172, no. 6, pp. 697–705, 2015.

[24] S. Jahnavi, V. Poovazhagi, S. Kanthimathi, V. Gayathri, V. Mohan, and V. Radha, "EIF2AK3 mutations in South Indian children with permanent neonatal diabetes mellitus associated with Wolcott-Rallison syndrome," *Pediatric Diabetes*, vol. 15, no. 4, pp. 313–318, 2014.

[25] P. Proks, C. Girard, S. Haider et al., "A gating mutation at the internal mouth of the Kir6.2 pore is associated with DEND syndrome," *EMBO Reports*, vol. 6, no. 5, pp. 470–475, 2005.

Hindawi Publishing Corporation
Journal of Diabetes Research
Volume 2016, Article ID 2108909, 10 pages
http://dx.doi.org/10.1155/2016/2108909

Research Article

Tyrosine Is Associated with Insulin Resistance in Longitudinal Metabolomic Profiling of Obese Children

Christian Hellmuth,[1] Franca Fabiana Kirchberg,[1] Nina Lass,[2] Ulrike Harder,[1] Wolfgang Peissner,[1] Berthold Koletzko,[1] and Thomas Reinehr[2]

[1]*Division of Metabolic and Nutritional Medicine, Dr. von Hauner Children's Hospital, Ludwig-Maximilians-University of Munich, Lindwurmstraße 4, 80337 Munich, Germany*
[2]*Department of Pediatric Endocrinology, Diabetes and Nutrition Medicine, Vestische Hospital for Children and Adolescents, University of Witten-Herdecke, Dr. Friedrich Steiner Strasse 5, 45711 Datteln, Germany*

Correspondence should be addressed to Berthold Koletzko; office.koletzko@med.uni-muenchen.de

Received 10 July 2015; Revised 28 August 2015; Accepted 6 September 2015

Academic Editor: Francisco J. Ruperez

In obese children, hyperinsulinaemia induces adverse metabolic consequences related to the risk of cardiovascular and other disorders. Branched-chain amino acids (BCAA) and acylcarnitines (Carn), involved in amino acid (AA) degradation, were linked to obesity-associated insulin resistance, but these associations yet have not been studied longitudinally in obese children. We studied 80 obese children before and after a one-year lifestyle intervention programme inducing substantial weight loss >0.5 BMI standard deviation scores in 40 children and no weight loss in another 40 children. At baseline and after the 1-year intervention, we assessed insulin resistance (HOMA index), fasting glucose, HbA1c, 2 h glucose in an oral glucose tolerance test, AA, and Carn. BMI adjusted metabolite levels were associated with clinical markers at baseline and after intervention, and changes with the intervention period were evaluated. Only tyrosine was significantly associated with HOMA ($p < 0.05$) at baseline and end and with change during the intervention ($p < 0.05$). In contrast, ratios depicting BCAA metabolism were negatively associated with HOMA at baseline ($p < 0.05$), but not in the longitudinal profiling. Stratified analysis revealed that the children with substantial weight loss drove this association. We conclude that tyrosine alterations in association with insulin resistance precede alteration in BCAA metabolism. This trial is registered with ClinicalTrials.gov Identifier NCT00435734.

1. Introduction

Obesity in childhood is strongly associated with cardiovascular risk factors (CRFs) including dyslipidemia, hyperglycaemia, and hypertension [1]. In obese children hyperinsulinaemia and other CRFs are far more commonly found than in normal weight children and adolescents [2–4]. Most metabolic consequences appear to be mediated through insulin resistance (IR) [5]; therefore improving insulin sensitivity seems even more important than weight loss [6]. "Omics" platforms, such as proteomics, transcriptomics, epigenomics, and metabolomics, provide insights into molecular changes and allow assessing biochemical alterations in the development of obesity and IR [7, 8]. While new targets or potential biomarkers are identified in humans with these approaches [9, 10], the role of known metabolites still needs to be evaluated. Particularly, the influence of amino acid (AA) metabolism on the onset of IR still needs clarification. Two recent studies have reported on the untargeted metabolomic approach to study the relation of metabolites to IR in older adults [11] and children [12]. Untargeted metabolomics involves an unbiased screening of all metabolites present in a specimen regardless of chemical class. Targeted metabolomic techniques facilitate the profiling of specific metabolites of interest in a given population, to aid in-depth analysis of metabolic processes in the context of preformed findings. Thus, clinical targeted metabolomics platforms are suitable tools to reveal associations between AA and IR. Different studies depicted associations between IR or type 2 diabetes mellitus (T2DM) and branched-chain amino acids (BCAA), aromatic amino acids (AAA), sulphur containing AA, and other AAs as well as short-chain acylcarnitines (Carn)

involved in AA metabolism in adults [13–23]. BCAA were found to be positively associated with homeostasis model assessment (HOMA), an IR index, in nonobese Chinese men [15] and young Finn adults [16]. Mohorko et al. recently reported elevated serum levels of cysteine (Cys) and tyrosine (Tyr) as early biomarkers for metabolic syndrome in young adults [14]. Newgard et al. showed that BCAA and short-chain Carn derived from BCAA contribute to the development of obesity-associated IR [13]. However, the majority of these studies describe relations of clinical markers to metabolites in cross-sectional settings. Furthermore, such associations are susceptible to confounders, like dietary protein intake that was shown to be higher in obese subjects than in normal weight subjects [15]. A few studies describe the prediction potential of BCAA and AAA for the onset of IR [16, 18, 24]. Although metabolomic analyses in children yield the potential to investigate the early onset of metabolic disease, studies on obese children are lacking. Recently, Newbern et al. reported an association of HOMA with a metabolic signature containing BCAA, uric acid, and long-chain Carn in adolescent boys in a cross-sectional study [25]. A combination of BCAA and AAA was associated with HOMA in obese Hispanic children [26], but only BCAA in Korean children [27]. BCAA pattern and androgen hormone pattern were associated with childhood adiposity and cardiometabolic risk, like HOMA, in another recently published cross-sectional study [12]. Longitudinal studies are necessary to explore stronger association between IR and metabolic alterations. To our knowledge, two longitudinal studies in children have been published so far, showing an association of baseline BCAA with HOMA in healthy American children [28] and in Korean children [27].

We embarked on a longitudinal study on obese children participating in a lifestyle intervention for inducing weight loss to explore the relationship between changes in AA metabolism and IR in the fasting state and after an oral glucose tolerance test (oGTT) in obese European children. Additionally, we analysed the obesity-independent associations of changes during the intervention period in makers of IR, hemoglobin A1c (HbA1c), 2 h glucose in oGTT, and changes of AA and Carn.

2. Methods

2.1. Study. Written informed consent was obtained from all parents of the participants prior to inclusion in the study. The study has been performed according to the Declaration of Helsinki. The local ethics committee of the University of Witten/Herdecke in Germany approved the study (ClinicalTrials.gov Identifier NCT00435734). We studied 80 obese Caucasian children participating in the one-year lifestyle intervention "Obeldicks," which has been described in detail elsewhere [29]. Briefly, this outpatient intervention program is based on promoting regular physical activity, nutrition education, and behavior therapy including individual psychological care of the children and their families. The one-year training program was divided into three phases. In the first one, intensive phase (3 months), the children took part in the nutritional course and in the eating-behavior course in six group-sessions, each lasting for 1.5 hours. Parents were invited to attend six evening classes. In the establishing phase (6 months), individual psychological family therapy was provided (30 minutes/month). In the last phase of the program (accompanying the families back to their everyday lives) (3 months), further individual care was possible, if and when necessary. None of the children in the current study were smokers, took any drugs, or suffered from endocrine disorders or syndromal obesity such as Prader Willi syndrome [30]. Also MC4 receptor mutation was excluded. The children studied were selected at random from the Obeldicks cohort reported previously [30] choosing 40 obese children with substantial weight loss and 40 obese children without weight loss of similar age, gender, pubertal stage, and degree of overweight. We included only children who participated in oGTT both at baseline and after one year. Substantial reduction of overweight was defined by a decrease in standard deviation score of body mass index (BMI-SDS) ≥ 0.5 based on previous studies [31], whereas no reduction of overweight was defined by a decrease in BMI-SDS < 0.15. The metabolomic profile of these children in respect to obesity status and weight loss was previously reported [32].

2.2. Measurements and Sampling. Height was measured to the nearest millimeter using a rigid stadiometer. Weight was measured unclothed to the nearest 0.1 kg using a calibrated balance scale. BMI was calculated as weight in kilograms (kg) divided by the square of height in meters (m^2). The degree of overweight was quantified using Cole's LMS method, which normalized the BMI skewed distribution and expressed BMI as a standard deviation score (BMI-SDS) [33]. Reference data for German children were used [34]. Waist circumference was measured halfway between lower rib and iliac crest.

For longitudinal analysis, blood samples were collected in the fasting state before the intervention and after 1 year. Furthermore, oGTT were performed according to current guidelines [35]. The glucose load was 1.75 g/kg with a maximum of 75 g. Blood samples were taken at 8 a.m. after overnight fasting for at least 10 hours. Following coagulation at room temperature, blood samples were centrifuged for 10 min at 8000 rpm at room temperature and aliquoted. Glucose (Boehringer, Mannheim, Germany), HbA1c (Germany Tinaquant Hemoglobin A1c Gen), and insulin (Abbott, Wiesbaden, Germany) were measured in serum by using commercially available test kits directly. Intra-assay and interassay CVs of glucose, HbA1c, and insulin were less than 5%. HOMA was used to detect the degree of IR [36]. Furthermore, serum samples were stored at −81°C and thawed at room temperature for the metabolomics assay only once.

2.3. Biochemical Measures. Metabolites were qualified and quantified with the Absolute IDQ p 150 kit (Biocrates Life Sciences AG, Innsbruck, Austria) as described previously [32]. Briefly, 10 μL of blood serum was analysed with a flow injection tandem mass spectrometer (FIA-MS/MS). An Agilent 1200 SL series high-performance liquid chromatography system (Agilent, Waldbronn, Germany) was coupled to a hybrid quadrupole mass spectrometer (QTRAP 4000, AB Sciex, Darmstadt, Germany). MS/MS analysis was run in

Table 1: Characteristics of participating children at start and end point of the 1-year intervention period. Characteristics are shown for all obese children ($n = 80$), children with substantial weight loss (WL, $n = 40$), and children without substantial weight loss (nWL, $n = 40$) as mean ± SD unless stated otherwise.

Parameter	All start (%)	All end (%)	WL start (%)	WL end (%)	nWL start (%)	nWL end (%)
Sex, male	36 (45%)		18 (45%)		18 (45%)	
Age (years)	11.5 ± 2.42	12.5 ± 2.42	10.6 ± 2.54	11.6 ± 2.54	12.4 ± 1.9	13.4 ± 1.9
Prepubertal	34 (42%)	26 (32%)	23 (58%)	18 (45%)	11 (28%)	8 (20%)
Early pubertal	42 (52%)	44 (55%)	17 (42%)	22 (55%)	25 (62%)	22 (55%)
Postpubertal	4 (5%)	10 (12%)	—	—	4 (10%)	10 (25%)
BMI-SDS	2.4 ± 0.45	2.1 ± 0.63*	2.4 ± 0.44	1.7 ± 0.58*	2.4 ± 0.46	2.4 ± 0.47*
Waist circumference (cm)	91.7 ± 14	89.3 ± 13.89*	87 ± 13.59	81 ± 10.99*	96.5 ± 12.88	97.3 ± 11.55
Insulin (mU/L)	19.9 ± 15.01	17 ± 12.39	18 ± 12.01	9.3 ± 3.87*	21.9 ± 17.44	25.1 ± 13.14*
Fasting glucose (mg/dL)	86.3 ± 7.38	87.1 ± 6.39	84.8 ± 7.05	85.5 ± 5.76	87.8 ± 7.47	88.8 ± 6.65
2-hour oGTT glucose (mg/dL)	132.7 ± 25.02	113.9 ± 23.94*	133.9 ± 24.26	98.9 ± 10.42*	131.4 ± 25.99	128.9 ± 24.28
HbA1C (mmol/mol Hb)	373.43 ± 32.92	372.81 ± 37.98	364.16 ± 30.12	363.77 ± 30.81	382.95 ± 33.32	382.61 ± 42.78
HOMA	4.29 ± 3.1	3.79 ± 3.2	4.01 ± 3	1.96 ± 0.81*	4.58 ± 3.21	5.67 ± 3.64*

*Significant different means between start and end point ($p < 0.05$, paired Wilcoxon rank sum test).

Multiple Reaction Monitoring mode with electrospray ionization used in both positive and negative modes. Data acquisition on the mass spectrometer was controlled by Analyst 1.5 software (AB Sciex, Darmstadt, Germany). For raw data processing, peak integration, isotope correction, calibration, and quality control, the Met IQ software package (Biocrates Life Sciences AG, Innsbruck, Austria) was used, which is an integral part of the Absolute *IDQ* kit quantifying a total of 163 metabolites. Middle- and long-chain Carn, sphingomyelins (SM), acyl-linked phosphatidylcholines, ether-linked phosphatidylcholines, and lysophosphatidylcholines were not used for the data analysis of this work, since the presented study focused on alterations in AA metabolism with respect to IR. For the presented work, we analyzed 14 short-chain Carn (Cx:y, hydroxyl acylcarnitines Cx:y-OH, oxoacylcarnitines Cx:y-oxo, and dicarboxylacylcarnitines Cx:y-DC), free carnitine (Carn C0), and 14 AA. Cx:y abbreviates the lipid side chain composition, x and y denoting the number of carbons and double bonds, respectively. The sum of leucine (Leu) and isoleucine (Ile) is expressed as xLeu. Samples were integrated with the Met IQ software by automated calculation of metabolite concentrations. For the data analysis performed here, only short-chain Carn, Carn C0, and AA are used. The sum of xLeu and valine (Val) is expressed as BCAA sum. The sum of phenylalanine (Phe), tryptophan (Trp), and Tyr is expressed as AAA sum. We report all metabolite concentrations in μmol/L. In addition to the 29 metabolite concentrations and two sum parameters, eleven metabolite ratios were calculated resulting in a total of 42 metabolites and metabolite ratios.

2.4. Statistics. All statistical analyses were performed using the statistical software R (3.0.2) [37]. In a first step, we graphically screened for outliers and normality. An absolute metabolite concentration that lay greater than 1 standard deviation (SD) away from its nearest neighbor was considered to be an outlier and this measurement was excluded from the analysis. Principal component analysis score plots were used as a complementary tool to ensure that no outliers remained undetected.

Differences in clinical parameters between baseline and follow-up were calculated using the paired Wilcoxon rank test. Associations between markers for insulin and glucohomeostasis were quantified using Spearman rank correlation coefficients.

The changes in the clinical markers, metabolite concentrations, and metabolite ratios over the one-year intervention are expressed as the relative difference of baseline and follow-up measurements (with the baseline values being the reference). For each time point (baseline and follow-up) as well as for the relative change, we calculated the following model to assess the association between the metabolites and the clinical parameters: (1) firstly, in order to account for the effect of obesity status on the metabolite level, we fitted age and sex adjusted robust regression models of the BMI on the metabolite using the M-estimator with Huber bisquare weighting (R package MASS); (2) subsequently, we regressed the obtained metabolite residuals on markers for IR with robust regression models using the M-estimator with Huber bisquare weighting (R package MASS). p values and estimates are taken as proxies for the strengths and directions of the associations. Results of selected clinical outcomes are represented graphically in Manhattan plots, where the $\log_{10}(p)$ values are plotted and the sign is used to indicate the direction of the relationship, as assessed by the robust regression model. Due to the small sample size and in order not to veil differences in p values, we will report the raw (unadjusted) p values. The significance level was thus set at $p < 0.05$. Bonferroni corrected p values can be obtained by multiplying the reported p values with the factor 42 (number of analytes tested). The Bonferroni corrected significance level is 0.0012.

3. Results

3.1. Population Characteristics. Characteristics of participating children are presented in Table 1. In all obese children,

Table 2: Spearman correlation coefficients of markers of insulin homeostasis in all obese children ($n = 80$) at baseline.

	Fasting glucose (mg/dL)	2-hour oGTT glucose (mg/dL)	HbA1C (mmol/mol Hb)	Insulin (mU/L)	HOMA	BMI-SDS	Waist circumference (cm)
Fasting glucose (mg/dL)	1	0.246	0.231	0.091	0.154	−0.001	0.241
2-hour oGTT glucose (mg/dL)		1	0.188	0.113	0.135	0.153	0.164
HbA1C (mmol/mol Hb)			1	0.120	0.176	0.116	0.234
Insulin (mU/L)				1	0.984	0.343	0.586
HOMA					1	0.402	0.669
BMI-SDS						1	0.445
Waist circumference (cm)							1

waist circumference and 2-hour oGTT glucose decreased significantly during the intervention period. Additionally, insulin levels and HOMA decreased in the group of 40 obese children with substantial weight loss. In contrast, insulin levels and HOMA increased in the group of obese children without substantial weight loss. Since HOMA and insulin were strongly correlated (Table 2) and HbA1C and fasting glucose showed no changes between the two time points in any of the groups, in contrast to HOMA, waist circumference, and 2 h glucose in oGTT (Table 1), we focused our data analysis on HOMA, 2-hour oGTT glucose, and waist circumference. Waist circumference showed no significant association with the metabolites. No difference between puberty and HOMA status was found at baseline ($p = 0.44$), but after the intervention period ($p = 0.036$) with pubertal children having higher HOMA values.

Associations of all clinical parameters and metabolites are reported in the Supplementary Material (available online at http://dx.doi.org/10.1155/2016/2108909).

3.2. HOMA. At baseline, HOMA was positively associated with Tyr ($p = 0.004$, Figure 2), Trp ($p = 0.007$), sum of AAA ($p = 0.013$), ornithine (Orn, $p = 0.026$), and threonine (Thr, $p = 0.036$) and negatively associated with Carn C3-OH ($p = 0.036$) and the ratios of Carn C5:1/Carn C5 ($p = 0.014$) and Carn C6-oxo/xLeu ($p = 0.044$) in all obese children (Figure 1). After the end of the intervention, only Tyr was associated with HOMA in all obese children ($p = 0.044$, Figures 2 and 3). In a stratified analysis including the 40 children with substantial weight loss, HOMA was negatively associated with the ratio of Carn C6-oxo/xLeu ($p = 0.011$), Carn C6-oxo ($p = 0.023$), and Carn C4 ($p = 0.031$) and positively associated with Carn C4/Carn C5-oxo ($p = 0.041$) and Tyr ($p = 0.047$, Figure 2) at baseline. After the intervention, only Tyr was associated with HOMA ($p = 0.041$) in the children with substantial weight loss (Figures 2 and 3). Children without substantial weight loss showed different associations for HOMA. Thr ($p < 0.001$) and proline (Pro, $p = 0.0322$) were positively associated with HOMA, while the ratios of Carn C5:1/Carn C5 ($p = 0.030$) and Carn C4/Val ($p = 0.033$) were negatively associated at baseline. After the intervention, only the ratio of Carn C5-OH/Carn C5:1 was associated with HOMA ($p = 0.048$) in children without substantial weight loss (Figure 3). The significant associations

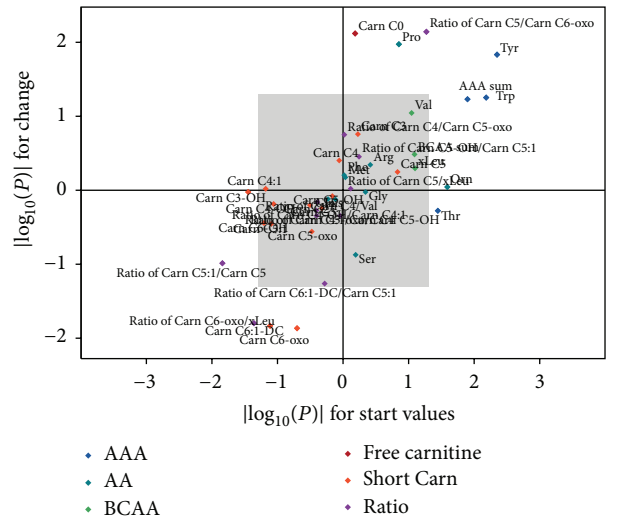

Figure 1: Associations of amino acids (AA) and acylcarnitines (Carn) with HOMA. Associations were calculated at baseline (x-axis) and for changes of AA and Carn to changes of HOMA during the intervention (y-axis) period in all children ($n = 80$). Displayed are the absolute $\log(p)$ values of the applied obesity-independent robust regression models for both associations. AAA, aromatic amino acids; BCAA, branched-chain amino acids.

between the relative change of HOMA during the intervention period and the relative change of AA and Carn are shown in Table 3 for all obese children (Figure 1), children with substantial weight loss, and children without substantial weight loss. The change of ratio of Carn C5/Carn C6-oxo was positively associated with change of HOMA in all three groups, while this was true for the ratio of Carn C4/Carn C5-oxo only in children with substantial weight loss. Changes of Tyr were again positively correlated with changes in HOMA in all children and children with substantial weight loss.

3.3. Two-Hour oGTT Glucose. Two-hour oGTT glucose showed different associations compared to HOMA, particularly in children with substantial weight loss. At baseline, the ratios of Carn C4:1/Carn C4 ($p = 0.011$, negative), Carn C4/Carn C5-oxo ($p = 0.023$, positive), and Carn C4/Val ($p = 0.05$, positive) as well as histidine (His, $p = 0.040$,

Table 3: Estimates and p values (p) of changes in metabolite concentrations which are significantly associated with changes in HOMA in at least one (sub)group (All, WL, and nWL). Change is defined as the relative change over the one-year intervention. Estimates are given with 95% confidence interval (CI). Estimates, confidence intervals, and p values were calculated with robust regression models. WL, children with substantial weight loss; nWL, children without substantial weight loss; AAA, aromatic amino acids; Carn, acylcarnitine; Pro, proline; Trp, tryptophan; Tyr, tyrosine; Val, valine, xLeu, sum of leucine and isoleucine.

Analyte	All ($n = 80$)		WL ($n = 40$)		nWL ($n = 40$)	
	Estimate [95% CI]	p	Estimate [95% CI]	p	Estimate [95% CI]	p
AAA sum	0.79 [−0.04; 1.60]	0.059	1.04 [0.29; 1.80]	0.009	0.27 [−1.40; 1.90]	0.742
Carn C0	1.10 [0.29; 1.90]	0.008	1.71 [0.88; 2.50]	<0.001	0.24 [−1.30; 1.70]	0.751
Carn C3	0.34 [−0.16; 0.83]	0.174	0.49 [0.03; 0.96]	0.036	0.24 [−0.72; 1.20]	0.615
Carn C6:1-DC	−0.33 [−0.59; −0.06]	0.015	−0.29 [−0.47; −0.10]	0.003	−0.37 [−1.10; 0.38]	0.342
Carn C6-oxo	−0.24 [−0.43; −0.05]	0.014	−0.21 [−0.35; −0.08]	0.003	−0.21 [−0.73; 0.31]	0.438
Pro	0.81 [0.19; 1.40]	0.011	0.72 [0.11; 1.30]	0.023	0.88 [−0.08; 1.80]	0.067
Ratio of Carn C4/Carn C5-oxo	0.23 [−0.09; 0.55]	0.177	0.48 [0.18; 0.77]	0.003	−0.21 [−0.86; 0.45]	0.530
Ratio of Carn C5/Carn C6-oxo	0.24 [0.07; 0.41]	0.007	0.22 [0.08; 0.35]	0.002	0.29 [0.02; 0.57]	0.041
Ratio of Carn C6:1-DC/Carn C5:1	−0.27 [−0.54; 0.01]	0.055	−0.22 [−0.41; −0.03]	0.024	−0.39 [−1.10; 0.37]	0.321
Ratio of Carn C6-oxo/xLeu	−0.19 [−0.34; −0.03]	0.016	−0.15 [−0.25; −0.04]	0.007	−0.24 [−0.84; 0.37]	0.442
Trp	0.93 [−0.02; 1.90]	0.056	1.13 [0.14; 2.10]	0.027	0.44 [−1.30; 2.20]	0.613
Tyr	0.79 [0.17; 1.40]	0.015	1.09 [0.51; 1.70]	0.001	0.28 [−0.99; 1.50]	0.651
Val	0.65 [−0.11; 1.40]	0.090	0.73 [0.07; 1.40]	0.033	0.48 [−1.10; 2.10]	0.544

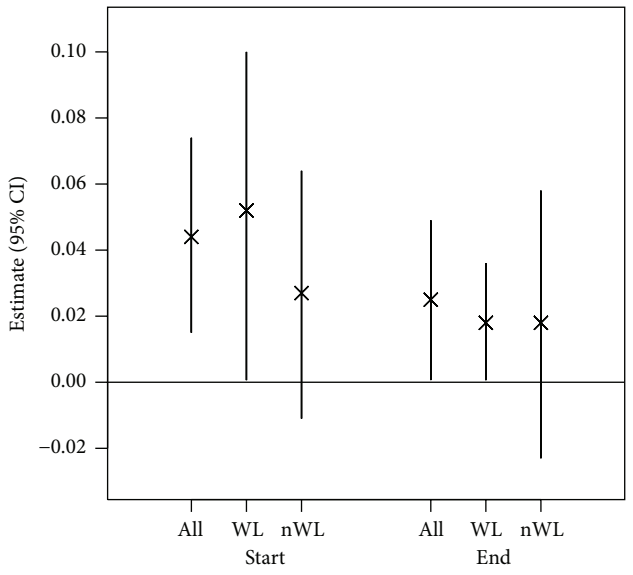

Figure 2: Estimates (95% CI) for associations of tyrosine with HOMA. Associations were calculated at baseline (Start) and after the intervention (End). Associations were calculated for all obese children ($n = 80$), children with substantial weight loss (WL, $n = 40$), and children without substantial weight loss (nWL, $n = 40$). 95% CI: 95% confidence interval.

negative), serine (Ser, $p = 0.043$, negative), and Carn C4 ($p = 0.049$, positive) were associated with 2-hour oGTT glucose in children with substantial weight loss, while children without substantial weight loss showed only positive associations between arginine (Arg) and 2-hour oGTT glucose at baseline. After the intervention, 2-hour oGTT glucose was associated negatively with Ser ($p = 0.048$) and Orn ($p = 0.039$) in children with substantial weight loss and with glutamine (Gln, $p = 0.011$) and Carn C3-OH ($p = 0.012$) in children without substantial weight loss. Interestingly, changes of 2-hour oGTT glucose during the one-year intervention period were not significantly associated with changes of any of the measured metabolites, ratios, or sums in any of the groups.

4. Discussion

To our knowledge, this is the first longitudinal study analysing the relationships between metabolites and markers of glucose metabolism in obese children. Tyr is the only metabolite which was significantly associated with HOMA at baseline and after intervention. Changes of Tyr over time were also positively associated with changes of HOMA in our obesity-independent model. Thus, Tyr, rather than BCAA, seems to be associated with IR. This is in accordance with a recent study where Tyr was identified as the most important metabolite in a random forest analysis in obese children [26]. In the same study, a combination of BCAA and AAA was most strongly related to HOMA. Furthermore, Tyr was found to be a strong predictor for diabetes in South Asian men [21]. Tyr is biosynthesised endogenously by hydroxylation of Phe by phenylalanine hydroxylase in mammals [38]. Since Phe was not associated with HOMA in any of the groups at any time point, we assume that there is no confounding dietary effect on Tyr levels. Tyr stimulates insulin secretion, but other AAs are more effective in stimulating insulin release [39]. In contrast, Michaliszyn et al. showed a positive association of β-cell function and all AAs except for Tyr and citrulline in adolescents [40]. The same group reported lower AA plasma levels, except for Tyr, in diabetic adolescents [41], which is in contrast to the role of elevated AA in IR [42]. However, the effect on insulin secretion should not be driving the relation between Tyr and HOMA. An influence on Tyr metabolism appears more likely. Insulin is known to increase

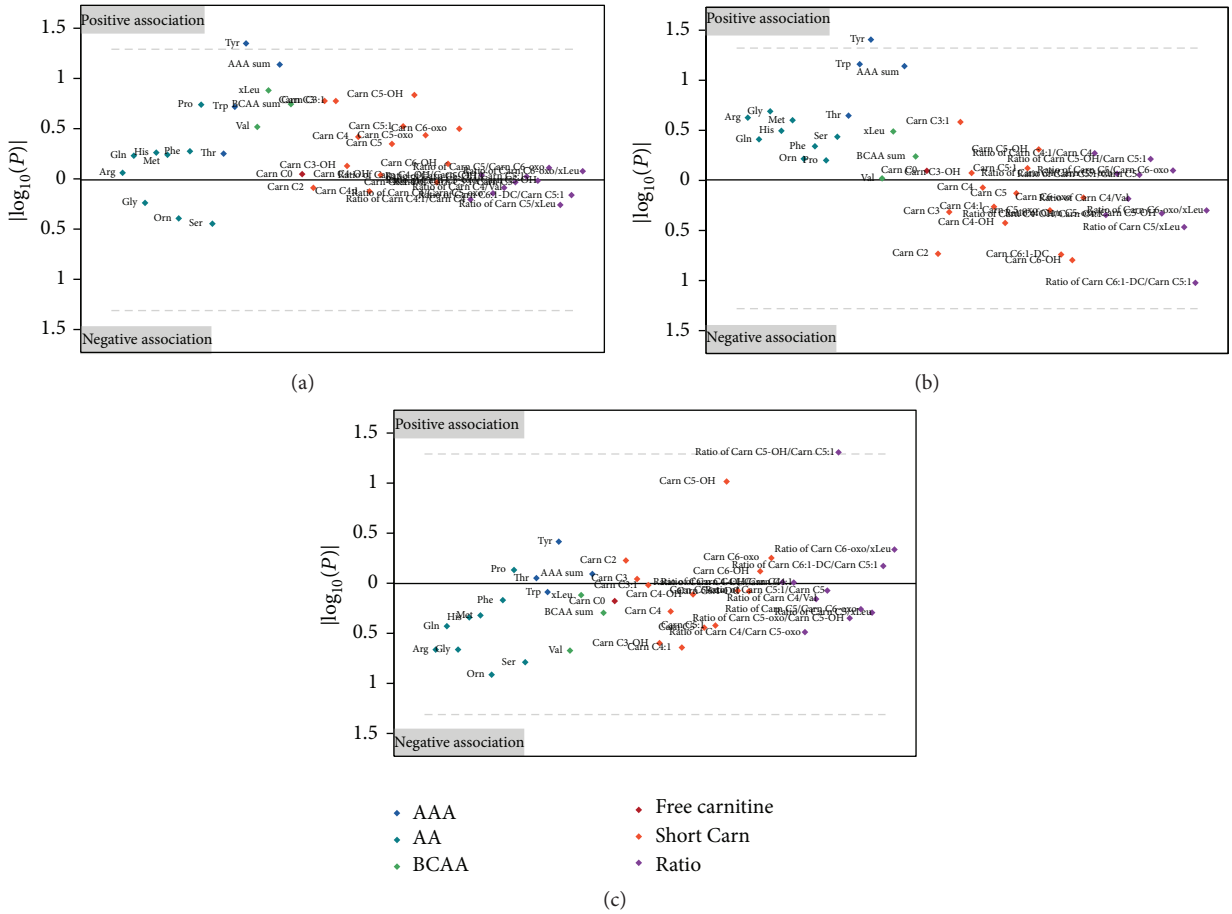

Figure 3: Manhattan plot for associations of amino acids (AA) and acylcarnitines (Carn) with HOMA after the one-year lifestyle intervention for all obese children (a), children with substantial weight loss (b), and children without substantial weight loss (c). Plotted are the $\log_{10}(p)$ values and the sign is used to indicate the direction of the relationship, as assessed by the robust regression model. The area below or above the dashed lines contains metabolites that are significantly related to HOMA (p values < 0.05). AAA, aromatic amino acids; BCAA, branched-chain amino acids.

tyrosine aminotransferase (TAT) activity in rat liver [43], probably by selectively slowing down the rate of degradation of TAT [44]. TAT catalyses the transamination of Tyr to p-hydroxyphenylpyruvate. This should result in lower Tyr levels. A possible inhibition of TAT may occur due to higher Cys levels. Cys is an inhibitor of TAT [19, 45]. In a recent study, only Cys and Tyr were found to be increased in nonobese adults who had one symptom of the metabolic syndrome [14]. With further progression of the metabolic syndrome, BCAA and Phe were enhanced in subjects with two or more symptoms of the metabolic syndrome. It seems that alterations in Cys and Tyr metabolism precede changes in BCAA metabolism. Thus, Tyr is a potential early marker for the onset of IR. Higher insulin levels in the IR state may still cover demands to ensure adequate glucose metabolism, but Tyr may be affected and Tyr may present an early biomarker for the onset of IR in obese children. This predictive value of Tyr was shown in previous studies in adults, along with BCAA in young adults [16, 18]. In the presented study, we could not investigate Tyr as predictor for later IR, since the "Obeldicks" study has an interventional design not a prospective one. Contrarily, Lee et al. found BCAA, and not AAA, as predictive marker for IR in Korean children [27]. Thus, further prospective, longitudinal studies are required to unravel associations between AA and IR with respect to sex and ethnicity.

Furthermore, Tyr can affect BCAA levels, since BCAA and AA compete for the same neutral AA transporter for cellular uptake [46]. Thus, prolonged elevated Tyr levels may also result in elevated BCAA level. Many studies found altered levels of BCAA when studying obesity in adults [9], but also when looking at IR and T2DM in adults [13, 15–18, 42]. Similar results were found in a few cross-sectional studies in children [12, 25]. We found no association between HOMA and BCAA, neither at baseline nor after the intervention. A previous cross-sectional metabolomic analysis of the presented population did not find different BCAA levels between obese and normal weight children [47]. Levels of BCAA, being essential AAs, are mainly defined by the diet. Thus, higher BCAA levels later in life may result from competition for the neutral AAs transport [46], higher protein intake, and/or disturbed BCAA clearance [48]. During BCAA degradation, Val, Leu, and Ile are first degraded to the α-keto acids

C5-oxo and C6-oxo by the branched-chain amino transferase (BCAT). These keto acids are subsequently reduced by branched-chain α-keto acid dehydrogenase (BCKDH) in the rate limiting step [49]. To identify alterations of BCAA metabolism in obesity and IR, we calculated the ratios of the different steps in the BCAA degradation pathway. We found that the ratio of C6-oxo to C5 was positively associated with HOMA at baseline and in the change during the intervention period in all three groups. The ratio of C5-oxo to C4 was positively associated with HOMA only in children with substantial weight loss only. Both ratios are markers for the second, rate limiting degradation step of BCAA which is regulated by BCAA itself to keep BCAA concentrations at a constant level. Thus, this pathway may have been upregulated in our study resulting in BCAA levels not associated with HOMA. In contrast, all other ratios showed no significant association with HOMA or were negatively associated with HOMA, particularly the first step of xLeu degradation to methylketopentanoate (C6-oxo) by BCAT. It was shown recently that IR subjects have a significant reduction in BCAT expression and other enzymes involved in BCAA metabolism in the adipose tissue compared to none-IR subjects [50]. Additionally, BCAT2 (mitochondrial) was significantly downregulated, whereas BCAT1 (cytosolic) was significantly upregulated in the adipose tissue of obese subjects [51]. Other mitochondrial genes of BCAA metabolism were also downregulated in adipose tissue, but not in liver or muscle tissue. Our study showed that the reduction of BCAA degradation seems to precede elevated BCAA levels in IR state or obesity in children, since no elevated BCAA were found but alterations in BCAA metabolite ratios. Thus, insulin negatively alters BCAA metabolism resulting in higher plasma BCAA in later life, when BCAA concentrations overcome their own degradation and contribute to the vicious circle of IR [52]. The analysis of metabolite profiles in children allowed us to study this early development effect of IR, but far more studies in children and early adulthood are needed to investigate the molecular changes in the early state of obesity and IR. However, BCAA and BCAA metabolism are more affected by protein-rich diet than other AAs [53], and thus diet is a known confounder, especially in obese patients with higher protein intake [15, 22]. After the intervention, in a state of homogenous lifestyle and diet, the BCAA ratios were no longer significantly associated with HOMA, except for the ratio of Carn C5-OH to Carn C5:1, which was positively associated with HOMA in children without substantial weight loss. Thus, lifestyle may have strong effect on BCAA metabolism, and the results found at baseline were hidden by the homogenous lifestyle of the studied cohort. This possible confounding effect of diet and lifestyle on BCAA metabolism has to be investigated in further studies. The nonsignificant association of HOMA and BCAA could also be result of less power of our study. Tai et al. depicted the same challenge when they found an association of IR with BCAA in a large group of Chinese men, but not in a smaller group of Indian Asian men [15]. Two-hour oGTT glucose showed different associations with AA and AA derivatives compared to HOMA. Particularly, Ser was negatively associated with 2-hour oGTT glucose. Since fewer studies exist on relations of 2-hour oGTT glucose to metabolites, we can only speculate about the underlying mechanisms. Ser and glycine (Gly) were found to be decreased in obese Hispanic children [26] and in obese Korean children [27]. The concentrations of Gly and Ser were found to be lower in diabetic than in fasted normal rats [54]. The authors concluded that the contribution of Ser to gluconeogenesis becomes proportionally higher in diabetes. Thus, an increased gluconeogenesis rate in diabetic or prediabetic patients most likely leads to decreased Ser levels. In this case, Ser seems to be the AA which is first affected by higher gluconeogenesis rate. But to unravel this relation, further studies are needed. Another explanation is the use of consumed Ser for SM synthesis, since SM are elevated in IR state [55]. Furthermore, we have to recall the relatively low reliability of 2 h glucose in oGTT [56]. Additionally, elevated 2 h glucose levels in obese children tend to normalize in follow-up even without weight loss as also demonstrated in our study [57, 58].

All the described relations between metabolites and HOMA or 2-hour oGTT glucose were driven by children with substantial weight loss. Children without substantial weigh loss showed fewer and different associations. Thus, it is plausible that different metabolomic changes are associated with different types of IR. However, HOMA and 2-hour oGTT glucose did not change significantly in children without substantial weight loss during the intervention period, and thus the information in these parameters may be too little to depict associations between metabolites and clinical parameters in this group. Nevertheless, estimates for the associations between metabolites and HOMA were different at baseline, in change, and at follow-up, assuming different metabolic pattern which could be related to IR, the intervention, or weight loss. Thus, further prospective studies should focus on the relation of IR to different metabolomic patterns.

However, we were not able to differentiate the effect of diet, increased physical exercise, and weight loss on metabolites and their ratio concentrations due to our study protocol. Unfortunately, we could not perform stratified analyses to the influence of pubertal status on the associations of metabolites with IR. An explorative statistical approach showed no influence on the association of IR with Tyr, but on Carn. Further studies with larger sample number are required to determine differences in IR development with respect to puberty status. A limitation of our study is that BMI percentiles were used to classify overweight. Although BMI is a good measure for overweight, it is not a precise measure of body fat mass. Furthermore, the degree of obesity was relatively homogeneous in our obese children. Additionally, the HOMA model is only an assessment of IR [59]. Clamp studies are actually the gold standard for analysing IR. In addition to the small sample number, these facts reduced the odds to detect associations between metabolites and clinical outcomes. The relatively low sample number also reduced the statistical power of the presented data analysis, which kept us from correction for multiple testing. Among the strengths of our study are the longitudinal design and the analysed children that were naïve to drugs and other diseases and had similar lifestyle during the one-year intervention. The additional focus on ratios allowed for a closer insight

into degradation pathways associated with obesity-related IR. Thus, the influence of diet and physical activity on changes of metabolite levels should be limited.

5. Conclusions

This study provides novel insights into the longitudinal interrelations of IR and obesity markers to metabolites and generates possible questions for further mechanistic studies of IR in obese children. Our cross-sectional and longitudinal analyses confirm a relationship between the Tyr and HOMA in obese children. So, Tyr and the Tyr metabolism should be focused more on in studies searching for early biomarkers and predictors in the switch from obesity to IR. In contrast, BCAA levels were negatively related to IR in cross-sectional analyses, while there was no significant association in the longitudinal analysis, which does not support a causal role of BCAA in inducing IR. Furthermore, responders to the intervention showed different associations between HOMA and AA compared to nonresponders, which appears to reflect different mechanisms for the development of obesity-induced IR. Further studies should also explore other analytes which were not determined in our study, such as p-hydroxyphenylpyruvate, fumarate, or acetoacetate that are involved in Tyr metabolism and sulfur containing AA.

Conflict of Interests

The authors declare that there is no conflict of interests regarding the publication of this paper.

Acknowledgments

The authors thank the participating children in this study. The research leading to these results has received funding from the European Union's Seventh Framework Programme (FP7/2007–2013), project EarlyNutrition under Grant Agreement no. 289346, and the European Research Council Advanced Grant ERC-2012-AdG, no. 322605 METAGROWTH. The research leading to these results has received support from the Innovative Medicines Initiative Joint Undertaking under EMIF Grant Agreement no. 115372, resources of which are composed of financial contribution from the European Union's Seventh Framework Programme (FP7/2007–2013) and EFPIA companies in kind contribution. This paper does not necessarily reflect the views of the Commission and in no way anticipates the future policy in this area. Further grant support by the German Ministry of Education and Research (Obesity Network: Grant nos. 01 01GI1120A, 01GI 1120B, and 001 GI 0825) is gratefully acknowledged.

References

[1] E. R. Pulgarón, "Childhood obesity: a review of increased risk for physical and psychological comorbidities," *Clinical Therapeutics*, vol. 35, no. 1, pp. A18–A32, 2013.

[2] G. Csábi, K. Török, D. Molnár, and S. Jeges, "Presence of metabolic cardiovascular syndrome in obese children," *European Journal of Pediatrics*, vol. 159, no. 1-2, pp. 91–94, 2000.

[3] D. S. Freedman, W. H. Dietz, S. R. Srinivasan, and G. S. Berenson, "The relation of overweight to cardiovascular risk factors among children and adolescents: the Bogalusa Heart study," *Pediatrics*, vol. 103, no. 6, part 1, pp. 1175–1182, 1999.

[4] T. Reinehr, W. Andler, C. Denzer, W. Siegried, H. Mayer, and M. Wabitsch, "Cardiovascular risk factors in overweight German children and adolescents: relation to gender, age and degree of overweight," *Nutrition, Metabolism and Cardiovascular Diseases*, vol. 15, no. 3, pp. 181–187, 2005.

[5] F. M. Biro and M. Wien, "Childhood obesity and adult morbidities," *The American Journal of Clinical Nutrition*, vol. 91, no. 5, pp. 1499S–1505S, 2010.

[6] T. Reinehr, G. de Sousa, and W. Andler, "Longitudinal analyses among overweight, insulin resistance, and cardiovascular risk factors in children," *Obesity Research*, vol. 13, no. 10, pp. 1824–1833, 2005.

[7] S. S. Coughlin, "Toward a road map for global -omics: a primer on -omic technologies," *American Journal of Epidemiology*, vol. 180, no. 12, pp. 1188–1195, 2014.

[8] N. M. R. Sales, P. B. Pelegrini, and M. C. Goersch, "Nutrigenomics: definitions and advances of this new science," *Journal of Nutrition and Metabolism*, vol. 2014, Article ID 202759, 6 pages, 2014.

[9] S. Rauschert, O. Uhl, B. Koletzko, and C. Hellmuth, "Metabolomic biomarkers for obesity in humans: a short review," *Annals of Nutrition and Metabolism*, vol. 64, no. 3-4, pp. 314–324, 2014.

[10] S. Demine, N. Reddy, P. Renard, M. Raes, and T. Arnould, "Unraveling biochemical pathways affected by mitochondrial dysfunctions using metabolomic approaches," *Metabolites*, vol. 4, no. 3, pp. 831–878, 2014.

[11] M. S. Lustgarten, L. Lyn Price, E. M. Phillips, and R. A. Fielding, "Serum glycine is associated with regional body fat and insulin resistance in functionally-limited older adults," *PLoS ONE*, vol. 8, no. 12, Article ID e84034, 2013.

[12] W. Perng, M. W. Gillman, A. F. Fleisch et al., "Metabolomic profiles and childhood obesity," *Obesity*, vol. 22, no. 12, pp. 2570–2578, 2014.

[13] C. B. Newgard, J. An, J. R. Bain et al., "A branched-chain amino acid-related metabolic signature that differentiates obese and lean humans and contributes to insulin resistance," *Cell Metabolism*, vol. 9, no. 4, pp. 311–326, 2009.

[14] N. Mohorko, A. Petelin, M. Jurdana, G. Biolo, and Z. Jenko-Pražnikar, "Elevated serum levels of cysteine and tyrosine: early biomarkers in asymptomatic adults at increased risk of developing metabolic syndrome," *BioMed Research International*, vol. 2015, Article ID 418681, 14 pages, 2015.

[15] E. S. Tai, M. L. S. Tan, R. D. Stevens et al., "Insulin resistance is associated with a metabolic profile of altered protein metabolism in Chinese and Asian-Indian men," *Diabetologia*, vol. 53, no. 4, pp. 757–767, 2010.

[16] P. Wurtz, P. Soininen, A. J. Kangas et al., "Branched-chain and aromatic amino acidsare predictors of insulinresistance in young adults," *Diabetes Care*, vol. 36, no. 3, pp. 648–655, 2013.

[17] O. Fiehn, W. T. Garvey, J. W. Newman, K. H. Lok, C. L. Hoppel, and S. H. Adams, "Plasma metabolomic profiles reflective of glucose homeostasis in non-diabetic and type 2 diabetic obese African-American women," *PLoS ONE*, vol. 5, no. 12, Article ID e15234, 2010.

[18] S. H. Shah, D. R. Crosslin, C. S. Haynes et al., "Branched-chain amino acid levels are associated with improvement in insulin resistance with weight loss," *Diabetologia*, vol. 55, no. 2, pp. 321–330, 2012.

[19] S. H. Adams, "Emerging perspectives on essential amino acid metabolism in obesity and the insulin-resistant state," *Advances in Nutrition*, vol. 2, no. 6, pp. 445–456, 2011.

[20] H.-H. Chen, Y. J. Tseng, S.-Y. Wang et al., "The metabolome profiling and pathway analysis in metabolic healthy and abnormal obesity," *International Journal of Obesity*, vol. 39, no. 8, pp. 1241–1248, 2015.

[21] T. Tillin, A. D. Hughes, Q. Wang et al., "Diabetes risk and amino acid profiles: cross-sectional and prospective analyses of ethnicity, amino acids and diabetes in a South Asian and European cohort from the SABRE (Southall And Brent REvisited) Study," *Diabetologia*, vol. 58, no. 5, pp. 968–979, 2015.

[22] P. Würtz, V.-P. Mäkinen, P. Soininen et al., "Metabolic signatures of insulin resistance in 7,098 young adults," *Diabetes*, vol. 61, no. 6, pp. 1372–1380, 2012.

[23] J. Villarreal-Pérez, J. Villarreal-Martínez, F. Lavalle-González et al., "Plasma and urine metabolic profiles are reflective of altered beta-oxidation in non-diabetic obese subjects and patients with type 2 diabetes mellitus," *Diabetology & Metabolic Syndrome*, vol. 6, article 129, 2014.

[24] T. J. Wang, M. G. Larson, R. S. Vasan et al., "Metabolite profiles and the risk of developing diabetes," *Nature Medicine*, vol. 17, no. 4, pp. 448–453, 2011.

[25] D. Newbern, P. G. Balikcioglu, M. Balikcioglu et al., "Sex differences in biomarkers associated with insulin resistance in obese adolescents: metabolomic profiling and principal components analysis," *Journal of Clinical Endocrinology and Metabolism*, vol. 99, no. 12, pp. 4730–4739, 2014.

[26] N. F. Butte, Y. Liu, I. F. Zakeri et al., "Global metabolomic profiling targeting childhood obesity in the Hispanic population," *The American Journal of Clinical Nutrition*, vol. 102, no. 2, pp. 256–267, 2015.

[27] A. Lee, H. B. Jang, M. Ra et al., "Prediction of future risk of insulin resistance and metabolic syndrome based on Korean boy's metabolite profiling," *Obesity Research & Clinical Practice*, 2014.

[28] S. E. Mccormack, O. Shaham, M. A. Mccarthy et al., "Circulating branched-chain amino acid concentrations are associated with obesity and future insulin resistance in children and adolescents," *Pediatric Obesity*, vol. 8, no. 1, pp. 52–61, 2013.

[29] T. Reinehr, G. de Sousa, A. M. Toschke, and W. Andler, "Long-term follow-up of cardiovascular disease risk factors in children after an obesity intervention," *American Journal of Clinical Nutrition*, vol. 84, no. 3, pp. 490–496, 2006.

[30] T. Reinehr, A. Hinney, G. de Sousa, F. Austrup, J. Hebebrand, and W. Andler, "Definable somatic disorders in overweight children and adolescents," *The Journal of Pediatrics*, vol. 150, no. 6, pp. 618.e5–622.e5, 2007.

[31] T. Reinehr, W. Kiess, T. Kapellen, and W. Andler, "Insulin sensitivity among obese children and adolescents, according to degree of weight loss," *Pediatrics*, vol. 114, no. 6, pp. 1569–1573, 2004.

[32] T. Reinehr, B. Wolters, C. Knop et al., "Changes in the serum metabolite profile in obese children with weight loss," *European Journal of Nutrition*, vol. 54, no. 2, pp. 173–181, 2015.

[33] T. J. Cole, "The LMS method for constructing normalized growth standards," *European Journal of Clinical Nutrition*, vol. 44, no. 1, pp. 45–60, 1990.

[34] K. Kromeyer-Hauschild, M. Wabitsch, D. Kunze et al., "Perzentile für den Body-mass-Index für das Kindes- und Jugendalter unter Heranziehung verschiedener deutscher Stichproben," *Monatsschrift Kinderheilkunde*, vol. 149, no. 8, pp. 807–818, 2001.

[35] American Diabetes Association, "Type 2 diabetes in children and adolescents," *Diabetes Care*, vol. 23, no. 3, pp. 381–389, 2000.

[36] D. R. Matthews, J. P. Hosker, A. S. Rudenski, B. A. Naylor, D. F. Treacher, and R. C. Turner, "Homeostasis model assessment: insulin resistance and β-cell function from fasting plasma glucose and insulin concentrations in man," *Diabetologia*, vol. 28, no. 7, pp. 412–419, 1985.

[37] The R Project for Statistical Computing, http://www.r-project.org/.

[38] S. L. C. Woo, A. S. Lidsky, F. Guttler, T. Chandra, and K. J. Robson, "Cloned human phenylalanine hydroxylase gene allows prenatal diagnosis and carrier detection of classical phenylketonuria," *Nature*, vol. 306, no. 5939, pp. 151–155, 1983.

[39] T. Kuhara, S. Ikeda, A. Ohneda, and Y. Sasaki, "Effects of intravenous infusion of 17 amino acids on the secretion of GH, glucagon, and insulin in sheep," *American Journal of Physiology—Endocrinology and Metabolism*, vol. 260, no. 1, pp. E21–E26, 1991.

[40] S. F. Michaliszyn, L. A. Sjaarda, S. J. Mihalik et al., "Metabolomic profiling of amino acids and β-cell function relative to insulin sensitivity in youth," *The Journal of Clinical Endocrinology & Metabolism*, vol. 97, no. 11, pp. E2119–E2124, 2012.

[41] S. J. Mihalik, S. F. Michaliszyn, J. de las Heras et al., "Metabolomic profiling of fatty acid and amino acid metabolism in youth with obesity and type 2 diabetes: evidence for enhanced mitochondrial oxidation," *Diabetes Care*, vol. 35, no. 3, pp. 605–611, 2012.

[42] K. M. Huffman, S. H. Shah, R. D. Stevens et al., "Relationships between circulating metabolic intermediates and insulin action in overweight to obese, inactive men and women," *Diabetes Care*, vol. 32, no. 9, pp. 1678–1683, 2009.

[43] F. Labrie and A. Korner, "Effect of glucagon, insulin, and thyroxine on tyrosine transaminase and tryptophan pyrrolase of rat liver," *Archives of Biochemistry and Biophysics*, vol. 129, no. 1, pp. 75–78, 1969.

[44] C. J. Spencer, J. H. Heaton, T. D. Gelehrter, K. I. Richardson, and J. L. Garwin, "Insulin selectively slows the degradation rate of tyrosine aminotransferase," *Journal of Biological Chemistry*, vol. 253, no. 21, pp. 7677–7682, 1978.

[45] J. L. Hargrove, J. F. Trotter, H. C. Ashline, and P. V. Krishnamurti, "Experimental diabetes increases the formation of sulfane by transsulfuration and inactivation of tyrosine aminotransferase in cytosols from rat liver," *Metabolism*, vol. 38, no. 7, pp. 666–672, 1989.

[46] J. D. Fernstrom, "Branched-chain amino acids and brain function," *Journal of Nutrition*, vol. 135, supplement 6, pp. 1539S–1546S, 2005.

[47] S. Wahl, Z. Yu, M. Kleber et al., "Childhood obesity is associated with changes in the serum metabolite profile," *Obesity Facts*, vol. 5, no. 5, pp. 660–670, 2012.

[48] G. Marchesini, G. P. Bianchi, H. Vilstrup, M. Capelli, M. Zoli, and E. Pisi, "Elimination of infused branched-chain aminoacids from plasma of patients with non-obese type 2 diabetes mellitus," *Clinical Nutrition*, vol. 10, no. 2, pp. 105–113, 1991.

[49] J. T. Brosnan and M. E. Brosnan, "Branched-chain amino acids: enzyme and substrate regulation," *Journal of Nutrition*, vol. 136, no. 1, supplement, pp. 207S–211S, 2006.

[50] A. E. Serralde-Zúñiga, M. Guevara-Cruz, A. R. Tovar et al., "Omental adipose tissue gene expression, gene variants, branched-chain amino acids, and their relationship with metabolic syndrome and insulin resistance in humans," *Genes and Nutrition*, vol. 9, no. 6, article 431, 2014.

[51] A. Mardinoglu, C. Kampf, A. Asplund et al., "Defining the human adipose tissue proteome to reveal metabolic alterations in obesity," *Journal of Proteome Research*, vol. 13, no. 11, pp. 5106–5119, 2014.

[52] T. M. O'Connell, "The complex role of branched chain amino acids in diabetes and cancer," *Metabolites*, vol. 3, no. 4, pp. 931–945, 2013.

[53] F. F. Kirchberg, U. Harder, M. Weber et al., "Dietary protein intake affects amino acid and acylcarnitine metabolism in infants aged 6 months," *The Journal of Clinical Endocrinology & Metabolism*, vol. 100, no. 1, pp. 149–158, 2015.

[54] G. Hetenyi Jr., P. J. Anderson, M. Raman, and C. Ferrarotto, "Gluconeogenesis from glycine and serine in fasted normal and diabetic rats," *Biochemical Journal*, vol. 253, no. 1, pp. 27–32, 1988.

[55] J. M. R. Gill and N. Sattar, "Ceramides: a new player in the inflammation-insulin resistance paradigm?" *Diabetologia*, vol. 52, no. 12, pp. 2475–2477, 2009.

[56] I. M. Libman, E. Barinas-Mitchell, A. Bartucci, R. Robertson, and S. Arslanian, "Reproducibility of the oral glucose tolerance test in overweight children," *Journal of Clinical Endocrinology and Metabolism*, vol. 93, no. 11, pp. 4231–4237, 2008.

[57] M. Kleber, G. deSousa, S. Papcke, M. Wabitsch, and T. Reinehr, "Impaired glucose tolerance in obese white children and adolescents: three to five year follow-up in untreated patients," *Experimental and Clinical Endocrinology and Diabetes*, vol. 119, no. 3, pp. 172–176, 2011.

[58] M. Kleber, N. Lass, S. Papcke, M. Wabitsch, and T. Reinehr, "One-year follow-up of untreated obese white children and adolescents with impaired glucose tolerance: high conversion rate to normal glucose tolerance," *Diabetic Medicine*, vol. 27, no. 5, pp. 516–521, 2010.

[59] G. I. Uwaifo, E. M. Fallon, J. Chin, J. Elberg, S. J. Parikh, and J. A. Yanovski, "Indices of insulin action, disposal, and secretion derived from fasting samples and clamps in normal glucose-tolerant black and white children," *Diabetes Care*, vol. 25, no. 11, pp. 2081–2087, 2002.

Hindawi Publishing Corporation
Journal of Diabetes Research
Volume 2016, Article ID 2391592, 14 pages
http://dx.doi.org/10.1155/2016/2391592

Research Article

An Investigation into the Antiobesity Effects of *Morinda citrifolia* L. Leaf Extract in High Fat Diet Induced Obese Rats Using a ^{1}H NMR Metabolomics Approach

Najla Gooda Sahib Jambocus,[1] Nazamid Saari,[1] Amin Ismail,[2] Alfi Khatib,[3] Mohamad Fawzi Mahomoodally,[4] and Azizah Abdul Hamid[1,5]

[1]*Faculty of Food Science and Technology, Universiti Putra Malaysia, 43400 Serdang, Selangor, Malaysia*
[2]*Faculty of Medicine and Health Sciences, Universiti Putra Malaysia, 43400 Serdang, Selangor, Malaysia*
[3]*Department of Pharmaceutical Chemistry, Kulliyyah of Pharmacy, International Islamic University Malaysia, 25200 Kuantan, Pahang, Malaysia*
[4]*Department of Health Sciences, Faculty of Science, University of Mauritius, 230 Réduit, Mauritius*
[5]*Halal Products Research Institute, Universiti Putra Malaysia, 43400 Serdang, Selangor, Malaysia*

Correspondence should be addressed to Najla Gooda Sahib Jambocus; najla.goodasahib@gmail.com and Azizah Abdul Hamid; azizahah@upm.edu.my

Received 14 June 2015; Revised 13 September 2015; Accepted 13 September 2015

Academic Editor: Michal Ciborowski

The prevalence of obesity is increasing worldwide, with high fat diet (HFD) as one of the main contributing factors. Obesity increases the predisposition to other diseases such as diabetes through various metabolic pathways. Limited availability of antiobesity drugs and the popularity of complementary medicine have encouraged research in finding phytochemical strategies to this multifaceted disease. HFD induced obese Sprague-Dawley rats were treated with an extract of *Morinda citrifolia* L. leaves (MLE 60). After 9 weeks of treatment, positive effects were observed on adiposity, fecal fat content, plasma lipids, and insulin and leptin levels. The inducement of obesity and treatment with MLE 60 on metabolic alterations were then further elucidated using a ^{1}H NMR based metabolomics approach. Discriminating metabolites involved were products of various metabolic pathways, including glucose metabolism and TCA cycle (lactate, 2-oxoglutarate, citrate, succinate, pyruvate, and acetate), amino acid metabolism (alanine, 2-hydroxybutyrate), choline metabolism (betaine), creatinine metabolism (creatinine), and gut microbiome metabolism (hippurate, phenylacetylglycine, dimethylamine, and trigonelline). Treatment with MLE 60 resulted in significant improvement in the metabolic perturbations caused obesity as demonstrated by the proximity of the treated group to the normal group in the OPLS-DA score plot and the change in trajectory movement of the diseased group towards the healthy group upon treatment.

1. Introduction

The new understanding of obesity and its related disorders has resulted in a renewed interest in finding antiobesity agents from nature, with partial success [1]. An established antiobesity agent, such as green tea polyphenols, is one of the few plants extracts reported to reduce weight in both animals and human subjects [2–4]. Others include extracts of Nomame Herba, cocoa, and chitin/chitosan [5–7]. While these studies yielded significant information on the effect of those plants on diet induced obesity and its biochemical changes, the overall effect on metabolic responses is relatively unknown.

Metabolomics as a new bioanalytical technique in obesity research is still largely unexplored. This "omics" technique is concerned with the high throughput identification and quantification of small molecules (<1500 Da) in the metabolome, the collection of small metabolites present in a cell, organ, or organism [8]. So far, the main application of the metabolomics approach has been in toxicological and pharmaceutical research, having the potential of

"bridging Traditional Chinese Medicine (TCM) and molecular pharmacology" [9]. Metabolomics has been applied for extracts characterisation and quality control of herbal supplements [10]. In regard to disease biomarkers discovery, metabolomics, in combination with multivariate data analysis, has been used for the profiling of various biofluids [11, 12]. More specifically to obesity research, it has been used to discriminate between metabolites of the obese models and the healthy models [13–15]. Metabolites such as betaine, taurine, acetone/acetoacetate, phenylacetylglycine, pyruvate, lactate, and citrate were the main discriminating metabolites between the obese and lean groups [13]. There is also the emerging trend of using metabolomics as a platform to study the holistic efficacy of traditional medicine. ^{1}H NMR based metabolomics approach was used to assess the effect of Xue-Fu-Zhu-Yu decoction (XFZYD) on high fat diet induced hyperlipidemia in rats. Metabolomics analysis of the plasma, combined with multivariate data analysis, revealed that XFZYD improved hyperlipidemia by regulating major metabolic pathways such as decreasing the accumulation of ketone bodies, enhancing glutathione biosynthesis, and reversing disturbances in lipid and energy metabolism [16].

Morinda citrifolia L., commonly called noni or Indian Mulberry, was discovered by the Polynesians more than 2000 years ago and brought to southeast Asia during migration [17]. Different parts of the plant have a long history of safe use and were reported to have many health promoting properties [18] including antidyslipidemic effects in rats [19] and inhibition of digestive and metabolic lipases *in vitro* [20–22]. We recently showed (results under publication) that a rutin rich extract of *Morinda citrifolia* leaves (MLE60) prevented weight and fat mass gain in lean Sprague-Dawley rats fed with a high fat diet with an improvement in plasma lipids, leptin, and insulin profiles and increased fecal fat output.

In this study, we assessed the effects of the leaf extract in high fat diet induced obese male Sprague-Dawley rats, using a ^{1}H NMR metabolomics approach, analysing urine and serum for markers metabolites.

2. Methodology

2.1. Preparation of Morinda citrifolia Leaf Extract (MLE 60). Mature *M. citrifolia* leaves were obtained from 5 representative trees from Bukit Expo, Universiti Putra Malaysia, Serdang, Selangor, Malaysia. Voucher specimens were deposited at the herbarium, Institute of Bioscience, Universiti Putra Malaysia (SK2197/13), and species were confirmed as *M. citrifolia* L. The leaves were immediately quenched using liquid nitrogen and lyophilised under pressure (−50°C, 48–72 hours, LABONCO, Labonco Corporation, Kansas City, Missouri, USA) until constant weight. The dried plant sample was ground using a commercial grinder, sieved, and stored at −80°C until further use.

Dried plant materials were extracted with 60% ethanol at room temperature for 72 hours. Filtrate was collected every 24 hours and the pooled filtrate was rotary-evaporated under vacuum until being concentrated. The aqueous phase was frozen at −80°C and lyophilised under pressure (−50°C, 48 hours) and stored at −80°C until future use. Extracts were prepared by dissolving weighed amount of extract in 0.03% carboxymethyl cellulose (CMC).

2.2. Animal Experiment. Male Sprague-Dawley rats (3 weeks old) were purchased from Sapphire Enterprise, Malaysia, and acclimatized for 10 days under standard laboratory conditions (12 h light/dark cycle, 55–60% relative humidity, 23–25°C). After acclimatization, rats were randomly divided into 2 groups based on assigned diets: standard rat chow (Gold Coin, Malaysia) and a high saturated fat diet for 12 weeks (MP Diets, USA). The body weight of each rat in both groups was recorded weekly to ensure development of obesity in the HFD group. After 12 weeks of the assigned diet, rats in the HFD group were then further divided into the following groups ($n = 6$), based on supplementation or nonsupplementation with MLE 60/Orlistat, and rats in both HFD and ND groups were continued on their respective diets:

(i) ND: normal diet only.

(ii) HFD: high fat diet only.

(iii) HFD + 250: high fat diet + 250 mg/kg body weight MLE 60.

(iv) HFD + 500: high fat diet + 500 mg/kg body weight MLE 60.

(v) HFD + OR: high fat diet + 30 mg/kg body weight Orlistat.

Orlistat, the currently available pancreatic lipase inhibitor, was used as positive control. An overview of the experiment is given in Figure 1.

2.3. Administration of MLE 60. Animals were allowed their respective diets *ad libitum* and required dosage of MLE 60 was given through gastric intubation. Volume of extracts given per day did not exceed 3 mL. Control groups (ND and HFD) received the vehicle (0.03% CMC) through gastric intubation. Body weight and food intake of each rat were recorded weekly.

2.4. Urine, Serum, and Feces Collection. Animals were placed in individual metabolic cages at the initial, middle, and final stages of the experiment. Urine was collected over 24 hours in tubes containing 1% sodium azide, transferred to urine specimen bottles, and stored at −80°C until being analysed. Blood samples were collected by cardiac puncture and serum and plasma samples were separated at 1500 ×g for 15 minutes and stored at −80°C for further analysis. Feces were collected and stored in airtight containers at −80°C for further analysis.

2.5. Sacrifice of Animals. After 12 weeks of obesity induction and 9 weeks of treatment, animals were weighed and sacrificed by cardiac puncture under an anaesthetic effect (xylazine + ketamine). Rats were deprived of food for 12 h prior to sacrifice. Serum and plasma samples were separated at 1500 ×g for 15 minutes and stored at −80°C

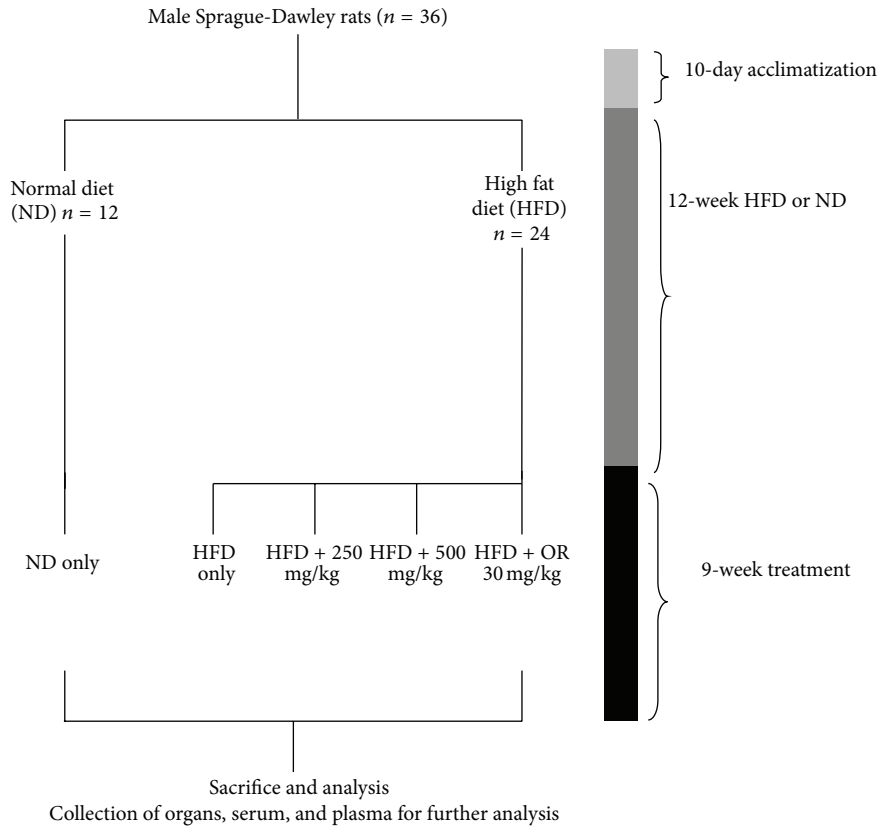

Figure 1: Schematic diagram of the experimental design to assess the antiobesity effect of MLE 60 in HFD induced obese male Sprague-Dawley rats.

for further analysis. All animals were handled according to the international principles of the Use and Handling of Experimental Animals (United States National Institute of Health, 1985) and all the protocols were approved by the Animal House and Use Committee of the Faculty of Medicine and Health Sciences, Universiti Putra Malaysia (Approval number UPM/FPSK/PADS/BR.UUH/00462).

2.6. Clinical Chemistry Measurements. Various biochemical parameters were measured, including blood glucose (One Touch Basic glucose monitor, LifeScan), lipids profiles (Roche Diagnostics GmbH, Sandhofer Strasse, Mannheim), total cholesterol (TC), total triglycerides (TG), low density lipoprotein (LDL), high density lipoprotein (HDL), kidney function tests (creatinine and urea), liver function tests γ-glutamyltransferase (GGT), alanine aminotransferase (ALT), aspartate aminotransferase (AST), alkaline phosphatase (ALP), leptin (RayBio Rat Leptin ELISA kit, Cat# ELR-Leptin-001, Norcross, GA, USA), insulin (Mercodia Rat Insulin ELISA, Uppsala, Sweden), adiponectin (Assay-Max Rat Adiponectin ELISA kit, Cat# ERA2500-1), and ghrelin (RayBio Rat Ghrelin ELISA kit, Cat# EIA-GHR-1, Norcross, GS, USA). All procedures were carried out in accordance with the manufacturers' instruction.

2.7. Determination of Fecal Fat Content. Fecal lipid content was determined according to a modified method of Tsujita et al. [23]. Feces were collected at the initial and final stages of the experiment and stored at −80°C until further analysis. Feces (0.5 g) were soaked in 2 mL of deionized water for 24 hours at 4°C, followed by homogenisation by vortexing at high speed for 60 seconds. Lipids were extracted with 7.5 mL of methanol : chloroform (2 : 1, v : v) and shaken for 30 minutes, followed by addition of 2.5 mL of deionized water and 2.5 mL of chloroform and further shaking for 30 minutes. Mixture was then centrifuged at 2000 g for 15 min and the lipophilic layer from the extraction was collected and dried under vacuum. Total fat content was weighed using a laboratory balance.

2.8. ^{1}H NMR Analysis of Urine and Serum. ^{1}H NMR analysis of urine and serum was carried out following the method of Beckonert et al. [12]. Urine samples were thawed and centrifuged at 12 000 ×g for 10 minutes. 400 μL of the supernatant was mixed with 200 μL phosphate buffer solution consisting of 0.1% of 3-trimethylsilyl propionic-2,2,3,3-d4 acid sodium salt (TSP) as internal standard (adjusted to pH 7.4 using NaOD) and transferred into 5 mm NMR tubes. Spectra were acquired at 27°C on a Varian Unity INOVA 500 MHz spectrometer (Varian Inc., CA), with a frequency of 499.887 MHz. Standard one-dimensional (1D) NOESY-presat pulse sequence was used for suppression of the water peak. For each sample, 64 scans were recorded with an acquisition

time of 1.36 s, pulse width of 3.75 μs, and relaxation delay of 1.0 s.

For serum, thawed samples were centrifuged at 12 000 ×g for 10 minutes and 200 μL of the supernatant was mixed with 400 μL of phosphate buffer containing 0.2% TSP and transferred into 5 mm NMR tubes. In addition to the NOESY-presat experiments, water suppressed Carr-Purcell-Meiboom-Gill (CPMG) spin-echo pulse was performed to suppress broad signals from macromolecules. The CPMG spectra were acquired with 128 transients, with an acquisition time of 1.36 s, relaxation delay of 2.0 s, and number of loops of $n = 80$.

Additional two-dimensional ^{1}H-^{1}H J resolved and ^{1}H-^{13}C HMBC analysis was performed to confirm the identity of certain metabolites.

2.9. NMR Spectral Data Reduction and Multivariate Data Analysis. Chenomx NMR Suite (Chenomx, Calgary, Canada) was used for metabolite identification and quantification. Nonzero filled spectra were manually phased and baseline corrected, calibrated to TSP at 0.00 ppm. Processed spectra (δ 0–10 ppm) were segmented (0.04 ppm) using the profiler module. Residual signals of water (δ 4.75–δ 4.85) and urea (δ 5.50–δ 6.00 ppm) were excluded from analysis. Remaining bins were normalized to the sum of spectral integrals, extracted with Microsoft Excel, and imported into Simca-P software (Umetrics, Umeå, Sweden) for multivariate data analysis.

Multivariate data analysis was performed using the mean centering with Pareto scaling. Principal component analysis (PCA) was selected as the initial clustering method. Partial Least Squares Discriminant Analysis (PLS-DA) was further performed as a supervised pattern recognition analysis, which maximizes the variation between the different groups and identifies variables responsible for the separation. Orthogonal projections to latent structures-discriminant analysis (OPLS-DA) were also performed for biomarkers analysis between the obese and lean groups and any metabolite changes associated with MLE 60 treatment [24].

2.10. Statistical Analysis. Data are expressed as mean ± standard deviation (SD). Difference between groups was determined by one-way analysis of variance (ANOVA, Minitab Version 14.0). Values were considered to be significantly different at the level of $p < 0.05$. For analysis of fecal fat content (week 6 and week 12) and body weight (before and after treatment), significance was further confirmed with one-sample t-test.

3. Results and Discussion

3.1. Induction of Obesity in Sprague-Dawley Rats Using a High Saturated Fat Diet. After 12 weeks of either the HFD or the ND, rats on the HFD had significantly higher weight gain as compared to rats on the ND. Sprague-Dawley rats on the HFD put on 157.54 ± 39.54% of their original weight whereas rats on the ND gained 93.34 ± 13.82%. Other obesity related biomarkers such as total triglycerides (TG), total cholesterol (TC), low density lipoprotein (LDL), and high density lipoprotein (HDL) levels in the plasma were also affected by the diet intervention (Table 1). Obese rats had lower HDL level (0.65 ± 0.08 mmol/L) as compared to lean rats (0.986 ± 0.16). There was no significant difference in the plasma TC and LDL content in both groups. The TG level was significantly ($p < 0.05$) elevated in the group fed the HFD (0.908±0.15 mmol/L) as compared to rats fed the ND (0.432± 0.07). Obese rats had higher fasting glucose levels than lean rats, though still in the normal range. Other obesity related adipocytic factors such as leptin and insulin were elevated in the obese models. Kidney function tests as measured by plasma urea and creatinine levels appeared normal, with no significant difference between the groups. In terms of liver function, GGT, ALT, and ALP levels were increased in obese rats fed the HFD. Hypercaloric diets ranging from 3.7 to 5.5 kcal/g result in models of obesity, which represent the aetiology of obesity at its best and reproduce its pathophysiological characteristics [25]. The increase in weight gain is gradual as the intervention progresses. Based on the changes in lipid profiles and other plasma biochemistries, our study, which uses HFD containing 36% of total calories from coconut oil, supports the theory that coconut/lard based high fat diets do model the metabolic disorders of human obesity in rodents [26, 27]. More specifically, a hydrogenated coconut oil (HCO) based HFD has previously caused weight gain, increased liver weight, and hyperlipidaemia in rats [28]. Based on the significant increase in body weight and other biochemical parameters measured, we can conclude that high fat diet induced obesity was successfully achieved in male Sprague-Dawley rats after a feeding period of 12 weeks.

Table 1: The plasma biochemistry of rats fed a normal diet (ND) or a high fat diet (HFD) for 12 weeks to induce obesity.

	ND	HFD
Total cholesterol (mmol/L)	1.28 ± 0.15^a	1.16 ± 0.09^a
HDL (mmol/L)	0.99 ± 0.16^a	0.66 ± 0.08^b
LDL (mmol/L)	0.28 ± 0.02^a	0.23 ± 0.03^a
Triglycerides (mmol/L)	0.43 ± 0.07^a	0.91 ± 0.15^b
Leptin (pg/mL)	719.30 ± 150.1^a	1819.50 ± 150.1^b
Insulin (μg/L)	0.20 ± 0.02^a	1.30 ± 0.09^b
Adiponectin (ng/mL)	7.40 ± 0.50^a	6.11 ± 0.07^b
Glucose (mmol/L)	5.68 ± 0.33^a	6.26 ± 0.13^b
Urea (μmol/L)	6.26 ± 0.81^a	5.14 ± 0.80^a
Creatinine (mmol/L)	55.20 ± 2.17^a	51.60 ± 2.41^a
GGT (U/L)	1.00 ± 0.00^a	6.00 ± 0.84^b
AST (U/L)	76.36 ± 3.16^a	75.40 ± 1.29^a
ALT (U/L)	37.64 ± 5.26^a	30.82 ± 1.48^b
ALP (U/L)	69.14 ± 9.98^a	127.20 ± 5.07^b

Different small letters indicate significant difference ($p < 0.05$) between ND and HFD groups as shown by analysis of variance (ANOVA) using Minitab Version 14.

3.2. ^{1}H NMR Spectra of Urine and Serum Metabolites of Sprague-Dawley Rats Fed HFD or ND for 12 Weeks. Representatives of ^{1}H NMR spectra for the serum and urine samples

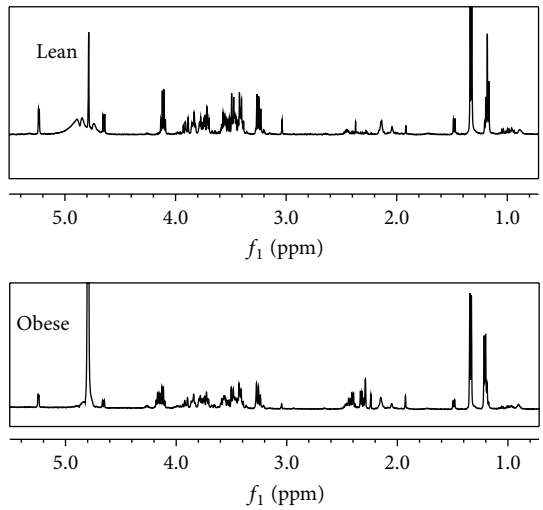

Figure 2: Typical 500 MHz ^{1}H NMR spectra of serum collected from a Sprague-Dawley rat fed a normal diet (lean) and a Sprague-Dawley rat fed a high fat diet (obese).

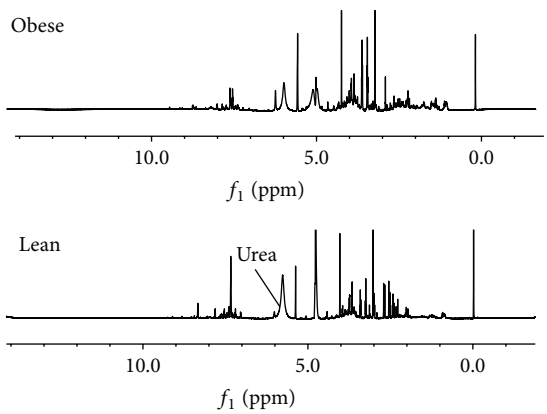

Figure 3: Typical 500 MHz ^{1}H NMR spectra of urine collected from a Sprague-Dawley rat fed a high fat diet (obese) and a Sprague-Dawley rat fed a normal diet (lean).

from an obese rat fed HFD and a lean rat fed ND for 12 weeks are shown in Figures 2 and 3, respectively. Expanded regions for better comparison are available in Supplementary Data sections in Supplementary Material available online at http://dx.doi.org/10.1155/2016/2391592. Metabolites were assigned based on previous studies [29, 30], the Chenomx NMR Suite, Version 7.7 (Chenomx Inc., Edmonton, AB, Canada), and the Human Urine and Serum Metabolome Databases [31, 32]. Additional two-dimensional ^{1}H-^{1}H J resolved and HMBC analysis was performed to aid in the identification of certain metabolites. A list of the identified metabolites, including their chemical shifts, is represented in Table 2.

CV ANOVA was used to test the significance of the models, whereby significance is achieved with a p value less than 0.05. Both PLS-DA and OPLS-DA models for urine and serum were validated accordingly (Table 3).

Table 2: ^{1}H NMR assignments of metabolites in rat's serum and urine.

Metabolites	Assignments	Chemical shifts	Samples
Urea	NH_2	5.78 (s)	U
Phenylacetylglycine	2,6-CH	7.42 (m)	U
	3,5-CH,	7.57 (m)	
	7-CH	7.65 (m)	
	10-CH	7.84 (m)	
Trigonelline	γCH_3	4.43 (s)	U
	C_2H	8.1 (m)	
	C_4H	8.8 (m)	
	C_5H,	9.1 (s)	
Hippurate	CH_2,	3.98 (d)	U
	CH	7.54 (d)	
	CH	7.65 (t)	
Acetate	CH_3	1.93 (s)	U, S
Dimethylamine	CH_3	2.71 (s)	U
Citrate	$1/2CH_2$	2.54 (d)	U
	$1/2CH_2$	2.66 (d)	
2-Oxoglutarate	CH_2	2.45 (t)	U
	CH_3	3.02 (t)	
Creatinine	CH_3,	3.06 (s)	U
	CH_2	4.06 (s)	
Lactate	CH_3,	1.34 (d)	U, S
	CH	4.11 (dd)	
B-Glucose	1-CH	4.66 (d)	U, S
α-Glucose	1-CH	5.22 (d)	U, S
Allantoin	CH	5.38 (s)	U
Glycine	CH_2	3.57 (s)	U
Taurine	CH_2S,	3.26 (t)	U, S
	CH_2-N	3.40 (t)	
TMAO	$N(CH_3)_3$	3.26 (s)	U
Alanine	βCH_3,	3.78 (dd)	S
	αCH	1.48 (d)	
Pyruvate	βCH_3	2.38 (s)	S
Succinate	CH	2.41 (s)	S
Acetoacetate	CH_3	2.27 (s)	S
3-Hydroxybutyrate	γCH_3	1.18 (d)	S
	βCH	4.23 (m)	
	αCH_2	2.31 (d)	
	αCH_2	2.38 (dd)	
2-Hydroxyisobutyrate	CH_3	1.34 (s)	S
Lipoprotein	$CH_3(CH_2)_n$	0.89 (m)	S
LDL/VLDL	$CH_3CH_2CH_2C=$	1.2–1.30 (m)	S

s: singlet; d: doublet; t: triplet; dd: doublet of doublets; m: multiplet.
S: serum; U: urine.

The variable importance in project (VIP) plots were generated to identify metabolites contributing significantly to the separation of the obese and the lean groups. A cut-off value of 0.7-0.8 for the VIP is generally acceptable. In this study, the cut-off value was set at 1.0 [24].

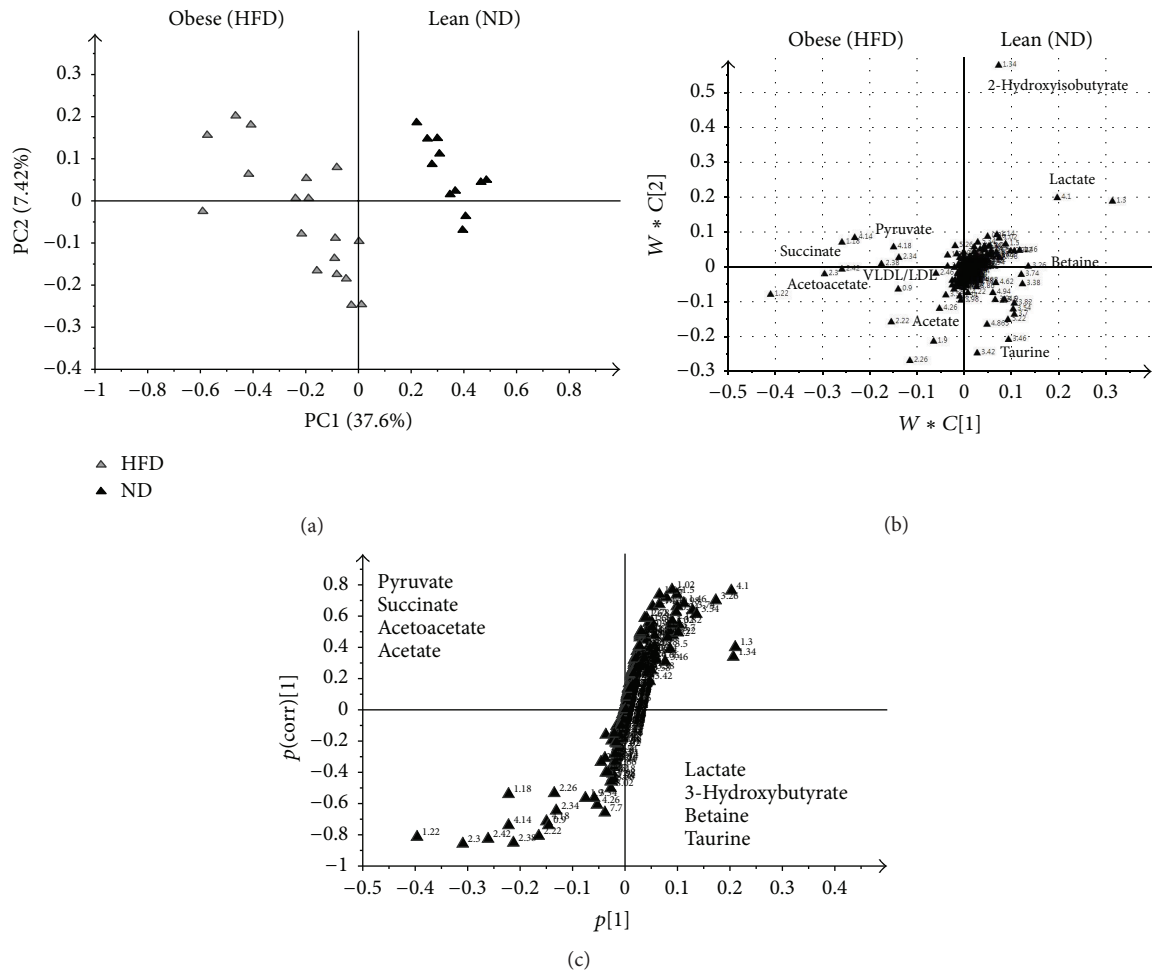

Figure 4: OPLS-DA derived score plot (a), loading plot (b), and *S* plot (c) obtained using ^{1}H NMR data for serum samples from Sprague-Dawley rats fed a high fat diet (HFD) or a normal diet (ND) for 12 weeks.

Table 3: PLSDA and OPLS-DA models validation for serum and urine of Sprague-Dawley rats fed a high fat diet (HFD) or a normal diet (ND) for 12 weeks.

Samples/models	R^2Y	Q^2Y	p CV ANOVA	Number of components
Serum				
PLS-DA	0.830	0.752	3.32×10^{-6}	2
OPLS-DA	0.987	0.936	4.26×10^{-7}	2
Urine				
PLS-DA	0.917	0.874	3.18×10^{-12}	3
OPLS-DA	0.959	0.923	1.89×10^{-12}	3

An OPLS-DA model was used to identify discriminating metabolites between the 2 groups fed the different diets. The OPLS-DA method is useful for biomarkers identification. The *S* plot was further used to visualise the influence of the variables in the model by considering both covariance $p(1)$ and correlation $p(\text{corr})$ loadings profiles from the OPLS-DA model. This enables filtering interesting metabolites in the projection. Ideal biomarkers have high magnitude and reliability values (Figures 4 and 5).

Induction of obesity was associated with increased serum levels of acetate, succinate, pyruvate, VLDL/LDL, and acetoacetate and decreased levels of lactate, 2-hydroxyisobutyrate, and betaine, among others (Figure 4). The same principle was applied to the analysis of urine and clear separation was obvious in the ^{1}H NMR profiles (Figure 5). Among the increased metabolites in the HFD group were the levels of creatinine, allantoin, taurine, and phenylacetylglycine, while the levels of 2-oxoglutarate, dimethylamine, citrate, and hippurate were decreased.

After 12 weeks of feeding on the HFD, male Sprague-Dawley rats had a significantly ($p < 0.05$) higher increase in body weight as compared to rats fed ND. Obese rats had higher plasma level of TG and lower level of HDL as compared to their lean counterparts. TC and LDL levels were not significantly changed in the 2 groups fed ND and HFD. ^{1}H NMR analysis of urine and serum revealed additional metabolic changes, beyond the measured small set of parameters. OPLS-DA analysis of serum ^{1}H NMR spectra revealed increased succinate, pyruvate, VLDL/LDL,

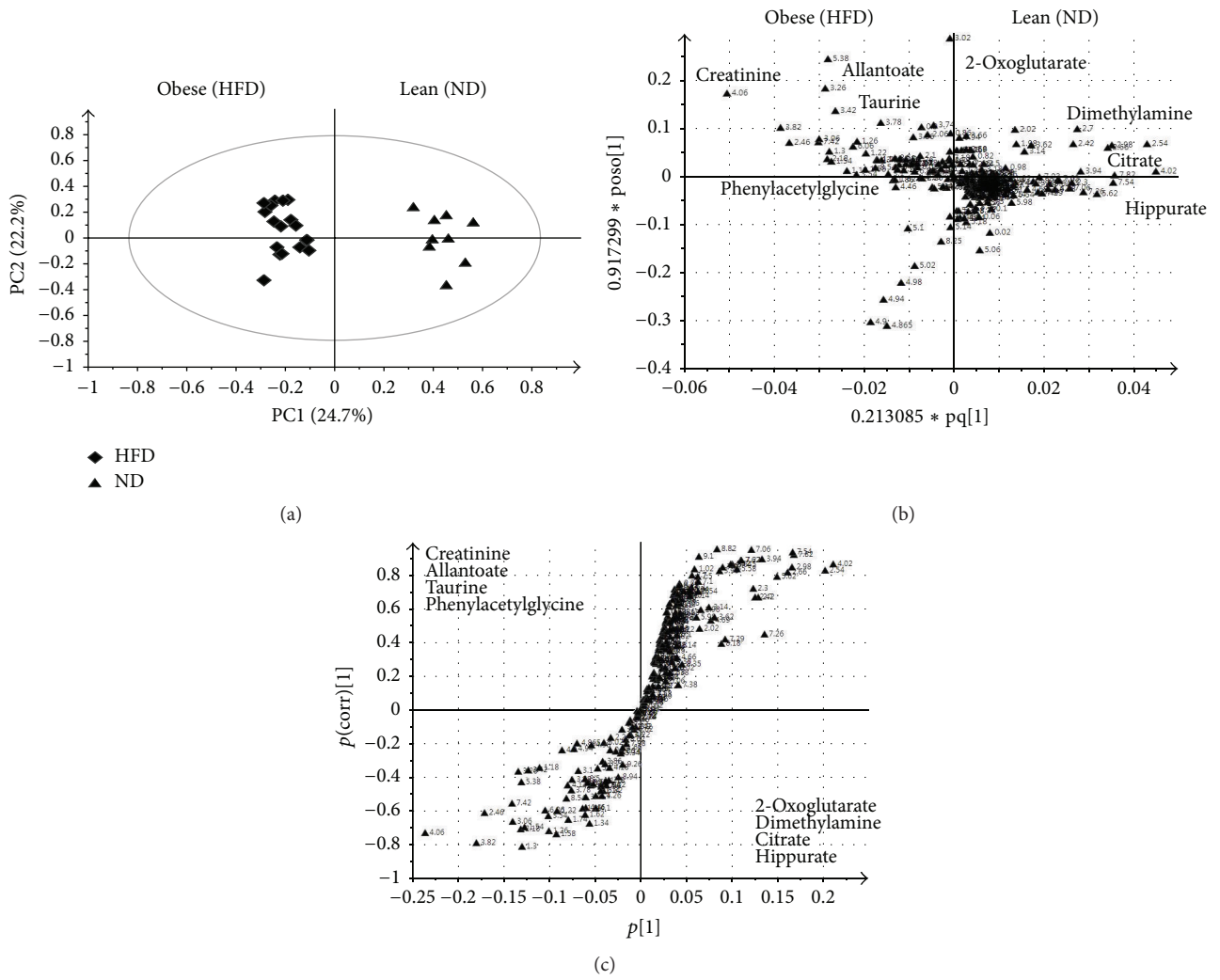

Figure 5: OPLS-DA derived score plot (a), loading plot (b), and *S* plot (c) obtained using ^{1}H NMR data for urine samples from Sprague-Dawley rats fed a high fat diet (HFD) or a normal diet (ND) for 12 weeks.

and acetoacetate and decreased lactate, betaine, and taurine levels in the HFD group. OPLS-DA analysis of urine samples showed that rats fed HFD had higher urinary content of creatinine, allantoin, taurine, and phenylacetylglycine and decreased levels of 2-oxoglutarate, dimethylamine, citrate, and hippurate.

All of these identified metabolites are related to various metabolic pathways, namely, the glucose metabolism and tricarboxylic acid (TCA) cycle, lipid metabolism, choline metabolism, amino acids metabolism, and creatinine metabolism.

Glucose Metabolism and TCA Cycle. Obese rats had higher succinate, pyruvate, acetoacetate, and acetate levels and decreased levels of lactate, 2-oxoglutarate, and citrate, all metabolites related to the glucose metabolism and the TCA cycle. These findings are consistent with other reports on the metabolomics studies of obesity [14, 33, 34]. This current study showed decreased serum lactate in obese rats fed HFD for 12 weeks, which is similar to the study of Song et al. [16] where hyperlipidemic mice fed HFD had decreased level of lactate. The urine of Zucker rats and the serum of HFD mice also had lower lactate content than the normal weight rats and the serum [14, 35]. The reduced lactate levels can be explained by factors other than HFD induced obesity, including young age and activity [36].

HFD induced obese rats had lower urinary content of 2-oxoglutarate and citrate as compared to the lean rats. Previously, Schirra et al. [37] reported a decreased level of 2-oxoglutarate in 2 mutants groups studied for altered liver metabolism. The level of citrate in the plasma is regulated by insulin, glucose levels, fatty acid utilization, and cholesterol synthesis [38] and is usually increased in HFD obese models [39] and diabetic models [40]. However, consistent with our findings, HFD induced rodents have decreased urinary citrate levels [37] which is associated with insulin resistance in humans [41]. Independent measurement of plasma insulin in this study showed a 6-fold increase in the insulin level of HFD fed obese rats (1.29 μg/L) as opposed to the ND fed lean rats (0.21 μg/L), which indicates that the HFD not only

induced obesity in the rodents, but also caused the model to be insulin resistant, most likely caused by decreased urinary citrate excretion due to an increase in metabolic acidosis [42].

With lactate being the precursor for gluconeogenesis, any fluctuation in lactate levels indicates perturbations in glucose production and lipid synthesis in the liver [43]. The downregulation of pyruvate dehydrogenase phosphatase in obese subjects has been reported to be a defect, which signals insulin resistance [44]. Elevated concentrations of pyruvate suggest increased glycogenolysis and glycolysis to meet exceeding energy demands, similarly to the observation of serum profile of obese growing pigs [45].

Lipid Metabolism. The levels of betaine and taurine were changed as a result of the HFD, revealing changes in lipid metabolic pathways. Serum profiles showed lower levels of taurine, while there was an increased level of urinary taurine content. Previous studies have reported reduced taurine content in the serum, urine, and liver of various rodent models [14]. However, also in accordance with our findings, Kim et al. [13] reported increased levels of taurine in the urine of HFD fed rats. Taurine plays various biological roles in the conjugation of cholesterol, antioxidation of bile acids, osmoregulation, and calcium signalling pathways [46, 47]. The supplementation of taurine showed amelioration in obesity most likely mediated by the ability of taurine to increase fatty acid oxidation [48]. This study shows decreased taurine in the obese group, suggesting decreased fatty acids oxidation and inhibition of taurine biosynthetic enzymes related to obesity, as observed by increased levels of LDL/VLDL shown in both serum spectra and actual measured values.

Choline Metabolism. Pertaining to choline metabolism, the level of betaine was decreased in the HFD group, similarly to most metabolomics based obesity studies reporting decreased hepatic and urinary betaine content in HFD fed rodents [33, 34] and decreased hippurate in the serum of HFD mice [38]. In humans, lowered betaine levels are associated with obesity related disorders such as metabolic disorders, lipid disorders, and type 2 diabetes [49]. Supplementation of betaine causes increase in metabolites in the carnitine biosynthesis pathway, reduced accumulation of triglycerides in the liver, with no effect on body weight gain and increase in adipose tissue mass [50].

Creatinine Metabolism. Feeding of HFD diet for 12 weeks resulted in increased creatinine levels in the urine samples, in line with other reports [37, 51, 52].

Amino Acids Metabolism. High level of serum acetoacetate might be the indication of depletion in leucine level, an amino acid involved in insulin signalling, protein synthesis of muscle mass, and production of alanine and glutamine [53]. Alanine peaks were more prominent in the serum spectra of the lean rats as compared to obese subjects.

Gut Microbiome Metabolism. Changes in specific metabolites support the idea that there is a link between obesity and the gut microbiome. HFD induced obese rats showed high urinary content of phenylacetylglycine and decreased levels of hippurate and dimethylamines, metabolites involved in the gut microbiome metabolism. Hippurate is produced in the gut by microorganisms using glycine and benzoic acid as building blocks [54]. Increased hippurate level in the urine has been associated with leanness [34] and this study confirms the findings from other studies [38] that HFD induced obesity is associated with decreased urinary level of hippurate in rodent models of obesity. Increased levels of phenylacetylglycine in Sprague-Dawley rats fed HFD have been previously reported [13]. High gainers fed HFD were associated with increased levels of phenylacetylglycine as compared to low gainers on ND, which indicates an increase in the precursors produced by gut microorganisms [55]. Moreover, reduced dimethylamine levels in the obese group reflect changes in the gut microbiome derived metabolism, similarly to what is observed in leptin-deficient ob/ob mice [56]. Trigonelline was also identified in the urine samples of lean rats. It is an indicator of niacin metabolism, an essential vitamin needed as coenzyme in carbohydrate and lipid metabolism. The body's requirements for niacin can be met by dietary intake or endogenous biosynthesis through tryptophan-mediated metabolism carried out by the liver and the gut microorganisms [57]. Obesity related stress causes depletion in the glutathione stores and the decrease of trigonelline is related to depletion of *S*-adenosylmethionine, used to make up the energy stores [58]. A strong link between human gut microbiome and obesity was established with decreased urinary excretion of hippurate, trigonelline, and xanthine and increased urinary excretion of 2-hydroxybutyrate and bariatric surgery induced weight loss resulted in the loss of typical obese metabotype [59].

3.3. Effect of 9-Week Treatment with 250/500 mg/kg of MLE in the Obese Rats Models. After 12 weeks of inducing obesity, rats on the HFD were further divided and received either MLE 60 (250 and 500 mg/kg), Orlistat (30 mg/kg), or the carrier vehicle (CMC). Obese rats were kept on the HFD while lean rats were continued on the ND. Body weight and food intake were recorded weekly and the plasma biochemistry was analysed at the end of the experiment (Table 4).

Although there was no significant weight loss in the obese group, receiving MLE 60 or Orlistat, further weight gain was prevented in the HFD + 500 and HFD + OR group. Treatment resulted in reduced visceral fat, with the HFD group having the highest amount (6.62 ± 1.54%). The treated groups had a reduced % of visceral fat ranging from 3.34 ± 0.99 for the HFD + OR group to 4.87 ± 0.96% for the HFD + 500 group. There was no significant difference in decrease of visceral fat between the obese rats receiving 500 mg/kg MLE 60 and rats receiving standard antiobesity drug, Orlistat. No significant difference was recorded in the daily food intake among all groups. At baseline (before treatment), there was no significant difference in the fecal fat excretion in the lean and obese rats. Treatment with 500 mg/kg MLE increased the fecal fat excretion (12.64 ± 1.73%), with a comparable effect to treatment with Orlistat (15.89 ± 1.62%). The fecal fat content

Table 4: The body weight, % visceral fat, food intake, % fecal fat excretion, and plasma biochemistry of HFD induced obese rats after 9 weeks of treatment with MLE 60 at 250 mg/kg and 500 mg/kg body and 30 mg Orlistat/kg body weight.

	HFD	HFD + 250	HFD + 500	HFD + OR	ND
Body weight (g)					
Initial (week 12)	559.20 ± 25.89^{Bb}	546.85 ± 83.20^{Bb}	544.29 ± 78.74^{Bb}	537.25 ± 93.83^{Bb}	379.33 ± 34.82^{Aa}
Final (week 21)	614.20 ± 131.58^{Bb}	605.57 ± 101.50^{Bb}	565.85 ± 87.47^{Bb}	553.13 ± 98.93^{Bb}	417.16 ± 32.99^{Aa}
Visceral fat (%)	6.62 ± 1.54^{c}	5.18 ± 0.40^{bc}	4.87 ± 0.963^{b}	3.34 ± 0.99^{b}	1.70 ± 0.28^{a}
Food intake (g/rat/day)	20.00 ± 3.09^{a}	19.08 ± 2.29^{a}	19.38 ± 2.01^{a}	19.08 ± 0.86^{a}	20.17 ± 1.35^{a}
Fecal fat content (%)					
Initial	6.18 ± 1.19^{aA}	7.35 ± 1.14^{aA}	6.31 ± 1.40^{aA}	6.12 ± 1.52^{aA}	7.64 ± 0.70^{aA}
Final	7.23 ± 1.01^{aC}	9.44 ± 1.07^{aC}	12.64 ± 1.73^{bB}	15.89 ± 1.62^{bA}	8.99 ± 0.61^{aC}
Total cholesterol (mmol/L)	1.43 ± 0.08^{b}	1.04 ± 0.01^{a}	0.94 ± 0.02^{a}	0.92 ± 0.07^{a}	1.29 ± 0.13^{b}
HDL (mmol/L)	0.82 ± 0.06^{b}	0.57 ± 0.12^{bc}	0.69 ± 0.07^{b}	0.56 ± 0.01^{c}	1.02 ± 0.09^{a}
LDL (mmol/L)	0.33 ± 0.07^{b}	0.22 ± 0.03^{ab}	0.17 ± 0.03^{a}	0.20 ± 0.04^{a}	0.21 ± 0.05^{a}
Triglycerides (mmol/L)	0.93 ± 0.16^{c}	0.72 ± 0.12^{bc}	0.50 ± 0.11^{ab}	0.58 ± 0.01^{ab}	0.42 ± 0.09^{a}
Leptin (pg/mL)	2119.50 ± 176.3^{b}	1563.30 ± 556.9^{ab}	1050.00 ± 229.3^{a}	1263.30 ± 30.10^{a}	1125.00 ± 117.60^{a}
Insulin (μg/L)	1.83 ± 0.10^{c}	0.71 ± 0.01^{b}	0.37 ± 0.13^{a}	0.47 ± 0.22^{ab}	0.31 ± 0.01^{a}
Ghrelin (ng/mL)	25.7 ± 3.71^{c}	54.57 ± 4.19^{a}	35.74 ± 1.68^{b}	37.63 ± 0.98^{b}	53.01 ± 1.95^{a}
Adiponectin (ng/mL)	8.61 ± 0.77^{b}	9.50 ± 0.23^{ab}	9.25 ± 0.50^{ab}	8.25 ± 0.44^{b}	9.87 ± 0.20^{a}
Glucose (mmol/L)	7.70 ± 0.78^{c}	6.85 ± 0.71^{bc}	5.83 ± 0.53^{ab}	4.98 ± 0.17^{a}	6.03 ± 0.17^{b}

Different small letters indicate significant difference ($p < 0.05$) between different groups and different capital letters indicate significant difference among the same group at different time points, as shown by analysis of variance (ANOVA) using Minitab Version 14.

in the control group (HFD only) remained unchanged after 9 weeks (7.23 ± 1.01%).

Few plasma parameters were measured after 9 weeks of treatment (Table 4). With regard to lipid profiles, treatment with both 500 mg MLE 60/kg and Orlistat improved the plasma LDL level, reducing its levels to the LDL profile of lean rats. The treatment, however, failed to improve HDL levels, with the HFD + OR group having the lowest plasma HDL content of 0.56 ± 0.01 mmol/L. Lean rats on the ND have the highest level of HDL, 1.02 ± 0.09 mmol/L. The most marked effect was in the TG content, whereby HFD + 500 (0.50±0.11) significantly improved the plasma TG level as compared to rats receiving the HFD only (0.93 ± 0.12).

The plasma insulin level was significantly improved in the HFD + 500 group (0.37 ± 0.13), which was similar to the ND group (0.31 ± 0.02). Similarly, plasma leptin levels were significantly improved in both HFD + 500 group (1050 ± 229 pg/mL) and HFD + OR group (1263 ± 30.10 pg/mL) as compared with the HFD group (2119 ± 176 pg/mL). Ghrelin levels were improved in all treated groups, with 250 mg/kg dosage being more potent, restoring the ghrelin levels to 54.57 ng/mL, not significantly different from the lean group (53.01 ng/mL). Adiponectin levels were not significantly different in the lean groups and the treated groups (9.25–9.87 ng/mL), except in the group treated with Orlistat (8.25 ng/mL), where the adiponectin level was not significantly different from the obese group (8.61 ng/mL). Treatment with 30 mg/kg Orlistat and 500 mg/kg MLE 60 had the most significant improvement.

In the previous section, rats fed HFD were associated with higher acetate and pyruvate and surprisingly lower lactate levels as opposed to lean rats fed ND. After an additional 9 weeks, rats fed HFD were still associated with higher acetate and pyruvate and also higher lactate level. Lactate is one of the key metabolites related to glucose metabolism and the TCA cycle, which has been reported to be higher in obese humans [60]. Increased lactate concentration has been attributed to the upregulation in anaerobic glycolysis in obese subjects and the balance between lactate production and lactate removal [14, 61]. The adipose tissue is one of the sites of lactate production, together with the skeletal muscles, erythrocytes, and brain [61, 62]. Increased lactate production can also reflect perturbations in glucose and lipid production in the liver due to the involvement of lactate as a precursor in gluconeogenesis [43] with increased serum lactate being associated with increased risk of mortality [63]. In this study, increased serum lactate in the HFD group can be attributed to the higher percentage of body fat as compared to the lean rats. Lactate levels in obese subjects are also highly dependent on insulin resistance [64]. In a study by Chen et al., normal weight subjects with normal blood glucose had the lowest plasma lactate levels, obese subjects with normal blood glucose had intermediate plasma lactate levels, and obese subjects with impaired blood glucose had the highest lactate levels. Consistent with these reports, this study shows that, after 21 weeks of feeding HFD, rats had higher insulin levels (1.83 μg/L) as compared to after 12 weeks of feeding (1.30 μg/L), which explains the elevated lactate levels in the obese groups. Treated groups had significant decrease in % of body fat and plasma insulin levels, which contributes to the decreased lactate plasma content [65].

Another metabolite, which was found to be strongly associated with obesity, is 2-hydroxyisobutyrate. It is involved in the gut microbiome metabolism and has been reported to

Table 5: Relative quantification of significant discriminating metabolites based on the concentration of 0.1% of 3-trimethylsilyl propionic-2,2,3,3-d4 acid sodium salt (TSP) as internal standard and quantified using Chenomx NMR Suite.

Metabolites	Chemical shifts	VIP value	HFD	ND	HFD + 250	HFD + OR	p value
Lactate	1.34 (d) 4.11 (dd)	2.46	1662.9 ± 51.9^{c}	493.4 ± 73.1^{a}	482.1 ± 55.9^{a}	761.0 ± 33.6^{b}	0.000
Alanine	3.78 (dd) 1.48 (d)	1.63	94.0 ± 3.03^{b}	53.3 ± 13.48^{a}	55.6 ± 3.52^{a}	47.0 ± 2.50^{a}	0.002
3-Hydroxybutyrate	1.18 (d) 4.23 (m) 2.31 (d) 2.38 (dd)	3.48	316.8 ± 23.17^{b}	513.8 ± 74.20^{a}	368.7 ± 24.00^{ab}	396.9 ± 73.54^{ab}	0.023
2-Hydroxyisobutyrate	1.34 (s)	5.60	232.5 ± 25.36^{b}	153.8 ± 15.12^{a}	143.9 ± 21.54^{a}	182.1 ± 49.43^{ab}	0.036
Pyruvate	2.38 (s)	2.19	55.6 ± 3.62^{c}	18.7 ± 2.16^{a}	31.1 ± 1.03^{b}	28.3 ± 7.21^{b}	0.000
Creatinine/creatine	3.06 (s) 4.06 (s)	1.28	45.1 ± 2.43^{b}	25.6 ± 3.64^{a}	23.3 ± 0.60^{a}	39.5 ± 0.04^{b}	0.000
α-Glucose	5.22 (d)	1.09	1116.4 ± 27.4^{c}	458.1 ± 27.6^{b}	511.7 ± 20.6^{b}	206.4 ± 44.3^{a}	0.000
Acetate	1.93 (s)	1.28	38.9 ± 2.80^{b}	26.8 ± 4.42^{a}	35.4 ± 1.50^{b}	38.9 ± 2.61^{b}	0.013

Different small letters indicate significant difference ($p < 0.05$) between different groups as shown by the analysis of variance (ANOVA) using Minitab Version 14.

be altered in leptin-deficient ob/ob mice [56] and increased in obese patients [66].

Regarding amino acid metabolism, serum alanine was increased in HFD group as compared to the lean group, in line with previous studies reporting increased alanine in the serum and liver of HFD induced mice and rats [39].

Obesity was characterised by decreased levels of 3-hydroxybutyrate, a metabolite of amino acid metabolism, which is associated with leanness and weight loss, where obese patients expressed the highest 3-hydroxybutyrate levels following bariatric surgery [66]. Early studies have also reported on the link between obesity and 3-hydroxybutyrate. Administration of the compound in obese subjects on low energy diets resulted in improved fat : lean ratio while not affecting weight loss [67]. The roles of acetoacetate and 3-hydroxybutyrate were further studied in obese and insulin dependent diabetic humans using a kinetic approach, to investigate ketone body metabolism. Obese subjects had lower ketone body de novo synthesis, with no significant clearance of 3-hydroxybutyrate from the normal healthy subjects, with 3-hydroxybutyrate being an important determinant in diabetic ketoacidosis [68]. Moreover, 3-hydroxybutyrate has also been associated with reduced food intake in obese subjects [69] and involved in the short-term and long-term effects of high fat diet in mice [14]. Won et al. also reported the downregulation of 2-hydroxybutyrate in both male and female leptin-deficient ob/ob mice [56].

In the metabolites identification, OPLS-DA model consisting of 2 groups at a time was employed, followed by the Shared and Unique Structure (SUS) plots, to compare biomarkers from 2 models.

Key discriminating metabolites as potential biomarkers in rat serum based on ^{1}H NMR loading plots in the HFD, HFD + 500, and ND groups were quantified, relative to the TSP in the serum samples. Statistical analysis (Minitab Version 14) was further employed to detect significance. Focus was placed on metabolites with a VIP value of >1, as metabolites contributing more to the clustering of the different groups (Table 5).

There are limited studies, which have used a metabolomics approach to identify metabolic changes following intervention with drugs and therapeutics, including the phytochemical strategies for obesity, though the potential is vast [70]. However, there are few metabolomics based reports on weight loss as a result of weight loss intervention, including exercise and surgery. An energy-restricted diet for 8 weeks resulted in an improvement in glucose and lipid metabolism in overweight obese adults. Saturated fatty acids such as palmitic acid and stearic acid were significantly decreased as well as branched amino acid, isoleucine [71]. A lifestyle intervention in obese children, "Obeldicks," resulted in significant weight loss and abdominal obesity, modulated by the role of phosphatidylcholine metabolism. This particular study also highlights the large interindividual variation to lifestyle intervention and the possible need of a more individualised approach to lifestyle interventions [72]. ^{1}H NMR analysis also showed that while exercise can improve the metabolic disruptions associated with diet induced obesity, the effect cannot be cancelled out and diet predicts obesity better with a stronger influence on metabolites' profiles than exercise alone [14].

One of the few studies reporting the response of natural therapeutic agents in obese subjects assessed the effect of sea buckhorn and bilberry on serum metabolites in overweight women. No significant changes were observed in individual metabolites, though improvements in serum lipids and lipoproteins were observed [73]. The treatment of high fat diet induced hyperlipidemia with Xue-Fu-Zhu-Yu decoction was studied using a NMR based metabolomics approach. OPLS-DA analysis revealed the beneficial effects of the decoction, mainly through decrease in ketone bodies production, enhancement of biosynthesis, and modulation of

lipid metabolism [16]. Dietary intervention of black soybean peptides in overweight human showed an increase in betaine, benzoic acid, pyroglutamic acid, and pipecolic acid, among others. VIP analysis showed L-proline, betaine, and lyso-PCs to be more correlated to the discrimination before and after treatment [74].

Treatment with MLE 60 at 250 mg/kg body weight improved serum levels of lactate, alanine, pyruvate, creatinine, and α-glucose, bringing their levels closer to the normal control whereas the level of 3-hydroxyisobutyrate, 3-hydroxybutyrate, and acetate remained unchanged. Similar improvements were achieved in the groups receiving 30 mg/kg body weight of Orlistat. The relative concentration of α-glucose was found to be most reduced, consistent with the actual biochemical measurement done previously where the Orlistat treated group had significantly lower plasma glucose (4.97 mmol/L) as compared to the lean group (6.02 mmol/L). This is consistent with the literature reporting that Orlistat in a weight loss regimen can significantly improve glucose tolerance and slows down the progression of type 2 diabetes and impaired glucose tolerance in clinical cases of obesity [75, 76].

Based on the relative quantification of certain metabolites (lactate, pyruvate, and glucose) in the treated groups, it is apparent that treatment with MLE 60 improved perturbations in various metabolic pathways, predominantly in the glucose and TCA cycle as reflected by positive modulations in lactate, pyruvate, and glucose levels. Disruptions in the creatinine and amino acid metabolic pathways were also improved as indicated by a reduction of creatinine and alanine accumulation in the obese groups treated with MLE 60. The levels of 3-hydroxyisobutyrate, a metabolite of the gut microbiome metabolism, were unchanged in the treated groups, suggesting that MLE 60 did not impact on the obesity-induced disruptions in the gut microbiome. Similarly, the levels of 2-hydroxybutyrate, a metabolite of amino acid metabolism, were also unchanged.

Obesity has been characterised by an elevated TCA function in diet induced hepatic insulin and fatty liver as well as decreased brain glucose metabolism, predominantly through the TCA cycle [77, 78]. Treatment with MLE 60 improved serum creatinine profiles as shown by ^{1}H NMR measurement as compared to nonsignificance observed when blood creatinine level was measured. Poor creatinine clearance is associated with weight gain and central obesity due to increased metabolic abnormalities as risk factors [79]. An increase in creatine kinase and adenylate kinase 1 activity was observed in obese subjects, attributed to a compensatory effect of the downregulation of muscle mitochondrial function, associated with obesity [80].

Hence, antiobesity agent which can positively influence these pathways as well as other parameters such as adipocytes factors and weight loss shows promise for weight management.

4. Conclusion

Based on the reported health properties of *M. citrifolia*, including the antiobesity activities, the aim of this study was to further explore the effect of a leaf extract, MLE 60, on obesity using a ^{1}H NMR metabolomic approach. ^{1}H NMR spectroscopy and multivariate data analysis revealed clear metabolic differences in the urine and serum samples of the HFD induced obese and lean rats. An OPLS-DA method was chosen to project maximum separation between the groups and to identify discriminating biomarkers. All multivariate models including PLS-DA and OPLS-DA were duly validated, using permutation tests, R^2Y, Q^2Y, and p CV ANOVA values. Several metabolites were identified in both the serum and urine samples, which were the basis of difference among the groups. These metabolites were involved in the glucose metabolism and TCA cycle (lactate, 2-oxoglutarate, citrate, succinate, pyruvate, and acetate), amino acid metabolism (alanine, 2-hydroxybutyrate), choline metabolism (betaine), creatinine metabolism (creatinine), and gut microbiome metabolism (hippurate, phenylacetylglycine, dimethylamine, and trigonelline). Some key metabolites were identified and quantified showing a statistically ($p < 0.05$) significant improvement in this treated group (500 mg/kg). This study, therefore, confirms the metabolic alteration caused by HFD induced obesity in a rat model and the improvement in certain metabolic pathways, upon treatment with MLE 60. It also provides additional information that ^{1}H NMR metabolomics can be a good approach to study the development of disease and response to treatment in obese subjects.

Conflict of Interests

The authors declare that there is no conflict of interests regarding the publication of this paper.

References

[1] J. W. Yun, "Possible anti-obesity therapeutics from nature—a review," *Phytochemistry*, vol. 71, no. 14-15, pp. 1625–1641, 2010.

[2] A. G. Dulloo, C. Duret, D. Rohrer et al., "Efficacy of a green tea extract rich in catechin polyphenols and caffeine in increasing 24-h energy expenditure and fat oxidation in humans," *The American Journal of Clinical Nutrition*, vol. 70, no. 6, pp. 1040–1045, 1999.

[3] P. Chantre and D. Lairon, "Recent findings of green tea extract AR25 (Exolise) and its activity for the treatment of obesity," *Phytomedicine*, vol. 9, no. 1, pp. 3–8, 2002.

[4] C. Lu, W. Zhu, C.-L. Shen, and W. Gao, "Green tea polyphenols reduce body weight in rats by modulating obesity-related genes," *PLoS ONE*, vol. 7, no. 6, Article ID e38332, 2012.

[5] L.-K. Han, Y. Kimura, and H. Okuda, "Reduction in fat storage during chitin-chitosan treatment in mice fed a high-fat diet," *International Journal of Obesity*, vol. 23, no. 2, pp. 174–179, 1999.

[6] M. Yamamoto, S. Shimura, Y. Itoh, T. Ohsaka, M. Egawa, and S. Inoue, "Anti-obesity effects of lipase inhibitor CT-II, an extract from edible herbs, Nomame Herba, on rats fed a high-fat diet," *International Journal of Obesity*, vol. 24, no. 6, pp. 758–764, 2000.

[7] A. M. M. Jalil, A. Ismail, P. P. Chong, M. Hamid, and S. H. S. Kamaruddin, "Effects of cocoa extract containing polyphenols and methylxanthines on biochemical parameters of obese-diabetic rats," *Journal of the Science of Food and Agriculture*, vol. 89, no. 1, pp. 130–137, 2009.

[8] J. B. German, B. D. Hammock, and S. M. Watkins, "Metabolomics: building on a century of biochemistry to guide human health," *Metabolomics*, vol. 1, no. 1, pp. 3–9, 2005.

[9] M. Wang, R.-J. A. N. Lamers, H. A. A. J. Korthout et al., "Metabolomics in the context of systems biology: bridging traditional Chinese medicine and molecular pharmacology," *Phytotherapy Research*, vol. 19, no. 3, pp. 173–182, 2005.

[10] B. Wu, S. Yan, Z. Lin et al., "Metabonomic study on ageing: NMR-based investigation into rat urinary metabolites and the effect of the total flavone of *Epimedium*," *Molecular BioSystems*, vol. 4, no. 8, pp. 855–861, 2008.

[11] K. S. Solanky, N. J. C. Bailey, B. M. Beckwith-Hall et al., "Application of biofluid ^{1}H nuclear magnetic resonance-based metabonomic techniques for the analysis of the biochemical effects of dietary isoflavones on human plasma profile," *Analytical Biochemistry*, vol. 323, no. 2, pp. 197–204, 2003.

[12] O. Beckonert, H. C. Keun, T. M. D. Ebbels et al., "Metabolic profiling, metabolomic and metabonomic procedures for NMR spectroscopy of urine, plasma, serum and tissue extracts," *Nature protocols*, vol. 2, no. 11, pp. 2692–2703, 2007.

[13] S.-H. Kim, S.-O. Yang, H.-S. Kim, Y. Kim, T. Park, and H.-K. Choi, " ^{1}H-nuclear magnetic resonance spectroscopy-based metabolic assessment in a rat model of obesity induced by a high-fat diet," *Analytical and Bioanalytical Chemistry*, vol. 395, no. 4, pp. 1117–1124, 2009.

[14] G. E. Duggan, D. S. Hittel, C. C. Hughey, A. Weljie, H. J. Vogel, and J. Shearer, "Differentiating short- and long-term effects of diet in the obese mouse using ^{1}H-nuclear magnetic resonance metabolomics," *Diabetes, Obesity and Metabolism*, vol. 13, no. 9, pp. 859–862, 2011.

[15] E.-Y. Won, M.-K. Yoon, S.-W. Kim et al., "Gender specific metabolomic profiling of obesity in leptin deficient ob/ob mice by ^{1}H NMR spectroscopy," *PLoS ONE*, vol. 8, no. 10, Article ID e75998, 2013.

[16] X. Song, J. Wang, P. Wang, N. Tian, M. Yang, and L. Kong, " ^{1}H NMR-based metabolomics approach to evaluate the effect of Xue-Fu-Zhu-Yu decoction on hyperlipidemia rats induced by high-fat diet," *Journal of Pharmaceutical and Biomedical Analysis*, vol. 78-79, pp. 202–210, 2013.

[17] J. Gerlach, "Native or introduced plant species," *Phelsuma*, vol. 4, pp. 70–74, 1996.

[18] A. R. Dixon, H. McMillen, and N. L. Etkin, "Ferment this: the transformation of Noni, a traditional Polynesian medicine (*Morinda citrifolia*, Rubiaceae)," *Economic Botany*, vol. 53, no. 1, pp. 51–68, 1999.

[19] S.-U. R. Mandukhail, N. Aziz, and A.-H. Gilani, "Studies on antidyslipidemic effects of *Morinda citrifolia* (Noni) fruit, leaves and root extracts," *Lipids in Health and Disease*, vol. 9, article 88, 2010.

[20] M. S. Pak-Dek, A. Abdul-Hamid, A. Osman, and C. S. Soh, "Inhibitory effect of *Morinda citrifolia* L. on lipoprotein lipase activity," *Journal of Food Science*, vol. 73, no. 8, pp. C595–C598, 2008.

[21] N. G. Sahib, A. A. Hamid, D. Kitts, M. Purnama, N. Saari, and F. Abas, "The effects of *Morinda citrifolia*, *Momordica charantia* and *Centella asiatica* extracts on lipoprotein lipase and 3T3-L1 preadipocytes," *Journal of Food Biochemistry*, vol. 35, no. 4, pp. 1186–1205, 2011.

[22] N. Gooda Sahib, A. Abdul Hamid, N. Saari, F. Abas, M. S. Pak Dek, and M. Rahim, "Anti-pancreatic lipase and antioxidant activity of selected tropical herbs," *International Journal of Food Properties*, vol. 15, no. 3, pp. 569–578, 2012.

[23] T. Tsujita, H. Takaichi, T. Takaku, S. Aoyama, and J. Hiraki, "Antiobesity action of epsilon-polylysine, a potent inhibitor of pancreatic lipase," *Journal of Lipid Research*, vol. 47, no. 8, pp. 1852–1858, 2006.

[24] L. Ericksson, E. Johansson, N. Kettanen-Wold, J. Trygg, C. Wikstrom, and S. Wold, *Multi- and Megavariate Data Analysis, Part 1. Basic Principles & Applications*, Umetrics Academy, Umea, Sweden, 2006.

[25] V. Von Diemen, E. N. Trindade, and M. R. M. Trindade, "Experimental model to induce obesity in rats," *Acta Cirurgica Brasileira*, vol. 21, no. 6, pp. 425–429, 2006.

[26] S. C. Woods, R. J. Seeley, P. A. Rushing, D. D'Alessio, and P. Tso, "A controlled high-fat diet induces an obese syndrome in rats," *Journal of Nutrition*, vol. 133, no. 4, pp. 1081–1087, 2003.

[27] R. Buettner, J. Schölmerich, and L. C. Bollheimer, "High-fat diets: modeling the metabolic disorders of human obesity in rodents," *Obesity*, vol. 15, no. 4, pp. 798–808, 2007.

[28] P. Yaqoob, E. J. Sherrington, N. M. Jeffery et al., "Comparison of the effects of a range of dietary lipids upon serum and tissue lipid composition in the rat," *The International Journal of Biochemistry and Cell Biology*, vol. 27, no. 3, pp. 297–310, 1995.

[29] J.-S. Tian, B.-Y. Shi, H. Xiang, S. Gao, X.-M. Qin, and G.-H. Du, "^{1}H-NMR-based metabonomic studies on the anti-depressant effect of genipin in the chronic unpredictable mild stress rat model," *PLoS ONE*, vol. 8, no. 9, Article ID e75721, 2013.

[30] N. Tian, J. Wang, P. Wang, X. Song, M. Yang, and L. Kong, "NMR-based metabonomic study of Chinese medicine Gegen Qinlian Decoction as an effective treatment for type 2 diabetes in rats," *Metabolomics*, vol. 9, no. 6, pp. 1228–1242, 2013.

[31] S. Bouatra, F. Aziat, R. Mandal et al., "The human urine metabolome," *PLoS ONE*, vol. 8, no. 9, Article ID e73076, 2013.

[32] N. Psychogios, D. D. Hau, J. Peng et al., "The human serum metabolome," *PLoS ONE*, vol. 6, no. 2, Article ID e16957, 2011.

[33] N. J. Serkova, M. Jackman, J. L. Brown et al., "Metabolic profiling of livers and blood from obese Zucker rats," *Journal of Hepatology*, vol. 44, no. 5, pp. 956–962, 2006.

[34] A. Waldram, E. Holmes, Y. Wang et al., "Top-down systems biology modeling of host metabotype-microbiome associations in obese rodents," *Journal of Proteome Research*, vol. 8, no. 5, pp. 2361–2375, 2009.

[35] L.-C. Zhao, X.-D. Zhang, S.-X. Liao, H.-Y. Wang, D.-H. Lin, and H.-C. Gao, "A metabonomic comparison of urinary changes in Zucker and GK rats," *Journal of Biomedicine and Biotechnology*, vol. 2010, Article ID 431894, 6 pages, 2010.

[36] A. A. Mahdi, S. Annarao, S. Tripathi et al., "Correlation of age related metabonomic changes in ^{1}H NMR serum and urine profiles of rats with cognitive function," *The Open Magnetic Resonance Journal*, vol. 1, no. 1, pp. 71–76, 2008.

[37] H. J. Schirra, C. G. Anderson, W. J. Wilson et al., "Altered metabolism of growth hormone receptor mutant mice: a combined NMR metabonomics and microarray study," *PLoS ONE*, vol. 3, no. 7, Article ID e2764, 2008.

[38] J. Shearer, G. Duggan, A. Weljie, D. S. Hittel, D. H. Wasserman, and H. J. Vogel, "Metabolomic profiling of dietary-induced insulin resistance in the high fat-fed C57BL/6J mouse," *Diabetes, Obesity and Metabolism*, vol. 10, no. 10, pp. 950–958, 2008.

[39] H. Li, Z. Xie, J. Lin et al., "Transcriptomic and metabonomic profiling of obesity-prone and obesity-resistant rats under high fat diet," *Journal of Proteome Research*, vol. 7, no. 11, pp. 4775–4783, 2008.

[40] D. C. DeVilliers, P. K. Dixit, and A. Lazarow, "Citrate metabolism in diabetes. I. Plasma citrate in alloxan-diabetic rats and in clinical diabetes," *Metabolism*, vol. 15, no. 5, pp. 458–465, 1966.

[41] A. Cupisti, M. Meola, C. D'Alessandro et al., "Insulin resistance and low urinary citrate excretion in calcium stone formers," *Biomedicine & Pharmacotherapy*, vol. 61, no. 1, pp. 86–90, 2007.

[42] G. Souto, C. Donapetry, J. Calviño, and M. M. Adeva, "Metabolic acidosis-induced insulin resistance and cardiovascular risk," *Metabolic Syndrome and Related Disorders*, vol. 9, no. 4, pp. 247–253, 2011.

[43] B. Xie, M. J. Waters, and H. J. Schirra, "Investigating potential mechanisms of obesity by metabolomics," *Journal of Biomedicine and Biotechnology*, vol. 2012, Article ID 805683, 10 pages, 2012.

[44] M. Piccinini, M. Mostert, G. Alberto et al., "Down-regulation of pyruvate dehydrogenase phosphatase in obese subjects is a defect that signals insulin resistance," *Obesity Research*, vol. 13, no. 4, pp. 678–686, 2005.

[45] Q. He, P. Ren, X. Kong et al., "Comparison of serum metabolite compositions between obese and lean growing pigs using an NMR-based metabonomic approach," *Journal of Nutritional Biochemistry*, vol. 23, no. 2, pp. 133–139, 2012.

[46] H. Satoh, "Cardioprotective actions of taurine against intracellular and extracellular calcium-induced effects," *Advances in Experimental Medicine and Biology*, vol. 359, pp. 181–196, 1994.

[47] Y. Nakaya, A. Minami, N. Harada, S. Sakamoto, Y. Niwa, and M. Ohnaka, "Taurine improves insulin sensitivity in the Otsuka Long-Evans Tokushima Fatty rat, a model of spontaneous type 2 diabetes," *American Journal of Clinical Nutrition*, vol. 71, no. 1, pp. 54–58, 2000.

[48] N. Tsuboyama-Kasaoka, C. Shozawa, K. Sano et al., "Taurine (2-aminoethanesulfonic acid) deficiency creates a vicious circle promoting obesity," *Endocrinology*, vol. 147, no. 7, pp. 3276–3284, 2006.

[49] M. Lever and S. Slow, "The clinical significance of betaine, an osmolyte with a key role in methyl group metabolism," *Clinical Biochemistry*, vol. 43, no. 9, pp. 732–744, 2010.

[50] J. Pekkinen, K. Olli, A. Huotari et al., "Betaine supplementation causes increase in carnitine metabolites in the muscle and liver of mice fed a high-fat diet as studied by nontargeted LC-MS metabolomics approach," *Molecular Nutrition & Food Research*, vol. 57, no. 11, pp. 1959–1968, 2013.

[51] M. S. Klein, C. Dorn, M. Saugspier, C. Hellerbrand, P. J. Oefner, and W. Gronwald, "Discrimination of steatosis and NASH in mice using nuclear magnetic resonance spectroscopy," *Metabolomics*, vol. 7, no. 2, pp. 237–246, 2011.

[52] J. B. Walker, "Metabolic control of creatine biosynthesis. II. Restoration of transamidinase activity following creatine repression," *The Journal of Biological Chemistry*, vol. 236, pp. 493–498, 1961.

[53] S. R. Kimball and L. S. Jefferson, "Regulation of protein synthesis by branched-chain amino acids," *Current Opinion in Clinical Nutrition and Metabolic Care*, vol. 4, no. 1, pp. 39–43, 2001.

[54] J. K. Nicholson, E. Holmes, and I. D. Wilson, "Gut microorganisms, mammalian metabolism and personalized health care," *Nature Reviews Microbiology*, vol. 3, no. 5, pp. 431–438, 2005.

[55] A. N. Phipps, J. Stewart, B. Wright, and I. D. Wilson, "Effect of diet on the urinary excretion of hippuric acid and other dietary-derived aromatics in rat. A complex interaction between diet, gut microflora and substrate specificity," *Xenobiotica*, vol. 28, no. 5, pp. 527–537, 1998.

[56] E.-Y. Won, M.-K. Yoon, S.-W. Kim et al., "Gender specific metabolomic profiling of obesity in leptin deficient ob/ob mice by 1H NMR spectroscopy," *PLoS ONE*, vol. 8, no. 10, Article ID e75998, 2013.

[57] S. Rezzi, Z. Ramadan, F.-P. J. Martin et al., "Human metabolic phenotypes link directly to specific dietary preferences in healthy individuals," *Journal of Proteome Research*, vol. 6, no. 11, pp. 4469–4477, 2007.

[58] J. Sun, L. K. Schnackenberg, R. D. Holland et al., "Metabonomics evaluation of urine from rats given acute and chronic doses of acetaminophen using NMR and UPLC/MS," *Journal of Chromatography B*, vol. 871, no. 2, pp. 328–340, 2008.

[59] R. Calvani, A. Miccheli, G. Capuani et al., "Gut microbiome-derived metabolites characterize a peculiar obese urinary metabotype," *International Journal of Obesity*, vol. 34, no. 6, pp. 1095–1098, 2010.

[60] C. B. Newgard, J. An, J. R. Bain et al., "A branched chain amino acid-related metabolic signature that differentiates obese and lean humans and contributes to insulin resistance," *Cell Metabolism*, vol. 9, no. 4, pp. 311–326, 2009.

[61] R. A. Kreisberg, "Glucose-lactate inter-relations in man," *The New England Journal of Medicine*, vol. 287, no. 3, pp. 132–137, 1972.

[62] P.-A. Jansson, A. Larsson, U. Smith, and P. Lönnroth, "Lactate release from the subcutaneous tissue in lean and obese men," *The Journal of Clinical Investigation*, vol. 93, no. 1, pp. 240–246, 1994.

[63] J. Aduen, W. K. Bernstein, T. Khastagir et al., "The use and clinical importance of a substrate-specific electrode for rapid determination of blood lactate concentrations," *The Journal of the American Medical Association*, vol. 272, no. 21, pp. 1678–1685, 2004.

[64] J. Lovejoy, F. D. Newby, S. S. P. Gebhart, and M. DiGirolamo, "Insulin resistance in obesity is associated with elevated basal lactate levels and diminished lactate appearance following intravenous glucose and insulin," *Metabolism*, vol. 41, no. 1, pp. 22–27, 1992.

[65] Y. D. I. Chen, B. B. Varasteh, and G. M. Reaven, "Plasma lactate concentration in obesity and type 2 diabetes," *Diabete et Metabolisme*, vol. 19, no. 4, pp. 348–354, 1993.

[66] N. Friedrich, K. Budde, T. Wolf et al., "Short-term changes of the urine metabolome after bariatric surgery," *OMICS*, vol. 16, no. 11, pp. 612–620, 2012.

[67] G. L. S. Pawan and S. J. G. Semple, "Effect of 3-hydroxybutyrate in obese subjects on very-low-energy diets and during therapeutic starvation," *The Lancet*, vol. 321, no. 8314-8315, pp. 15–17, 1983.

[68] R. Nosadini, A. Avogaro, and R. Trevisan, "Acetoacetate and 3-hydroxybutyrate kinetics in obese and insulin-dependent diabetic humans," *The American Journal of Physiology—Regulatory Integrative and Comparative Physiology*, vol. 248, no. 5, part 2, pp. R611–R620, 1985.

[69] J. S. Fisler, M. Egawa, and G. A. Bray, "Peripheral 3-hydroxybutyrate and food intake in a model of dietary-fat induced obesity: effect of vagotomy," *Physiology & Behavior*, vol. 58, no. 1, pp. 1–7, 1995.

[70] N. Gooda Sahib, N. Saari, A. Ismail, A. Khatib, F. Mahomoodally, and A. Abdul Hamid, "Plants' metabolites as potential antiobesity agents," *The Scientific World Journal*, vol. 2012, Article ID 436039, 8 pages, 2012.

[71] A. Perez-Cornago, L. Brennan, I. Ibero-Baraibar et al., "Metabolomics identifies changes in fatty acid and amino acid profiles in serum of overweight older adults following a weight loss intervention," *Journal of Physiology and Biochemistry*, vol. 70, no. 2, pp. 593–602, 2014.

[72] S. Wahl, C. Holzapfel, Z. Yu et al., "Metabolomics reveals determinants of weight loss during lifestyle intervention in obese children," *Metabolomics*, vol. 9, no. 6, pp. 1157–1167, 2013.

[73] P. S. Larmo, A. J. Kangas, P. Soininen et al., "Effects of sea buckthorn and bilberry on serum metabolites differ according to baseline metabolic profiles in overweight women: a randomized crossover trial," *The American Journal of Clinical Nutrition*, vol. 98, no. 4, pp. 941–951, 2013.

[74] M. J. Kim, H. J. Yang, J. H. Kim et al., "Obesity-related metabolomic analysis of human subjects in black soybean peptide intervention study by ultraperformance liquid chromatography and quadrupole-time-of-flight mass spectrometry," *Journal of Obesity*, vol. 2013, Article ID 874981, 11 pages, 2013.

[75] J. M. Miles, L. Leiter, P. Hollander et al., "Effect of orlistat in overweight and obese patients with type 2 diabetes treated with metformin," *Diabetes Care*, vol. 25, no. 7, pp. 1123–1128, 2002.

[76] J. S. Torgerson, J. Hauptman, M. N. Boldrin, and L. Sjöström, "Xenical in the prevention of diabetes in obese subjects (XENDOS) study: a randomized study of orlistat as an adjunct to lifestyle changes for the prevention of type 2 diabetes in obese patients," *Diabetes Care*, vol. 27, no. 1, pp. 155–161, 2004.

[77] H. M. Sickmann, H. S. Waagepetersen, A. Schousboe, A. J. Benie, and S. D. Bouman, "Obesity and type 2 diabetes in rats are associated with altered brain glycogen and amino-acid homeostasis," *Journal of Cerebral Blood Flow & Metabolism*, vol. 30, no. 8, pp. 1527–1537, 2010.

[78] S. Satapati, N. E. Sunny, B. Kucejova et al., "Elevated TCA cycle function in the pathology of diet-induced hepatic insulin resistance and fatty liver," *Journal of Lipid Research*, vol. 53, no. 6, pp. 1080–1092, 2012.

[79] I. H. De Boer, S. D. Sibley, B. Kestenbaum et al., "Central obesity, incident microalbuminuria, and change in creatinine clearance in the epidemiology of diabetes interventions and complications study," *Journal of the American Society of Nephrology*, vol. 18, no. 1, pp. 235–243, 2007.

[80] D. S. Hittel, Y. Hathout, E. P. Huffman, and J. A. Houmard, "Proteome analysis of skeletal muscle from obese and morbidly obese women," *Diabetes*, vol. 54, no. 5, pp. 1283–1288, 2005.